Proceedings of Anticancer Research

Honorary Editor-in-Chief

Behnam Mahdavi

Department of Chemistry, Faculty of Science, Hakim Sabzevari University, Iran

Editor-in-Chief

Shixiang Guo

Chongqing General Hospital, China

Dongmei Guo

Qilu Hospital of Shandong University, China

Wenbin Zhang

The Affiliated Tumor Hospital of Xinjiang Medical University, China

BIO-BYWORD SCIENTIFIC PUBLISHING PTY LTD
(619 649 400)
Level 10
50 Clarence Street
SYDNEY NSW 2000
Copyright © 2025. Bio-Byword Scientific Publishing Pty Ltd.
Complimentary Copy

ISSN (ONLINE): 2208-3553
ISSN (PRINT): 2208-3545

Proceedings of Anticancer Research

Focus and Scope

Proceedings of Anticancer Research is an international peer-reviewed and open access journal, which is devoted to the rapid publication of high quality original articles, reviews, case reports, short communication and letters on all aspects of experimental and clinical oncology.

- Cellular research and bio-markers
- Identification of bio-targets and agents with novel mechanisms of action
- Preventative and integrated treatment for cancer patients
- Radiation and surgery
- Palliative care
- Patient adherence, quality of life, satisfaction
- Anticancer medicine

About Publisher

Bio-Byword Scientific Publishing is a fast-growing, peer-reviewed and open access journal publisher, which is located in Sydney, Australia. As a dependable and credible corporation, it promotes and serves a broad range of subject areas for the benefit of humanity. By informing and educating a global community of scholars, practitioners, researchers and students, it ndeavors to be the world's leading independent academic and professional publisher. To realize it, it keeps creative and innovative to meet the range of the authors' needs and publish the best of their work.

By cooperating with University of Sydney, University of New South Wales and other world-famous universities, Bio-Byword Scientific Publishing has established a huge publishing system based on hundreds of academic programs, and with a variety of journals in the subjects of medicine, construction, education and electronics.

PublisherHeadquarter

BIO-BYWORD SCIENTIFIC PUBLISHING PTYLTD Level 10
50 Clarence Street
Sydney NSW 2000
Website: www.bbwpublisher.com Email: info@bbwpublisher.com

2026, Volume 10, Issue 1

Table of Contents

1 **Analysis of the Application Effect of Laparoscopy Combined with Choledochoscopy in the Treatment of Difficult Cholelithiasis**
Dexin Xia

8 **Glucose-6-Phosphate Dehydrogenase is a Prognostic Biomarker and Correlated with Immune Infiltrates in Hepatocellular Carcinoma**
Yiming Niu, Qi Zhu, Jintang Jia

22 **A Review on the Association between Dyslipidemia, Glucose Tolerance, and Coronary Heart Disease Risk**
Xueling He, Yanyan Zhang, Qingkai Yan

33 **SIRT Visualization and Hotspot Analysis Based on The Web of Science Database for the Treatment of Liver Neoplasms**
Guangyuan Zhao, Mengyun Bai, Dengxiang Liu

48 **Single-cell Sequencing: Application in the Study of Disseminated Tumour Cells and Breast Cancer Treatment**
Mingyue Wang

54 **The Impact of Double-puncture Tympanic Membrane Puncture and Tympanic Cavity Drug Injection on the Complication Rate of Acute Secretory Otitis Media**
Wei Zheng

61 **Research Progress on Malnutrition and Nutritional Intervention in Children with Leukemia During Chemotherapy**
Xiangyan Cao, Shuang Zhang, Jialin Ye

69 **Advances in Proteolysis Targeting Chimeras**
Shili Liu, Yu Liu

84 **The Immunomodulatory, Anti-Tumor, and Metabolic Regulatory Effects of Fraction D of Polysaccharide from *Grifola frondosa*: Clinical Experiments and Mechanistic Insights**
Nurfarih Hanna, Mohd Zarif Fikri Bin Mohd, Muhammad Nabil Fikri Bin Mohd, Nurfarazuna Binti Mohd Fadrol

94 Imaging Findings of Sarcomatoid Carcinoma of the Ureter: A Case Report
Wenyu Cai, Xiaofen Ma

101 Analysis of Long-term Prognosis and Cosmetic Outcomes of Breast-conserving Surgery Combined with Sentinel Lymph Node Biopsy for Early-stage Breast Cancer
Yuedong Zhang

109 Cerebral Tuberculoma on the Left Frontal Lobe
Zixuan Zhou, Shanshan Wang

115 Observation on the Efficacy and Mechanism of Blood-Letting and Cupping Therapy in Improving Upper Limb Lymphedema after Breast Cancer Surgery
Dongli Zhang, Jia Liu, Qian Zheng

122 Expression and Clinical Significance of PKM2 and SERBP1 in Colorectal Cancer
Yijie Li, Ying Duan, Zhengyi Cheng, Weichen Zuo, Juan Yang, Hangrong Fang

130 Research on the Impact of Different Lymph Node Dissection Scopes on Postoperative Recurrence and Survival Rates in Patients with Early Gastric Cancer
Zhijun Mao, Yingdi Wei, Ganjie Yang, Pan Gao, Tong Hui

Proceedings of Anticancer Research, 2026, Volume 10, Issue 1
http://ojs.bbwpublisher.com/index.php/PAR
ISSN Online: 2208-3553
ISSN Print: 2208-3545

Analysis of the Application Effect of Laparoscopy Combined with Choledochoscopy in the Treatment of Difficult Cholelithiasis

Dexin Xia*

Xinghua People's Hospital, Taizhou 225700, Jiangsu, China

**Author to whom correspondence should be addressed.*

Copyright: © 2026 Author(s). This is an open-access article distributed under the terms of the Creative Commons Attribution License (CC BY 4.0), permitting distribution and reproduction in any medium, provided the original work is cited.

Abstract: *Objective*: To analyze the therapeutic effect of laparoscopy combined with choledochoscopy in the treatment of difficult cholelithiasis. *Methods*: A total of 60 patients with difficult cholelithiasis admitted for treatment from January 2022 to December 2024 were selected and evenly divided into two groups using a random number table. The combined group received laparoscopy combined with choledochoscopy treatment, while the single group received laparoscopy treatment alone. The total treatment efficacy, perioperative indicators, angiotensin (Ang) levels, quality of life scores, and complication rates were compared between the two groups. *Results:* The total treatment efficacy in the combined group was higher than that in the single group; except for operative time, the perioperative indicators in the combined group were superior to those in the single group; the Ang levels after treatment in the combined group were lower than those in the single group, and the quality of life scores were higher ($P < 0.05$). The complication rate in the combined group was lower than that in the single group ($P < 0.05$). *Conclusion:* Laparoscopy combined with choedochoscopy can enhance the treatment effectiveness for patients with difficult cholelithiasis, improve perioperative indicators, regulate their Ang levels, elevate quality of life, and demonstrate high surgical safety.

Keywords: Laparoscopy; Choledochoscopy; Difficult gallstones; Perioperative indicators; Complication rate

Online publication: February 4, 2026

1. Introduction

Difficult gallstones are a type of gallstone disease characterized by rapid onset, rapid progression, and significant difficulty in stone extraction, presenting symptoms such as pain in the right shoulder or upper right abdomen, and prone to causing adverse events such as cholecystitis or gallbladder cancer [1]. The primary treatment methods for this condition include oral medication or surgical intervention. The former mainly involves anti-inflammatory and cholagogic tablets or stone-dissolving drugs, which can alleviate symptoms but offer limited curative potential. Surgical treatment primarily employs laparoscopy, utilizing fiber-optic endoscopy to accurately locate the surgical area, comprehensively explore the abdominal cavity, and systematically perform procedures such as cholecystectomy

and stone extraction. While laparoscopic monotherapy offers a relatively short operative time, it is prone to leaving residual stones, thus presenting certain limitations [2]. Choledochoscopy, with its high imaging quality, can expand the surgical field of view during laparoscopy, efficiently remove small-volume stones, and, when combined with laparoscopy, achieves a high surgical success rate. Based on this, this study selected 60 patients with difficult gallstones to evaluate the overall efficacy of laparoscopic combined with choledochoscopic treatment.

2. Materials and methods

2.1. General information

A total of 60 patients with difficult gallstones admitted for treatment from January 2022 to December 2024 were selected and evenly divided into two groups using a random number table. The combined group consisted of 30 patients, including 18 males and 12 females, aged between 28 and 74 years old, with an average age of (43.15 ± 4.18) years old; the disease duration ranged from 1 to 8 months, with an average duration of (3.58 ± 0.74) months. The single group also had 30 patients, including 17 males and 13 females, aged between 26 and 71 years old, with an average age of (43.22 ± 4.34) years old; the disease duration ranged from 1 to 7 months, with an average duration of (3.40 ± 0.68) months. There were no significant differences in the data between the two groups ($P > 0.05$).

Inclusion criteria: Diagnosis of gallstones based on imaging techniques such as ultrasound or CT; meeting the indications for laparoscopic and choledochoscopic treatment; having complete basic patient information; possessing normal cognitive function; being informed about and consenting to the study. Exclusion criteria: Presence of surgical contraindications; having a history of biliary surgery; intrahepatic bile duct stones; cardiorenal and hepatic dysfunction; suffering from mental illnesses; withdrawing from the study midway.

2.2. Methods

Laparoscopic treatment for the single-treatment group: Prior to surgery, patients were instructed to fast and abstain from drinking for more than 6 hours, undergo skin preparation, and then, after general anesthesia, maintain a supine position with the head elevated and feet lowered, and the body tilted approximately 25° to the left. A 1 cm observation port was made below the umbilicus, and 1 cm and 0.5 cm working ports were made below the xiphoid process and below the right costal margin, respectively. A carbon dioxide pneumoperitoneum was established with a pressure of 12 mmHg, and a laparoscope and corresponding therapeutic instruments were inserted to comprehensively explore the abdominal cavity. The fundus of the gallbladder was grasped with grasping forceps and turned upward to expose the gallbladder triangle. The cystic artery and cystic duct were separated using an electrocautery hook, and a locking clip was applied near the common bile duct side, 0.5 cm from the common bile duct, and a titanium clip was applied near the gallbladder side. The cystic duct was then cut. The cystic artery was closed with a locking clip and cauterized and severed with electrocoagulation. The gallbladder was separated using an electrocautery hook for complete dissection and then resected. Active bleeding points were observed, and electrocoagulation hemostasis could be performed if necessary. Residual stones or bile in the abdominal cavity were cleared. The resected specimen was removed through the umbilical incision, the laparoscope and instruments were withdrawn, the carbon dioxide was evacuated, and the incision was sutured.

Combined laparoscopic and choledochoscopic treatment for the combined-treatment group: Preoperative preparation and anesthesia methods were the same as above. The patient was maintained in a supine position, and a 1 cm incision was made at the umbilicus. A 10 mm Trocar was inserted, and carbon dioxide gas was

injected to establish an artificial pneumoperitoneum with a pressure of 12 mmHg. Observation was conducted using the laparoscope, and a 0.5 cm incision was made below the right costal margin, into which a 5 mm Trocar was inserted; a 1 cm incision was made below the xiphoid process, into which a 10 mm Trocar was inserted. Keep the patient in a left oblique position with the head elevated and feet lowered, and examine the liver region and the gastroduodenal region. For patients with an excessively thick or tense gallbladder wall, incision and decompression are performed. The cystic triangle region is dissected to clarify the relationship between the three ducts and the ampulla, separate the ducts, insert a choledochoscope, evaluate the position of the cystic duct, determine the number, location, and size of stones, and remove them. The cystic artery is clamped with a lock clip, and the residual end of the cystic duct is also clamped. If the cystic duct is thick, it is ligated with a suture; if the residual end is short, it is sutured. The gallbladder tissue is stripped using a combination of anterograde and retrograde methods. Remove stones and resected tissues, and suture the incision.

2.3. Observation indicators

(1) Perioperative indicators: Observe indicators such as operation time, intraoperative blood loss, postoperative recovery time of gastrointestinal function, postoperative pain score at 7 days (using the Visual Analog Scale, with scores ranging from 0 to 10, where higher scores indicate greater pain intensity), and length of hospital stay.

(2) Ang levels: Fasting venous blood samples are collected at the same time periods, centrifuged for 10 minutes at a speed of 3000 r/min, and the supernatant is extracted. The levels of AngI, AngII, and Ang1-7 are evaluated using the enzyme-linked immunosorbent assay method [3].

(3) Quality of Life Score: The Generic Quality of Life Inventory (GQOLI) [4] was selected for evaluation, encompassing social function, psychological function, and physical function, each scored out of 100 points. Quality of life is positively correlated with the score.

(4) Complication Rate: The incidence rates of complications such as abdominal abscess, incision infection, bile leakage, intestinal adhesion, pulmonary infection, and bile duct injury were observed.

2.4. Efficacy evaluation criteria

Cure is defined as the disappearance of physical signs, normalization of blood test results, negative laboratory test results, and absence of residual stones on ultrasound. Significant efficacy is characterized by marked improvement in physical signs, generally normal blood test results, mostly negative laboratory test results, and no residual stones on ultrasound. Preliminary efficacy is indicated by improvement in physical signs, blood test results, and laboratory test results, with a small amount of residual stones visible on ultrasound. No efficacy is determined when there is no improvement in physical signs, blood test results, and laboratory test results, with a large amount of residual stones visible on ultrasound.

2.5. Statistical analysis

Data were analyzed using SPSS 26.0 statistical software. Count data were expressed as (n/%) and compared using the chi-square (χ^2) test. Measurement data were tested for normal distribution using the Kolmogorov-Smirnov (K-S) test and expressed as mean ± standard deviation (SD). Comparisons between groups were made using the independent samples t-test, while comparisons within groups were made using the paired t-test. A P-value less than 0.05 was considered statistically significant.

3. Results

3.1. Comparison of overall effectiveness rates between the two groups

The overall effectiveness rate in the combined group was higher than that in the single-treatment group ($P < 0.05$) (**Table 1**).

Table 1. Comparison of overall effectiveness rates between the two groups (*n*/%)

Group	n	Disease Cure	Marked Efficacy	Moderate Efficacy	No Efficacy	Overall Effective Rate
Combination Group	30	18 (60.00)	9 (30.00)	3 (10.00)	0	100.00 (30/30)
Single Agent Group	30	17 (56.67)	7 (23.33)	2 (6.67)	4 (13.33)	86.67 (26/30)
χ^2						4.286
P						0.038

3.2. Comparison of perioperative indicators between the two groups

Except for surgical duration, the perioperative indicators in the combined group were superior to those in the single-treatment group ($P < 0.05$) (**Table 2**).

Table 2. Comparison of perioperative indicators between the two groups (mean ± SD)

Group	n	Operative Time (min)	Intraoperative Blood Loss (mL)	Time to Gastrointestinal Function Recovery (h)	Pain Score at Postoperative Day 7	Length of Hospital Stay (days)
Combination Group	30	48.95 ± 6.48	45.39 ± 5.95	16.37 ± 1.77	2.20 ± 0.58	6.71 ± 0.51
Single Agent Group	30	47.11 ± 6.32	55.71 ± 5.82	17.82 ± 1.56	3.86 ± 0.67	7.09 ± 0.63
t		1.113	6.791	3.366	10.260	2.568
P		0.270	0.000	0.001	0.000	0.013

3.3. Comparison of quality of life scores between the two groups

One day before surgery, there was no significant difference in quality of life scores between the two groups ($P > 0.05$). Seven days after surgery, the quality of life score in the combined group was higher than that in the single-treatment group ($P < 0.05$) (**Table 3**).

Table 3. Comparison of quality of life scores between the two groups (mean ± SD, points)

Group	n	Social Functioning		Psychological Functioning		Physical Functioning	
		Preoperative	Postoperative	Preoperative	Postoperative	Preoperative	Postoperative
Combination Group	30	81.56 ± 4.91	92.11 ± 3.58	80.07 ± 3.54	93.57 ± 3.45	82.45 ± 3.66	92.85 ± 3.14
Single Agent Group	30	81.63 ± 4.95	87.02 ± 3.14	80.10 ± 3.56	90.01 ± 3.41	82.19 ± 3.62	88.02 ± 3.10
t		0.055	5.855	0.033	4.020	0.277	5.996
P		0.956	0.000	0.974	0.000	0.783	0.000

3.4. Comparison of Ang levels between the two groups

One day before surgery, there was no significant difference in Ang levels between the two groups ($P > 0.05$). Seven days after surgery, the Ang level in the combined group was lower than that in the single-treatment group ($P < 0.05$) (**Table 4**).

Table 4. Comparison of Ang levels between the two groups (mean ± SD)

Group	n	Ang I (ng/mL)		Ang II (ng/L)		Ang-(1-7) (ng/L)	
		Preoperative	Postoperative	Preoperative	Postoperative	Preoperative	Postoperative
Combination Group	30	7.51 ± 1.74	10.33 ± 1.89	37.29 ± 5.11	54.28 ± 4.15	310.75 ± 28.41	411.53 ± 32.48
Single Agent Group	30	7.53 ± 1.76	14.52 ± 1.94	37.31 ± 5.08	66.12 ± 4.18	311.02 ± 28.39	520.19 ± 38.76
t		0.044	8.473	0.015	11.010	0.037	11.769
P		0.965	0.000	0.988	0.000	0.971	0.000

3.5. Comparison of complication rates between the two groups

The complication rate in the combined group was lower than that in the single-treatment group ($P < 0.05$) (**Table 5**).

Table 5. Comparison of complication rates between the two groups (*n*/%)

Group	n	Intra-abdominal Abscess	Incisional Infection	Bile Leak	Intestinal Adhesion	Pulmonary Infection	Bile Duct Injury	Overall Complication Rate
Combination Group	30	0 (0.00)	1 (3.33)	0	0	0	0	3.33 (1/30)
Single Agent Group	30	1 (3.33)	1 (3.33)	1 (3.33)	1 (3.33)	1 (3.33)	1 (3.33)	20.00 (6/30)
χ^2								4.043
P								0.044

4. Discussion

The pathogenic factors of gallstones are complex, encompassing long-term skipping breakfast, genetic factors, low physical activity, or cirrhosis, among others. The pathological basis includes increased bile concentration and an imbalance in the ratio of bile acids to cholesterol in the bile, which hinders the smooth excretion of bile and leads to stone formation. The symptoms of this disease are influenced by the location of the stones, the degree of inflammatory response, and the size of the stones, with pain in the upper right abdomen and right shoulder being the primary manifestations. Difficult gallstones refer to a type of gallstone characterized by a complex pathological environment or anatomical structure where the stones are located, large stone size, high risk associated with endoscopic or surgical treatment, and a higher incidence of postoperative complications. These stones may induce symptoms such as indigestion and belching, necessitating early surgical intervention.

Laparoscopic surgery is a commonly used procedure for difficult gallstones. It involves a laparoscope equipped with a miniature camera and is composed of a CO2 pneumoperitoneum system, a video recording system, an electrocautery system, and surgical instruments. During the operation, an artificial pneumoperitoneum can be created under the guidance of a laparoscope, followed by trocar puncture and cholecystotomy, ensuring

a high degree of surgical precision. However, laparoscopic surgery may not efficiently remove stones that are concealed or small in size, presenting certain surgical limitations. Cholangioscopy, a new type of optical endoscope, consists of an optical image transmission system, an objective lens system, and an eyepiece system, and includes flexible and rigid cholangioscopes, among other specifications. It can expand the surgical field of view and ensure a safe and reliable treatment process [5]. The combination of these two techniques can fully leverage their respective advantages and improve the stone clearance effect, resulting in remarkable therapeutic outcomes.

The results showed that the overall effective rate of the combined group was higher than that of the single-technique group, and apart from operative time, the perioperative indicators of the combined group were superior to those of the single-technique group ($P < 0.05$). The reasons for this are as follows: laparoscopy combined with cholangioscopy can magnify the surgical field, accurately locate impacted stones within the ducts, and determine the number of stones, thereby preventing stone omission and enhancing surgical efficacy. Stone removal under direct cholangioscopic visualization can increase the stone clearance rate and effectively prevent disease recurrence [6].

Additionally, the combined surgery is highly applicable to special conditions such as thickened gallbladder walls and increased tension, enabling the clarification of the relationships among the three ducts and the ampulla, preventing bile duct injury, and accurately separating adhesive tissues to ensure surgical precision. More importantly, the combined surgery is minimally invasive, which can reduce surgical trauma and thus promote postoperative recovery [7,8]. The level of Ang in the combined group was lower than that in the single-procedure group 7 days after surgery, the quality of life score was higher, and the complication rate was lower ($P < 0.05$). The reason is that the combined surgery can prevent massive activation of the Ang system and improve patients' tolerance to surgical treatment. Moreover, the magnifying effect of the combined surgery can enhance the accuracy during cholecystectomy and stone removal, reducing stimulation of the renin-angiotensin-aldosterone system (RAS). Consequently, it can improve Ang levels and reduce the risk of postoperative complications [9,10]. Based on the aforementioned surgical treatment, patients recover faster postoperatively, experience mild stress responses, and can resume normal life as soon as possible, thereby enjoying a higher quality of life.

5. Conclusion

In summary, laparoscopic combined with choledochoscopic treatment for patients with difficult gallstones demonstrates a high overall effectiveness rate, accelerates postoperative recovery, protects the patients' Ang system, significantly improves their future quality of life, and is associated with fewer postoperative complications.

Disclosure statement

The author declares no conflict of interest.

References

[1] Jia S, 2025, Study on the Effect of Laparoscopy Combined with Choledochoscopy in Patients with Gallstones and Its Impact on VAS Scores. Journal of Rare and Uncommon Diseases, 32(8): 101–103.

[2] Zhang R, 2023, The Effect of Laparoscopic Combined with Choledochoscopic Common Bile Duct Exploration and

Lithotomy for Primary Suture of the Common Bile Duct in the Treatment of Extrahepatic Gallstones. Chinese Journal of Practical Rural Physicians, 30(6): 43–46.

[3] Song W, 2022, Therapeutic Effect of Laparoscopic Cholecystectomy on Patients with Gallstones. Electronic Journal of Clinical Medical Literature, 9(14): 100–102 + 87.

[4] Li L, Yang D, Zhou L, et al., 2003, Reliability and Validity Study of the World Health Organization Quality of Life Questionnaire in China. Chinese Journal of Psychiatry, 36(3): 143–147.

[5] Xu J, Zhang J, Zhang S, 2021, The Effect of Laparoscopic Combined with Choledochoscopy in the Treatment of Gallstones and Its Impact on Gallbladder Function. Chinese Journal of Current Advances in General Surgery, 24(12): 980–981 + 984.

[6] Wu B, Wu H, 2025, Comparative Study on the Clinical Effects of Laparoscopic Choledochotomy with Fiber Choledochoscope Lithotomy and T-Tube Drainage Versus Open Cholecystectomy for the Treatment of Gallstones. China Practical Medicine, 20(18): 41–43.

[7] Zhang J, Su Z, Fei H, et al., 2021, Analysis and Exploration of the Value of Laparoscopy Combined with Choledochoscopy in the Treatment of Gallstones. China Medical Device Information, 27(4): 70–71.

[8] Zhang L, 2021, Observation on the Application Effect of Personalized Nursing in Laparoscopy Combined with Choledochoscopy for the Treatment of Gallstones. China Health Care & Nutrition, 31(6): 233.

[9] Zhou Q, 2021, Analysis of the Effect of Laparoscopy Combined with Choledochoscopy in the Surgical Treatment of Gallstones. Chinese Journal of Modern Drug Application, 15(2): 59–61.

[10] Sun Q, 2021, Observation on the Clinical Efficacy of Laparoscopy Combined with Choledochoscopy in the Treatment of Gallstones. Intelligent Health, 7(30): 72–74.

Publisher's note

Bio-Byword Scientific Publishing remains neutral with regard to jurisdictional claims in published maps and institutional affiliations.

Proceedings of Anticancer Research, 2026, Volume 10, Issue 1
http://ojs.bbwpublisher.com/index.php/PAR
ISSN Online: 2208-3553
ISSN Print: 2208-3545

Glucose-6-Phosphate Dehydrogenase is a Prognostic Biomarker and Correlated with Immune Infiltrates in Hepatocellular Carcinoma

Yiming Niu, Qi Zhu, Jintang Jia

Gansu Provincial Maternity and Child-care Hospital / Gansu Provincial Central Hospital, Lanzhou 730000, Gansu, China

Copyright: © 2026 Author(s). This is an open-access article distributed under the terms of the Creative Commons Attribution License (CC BY 4.0), permitting distribution and reproduction in any medium, provided the original work is cited.

Abstract: *Objective*: To investigate the correlation between the expression of glucose-6-phosphate dehydrogenase (G6PD) and the clinicopathological characteristics, prognosis and immune cell infiltration of hepatocellular carcinoma (HCC). *Methods*: The expression of G6PD in liver cancer tissues and normal tissues is extracted from TCGA and GEO databases, validated by immunohistochemistry, and the correlation between G6PD expression and clinical features is analyzed. The clinical significance of G6PD in liver cancer is assessed by Kaplan-Meier, Cox regression, and prognostic line graph models. Functional enrichment analysis is performed by protein-protein interaction (PPI) network, GO/KEGG, GSEA and for G6PD-associated differentially expressed genes (DEGs). TIMER and ssGSEA packages are used to assess the correlation between expression and the level of immune cell infiltration. *Results:* Analysis of TCGA and GEO datasets revealed that G6PD expression is significantly upregulated in hepatocellular carcinoma tissues ($P < 0.001$). G6PD expression is associated with histological grade, pathological stage, T-stage, vascular infiltration, and AFP level ($P < 0.05$); HCC patients in the low G6PD expression group had longer overall survival and better prognosis compared with the high G6PD expression group ($P < 0.05$). The level of G6PD expression affects the levels of macrophages, dendritic cells, B cells, and follicular helper T cells in the tumor microenvironment. *Conclusion:* High expression of G6PD is a potential biomarker for poor prognosis of hepatocellular carcinoma, and G6PD may be a target for immunotherapy of HCC.

Keywords: Hepatocellular carcinoma; G6PD; Immunization; Prognosis; Bioinformatics analysis

Online publication: February 6, 2026

1. Introduction

Primary liver cancer is the sixth most common cancer in the world and the third most common cause of cancer mortality, with approximately 906,000 new cases and 830,000 deaths each year. Primary liver cancers include hepatocellular carcinoma (HCC) (75%-85% of cases) and intrahepatic cholangiocarcinoma (10–15%) and mixed [1]. Chronic infection with hepatitis B virus (HBV) or hepatitis C virus (HCV), aflatoxin, alcohol consumption, obesity, type 2 diabetes, and smoking are main risk factors for developing hepatocellular carcinoma (HCC).

Surgical resection, liver transplantation and percutaneous hepatic artery embolization are still the main treatment modalities for HCC, with a 5-year recurrence rate exceeding 70–80% [2]. HCC is prone to relapse, metastasis is the main cause of death, and to date, there is no effective treatment for metastatic HCC. Clinically proven poor response of hepatocellular carcinoma to molecularly targeted drugs (sorafenib, etc.) with limited survival benefit for patients. Immune checkpoint blockers are the most rapidly developing immunotherapy in recent years, mainly using PD1/PDL1 and CTLA4 as therapeutic targets to kill tumors by restoring the function of suppressed T cells [3], while the study found less than 20% anti-PD-1 response rate in liver cancer [4,5].

Existing research shows that the energy metabolic requirements of tumor cells are exceptionally complex compared with normal cells, and abnormal metabolism of many pathways complements the energy requirements of tumor cells. Changes in abnormal glucose metabolism can be observed in many cancer cells, including HCC [5]. Therefore, a better understanding of the metabolic abnormalities of HCC cells is crucial for improving the early diagnosis and treatment of HCC. The pentose phosphate pathway (PPP) is an important component of cellular energy metabolism. It is important for maintaining carbon homeostasis, providing precursors for nucleotide and amino acid biosynthesis, supplying reducing molecules for anabolism, and resisting oxidative stress [6]. *G6PD* is an prominent rate-limiting enzyme in PPP [8], Involves in regulating the synthesis of ribulose-5-phosphate (R-5-P) and reduces coenzyme II (NADPH), of which R-5-P is a precursor for the synthesis of ATP, ADP, AMP, coenzyme A, NAD, etc. [8] NADPH is involved in various metabolic reactions as a hydrogen donor such as tetrahydrofolate, biotransformation of drugs and hormones, and maintenance of reduced glutathione(GSH) [6]. This study analyses the level of *G6PD* expression and prognostics of HCC patients in the Cancer Genome Atlas (TCGA) (https://tcga-data.nci.nih.gov/tcga/) and other public databases. It is aimed at assessing the correlation between *G6PD*-related genes and clinicopathological features, prognosis, and immune infiltration, and providing possible theoretical support for exploring anti-*G6PD* therapy to improve the efficacy of hepatocellular carcinoma.

2. Methods

2.1. Data collection

Gene expression profile tertiary data of hepatocellular carcinoma were downloaded from the TCGA database (https: //portal.gdc.cancer.gov/) and normalized to extract *G6PD* gene expression information. Download clinical information on patients from the cBioportal database (https://www.cbioportal.org/). A total of 374 liver cancer samples and 50 paracancerous tissue samples were included in the study after excluding samples with incomplete clinical information and survival data. This study does not require the approval of the local ethics committee due to the fact that TCGA data are publicly available. In addition, gene expression profiles of the GSE39791 and GSE62232 datasets were collected from the GEO database to verify the expression levels of *G6PD* in normal and tumor tissues. the IHC data from THPA （https://www.proteinatlas.org/） is used to observe the distribution and subcellular localization of *G6PD* and expression in HCC.

2.2. Statistical analysis

SPSS 26.0 statistical software was applied for analysis, and the count data were analyzed by χ^2 test. The diagnostic and prognostic value of *G6PD* in HCC patients was analyzed using the subject operating characteristic curve (ROC) and Kaplan- Meier survival curve. Univariate and multifactorial COX regression analyses illustrated the relationship between *G6PD* expression and overall survival (OS) in HCC patients. $P < 0.05$ was considered to be

statistically significant.

2.3. Protein–protein interaction (PPI) and enrichment analysis

Based on the data of protein-protein interaction (*PPI*) in the online STRING database, we constructed the *PPI* network of differentially expressed proteins. Gene Ontology (GO) and Kyoto Encyclopedia of Genes and Genomes (KEGG) pathway enrichment analysis of *G6PD* and its related genes were performed using the clusterProfiler package in R language to analyze the sites and pathways of action of *G6PD* and its related proteins on HCC. Enrichment analysis of *G6PD*-related biological functions and signaling pathways was performed using the GSEA tool with the ggplot2 package in R language, and gene sets with FDR (false discovery rate) < 0.25 and $P < 0.05$ were considered as significantly enriched gene sets.

2.4. Correlation analysis of immune cell infiltration

The relationship between *G6PD* and tumor purity and several immune cells, including B cells, neutrophils, macrophages, dendritic cells, CD4+ T cells and CD8+ T cells, was assessed by using the Tumor Immune Evaluation Resource (TIMER). Spearman correlation analysis was used to investigate the correlation between *G6PD* and immune cell infiltration.

3. Results

3.1. Clinical data collection

As shown in **Table 1**, the clinical data of 374 patients with HCC in TCGA were statistically analyzed. The results showed that the differences of *G6PD* expression levels in gender, age, BMI, Child stage, liver fibrosis score and tumor status were not statistically significant ($P > 0.05$), and the differences of *G6PD* expression levels in AFP level, T stage, pathological stage, histological stage and vascular invasion were statistically significant ($P < 0.05$).

Table 1. Clinical characteristics of patients with liver cancer based on TCGA

Characteristics	Expression of G6PD		*P*-value
	Low (*n* = 187)	High (*n* = 187)	
Gender, n (%)			
Female	63 (16.8%)	58 (15.5%)	0.658
Male	124 (33.2%)	129 (34.5%)	
Age, n (%)			
≤ 60	89 (23.9%)	88 (23.6%)	1.00
> 60	98 (26.3%)	98 (26.3%)	
BMI, n (%)			
≤ 25	84 (24.9%)	93 (27.6%)	0.246
> 25	87 (25.8%)	73 (21.7%)	
AFP (ng/mL), n (%)			
≤ 400	120 (42.9%)	95 (33.9%)	0.011
> 400	24 (8.6%)	41 (14.6%)	

Table 1 (Continued)

Characteristics	Expression of G6PD		*P*-value
	Low (*n* = 187)	High (*n* = 187)	
Child-Pugh grade, n (%)			
A	123 (51%)	96 (39.8%)	
B	11 (4.6%)	10 (4.1%)	0.899
C	1 (0.4%)	0 (0%)	
Fibrosis Ishak core, n (%)			
0	52 (24.2%)	23 (10.7%)	
1/2	17 (7.9%)	14 (6.5%)	0.080
3/4	15 (7%)	13 (6%)	
5/6	40 (18.6%)	41 (19.1%)	
T stage, n (%)			
T1	107 (28.8%)	76 (20.5%)	
T2	37 (10%)	58 (15.6%)	0.007
T3	37 (10%)	43 (11.6%)	
T4	4 (1.1%)	9 (2.4%)	
Histologic grade, n (%)			
G1	39 (10.6%)	16 (4.3%)	
G2	98 (26.6%)	80 (21.7%)	< 0.001
G3	44 (11.9%)	80 (21.7%)	
G4	4 (1.1%)	8 (2.2%)	
Pathologic stage, n (%)			
Stage I	101 (28.9%)	72 (20.6%)	
Stage II	36 (10.3%)	51 (14.6%)	0.017
Stage III	36 (10.3%)	49 (14%)	
Stage IV	2 (0.6%)	3 (0.9%)	
Vascular invasion, n (%)			
No	118 (37.1%)	90 (28.3%)	0.035
Yes	48 (15.1%)	62 (19.5%)	
Tumor status, n (%)			
Tumor free	112 (31.5%)	90 (25.4%)	0.052
With tumor	68 (19.2%)	85 (23.9%)	

3.2. G6PD expression in HCC

G6PD mRNA levels were expressed in breast cancer (BRCA), cholangiocarcinoma (CHOL), colon cancer (COAD), esophageal cancer (ESCA), glioblastoma multiforme (GBM), renal papillary cell carcinoma (KIRP), acute myeloid leukemia (LAML), low-grade glioma of the brain (LGG), Hepatocellular carcinoma (HCC), lung

adenocarcinoma (LUAD), lung squamous cell carcinoma (LUSC), ovarian plasmacytoid cystic adenocarcinoma (OV), pancreatic adenocarcinoma (PAAD), rectal adenocarcinoma (READ), sarcoma (SARC), cutaneous melanoma (SKCM), gastric adenocarcinoma (STAD), testicular germ cell tumor (TGCT), thyroid carcinoma (THCA), uterine carcinosarcoma (UCS), lymphoid tumor diffuse large b-cell lymphoma (DLBC), head and neck squamous cell carcinoma (HNSC), renal pheochromocytic carcinoma (KICH), prostate adenocarcinoma (PRAD) and other tumor tissues and normal tissues (**Figure 1A**). *G6PD* expression levels were higher in HCC tissues compared to normal tissues ($p < 0.05$). Correlation analysis showed that *G6PD* was statistically different from tissue grade ($p < 0.05$), vascular infiltration ($p < 0.05$), AFP level ($p < 0.05$), pathological stage ($p < 0.05$), and T stage (**Figure 1B**). G6PD expression was verified in GSE60502 and GSE62232 ($p < 0.001$) (**Figure 2A–B**). Further analysis showed agreement with IHC results (**Figure 2C–D**).

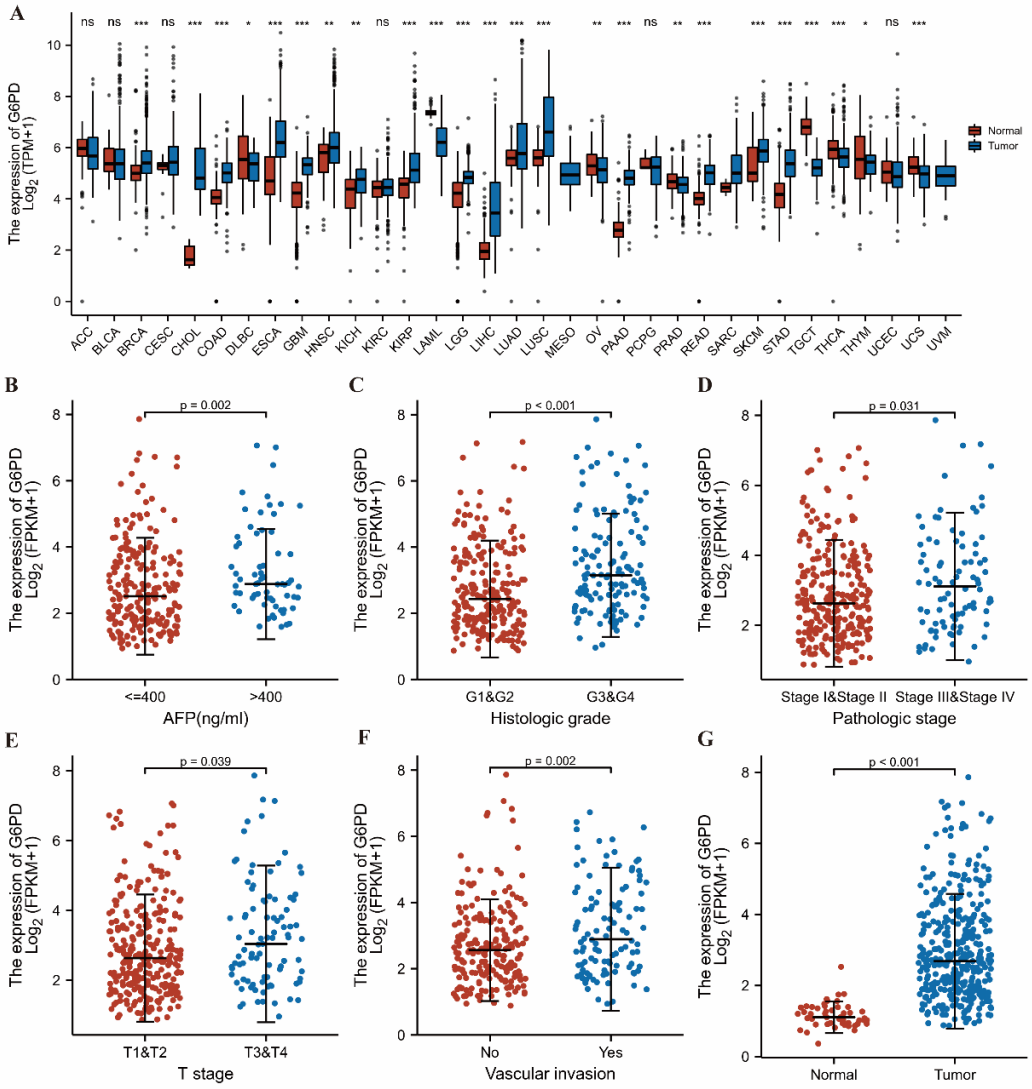


Figure 1. Expression levels of G6PD in cancer. (A) The expression levels of G6PD in different cancer tissues are different from the corresponding normal tissues. (B–F) Association between G6PD and clinical manifestations of HCC. The results showed that high expression of G6PD was associated with higher histological grade, higher pathological stage, T-stage, vascular infiltration and AFP level ($p < 0.05$). (G) The expression level of G6PD was significantly higher in HCC tissues compared to normal tissues ($p < 0.01$).

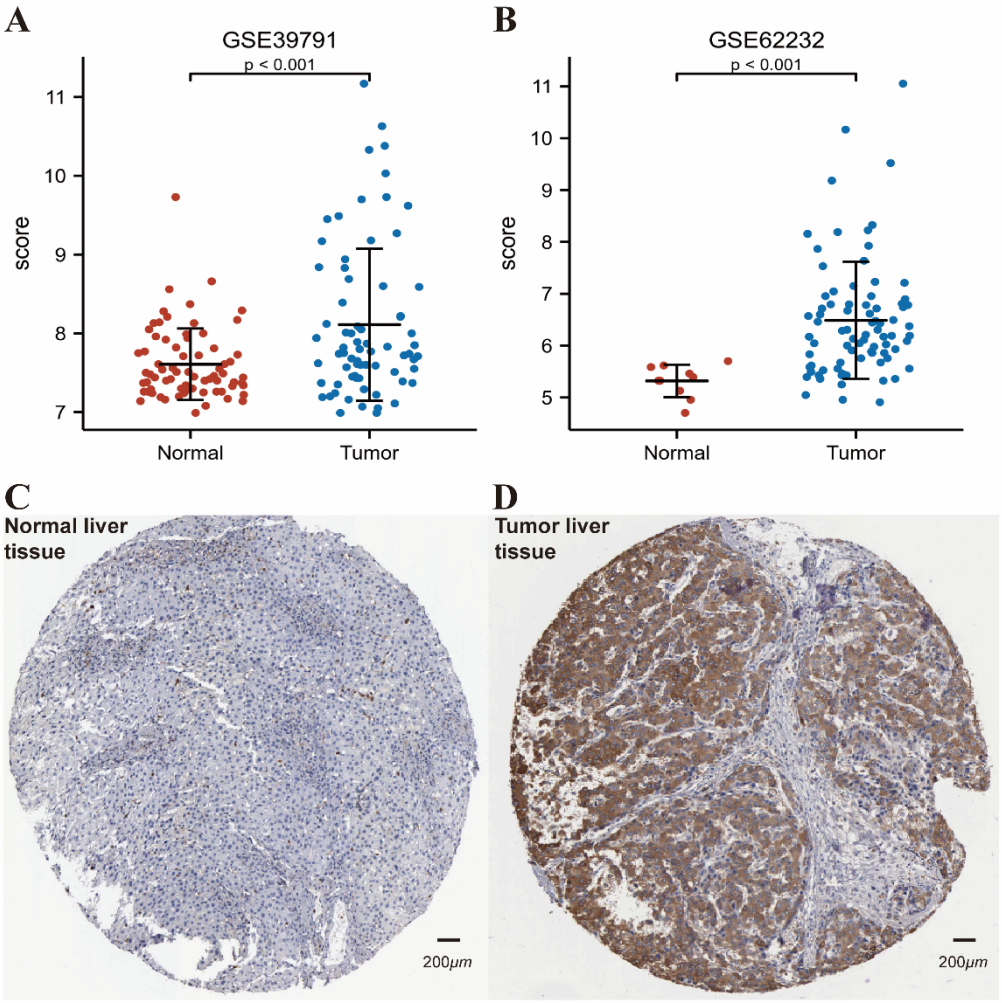


Figure 2. (A–B) *G6PD* is overexpressed in HCC. *G6PD* expression was higher in GSE 39791 and GSE 62232 than in normal tissues ($p < 0.001$). (C–D) The level of *G6PD* protein was higher in HCC than in normal tissues.

3.3. Prognostic correlation analysis of G6PD and HCC

Plotting the ROC curve yields an AUC value of 0.944, from which it can be concluded that *G6PD* can distinguish between normal and tumor tissues. Meanwhile, the Kaplan-Meier curve showed that high *G6PD* levels were associated with poor prognosis (**Figure 3**). The univariate Cox regression model showed that *G6PD* level, T-stage, tumor status, and pathological stage were associated with the prognosis of HCC patients ($p < 0.01$). Multivariate Cox regression analysis showed that tumor status and *G6PD* level were independent risk factors for survival of HCC patients ($p < 0.01$; **Figure 4**). Nomogram column line plots were constructed using the RMSR package based on the results of Cox regression analysis to further predict the 1-, 3-, and 5-year survival rates of HCC patients (**Figure 5**).

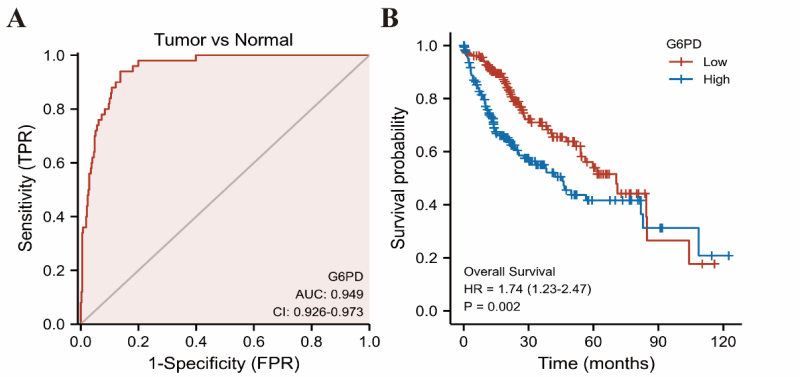


Figure 3. (A) ROC curve and Kaplan-Meier curve of G6PD. ROC curve analysis showed that G6PD was able to accurately identify tumor and normal tissue with an AUC of 0.949; (B) Kaplan-Meier survival curve showed poor prognosis of HCC patients with higher G6PD levels.

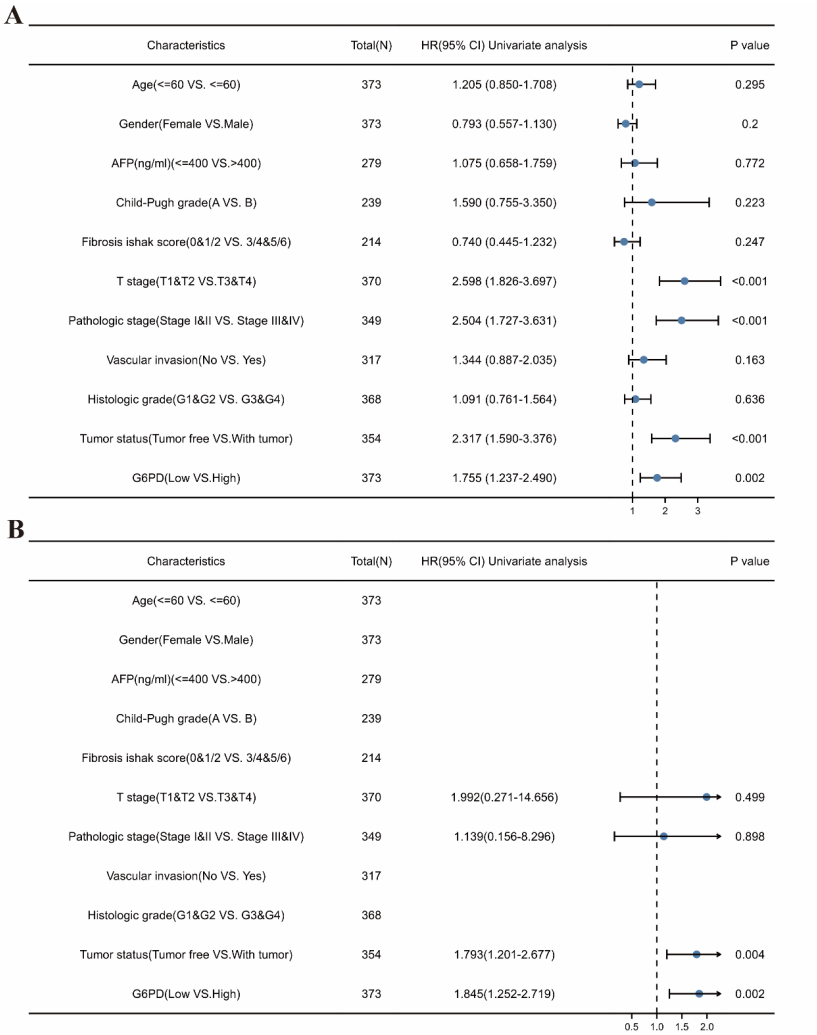


Figure 4. Univariate and multifactorial regression analyses were calculated for *G6PD* expression and other OS clinicopathological factors in HCC. (A) The univariate Cox regression model. Among these factors, T-stage, tumor status, and pathological stage were determined to be statistically significantly associated with the likelihood of OS. (B) Multiple Cox regression analysis in which tumor status and *G6PD* level were independent risk factors for survival in HCC patients.

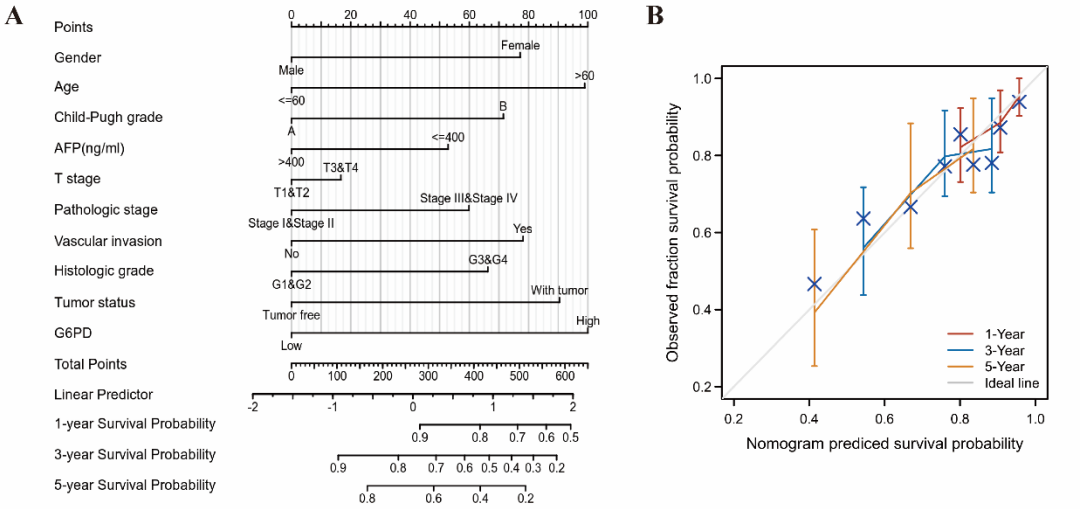
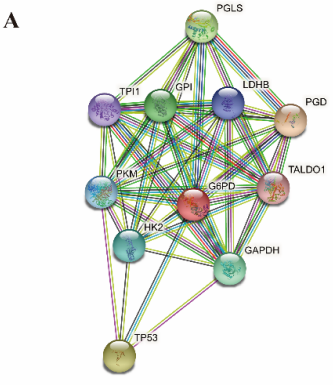


Figure 5. Nomogram plot: 1, 3, and 5-year survival rates of HCC patients can be predicted based on the column line plot.

3.4. PPI networks and enrichment analysis

In this study, we constructed a network of *G6PD* and its related genes using the STRING tool. the *G6PD*-related genes included GAPDH, TPI1, PGLS, TP53, PGD, PKM, TALDO1, LDHB, GPI. Their scores were greater than 0.9 (**Figure 6**). Based on the clusterProfiler package and ggplot2 package in R language, we enriched the differential genes in tumor tissues and normal tissues, and the results of GO functional enrichment analysis showed that *G6PD*-related genes were mainly involved in the metabolism of pyridine compounds, nicotinamide nucleotides, pyridine nucleotides, carbohydrate binding, monosaccharide binding, and NADP binding in biological processes. and NADP binding. KEGG results suggest that *G6PD*-related genes are enriched in the biological processes of carbon metabolism, gluconeogenesis and pentose phosphate pathway, among which *G6PD*, NAPDH, GPI, HK2, PGD, PKM, TALDO1, TPL1 and PGLS are enriched in the carbon metabolism pathway (**Figure 7**). GSEA analysis results suggested a high *G6PD* gene expression phenotype significantly enriched in the REACTOME_INNATE_IMMUNE_SYSTEM gene set (NES = 1.997; p.adjust = 0.017; FDR = 0.012); in the EACTOME_INFECTIOUS_DISEASE gene set (NES = 2.124; p.adjust = 0.017; FDR = 0.012) (NES = 2.124; p.adjust = 0.017; FDR = 0.012).



B

Gene symbol	Annotation	Score
GAPDH	glyceraldehyde phosphate dehydrogenase	0.975
TPI1	Triosephosphate isomerase 1	0.957
PGLS	6-phosphogluconolactonase	0.995
TP53	Tumor Protein53	0.996
PGD	phosphogluconate dehydrogenase	0.998
HK2	hexokinase 2	0.965
PKM	Pyruvate kinase PKM	0.962
TALDO1	transaldolase 1	0.954
LDHB	lactate dehydrogenase B	0.961
GPI	glucose-6-phosphate isomerase	0.992

Figure 6. (A) Comprehensive analysis of *G6PD*-related protein interactions. The network of *G6PD* and its potential co-expressed genes was analyzed using the STRING tool. The results are shown in the bubble diagram. (B) Details of *G6PD*-related genes are listed.

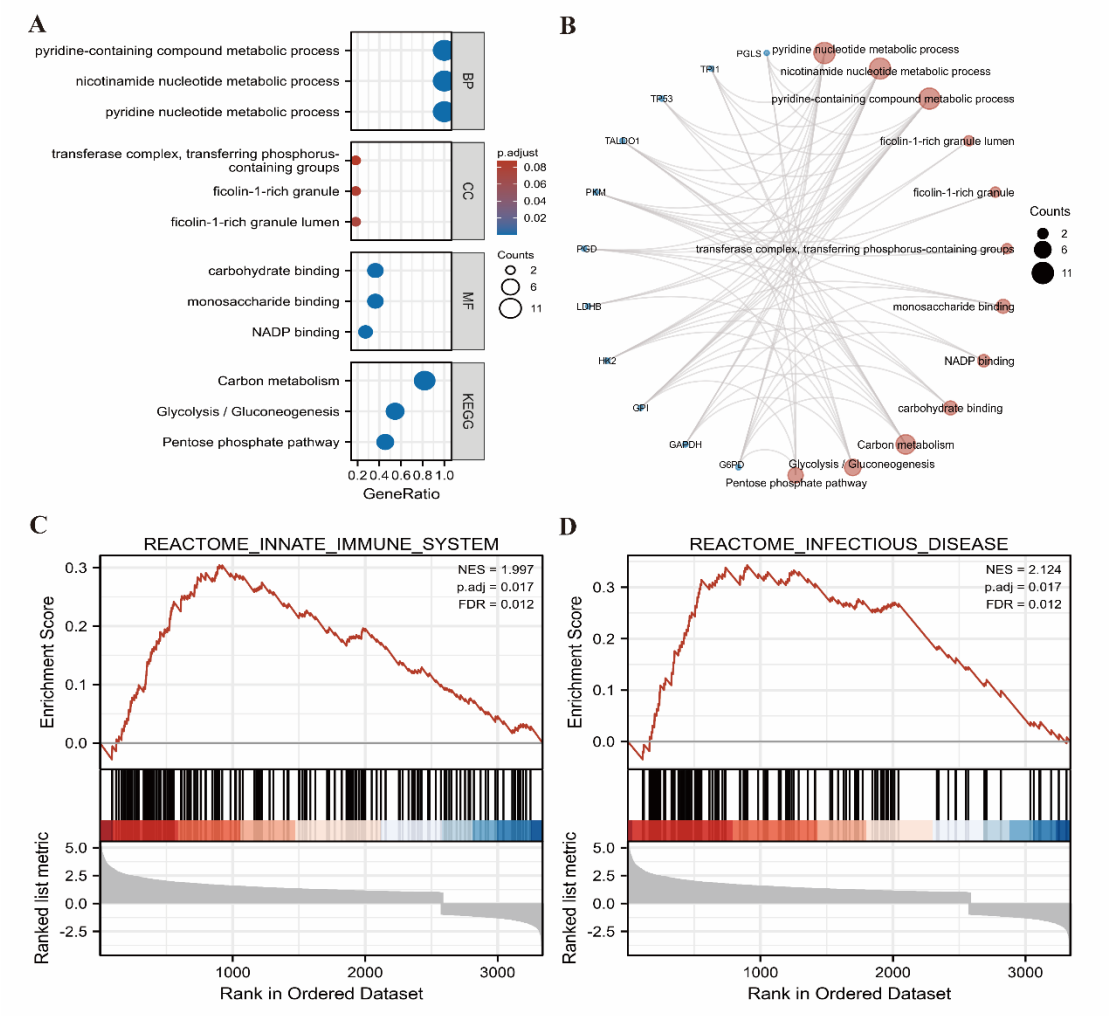


Figure 7. Enrichment analysis of *G6PD*.

3.5. Correlation analysis of immune cell infiltration

Hepatocellular carcinoma is considered to be an immunogenic tumor, which is closely associated with viral infection and inflammatory environment. TIMER data suggested statistically significant differences between *G6PD* and B cells, CD4+ T cells, CD4+ T cells, neutrophils, macrophages, and dendritic cells (all $p < 0.05$). Compared with *G6PD* low expression group, B cells, CD4+ T cells, CD4 + T cells, neutrophils, macrophages and dendritic cells in *G6PD* high expression group were significantly increased (all $P < 0.05$). Meanwhile, ssGESA analysis showed: Helper T cells, TFH cells, Th1 cells, and Th2 cells were elevated in the *G6PD* high expression group compared to the low expression group ($p < 0.05$. In contrast, Th17 cells and TReg cells ($p < 0.01$) were decreased in the high expression group compared to the low expression group.

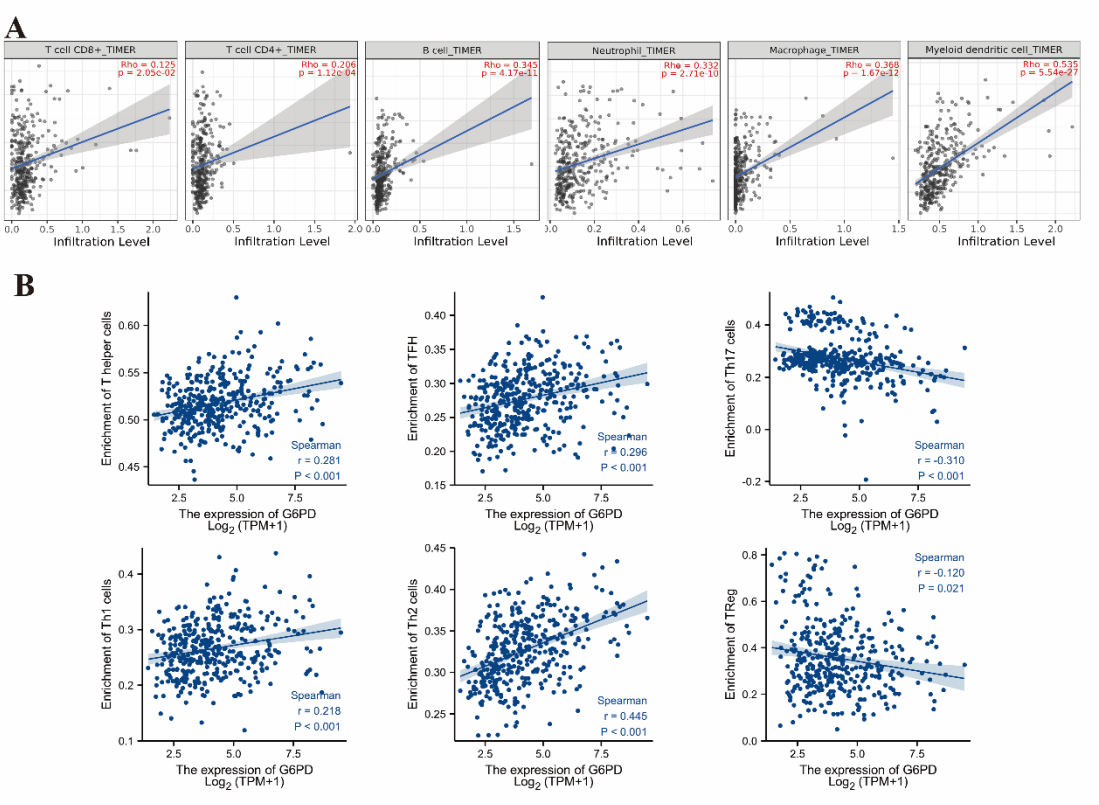


Figure 8. (A) Correlation of *G6PD* expression with immune cell infiltration in HCC. Correlation of *G6PD* expression with tumor purity and six immune cells was analyzed by TIMER database. (B) Correlation between *G6PD* and other immune cells was calculated by ssGSEA.

4. Discussion

Recurrence and metastasis of HCC are still the primary causes of patients' death, and these factors are closely related to the proliferation and invasion capacities of tumor cells. Recently, a lot of progress has been made in the pathogenesis of HCC. Therefore, exploring new therapeutic targets for hepatocellular carcinoma is of great significance to improve postoperative survival rates and to ameliorate the survival prognosis of patients. As a key enzyme in the PPP process, the main role of *G6PD* is to provide sufficient reducing capacity to support cell growth and keep cells in redox homeostasis. Its product, NADPH, acts as a pro-oxidant, generating reactive oxygen species (ROS) and reactive nitrogen species (RNS), which help ameliorate tumor cell proliferation and metastasis, as well as regulate the cell cycle and apoptosis. Severe deficiency of *G6PD* can impair embryonic development and retard the growth of the organism. Hence, altering the activity of *G6PD* is associated with pathophysiology such as autophagy, insulin resistance, infection, inflammation, diabetes, hypertension, etc. Besides, abnormal activation of *G6PD* can also lead to cell proliferation in many cancers [9]. In the current study, *G6PD* activity is significantly increased in tumor tissues of gastric cancer, breast cancer, bladder cancer, cervical cancer, and colorectal cancer [10–14]. This is consistent with the result that *G6PD* is highly expressed in pan-cancer in the TCGA data. Therefore, *G6PD* is also considered a potential effective target for tumor treatment [15–17].

As an independent predictor of prognosis for gastric cancer patients, *G6PD* expression was higher in gastric cancer tissues than in paired normal gastric mucosa groups, and high *G6PD* expression was closely associated

with tumor size, depth of infiltration and tumor size, lymph node metastasis, distant metastasis, TNM stage, and survival rate in previous studies [10]. Zhang et al. found that intracellular high expression of *G6PD* decreased matrix metalloproteinase expression through the *G6PD* /HIF-1α/ Notch1 axis and promoted the migration of tumor cells [18]. Chen J et al. showed that *G6PD*-based metabolic markers can be used as predictors of prostate cancer metastasis [19]. *G6PD* was expressed at high levels in melanoma. In animal models, wild-type nude mice models had faster tumor growth, larger tumor size, and higher malignancy compared with G6PD-deficient nude mice [20]. Hong et al. found that high *G6PD* expression was significantly associated with poor prognosis in HCC, especially in HCC patients who are in the advanced stages of HCC treated with sorafenib after hepatocellular carcinoma surgery. High *G6PD* expression was significantly associated with worse PFS and OS. This may also have a link with PPP and tumor cell resistance [21]. Yin X et al. found that Inhibitor of Differentiation 1(ID1) in HCC cells leads to reduce *G6PD* and NADPH activity and increase ROS production, and transfection of *G6PD* into ID1 knockdown HCC cells reversed these changes and induced oxaliplatin resistance, and the above evidence also provides new ideas for the study of hepatocellular carcinoma in terms of resistance to sorafenib and oxaliplatin [22]. In our research, *G6PD* expression is associated with histological grading, pathological stage, T-stage, vascular infiltration, and AFP levels ($P < 0.05$). HCC patients in the *G6PD* low expression group have longer overall survival and better prognosis than the *G6PD* high expression group ($P < 0.05$), and high *G6PD* expression is a potential biomarker for poor prognosis of hepatocellular carcinoma. In addition, we combined *G6PD* with age, AFP, and Child classification to construct columnar line graph prognostic plots to obtain a more accurate prognostic prediction model, and the C-index *G6PD*-related Cox model predicted OS of 0.686 (0.645–0.728). The calibration plots show that the best agreement between the predictions of the column line graphs is associated with *G6PD* and the actual observations of the 1-year, 3-year and 5-year OS probabilities. Thus, our model can provide personalized scoring for HCC patients.

In this study, the PPI network was used to identify co-expressed proteins of *G6PD*, and we identified *G6PD*-related genes, including GAPDH, TPI1, PGLS, TP53, PGD, PKM, TALDO1, LDHB, and GPI. Among them, P53 has become a key antitumor factor since its discovery, and P53 can be activated under conditions of genotoxic stress, oncogene activation, ribosomal stress, hypoxic state, and abnormal energy metabolism. Furthermore, the MDM2-p53 axis may play a dual role in hepatocyte glycolipid metabolism, which is manifested by enhanced glycolipid catabolism, but in early and late stages of the disorder, promoting hepatocyte injury in a study by Cao H et al. [23] The MDM2-p53 axis may play a dual role in hepatocyte glycolipid metabolism, which is manifested by enhanced glycolipid catabolism, but in early and late stages of the disorder, promoting hepatocyte injury [24]. Oxidative stress, steatosis and abnormal cell growth can be detected in hepatocytes with disorders of glucolipid metabolism, all of which may contribute to the development of HCC [23]. GAPDH and LDHB are all glycolysis-related genes, and it has been shown that TFB2M activates aerobic glycolysis in hepatocellular carcinoma cells through NAD /SIRT3/HIF-1α Signaling pathway [25]. Among them, TFB2M (mitochondrial transcription factor B2) is a core mitochondrial transcription factor, and its overexpression is significantly associated with the malignancy and prognosis of hepatocellular carcinoma [26]. Enrichment analysis of differential genes in tumor tissues and normal tissues based on the DAVID database was performed, and the results of GO functional enrichment analysis showed that *G6PD*-related genes were enriched in metabolism of pyridine compounds, metabolism of nicotinamide nucleotides, metabolism of pyridine nucleotides, carbohydrate binding, monosaccharide binding, and NADP binding. Among them, nicotinamide ribonucleotide (NMN) is a precursor of coenzyme 1NAD+ (nicotinamide adenine dinucleotide), which is not only a coenzyme involved in intracellular redox reactions, but

also involved as a substrate in regulating apoptosis, DNA repair, immune response, and many other physiological roles [27].

Moreover, due to the high rate of tumor cell proliferation and DNA repair, the demand for NAD is increased, and some studies have shown an important role of nicotinamide phosphoribosyl transferase (NAMPT)-mediated NAD remediation pathway in the energy homeostasis of hepatocellular carcinoma cells and suggested that NAMPT inhibition is a potential therapeutic option for hepatocellular carcinoma [28]. KEGG results suggest that *G6PD*-related genes are enriched in carbon metabolism, gluconeogenesis, and the pentose phosphate pathway (PPP), which is consistent with the function of *G6PD*. The pentose phosphate pathway (PPP) is the first step reaction of glycolysis, and its product NADPH, has an important role in biosynthesis as well as in maintaining cellular redox homeostasis. ROS is a collective term for a variety of oxygen radicals in intracellular metabolic processes, which can promote normal cell proliferation when ROS levels are low, and trigger apoptosis when ROS levels are too high [29]. The significance of PPP at this time lies largely in reducing excess ROS and maintaining cellular energy metabolism in a redox homeostasis. In tumor cells, making PPP at high levels is able to induce ROS-induced apoptosis [30]. In hepatocellular carcinoma cells, high expression of the G6PDH gene is closely related to the occurrence, development, metastasis and prognosis of hepatocellular carcinoma [31]. In addition, tumor cell metabolic reprogramming is involved in tumor immune regulation, and metabolic reprogramming plays a crucial role in antitumor immunotherapy. Tumor cells require large amounts of energy during proliferation, but the body has to compete with tumor cells for these nutrients through tumor-infiltrating effector cells, CD8+ T lymphocytes (CD8TILs), in order to fight tumors. Studies have shown that sustained antitumor immunity can be triggered by upregulating glycolysis and oxidative phosphorylation in CD8TILs [32].

T cells also play an important role in the immune microenvironment against infections and tumors [33], Naïve T cells have a low metabolic demand and rely mainly on oxidative phosphorylation for energy production, but with the onset of infections and tumors, Naïve T cells will be activated, and activated T cell energy metabolism will shift to aerobic glycolysis and increase oxidative phosphorylation, which is essential for effector T cell production and function [34,35]. Gu M et al. found that the G6PD-NADPH redox system plays an important role in the stability and metabolism of hexokinase 2 (HK2) in activated T cells [36]. However, there are few studies on the relationship between *G6PD* and immune cells in HCC. In the present study, the correlation between *G6PD* and immune cell infiltration was assessed using TIMER and ssGSEA. Our results showed significant differences between *G6PD* and $CD8^+$ T lymphocytes, $CD4^+$ T lymphocytes, B cells, neutrophils, macrophages, dendritic cells, helper T cells, follicular helper T cells, Th1, Th2, Th17, and regulatory T cells (Treg). This also provides new ideas for immunotherapy in HCC patients with elevated *G6PD*. However, there are some limitations in this study, such as the relatively small sample size in the TCGA database and the hypothesis of this study was not validated using animal models. Therefore, we will conduct further cellular assays to further prove this in the following studies.

5. Conclusion

In conclusion, our study confirmed that *G6PD* expression levels were significantly associated with the prognosis of HCC patients and that *G6PD* expression levels were significantly associated with immune cell infiltration. Thus, our findings suggest that *G6PD* expression may have a unique prognostic value in HCC patients and may be a potential target for HCC immunotherapy.

Disclosure statement

The authors declare no conflict of interest.

References

[1] Sung H, Ferlay J, Siegel R, et al., 2021, Global Cancer Statistics 2020: GLOBOCAN Estimates of Incidence and Mortality Worldwide for 36 Cancers in 185 Countries. CA: A Cancer Journal for Clinicians, 71(3): 209–249.

[2] Llovet J, Kelley R, Villanueva A, et al., 2021, Hepatocellular Carcinoma. Nature Reviews Disease Primers, 7(1): 6.

[3] Chu P, Chan S, 2021, Cure the Incurable? Recent Breakthroughs in Immune Checkpoint Blockade for Hepatocellular Carcinoma. Cancers, 13(21): 5295.

[4] Marrero J, Kulik L, Sirlin C, et al., 2018, Diagnosis, Staging, and Management of Hepatocellular Carcinoma: 2018 Practice Guidance by the American Association for the Study of Liver Diseases. Hepatology, 68(2): 723–750.

[5] Boroughs L, DeBerardinis R, 2015, Metabolic Pathways Promoting Cancer Cell Survival and Growth. Nature Cell Biology, 17(4): 351–359.

[6] Wood T, 1986, Physiological Functions of the Pentose Phosphate Pathway. Cell Biochemistry and Function, 4(4): 241–247.

[7] Wang A, Chen B, Jian S, et al., 2021, miR-206-G6PD Axis Regulates Lipogenesis and Cell Growth in Hepatocellular Carcinoma Cell. Anti-Cancer Drugs, 32(5): 508–516.

[8] Yan Y, Wang J, Dong X, et al., 2022, Quantitative Proteomic Analysis of Hepatic Tissue in Allotetraploid Hybridized from Red Crucian Carp and Common Carp Identified Crucial Proteins and Pathways Associated with Metabolism and Growth Rate. Proteomics, 22(4): e2100115.

[9] Yang H, Wu Y, Yen W, et al., 2019, The Redox Role of G6PD in Cell Growth, Cell Death, and Cancer. Cells, 8(9): 1055.

[10] Wang J, Yuan W, Chen Z, et al., 2012, Overexpression of G6PD Is Associated with Poor Clinical Outcome in Gastric Cancer. Tumour Biology, 33(1): 95–101.

[11] Dong T, Kang X, Liu Z, et al., 2016, Altered Glycometabolism Affects Both Clinical Features and Prognosis of Triple-Negative and Neoadjuvant Chemotherapy-Treated Breast Cancer. Tumour Biology, 37(6): 8159–8168.

[12] Ohl F, Jung M, Radonić A, et al., 2006, Identification and Validation of Suitable Endogenous Reference Genes for Gene Expression Studies of Human Bladder Cancer. The Journal of Urology, 175(5): 1915–1920.

[13] Van Driel B, Valet G, Lyon H, et al., 1999, Prognostic Estimation of Survival of Colorectal Cancer Patients with the Quantitative Histochemical Assay of G6PDH Activity and the Multiparameter Classification Program CLASSIF1. Cytometry, 38(4): 176–183.

[14] Fang Z, Jiang C, Feng Y, et al., 2016, Effects of G6PD Activity Inhibition on the Viability, ROS Generation and Mechanical Properties of Cervical Cancer Cells. Biochimica et Biophysica Acta, 1863(9): 2245–2254.

[15] Budihardjo I, Walker D, Svingen P, et al., 1998, 6-Aminonicotinamide Sensitizes Human Tumor Cell Lines to Cisplatin. Clinical Cancer Research, 4(1): 117–130.

[16] Polimeni M, Voena C, Kopecka J, et al., 2011, Modulation of Doxorubicin Resistance by the Glucose-6-Phosphate Dehydrogenase Activity. The Biochemical Journal, 439(1): 141–149.

[17] Mele L, Paino F, Papaccio F, et al., 2018, A New Inhibitor of Glucose-6-Phosphate Dehydrogenase Blocks Pentose Phosphate Pathway and Suppresses Malignant Proliferation and Metastasis in Vivo. Cell Death & Disease, 9(5): 572.

[18] Zhang H, Zhang Z, Du G, et al., 2019, Nrf2 Promotes Breast Cancer Cell Migration via Up-Regulation of G6PD/HIF-1α/Notch1 Axis. Journal of Cellular and Molecular Medicine, 23(5): 3451–3463.

[19] Chen J, Cao S, Situ B, et al., 2018, Metabolic Reprogramming-Based Characterization of Circulating Tumor Cells in Prostate Cancer. Journal of Experimental & Clinical Cancer Research, 37(1): 127.

[20] Hu T, Zhang C, Tang Q, et al., 2013, Variant G6PD Levels Promote Tumor Cell Proliferation or Apoptosis via the STAT3/5 Pathway in the Human Melanoma Xenograft Mouse Model. BMC Cancer, 13: 251.

[21] Hong X, Song R, Song H, et al., 2014, PTEN Antagonises Tcl1/hnRNPK-Mediated G6PD pre-mRNA Splicing Which Contributes to Hepatocarcinogenesis. Gut, 63(10): 1635–1647.

[22] Yin X, Tang B, Li J, et al., 2017, ID1 Promotes Hepatocellular Carcinoma Proliferation and Confers Chemoresistance to Oxaliplatin by Activating Pentose Phosphate Pathway. Journal of Experimental & Clinical Cancer Research, 36(1): 166.

[23] Cao H, Chen X, Wang Z, et al., 2020, The Role of MDM2-p53 Axis Dysfunction in the Hepatocellular Carcinoma Transformation. Cell Death Discovery, 6: 53.

[24] Levine A, 2018, Reviewing the Future of the P53 Field. Cell Death and Differentiation, 25(1): 1–2.

[25] Chang H, Li J, Luo Y, et al., 2021, TFB2M Activates Aerobic Glycolysis in Hepatocellular Carcinoma Cells through the NAD^+/SIRT3/HIF-1α Signaling. Journal of Gastroenterology and Hepatology, 36(10): 2978–2988.

[26] Geng X, Geng Z, Li H, et al., 2020, Over-Expression of TFB2M Facilitates Cell Growth and Metastasis via Activating ROS–Akt–NF-κB Signalling in Hepatocellular Carcinoma. Liver International, 40(7): 1756–1769.

[27] Xu L, Yang C, Ma J, et al., 2021, NAMPT-Mediated NAD^+ Biosynthesis Suppresses Activation of Hepatic Stellate Cells and Protects against CCl_4-Induced Liver Fibrosis in Mice. Human & Experimental Toxicology, 40(12 Suppl): S666–S675.

[28] Schuster S, Penke M, Gorski T, et al., 2015, FK866-Induced NAMPT Inhibition Activates AMPK and Downregulates mTOR Signaling in Hepatocarcinoma Cells. Biochemical and Biophysical Research Communications, 458(2): 334–340.

[29] Lennicke C, Cochemé H, 2021, Redox Metabolism: ROS as Specific Molecular Regulators of Cell Signaling and Function. Molecular Cell, 81(18): 3691–3707.

[30] Simon-Molas H, Vallvé-Martínez X, Caldera-Quevedo I, et al., 2021, TP53-Induced Glycolysis and Apoptosis Regulator (TIGAR) Is Upregulated in Lymphocytes Stimulated with Concanavalin A. International Journal of Molecular Sciences, 22(14): 7436.

[31] Kowalik M, Guzzo G, Morandi A, et al., 2016, Metabolic Reprogramming Identifies the Most Aggressive Lesions at Early Phases of Hepatic Carcinogenesis. Oncotarget, 7(22): 32375–32393.

[32] Udono H, Nishida M, 2022, Pharmacological Effects on Anaplerotic Pathways Alter the Metabolic Landscape in the Tumor Microenvironment, Causing Unpredictable, Sustained Anti-Tumor Immunity. International Immunology, 34(3): 133–140.

[33] Durgeau A, Virk Y, Corgnac S, et al., 2018, Recent Advances in Targeting CD8 T-Cell Immunity for More Effective Cancer Immunotherapy. Frontiers in Immunology, 9: 14.

[34] Lim A, Rathmell W, Rathmell J, 2020, The Tumor Microenvironment as a Metabolic Barrier to Effector T Cells and Immunotherapy. eLife, 9: e55185.

[35] Odegaard J, Chawla A, 2013, The Immune System as a Sensor of the Metabolic State. Immunity, 38(4): 644–654.

[36] Gu M, Zhou X, Sohn J, et al., 2021, NF-κB-Inducing Kinase Maintains T Cell Metabolic Fitness in Antitumor Immunity. Nature Immunology, 22(2): 193–204.

Publisher's note

Bio-Byword Scientific Publishing remains neutral with regard to jurisdictional claims in published maps and institutional affiliations.

Proceedings of Anticancer Research, 2026, Volume 10, Issue 1
http://ojs.bbwpublisher.com/index.php/PAR
ISSN Online: 2208-3553
ISSN Print: 2208-3545

A Review on the Association between Dyslipidemia, Glucose Tolerance, and Coronary Heart Disease Risk

Xueling He, Yanyan Zhang, Qingkai Yan*

Department of Cardiology, Bishan Hospital of Chongqing Medical University, Chongqing 402760, China

**Corresponding author: Qingkai Yan, yangingkai@hotmail.com*

Copyright: © 2026 Author(s). This is an open-access article distributed under the terms of the Creative Commons Attribution License (CC BY 4.0), permitting distribution and reproduction in any medium, provided the original work is cited.

Abstract: As one of the main chronic diseases in modern society, coronary heart disease, as a major disease that affects people's lives and health, has the characteristics of hidden onset and sudden onset. Coronary heart disease has relatively clear risk factors. Among them, blood lipid levels and blood sugar levels, as two main risk factors, play an important role in promoting the onset of coronary heart disease. The two complement each other in a vicious cycle, synergize and promote each other, promote the process of coronary atherosclerosis, thereby causing coronary heart disease. Multiple components in blood lipids and poor management of long-term blood sugar levels play a major role in specific clinical problems. This article reviews the different components of blood lipids and the effects of hyperglycemia on coronary heart disease, and initially expounds the mechanism by which blood lipids and blood sugar levels synergize each other to aggravate the risk of coronary heart disease, and combines them with relevant clinical issues, in order to help clinicians guide the prevention of coronary heart disease in terms of blood lipids and blood sugar levels.

Keywords: Dyslipidemia; Coronary heart disease; Glucose tolerance; Risk

Online publication: February 6, 2026

1. Introduction

Coronary heart disease still tops the list of lethal conditions worldwide, and the bulk of these deaths root in risk factors that could, at least in theory, be altered. Among the most repeatedly verified culprits, dyslipidemia and impaired glucose tolerance stand out; they now occupy centre stage whenever clinicians reconstruct how CHD first takes hold. Dyslipidemia, a collective label for blood lipid levels that drift beyond the safe interval, accelerates atherosclerosis, the slow piling-up of material within arterial walls that eventually surfaces as clinical CHD. Impaired glucose tolerance, the metabolic phase that typically heralds type 2 diabetes, piles on cardiovascular danger even while fasting glucose stays short of the diabetic cut-off. The two disturbances frequently appear side by side and amplify one another, so teasing apart their interaction and sizing up their combined load on coronary

vessels has turned into a prerequisite if prevention schemes and therapeutic routines are to stay precise and deliver results.

After entering modern society, people's lifestyles have undergone significant changes, and dyslipidemia has become a long-term metabolic disorder affecting many individuals, posing serious health risks. The impact of long-term dyslipidemia on the human body is like an 'invisible bomb.' If patients do not pay attention and fail to intervene in time, the consequences are often severe, and it is highly likely to trigger various serious cardiovascular diseases, among which coronary heart disease is the most common and harmful. So, how closely is dyslipidemia linked to coronary heart disease? Dyslipidemia usually manifests as elevated low-density lipoprotein (LDL) and triglycerides, along with decreased high-density lipoprotein (HDL)[1]. In the human body, the metabolic internal environment is extremely complex, and when dyslipidemia occurs alongside conditions like insulin resistance that may cause blood sugar disturbances, the risk factors for developing coronary heart disease can be amplified [2].

Abnormal blood sugar levels are also quite common in today's society. Prolonged high blood sugar levels can simultaneously worsen and disrupt lipid levels, and abnormal blood sugar can also act as an independent risk factor contributing to the development of coronary heart disease [3,4]. In more extreme cases, when a patient with type 2 diabetes experiences significant lipid metabolism disorders, they may develop coronary heart disease as a complication [5].

Dyslipidemia and impaired glucose tolerance often lock together in a self-reinforcing loop, and the pattern is hardest to miss in patients who already carry the metabolic syndrome label or live with type 2 diabetes. Several cohort studies have shown that once the syndrome—recognised by the familiar triad of lipid anomalies, rising blood pressure, and IGT—takes hold, the odds of later coronary heart disease rise far beyond the level faced by people who escape this bundle of metabolic oddities [6]. Because the separate pieces so rarely appear alone, front-line clinicians have learned that isolating a single target seldom moves the needle; the cumulative threat to coronary arteries only contracts when several strands are reined in side by side. Routine practice, therefore turns into a coordinated bundle: steady guidance on food, activity, and weight, agents that act on both lipid and glucose pathways, and follow-up visits spaced closely enough to watch how overall cardiovascular risk drifts over time, all treated as indispensable if the heart is to stay insulated from the overlapping stress these linked disorders impose [7].

When the three elements of dyslipidemia, impaired glucose tolerance, and coronary heart disease are placed side by side, their mutual influence quickly reveals a maze rather than a straight line, because each disorder keeps feeding the others through overlapping metabolic and vascular disruptions. Dyslipidemia or IGT alone already nudges CHD risk upward, yet the moment they share the same body they amplify one another, so clinicians have to knit prevention and daily care into one coherent plan instead of letting the two drift along separate rails. The next layer of work is to chart, with far higher resolution, the molecular and cellular roads that tether lipid chaos to glucose swings, and then to run pragmatic trials of interventions that can strike both routes at the same time, hoping to tilt the cardiovascular future of high-risk cohorts toward a clearly brighter curve.

2. Main body

2.1. Definition and classification of dyslipidemia

Dyslipidemia is the label clinicians give when the blood levels of fat-like substances—chiefly cholesterol and triglycerides—drift outside the interval laboratories regard as normal, and the same label applies when HDL cholesterol slips below the value cardiologists would like to see. Physicians usually begin by deciding which lipid

component has wandered off course, and the first fork in the road separates primary from secondary varieties. Primary dyslipidemia, illustrated by disorders such as familial hypercholesterolemia, generally stems from germ-line DNA variants handed down through generations, while the secondary version follows in the wake of other illnesses—diabetes, adiposity, or a sluggish thyroid gland are typical culprits. After the main category is pinned down, the profile is sharpened into narrower subtypes: hypercholesterolemia when LDL or total cholesterol occupies centre stage, hypertriglyceridemia when triglycerides claim the spotlight, or an isolated HDL deficit when the good cholesterol alone is missing in action, allowing the therapeutic blueprint to focus on the exact pattern that is pushing cardiovascular risk upward and tangling the broader task of keeping the patient well [1].

2.1.1. Low-density lipoprotein cholesterol (LDL-C)

Low-density lipoprotein cholesterol, shortened in everyday notes to LDL-C, picked up the informal label “bad cholesterol” because it reliably appears at the exact spots where atherosclerotic plaques first take hold and where later cardiovascular problems quietly begin. When LDL-C lingers on the high side for years, the probability of coronary artery disease and a broader set of acute cardiac or cerebrovascular incidents rises in parallel. Because of this steady link, clinicians treat tight control of circulating LDL-C as one of the main handles for stopping atherosclerotic cardiovascular disease, or ASCVD, before it can gather speed. Present-day guidelines accordingly tell patients already classed as high-risk to push LDL-C under 70 mg/dL, a threshold that several large cohorts have tied to a visible fall in new cardiovascular events. Statins still serve as the routine first-line option for nudging LDL-C lower, yet daily experience shows that a noticeable minority of people—particularly those carrying familial hypercholesterolemia or those who cannot stomach statins—require additional help, most often from PCSK9 inhibitors or from ezetimibe, before the desired number finally slips into range [8]. Shifting to the laboratory bench, LDL-C can be measured in more than one way: the classic Friedewald equation continues to deliver an estimate by stripping HDL-C and a triglyceride-derived fraction away from total cholesterol, whereas direct homogeneous assays are now common and, in situations such as marked hypertriglyceridemia or non-fasting specimens, they usually hand back a more reliable figure [9].

2.1.2. High-density lipoprotein cholesterol (HDL-C)

High-density lipoprotein is widely labelled ‘good cholesterol’ by researchers, since it routinely lowers circulating triglycerides and ferries lipids back to the liver where they can be processed and cleared. This protection hinges on reverse cholesterol transport, a stepwise route that collects surplus cholesterol from peripheral tissues, shuttles it through plasma, and hands it to the liver for ultimate disposal in bile. Population studies have long linked higher HDL-C numbers with fewer heart attacks and strokes; yet fresh cohort data and Mendelian-randomisation papers now question the old assurance that simply raising HDL-C guarantees safety. A growing line of work contends that particle performance—its functionality—carries weight equal to, or greater than, the milligrams-per-decilitre figure. Chronic inflammation, oxidative pressure, or compositional remodelling can convert these supposedly anti-atherogenic spheres into dysfunctional ones that forfeit cholesterol-efflux power, turn pro-inflammatory, and erase the anticipated gain. Given these findings, many investigators hold that while HDL-C quantity still mirrors metabolic balance to some degree, markers such as cholesterol-efflux capacity or the HDL inflammatory index paint a more reliable portrait of personal cardiovascular risk [10]. Current guidelines avoid prescribing a fixed HDL-C threshold; they instead promote everyday habits—steady aerobic activity, swapping unsaturated fats for trans fats, light alcohol, and weight management—that usually lift HDL-C and, more critically, seem to revive

HDL performance [11].

2.1.3. Triglycerides (TG)

Triglycerides, often abbreviated as TG, serve the body both as a handy fuel depot and as one of the circulating lipid fractions, and once their plasma level drifts upward, it is usually read as a signal that overall health is slipping. Clinicians pay particular attention when these lipid molecules rise above the reference interval, because the shift becomes a clear cardiovascular warning, especially when low HDL-C and elevated LDL-C travel alongside, a trio that together is called atherogenic dyslipidemia. The upward drift of triglycerides rarely has a single cause; instead, it reflects a blend of everyday factors, with obesity, insulin resistance, and repeated heavy drinking heading the list. Holding the concentration within the desirable zone, therefore, matters above all for people who already carry a label of metabolic syndrome or diabetes, because values that stay high can trigger an episode of acute pancreatitis and, over the years, keep adding to long-term cardiovascular hazard. Current care paths open with lifestyle recalibration—tightening food choices and stepping up movement—and, if that is not enough, layer in medicines such as fibrates, omega-3 fatty acids, or newer agents that block triglyceride synthesis, all chosen to pull fasting TG under 150 mg/dL so that the linked threats recede. Laboratory checks spaced at regular intervals make sense for anyone with known cardiovascular disease or classified as high-risk, since the triglyceride figure also acts as a quick glimpse into broader lipid turnover and overall vascular health [12].

2.2. The relationship between dyslipidemia and coronary heart disease

Dyslipidemia, a catch-all label for any measurable departure of blood lipid values from their usual range, sits near the top of the list of modifiable culprits that quietly prepare the ground for coronary heart disease. The relationship between wayward lipids and CHD refuses to flatten into a single track; instead, several lipid sub-fractions join forces, amplifying hemorheological shifts and nudging the body's own clotting machinery off balance, with low-density lipoproteins leading the charge. When LDL climbs too high, the delicate inner coat of small arteries takes a direct hit, and the ordinary physiology of the intima begins to tilt toward dysfunction, inviting an eclectic mix of circulating elements to settle along the wall, a sequence that ends in stiffening and the slow build-up of atherosclerotic plaque. Those plaques, once established, act as an immediate pathological driver of severe cardiac events. Fragments can shear away, slip into the coronary stream and lodge further downstream, narrowing the lumen and deepening myocardial ischemia, a chain of events that lifts the risk of a catastrophic episode sharply upward. HDL-C, in contrast, earns its reputation as a cardioprotective player mainly by shepherging excess cholesterol out of the arterial wall, ferrying it through the reverse transport route, and finally delivering it to the liver for disposal. Clinicians who hope to ease the day-to-day weight of CHD still need to map the subtle tug-of-war between these opposing lipid camps and watch how the balance tips into tangible clinical endpoints, a step that underpins any prevention plan or treatment sequence worth implementing.

2.2.1. The impact of dyslipidemia on atherosclerosis

Dyslipidemia occupies the narrative core of atherosclerosis, since the instant LDL particles exceed what the arterial wall can clear, lipids begin to linger, fibrous debris mingles with immune cells that arrive as part of the inflammatory reaction, gradually knitting together the arterial plaque. Among the lipid cast, low-density lipoprotein sharpens this pathophysiological sequence most acutely: once it lodges beneath the endothelium it readily oxidises, delivers its cholesterol cargo to tissue macrophages, and powers a self-feeding inflammatory loop

that chips away at ordinary endothelial behaviour. An expanding collection of studies now indicates that long-standing dyslipidemia sustains both oxidative stress and inflammatory signalling inside the plaque milieu, twin forces that hasten lesion enlargement and undermine its stability [13]. In parallel, the unending lipid surplus trims nitric-oxide availability, loosens endothelial junctions and renders the arterial wall more porous, alterations that circle back to enlarge the plaque and further scramble local lipid management. Viewed as a whole, the reciprocal dance among climbing lipid concentrations, lingering inflammation and advancing endothelial harm clarifies why reining in dyslipidemia still serves as a workable keystone for curbing atherosclerotic hazard and, in turn, for heading off the cardiovascular events that erupt once a plaque finally breaks.

2.2.2. The correlation between LDL-C and coronary heart disease risk

For decades, clinicians have taken it as given that the concentration of LDL-cholesterol moves in step with the probability of coronary heart disease, and the literature has grown so large that every fresh meta-analysis merely sharpens the same outline: when low-density lipoprotein particles accumulate beyond their usual range, cardiac risk climbs in near-lockstep. Keeping that excess in place year after year erodes the mechanical integrity of the intima lining the smaller arteries, and once that lining weakens, the path toward arteriosclerosis needs no further invitation. Geneticists have added a sharper angle, pooling dozens of cohorts to show that individuals whose DNA nudges LDL-C upward carry a noticeably higher lifetime incidence of manifest CHD [14]. The mirror image appears in trials where statins or the newer lipid-lowering agents push the same metric downward, producing fewer events such as myocardial infarction or stroke, a symmetry that has turned the lipid hypothesis into common currency across cardiology departments. Abnormal lipid profiles therefore serve a dual role: they flag future risk and, more importantly, feed the disease process itself. The newest data refine the picture further, revealing that the impact of low-density lipoprotein can be tempered or amplified by existing atherosclerotic plaque and by the broader lipid landscape, a reminder that therapy should address the whole pattern rather than a solitary number in patients who already face high baseline hazard [15].

2.2.3. The protective role of HDL-C and its mechanisms

High-density lipoprotein cholesterol, abbreviated HDL-C, has long been casually called the “good cholesterol” because epidemiologists repeatedly observe that higher circulating amounts seem to wrap the vasculature in a buffer against atherosclerosis and its downstream companion, coronary heart disease. The maneuver most textbooks highlight is reverse cholesterol transport: the lipoprotein scours peripheral tissues for cholesterol that has wandered out of place, ferries the cargo through the bloodstream, and unloads it in the liver for ultimate excretion, a sequence that quietly prevents lipid from stacking inside arterial walls. Yet this cleanup operation is only one entry on its résumé; HDL also donates anti-inflammatory signals, supplies antioxidant enzymes, and shields the endothelial lining from stress, talents that together widen its cardioprotective footprint [16]. Recent cohort data, however, reveal that the HDL-C tale contains more wrinkles than earlier imagined, suggesting that the functional calibre of each particle can outweigh the sheer concentration measured in plasma. When the lipoprotein shifts into a “dysfunctional” state and its cholesterol efflux capacity slackens, cardiovascular hazard may paradoxically rise, a twist that redirects attention toward how effectively HDL operates rather than how many milligrams drift in the circulation [17]. Charting the intricate molecular choreography that underlies these protective maneuvers, therefore, stays high on the research agenda, because any future therapy that hopes to restore or amplify HDL performance will first need the granular map of what to fix before clinical benefit can follow.

2.3. Definition and clinical significance of abnormal glucose tolerance

Impaired glucose tolerance, abbreviated AGT, sits one step shy of outright diabetes. In this state the body can no longer keep blood sugar within a safe corridor for years on end, so glucose lingers at levels higher than ideal, quietly setting the scene for heavier downstream damage, above all type 2 diabetes mellitus and a cluster of cardiovascular diseases. Clinicians normally uncover AGT with a routine oral glucose tolerance test: two hours after the sweet drink, a plasma glucose value that stops anywhere from 140 to 199 mg/dL earns the label of impaired glucose tolerance, while a result that edges past 200 mg/dL crosses the line into outright diabetes. Doctors watch this narrow band so closely because AGT behaves like an early flare rather than a harmless flicker; cohort data keep showing that people who land here face roughly double or triple the risk of marching on to full T2DM when their long-term outcomes are lined up against peers whose two-hour values never leave the normal lane [18]. The glucose trouble seldom travels alone. Blood pressure drifts upward, lipids tilt toward dyslipidemia, and extra weight settles around the waist in the pattern of central obesity; these linked shifts steadily raise the probability that coronary artery disease will follow [19].

2.3.1. Diagnostic criteria for type 2 diabetes

Over the past decades, the yardsticks for labeling a person with T2DM have drifted noticeably, and both the American Diabetes Association and the World Health Organization now issue guidance that keeps hammering home the same message: unless the diagnosis is spot-on, any chance of starting therapy while the disease is still in its earliest chapter slips away. The ADA presently treats any one of four laboratory signals as decisive proof: a fasting plasma glucose that sits at 126 mg/dL or climbs higher, a two-hour reading that reaches 200 mg/dL or more during a standard oral glucose tolerance test, a hemoglobin A1c figure that lands at 6.5 % or above, or—when unmistakable hyperglycemic symptoms accompany the visit—a random plasma glucose that touches 200 mg/dL or beyond [2]. These thresholds quietly nudge clinicians to cast a wider screening net, especially over groups already freighted with extra risk, among them people whose glucose tolerance has begun to wobble and who, if no one intervenes, frequently tip into full-blown diabetes with unsettling speed. Picking up T2DM even a few months earlier than usual unlocks room for lifestyle adjustments and, should they prove insufficient, for pharmacologic help, a tandem that can trim the probability of later harm—think myocardial infarction, stroke, or a slow slide toward renal failure—by a clear margin [20].

2.3.2. Impact of abnormal glucose tolerance on cardiovascular health

Researchers have already traced the connection between abnormal glucose tolerance and cardiovascular health in considerable detail, and a steady stream of studies keeps sounding the same alarm: once blood sugar drifts into the impaired glucose tolerance zone, the likelihood of coronary heart disease climbs sharply. The problem rarely arrives unaccompanied; hypertension, hyperhomocysteinemia, and dyslipidemia usually tag along, and the resulting mix of elevated lipids, raised blood pressure, and other metabolic disturbances multiplies the baseline danger. Lipid panels offer a clear snapshot of this shift: individuals who have crossed into the AGT range tend to present with higher fasting triglycerides and, in the same breath, lower protective HDL-cholesterol, a pairing that clinicians recognise as a slow but steady eroder of arterial integrity [21]. The risk is not confined to laboratory figures; cohort data show that people with AGT register markedly more myocardial infarctions and ischaemic strokes, a trend that underlines why a glucose tolerance test ought to sit routinely within any thorough cardiovascular risk assessment. On a more hopeful note, targeted measures—structured exercise plans, careful

dietary tweaks, or glucose-lowering medication—can nudge tolerance back toward normal and, in the process, pare down a measurable slice of cardiac risk, implying that attentive control of AGT functions as a real, not merely theoretical, shield for the heart [22]. Spotting the condition promptly and responding without delay therefore emerges as a pivotal prevention move, above all in population segments already juggling a double load of metabolic and cardiovascular liabilities.

2.4. Interaction between glucose tolerance and dyslipidemia

When it comes to mechanism, the way dyslipidemia and erratic glucose values talk to each other has moved to the front of the current debate and carries weight both on the bench and at the bedside. Work to date shows that people who carry dyslipidemia almost always display measurable insulin resistance, a defect that then nudges fasting and post-prandial glucose further upward [1,2]. This two-way downward spiral, which also magnifies coronary risk, is most visible in individuals with marked obesity or with chronically low daily step counts. Metabolic chaos feeds itself, accelerating lipid-rich plaque growth within coronary trees and setting the stage for hard endpoints. For those who see patients every day, keeping an eye on metabolic read-outs and stepping in early—whether lipids are off or glucose tolerance is already wobbling—has become central to daily practice. More mapping of the molecular traffic between lipid and glucose circuits will clearly feed back into smarter molecules and into guidelines that are refreshed more often.

Insulin resistance quietly steers the entire derailment of lipid balance, and it does so by nudging liver cells away from their usual choreography; once the hepatic rhythm slips, the organ no longer finishes the daily task of sorting lipids with its former precision. Everyone who follows metabolic literature already accepts that insulin resistance sits at the hub of glucose intolerance, yet the same defect, while nudging glucose upward, also muffles the liver's talent for clearing low-density lipoprotein particles. When the liver's grip on lipid traffic loosens, triglycerides climb, high-density lipoprotein shrinks, and the twin stresses of hyperglycaemia and disordered lipids stir the clotting cascade inside the vessel wall, encouraging plaque to take root. The sequence makes it clear that dyslipidaemia can feed back into glucose intolerance, but the pivotal insult—insulin resistance—can just as easily push lipids further off course. A steady programme of everyday movement and deliberate lifestyle choices nudges both glucose and lipid figures back toward their usual corridors [23].

2.5. Prevention and intervention strategies

2.5.1. Lifestyle interventions

Day-to-day habits still give clinicians the clearest, least expensive line of defence against coronary heart disease and diabetes, particularly once fasting glucose edges into the impaired tolerance band. Study after study shows that when people edge their routines toward cardioprotective patterns, the likelihood of stepping into outright diabetes or landing in the emergency ward with a myocardial event shrinks in a visible way. The shield that research keeps pointing to is neither exotic nor new: it is a trio of ordinary moves—plate changes you can spot across the dinner table, minutes of movement you can tally on a watch face, and a final break with tobacco. One fresh meta-analysis, for instance, calculated that nudging meals toward a Mediterranean template—filling the weekly grocery list with intact grains, seasonal fruit, and pulses while treating meat as a side actor—restores lipids and fasting glucose well enough to trim coronary risk [24]. On the exercise ledger, accumulating a modest 150 min of brisk walking, cycling, or any activity that raises the pulse is repeatedly tied to fewer cardiac admissions and to welcome side benefits such as softer blood-pressure readings and a lipid panel that no longer alarms the laboratory [25]. When counsellors

add behavioural glue—perhaps a step-count wager among friends or a simple paper log of meals—participants usually stay with the regimen long enough for genuine shifts in risk to emerge [11]. Collectively, these strands of evidence show why community-wide lifestyle programmes merit front-row status in any serious plan to ease the shared burden of diabetes and heart disease, and they also clarify why public-health messages keep returning to the same quiet plea: eat a little more thoughtfully, move a little more often, and let the cigarettes go.

2.5.2. Recent advances in pharmacotherapy

Drug treatment has moved forward in the past few years, and the advance has given clinicians a noticeably firmer hold on coronary heart disease as well as on diabetes, particularly for individuals whose glucose tolerance is already beginning to slide. The newer classes—sodium-glucose co-transporter-2 inhibitors and glucagon-like peptide-1 receptor agonists—no longer stop at glycaemic control; they also hand clinicians measurable cardiovascular benefits that older agents could not deliver. Real-world trials illustrate the point: when an SGLT2 inhibitor is added to background therapy, the combined rate of heart-failure hospitalisations and major adverse cardiac events in adults with type 2 diabetes drops [7]. GLP-1 receptor agonists manage a comparable dual task, easing glucose levels downward, trimming excess weight, and still leaving patients with cleaner vascular endpoints [26]. Because these molecules interfere with several metabolic steps at once, they erode the tight bundle of risk factors that usually nourish both CHD and diabetes. While this is happening, investigators are busy testing cocktails that park the newcomers next to familiar workhorses—statins, ACE inhibitors, or beta-blockers—to learn whether the mixture can drive event curves still lower [1]. Clinics, for their part, are experimenting with personalised plans that fold age, renal function, body-mass index and other comorbidities into the equation before the first tablet is dispensed, a shift that should keep regimens from sliding into one-size-fits-all territory [27]. Viewed together, the shifting landscape of pharmacotherapy still looks like one of the more promising avenues for keeping high-risk patients clear of cardiac catastrophes.

2.5.3. Importance of regular screening

Keeping up a routine of cardiovascular and diabetes checks is still among the handful of measures that can pick up brewing problems before they gather speed, particularly for people whose years, body mass, or inherited background already nudge them into a clearly higher-risk lane. A pattern that surfaces again and again in the literature is that adults who carry impaired glucose tolerance—abbreviated simply as IGT—face a noticeably steeper probability of sliding into outright type 2 diabetes and, in parallel, of meeting some manifestation of cardiovascular illness, so identifying them at the earliest moment is not merely useful but close to decisive [4]. The workhorse investigations most outpatient rooms reach for—an overnight fasting glucose sample and the somewhat lengthier oral glucose tolerance procedure—manage reasonably well at highlighting these borderline persons, allowing counselling, dietary shifts, or even an initial pharmaceutical step to begin before injury fans out. Moving past glucose, watching the familiar cardiovascular cast—blood pressure numbers, a standard lipid profile, and a swift height-and-weight stop to derive body mass index—turns out to be equally indispensable for anyone who has already lived through a coronary episode or walks around with an established label of coronary heart disease [3]. Once clinics, or the wider health networks that support them, put in place a coherent screening timetable instead of leaving encounters to chance-driven appointments, the benefit shows up in plain figures: doctors can start discussions on modest lifestyle edits or hand out preventive prescriptions months, sometimes years, earlier, and that early lead converts into a measurable drop in heart attacks, strokes, and other major adverse cardiovascular

events as the calendar pages turn [28]. Professional guidelines drive the message home, recommending that every person who can check off either a first-degree family thread of cardiac disease or a constellation of textbook risk markers should turn up for these assessments on a tighter schedule, because the interval in which proactive care remains possible stays broader when surveillance is steady rather than sporadic [7]. Read side by side, the accumulated evidence offers a single pragmatic lesson: scheduled screening acts as the pivot on which worthwhile prevention turns, handing clinicians an opening to step in while the pathological process can still be reeled back and, by doing so, shifting the long-range prognosis toward a stretch of additional years free from complicated illness for those who stand closest to the fire.

3. Conclusion

Dyslipidemia and elevated glucose each push up coronary heart disease rates on their own, yet they also amplify one another inside the wider metabolic upset, piling up the danger in a joint fashion. The review first walks through the key clinical steps that mark how this illness begins and then expands. It offers fresh angles for bench scientists while urging front-line doctors to look harder at the overlap between disordered lipids and erratic glycemic readings.

Researchers who spend their days poring over lipid panels and fasting-glucose spreadsheets often remind newcomers that the published record on dyslipidemia and glucose intolerance resembles a patchwork quilt rather than a single seamless blanket. Dozens of papers draw a confident arrow between these twin metabolic glitches and coronary heart disease, yet the slope of that arrow tilts the moment you switch cohorts, so any clinic that wants to import the numbers into daily care has to keep one foot on the brake. A person's DNA, the ethnic story carried by grandparents, the small daily habits that never make it into a questionnaire, plus the air quality and neighbourhood income curve all steer how dyslipidemia or a blunted glucose spike will act once inside one particular body. With that mosaic in view, the coming studies could profit from slowing the camera down to single-human resolution, mapping how each tile fits, so that tomorrow's prevention recipe or drug sequence can be cut to exact measurements and, once applied, keep cardiovascular events low for good.

By threading endocrinology, cardiology, nutrition and neighbouring disciplines into the same fabric, we let the portrait of CHD thicken little by little, revealing a disorder that is nudged along by several intertwined influences rather than a single culprit. A habit of working across these boundaries lets teams assemble wider models that still keep an eye on how lipid shuttling, insulin signalling and the heart's moment-to-moment condition keep feeding back on one another. Once such living maps are in hand, they can serve as a day-to-day compass for sketching prevention bundles or therapy sequences that are trimmed to fit the exact risk fingerprint, daily routines and cultural habits that separate one population slice from another.

Researchers have sketched a fairly coherent outline of how dyslipidemia and impaired glucose tolerance jointly nudge coronary heart disease forward, yet a tangle of unanswered questions still dangles at the edges, so sustaining the investigative push remains every bit as urgent as it was at the outset. Tangible benefits will surface only if forthcoming studies keep refining preventive and therapeutic blueprints by quietly registering each person's idiosyncrasies while also scanning the broader population canvas on which those quirks appear. Once that delicate equilibrium is held, the clinical kit for intercepting—or at least tempering—CHD should gain a visibly keener edge, patients ought to face a lighter outlook, and the everyday burden this exceptionally prevalent condition imposes on hospitals, clinics, and households should ease a little.

Disclosure statement

The authors declare no conflict of interest.

References

[1] Xu S, Scott C, Coleman R, et al., 2021, Predicting the Risk of Developing Type 2 Diabetes in Chinese People Who Have Coronary Heart Disease and Impaired Glucose Tolerance. Journal of Diabetes, 13(10): 817–826.

[2] Cao L, Wang P, Luan H, et al., 2020, Elevated 1-H Postload Plasma Glucose Levels Identify Coronary Heart Disease Patients with Greater Severity of Coronary Artery Lesions and Higher Risk of 1-Year Re-Admission. Diabetes & Vascular Disease Research, 17(1): 1479164119896978.

[3] Welten S, van der Heijden A, Remmelzwaal S, et al., 2023, Prolongation of the QTc Interval Is Associated with an Increased Risk of Cardiovascular Diseases: The Hoorn Study. Journal of Electrocardiology, 80: 133–138.

[4] Cai X, Zhang Y, Li M, et al., 2020, Association Between Prediabetes and Risk of All-Cause Mortality and Cardiovascular Disease: Updated Meta-Analysis. BMJ, 370: m2297.

[5] Tsuchida K, Mitsuma W, Sato Y, et al., 2020, Impaired Glucose Tolerance and Future Cardiovascular Risk After Coronary Revascularization: A 10-Year Follow-Up Report. Acta Diabetologica, 57(2): 173–182.

[6] Wang B, Zhang H, Sun Y, et al., 2023, Association of Sleep Patterns and Cardiovascular Disease Risk Is Modified by Glucose Tolerance Status. Diabetes/Metabolism Research and Reviews, 39(6): e3642.

[7] Visco V, Forte M, Giallauria F, et al., 2025, Epigenetic Mechanisms Underlying the Beneficial Effects of Cardiac Rehabilitation: An Overview From the Working Groups of "Cellular and Molecular Biology of the Heart" and "Cardiac Rehabilitation and Cardiovascular Prevention" of the Italian Society of Cardiology (SIC). International Journal of Cardiology, 429: 133166.

[8] Pradhan A, Bhandari M, Vishwakarma P, et al., 2023, Bempedoic Acid: An Emerging Therapy for Uncontrolled Low-Density Lipoprotein (LDL) Cholesterol. Journal of Cardiovascular Development and Disease, 10(5): 195.

[9] Amarenco P, Kim J, Labreuche J, et al., 2020, Benefit of Targeting a LDL (Low-Density Lipoprotein) Cholesterol <70 mg/dL During 5 Years After Ischemic Stroke. Stroke, 51(4): 1231–1239.

[10] Tan M, Yang S, Xu X, 2023, High-Density Lipoprotein Cholesterol and Carcinogenesis. Trends in Endocrinology and Metabolism, 34(5): 303–313.

[11] Hayes M, 2024, Non-Insulin Medications for the Management of Type 2 Diabetes. Home Healthcare Now, 42(2): 72–77.

[12] Zachariah G, 2023, Management of Triglycerides, Non-High Density Lipoprotein Cholesterol and High Density Lipoprotein Cholesterol. Indian Heart Journal, 76(Suppl 1): S58–S64.

[13] Xiang Q, Tian F, Xu J, et al., 2022, New Insight Into Dyslipidemia-Induced Cellular Senescence in Atherosclerosis. Biological Reviews, 97(5): 1844–1867.

[14] Wu T, Chou C, Liu C, et al., 2025, Lipid Profiles and Their Association With Incident Carotid Atherosclerosis: A Community-Based Prospective Study in Taiwan. Nutrition, Metabolism and Cardiovascular Diseases, 35(6): 104023.

[15] Fukami H, Oike Y, 2025, ANGPTL3: A Breakthrough Target in Treatment for Dyslipidemia and Atherosclerosis. Journal of Atherosclerosis and Thrombosis, 32(9): 1071–1078.

[16] Xing L, Liu Y, Wang J, et al., 2023, High-Density Lipoprotein and Heart Failure. Reviews in Cardiovascular Medicine, 24(11): 321.

[17] Razavi A, Jain V, Grandhi G, et al., 2024, Does Elevated High-Density Lipoprotein Cholesterol Protect Against

Cardiovascular Disease? Journal of Clinical Endocrinology & Metabolism, 109(2): 321–332.

[18] Piccoli R, Simões W, Custódio S, et al., 2024, Sustainable Intervention: Grape Pomace Flour Ameliorates Fasting Glucose and Mitigates Streptozotocin-Induced Pancreatic Damage in a Type 2 Diabetes Animal Model. Pharmaceuticals, 17(11): 1530.

[19] Jose J, Madhu L, Bhongir A, et al., 2024, Evaluating Dyslipidemia and Atherogenic Indices as Predictors of Coronary Artery Disease Risk: A Retrospective Cross-Sectional Study. Cureus, 16(10): e71187.

[20] Najafipour H, Yousefzadeh G, Baneshi M, et al., 2021, Prevalence and 5-Year Incidence Rate of Dyslipidemia and Its Association With Other Coronary Artery Disease Risk Factors in Iran: Results of the Kerman Coronary Artery Disease Risk Factors Study (Phase 2). Journal of Research in Medical Sciences, 26: 99.

[21] Arvanitis M, Lowenstein C, 2023, Dyslipidemia. Annals of Internal Medicine, 176(6): ITC81–ITC96.

[22] Alhroub W, Jabareen M, Abu-Mayyaleh H, et al., 2025, Severe Left Main Coronary Artery Disease and STEMI in a 19-Year-Old Without Traditional Risk Factors: A Rare Case of Premature Coronary Artery Disease. SAGE Open Medical Case Reports, 13: 2050313X251321041.

[23] Wei Y, Xu W, 2019, Effect of Acarbose on Cardiovascular Events and New-Onset Diabetes in Patients With Coronary Heart Disease and Impaired Glucose Tolerance. Future Cardiology, 15(2): 127–133.

[24] de la Cruz-Ares S, Gutiérrez-Mariscal F, Alcalá-Díaz J, et al., 2021, Quality and Quantity of Protein Intake Influence Incidence of Type 2 Diabetes Mellitus in Coronary Heart Disease Patients: From the CORDIOPREV Study. Nutrients, 13(4): 1217.

[25] Zhan Q, Xie L, Wang C, 2023, Promoting Critical Care System and Capacity Building in Pulmonary and Critical Care Medicine Subspecialties. Zhonghua Yi Xue Za Zhi, 103(40): 3149–3151.

[26] Alshehri A, Guan D, Li P, et al., 2024, Trends in Utilization Patterns of Newer Glucose-Lowering Drugs in US Adults With Type 2 Diabetes and a History of Coronary Heart Disease or Heart Failure: 2005–2019. Primary Care Diabetes, 18(5): 561–563.

[27] Kumar S, Talwalkar P, Das S, et al., 2019, Cardiovascular Effects of Sodium Glucose Co-Transporter-2 Inhibitors in Patients With Type 2 Diabetes Mellitus. Indian Journal of Endocrinology and Metabolism, 23(1): 150–158.

[28] Vellapandian C, 2024, Exploring the Long-Term Effect of Artificial Sweeteners on Metabolic Health. Cureus, 16(9): e70043.

Publisher's note

Bio-Byword Scientific Publishing remains neutral with regard to jurisdictional claims in published maps and institutional affiliations.

Proceedings of Anticancer Research, 2026, Volume 10, Issue 1
http://ojs.bbwpublisher.com/index.php/PAR
ISSN Online: 2208-3553
ISSN Print: 2208-3545

SIRT Visualization and Hotspot Analysis Based on The Web of Science Database for the Treatment of Liver Neoplasms

Guangyuan Zhao[1,2]*, Mengyun Bai[1,2], Dengxiang Liu[2]*

[1] Graduate School of Hebei North University, Zhangjiakou 075000, Hebei, China
[2] Xingtai People's Hospital, Xingtai 054000, Hebei, China.

**Corresponding authors: Dengxiang Liu, rmyy666@163.com; Guangyuan Zhao, Light3330108@163.com*

Copyright: © 2026 Author(s). This is an open-access article distributed under the terms of the Creative Commons Attribution License (CC BY 4.0), permitting distribution and reproduction in any medium, provided the original work is cited.

Abstract: Selective internal radiation therapy using yttrium-90 has been used to treat hepatocellular carcinoma, intrahepatic cholangiocarcinoma, and other malignant tumors that have spread to the liver locally. The authors used the bibliometric approach in response to the neoplasms, using the keyword "Yttrium 90 AND Liver Neoplasms" as a search parameter and then looked up pertinent English-language literature in the Web of Science core collection database's self-built database through November 30, 2025. For statistical analysis and literature management, EndNote and Excel tools were utilized. In addition to co-citation and emergent keyword analysis of authors, VOSviewer and CiteSpace were utilized for social network and chronological order of countries, institutions, authors, and keywords. The aim of this study was to serve as a reference for future research by methodically sorting through the international research literature on Yttrium 90 treatment of liver neoplasms and summarizing the research status and hot trends in this field. In recent years, research focus has increasingly shifted toward high-quality, multi-center clinical trials that combine SIRT-targeted systemic therapy with hepatectomy following the descending stage. This approach is likely to remain a significant research trend in the field.

Keywords: Yttrium-90; Liver neoplasms; Web of Science; CiteSpace; VOSviewer; Bibliometric method; Therapeutics

Online publication: February 4, 2026

1. Introduction

From third highest in 2018 to second highest in 2020, hepatocellular carcinoma has emerged as the leading cause of cancer death [1]. Because the majority of liver malignant tumor treatment is based on the patient's tumor burden and cancer-related symptoms [2] (2), some patients may be able to undergo surgical resection or liver transplantation if their tumors shrink or their staging decreases as a result of Selective internal radiation therapy using yttrium-90 (^{90}Y-SIRT) [3]. It has been demonstrated that ^{90}Y-SIRT is a successful therapeutic approach for liver-directed therapy, which may enhance the results of local control or make tumor reduction more operable [4–9].

^{90}Y-SIRT has been extensively employed in the local management of primary and secondary liver malignancies [10]. But metastatic liver malignant tumors from other sites cannot be easily equated with hepatocellular carcinoma because of the biological features and treatment approaches that differ among malignant tumors from different sources. Research and therapy of malignant tumors of the liver are thus faced with obstacles. In the last 20 years, a significant number of studies have been published due to the growing application of ^{90}Y-SIRT in the treatment of malignant tumors of the liver. In order to sort through the English literature on the treatment of liver malignant tumors with Yttrium 90 and analyze the current publication status and hot topics in order to provide references for future research, the authors use the method of bibliometrics to more thoroughly comb the development status of ^{90}Y-SIRT in the treatment of liver malignant tumors.

2. Materials and methods

The Web of Science Core Collection (WoSCC) database was searched using the phrases "Yttrium-90 and Liver Neoplasms," and all citation indexes were chosen. Title, abstract, keywords, and other search terms are included in the "Subject" field search results. In addition, the time period is from the database's creation until November 30, 2025; the literary genre is restricted to treatises, conference papers, and reviews; and the language is only available in English. News stories, letters, communications, conference papers, information, and literature that do not fit the topic are among the exclusion criteria.

EndNote X9 and Excel 2010 were used to manage literature selection and data analysis, and literature citation frequency information in Web of Science citation reports was collected. VOSviewer 1.6.18 includes the country, institution, author, and keywords in each document and makes corresponding types of social network maps and time series maps, respectively. CiteSpace 6.1.R6 Select key-words and co-cited authors, set the screening threshold to "Top 5%," and make the corresponding graph. The number of instances is represented by the number of nodes in the graph. In VOSviewer's social network diagram, nodes belonging to distinct clusters are colored differently. With a darker node color indicating an earlier average publication year, the time average is used to generate the time series plan. CiteSpace nodes are colored and widened to indicate the quantity and time of occurrences. The incidence time increases with the darkness of the center color. The node that has a purple circle surrounding it signifies that its intermediary centrality is higher than 0.1, meaning it serves as a mediator between the other two nodes more frequently. The more connections, the greater the intermediary centrality, indicating that the analysis item represented by the node has an important influence in the field.

3. Result

3.1. Literature search results

There were 956 pieces of English literature that had been retrieved as of November 30, 2025. A total of 895 pieces of English literature, comprising 716 papers and 140 reviews, were acquired after duplicates and non-conforming literature were eliminated. The literature screening process is shown in **Figure 1**.

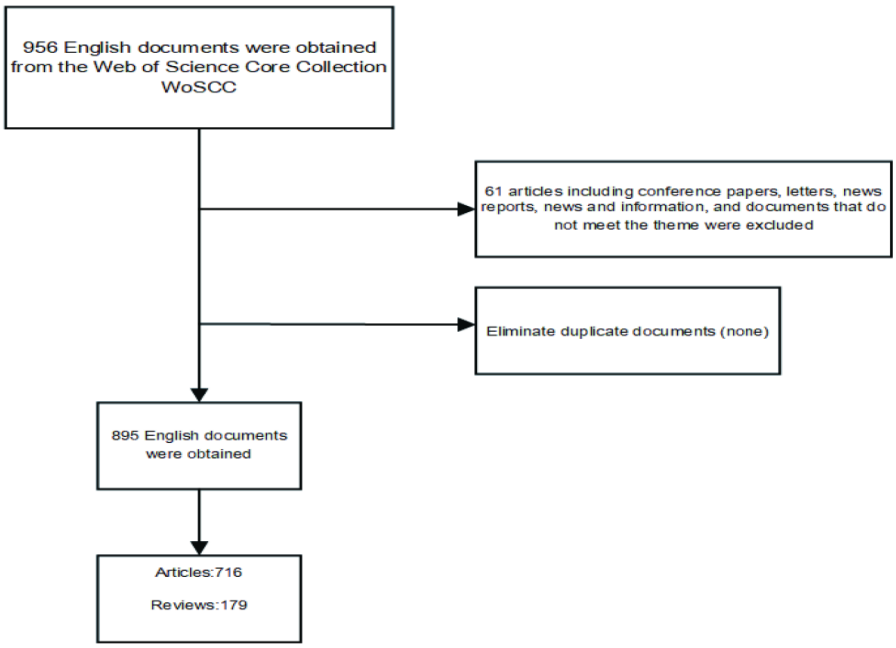


Figure 1. Flowchart for document screening.

3.2. Publication outputs and citation trends

The first article in the topic was published in 1991, and there were a total of 25 published before 2000. The number of publications per year is on the rise generally, reaching a peak in 2021. The change trend of the annual publication volume is shown in **Figure 2**.

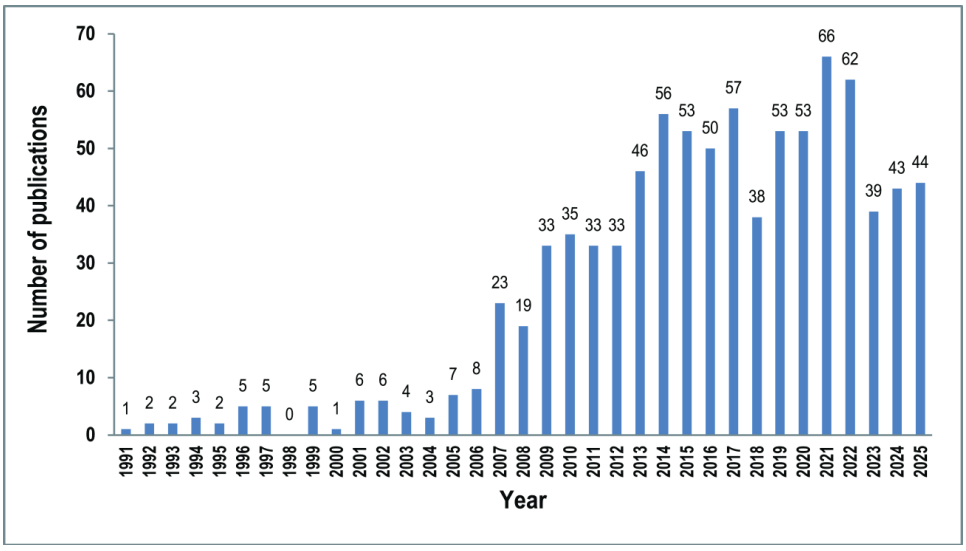


Figure 2. Annual number of publications on osteoporosis in selective internal radiation therapy research from 1991 to 2025.

The top three journals in terms of publication volume between 1991 and 2025 (**Table 1**) are the Journal of Vascular and Interventional Radiology (77 articles), the Cardiovascular and Interventional Radiology (58 articles) and the Journal of Gastrointestinal Oncology (24 articles). Nuclear medicine, interventional radiology, and cancer are the three professional publications that have published more than ten papers.

Table 1. Journals with more than 10 publications

Sources title	Output	% of 895	JIF (2024)
Journal of Vascular and Interventional Radiology	77	8.60	2.6
Cardiovascular And Interventional Radiology	58	6.48	2.9
Journal of Gastrointestinal Oncology	24	2.68	2.0
European Journal of Nuclear Medicine and Molecular Imaging	19	2.12	7.6
Nuclear Medicine Communications	15	1.68	1.3
Cancers	15	1.68	4.4
International Journal of Radiation Oncology Biology Physics	14	1.56	6.5
American Journal of Clinical Oncology Cancer Clinical Trials	14	1.56	1.8
European Radiology	13	1.45	4.7
Seminars In Interventional Radiolog	13	1.45	1.3
Medical Physics	12	1.34	3.2
Cancer Biotherapy and Radiopharmaceuticals	11	1.23	2.1
Frontiers In Oncology	11	1.23	3.8

The majority of the top 10 most cited publications (**Supplementary Table 1**) were written about phase III systemic therapy and dose, and they were all randomized controlled clinical trials, most were published after 2000.

Supplementary Table 1. The top 10 most cited works

No.	Title	First Author	Journal	Publication Year	Digital Object Identifier	Total Citations
1	Radioembolization for Hepatocellular Carcinoma Using Yttrium-90 Microspheres: A Comprehensive Report of Long-term Outcomes	Salem R	Gastroenterology	2010	10.1053/j.gastro.2009.09.006	802
2	Efficacy and safety of selective internal radiotherapy with yttrium-90 resin microspheres compared with sorafenib in locally advanced and inoperable hepatocellular carcinoma (SARAH): an open-label randomised controlled phase 3 trial	Vilgrain V	Lancet Oncology	2017	10.1016/S1470-2045(17)30683-6	638
3	Recommendations for radioembolization of hepatic malignancies using yttrium-90 microsphere brachytherapy: A consensus panel report from the Radioembolization Brachytherapy Oncology Consortium	Kennedy A	International Journal of Radiation Oncology Biology Physics	2007	10.1016/j.ijrobp.2006.11.060	544
4	Survival After Yttrium-90 Resin Microsphere Radioembolization of Hepatocellular Carcinoma Across Barcelona Clinic Liver Cancer Stages: A European Evaluation	Sangro B	Hepatology	2011	10.1002/hep.24451	519
5	Radioembolization Results in Longer Time-to-Progression and Reduced Toxicity Compared With Chemoembolization in Patients With Hepatocellular Carcinoma	Salem R	Gastroenterology	2011	10.1053/j.gastro.2010.10.049	510
6	Y90 Radioembolization Significantly Prolongs Time to Progression Compared With Chemoembolization in Patients With Hepatocellular Carcinoma	Salem R	Gastroenterology	2016	10.1053/j.gastro.2016.08.029	490

Supplementary Table 1 (Continued)

No.	Title	First Author	Journal	Publication Year	Digital Object Identifier	Total Citations
7	Randomised trial of SIR-Spheres® plus chemotherapy vs. chemotherapy alone for treating patients with liver metastases from primary large bowel cancer	Gray B	Annals of Oncology	2001	10.1023/A:1013569329846	402
8	Radioembolization with Yttrium-90 Glass Microspheres in Hepatocellular Carcinoma: European Experience on Safety and Long-Term Survival	Hilgard P	Hepatology	2010	10.1002/hep.23944	363
9	New therapies for hepatocellular carcinoma	Avila M.A.	Oncogene	2006	10.1038/sj.onc.1209550	333
10	Phase III Trial Comparing Protracted Intravenous Fluorouracil Infusion Alone or With Yttrium-90 Resin Microspheres Radioembolization for Liver-Limited Metastatic Colorectal Cancer Refractory to Standard Chemotherapy	Hendlisz,A	Journal Of Clinical Oncology	2020	10.1200/JCO.2010.28.5643	289

3.3. Number of publications issued by countries or regions

The top 10 countries in terms of publication volume are shown in **Table 2**. The United States (409 articles), Germany (82 articles), and England (58 articles) ranked in the top three. Among them, the United States was cited the most (14,799 times), followed by Germany (3,985 times) and Spain (3618 times).

Table 2. Top 10 countries with the most publications

Ranking	Country	Output	Total Citation
1	Usa	472	17481
2	Germany	88	4468
3	Italy	71	3237
4	England	63	3011
5	France	58	3061
6	Spain	54	4125
7	Australia	52	3436
8	Netherlands	49	1987
9	China	48	1052
10	Belgium	35	1892

3.4. Number of publications issued by research institutions

The top 10 research institutions in terms of the number of published papers are shown in **Table 3**. Among them, Northwestern University of the United States has the highest number of publications and citation frequency; Memorial Sloan Kettering Cancer Centre of the United States and Emory University of the United States rank second and third, respectively. Although the number of articles published by Hong Kong Chinese Hospital is small, it ranks 6th in the frequency of citations (17 articles, 1,089 citations).

Table 3. Top 10 institutions with the most publications

Ranking	Institution	Output	Total Citation
1	Northwestern Univ	86	5898
2	Mem Sloan Kettering Canc Ctr	29	532
3	Univ Texas Md Anderson Canc Ctr	25	1080
4	Emory Univ	23	722
5	Clin Univ Navarra	22	1185
6	Nw Mem Hosp	22	2522
7	Stanford Univ	22	669
8	Univ Med Ctr Utrecht	21	720
9	Singapore Gen Hosp	18	668
10	Chinese Univ Hong Kong	17	1089

3.5. Author's number of publications

The top 10 authors in the order of publication volume are shown in **Table 4**, all from the United States and Spain. The United States has the most authors, with nine. Salem R, the American author, ranked first in both the number of articles published and the number of citations (85 articles published and 6291 citations).

Table 4. Top 10 authors with the most publications

Ranking	Author	Country	Output	Total Citation
1	Salem,R	Usa	93	7343
2	Lewandowski,RJ	Usa	62	4697
3	Sangro,B	Spain	31	2295
4	Mulcahy,M	Usa	30	3744
5	Riaz,A	Usa	25	1917
6	Kulik,L	Usa	23	2732
7	Omary,RA	Usa	22	2938
8	Ryu,RK	Usa	21	2871
9	Sato,KT	Usa	19	2646
10	Gates,VL	Usa	19	1091

3.6. Author co-citation frequency ranking and co-citation network diagram

The authors with the top 10 citation frequencies are listed in **Supplementary Table 2**. Authors with greater co-citation frequencies have denser lines when combined with their co-cited social network (**Figure 3**). Nodes for Sangro B, Van Hazel G, Kennedy AS, Kennedy A, Riaz A, Lewandowski RJ, Salem R, Hendlisz A, Ho S, Jakobs TF, Kao YH, Van Cutsem E are surrounded by purple circles. The published papers are frequently utilized as a bridge to connect other publications, which has great cohesiveness and relevance in this subject, as seen by the eleven authors' median centrality of > 0.1.

Supplementary Table 2. The top 10 most cited authors

Ranking	Cited Author	Country	Centrality	Count
1	Salem,R	Usa	0.12	7343
2	Lewandowski,Rj	Usa	0.12	4697
3	Mulcahy,MF	Usa	0.01	3744
4	Omary,RA	Usa	0	2938
5	Ryu,RK	Usa	0.05	2871
6	Kulik,L	Usa	0.06	2732
7	Sato,KT	Usa	0.05	2646
8	Miller,F	Usa	0	2241
9	Sangro,B	Spain	0.23	2295
10	Atassi,B	Usa	0.01	1915

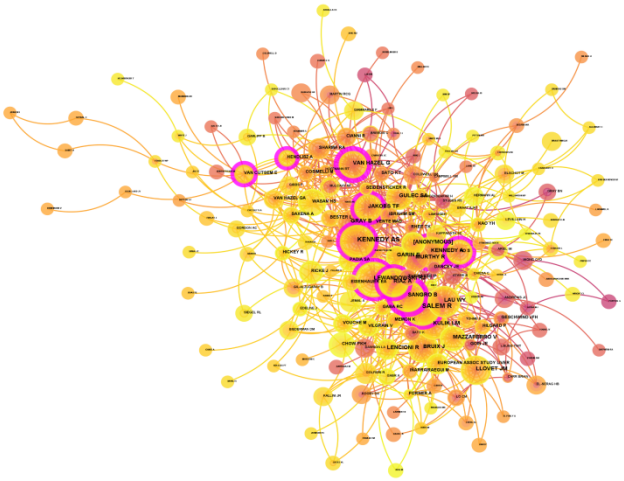


Figure 3. Co-citation analysis graph of authors (frequency ≥ 5).

3.7. Social network map and chronological map of a country or region

The social network map of countries or regions (**Figure 4a**) primarily divides countries or areas with cooperative interactions and a frequency of ≥ 5 times into five clusters: (1) The countries in red are those that work closely with Germany and the United States: Austria, Belgium, the United Kingdom, France, Italy, Spain, Switzerland, and Turkey. (2) The green areas are Australia, China, Singapore, South Korea, and close cooperation with the United States, Spain, Germany, and the United Kingdom. (3) The blue areas are Canada, Egypt, and Germany, which have close cooperation with Asian, European, and American countries. (4) The yellow area illustrates how the US, Japan, and Iran are all part of the same cluster and work closely with Australia as well as other Asian and European nations. (5) The purple area is the Netherlands, which has close cooperation with the United States, Germany, France, Belgium, and other countries.

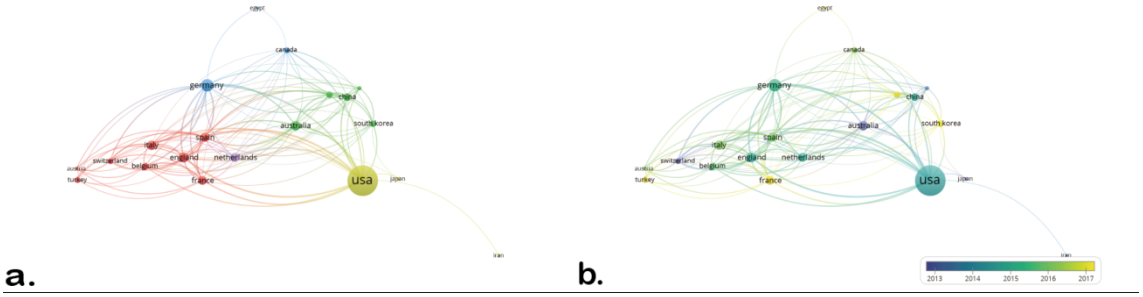


Figure 4. (a) Social networks of countries (frequency ≥ 5). (b) Sequence diagram of countries (frequency ≥ 5).

As shown in the time series diagram (**Figure 4b**), the average publication year of Australia, Switzerland, and other countries was earlier, around 2013; the average publication year of the United States, Germany, China, and other countries was around 2015; and France and Singapore have published a large number of articles since 2017.

3.8. The research institution social network map and sequence diagram

Eight clusters mostly comprise research institutions with a frequency of ≥ 5 times and collaborative relationships (**Figure 5**): (1) The red areas are: Northwestern University Memorial Hospital, Johns Hopkins University School of Medicine, University of New South Wales, etc. (2) The green areas are: the Chinese University of Hong Kong, Duke Medical School of the National University of Singapore, Hong Kong Sanatorium and Hospital, the National Cancer Institute of the United States, the National Cancer Center of Singapore, the University of Sydney, the University of Western Australia, etc. (3) The blue areas are: Emory University, Moffitt Cancer Center, Harvard Medical School, Mayo Medical Center, University of Texas MD Anderson Cancer Center, etc. (4) Yellow areas are: Institute of Barcelona, Spain; University of Hasetpe, Turkey; Munich City Hospital, Germany; University Hospital of Bologna, Italy; and University of Magdeburg, Germany. (5) Purple areas are: City of Hope National Medical Center, Stanford University, Utrecht University Medical Center in the Netherlands, Yonsei University in South Korea, etc. (6) The blue areas are: Christie NHS Foundation, Memorial Sloan Kettering Cancer Center, Seoul National University in South Korea, University of Rennes in France, Yale University School of Medicine, etc. (7) Orange areas are: the Netherlands Cancer Institute, the Technical University of Munich in Germany, the University of British Columbia in Canada, etc. (8) The brown areas are: North Carolina State University, Northwestern University, Imperial College London, the University of Navarra, Spain, and Wake Forest Baptist Comprehensive Cancer Center, USA.



Figure 5. (a) Social network of institutions (frequency ≥ 5). (b) Sequence diagram of institutions (frequency ≥ 5).

Northwestern Memorial Hospital and the Chinese University of Hong Kong published their works on average sooner, in 2012 or so. After 2001, some Chinese research institutes released publications, including the Chinese University of Hong Kong, among them releasing works somewhat sooner. In 2016, Northwestern University published a greater number of articles than any other university, with the highest frequency of citations. The Clinical School of the University of Navarra in Spain, the Duke Medical School of the National University of Singapore, and Harvard Medical School in the United States have all published related research recently.

3.9. The author's social network diagram and sequence diagram

The authors' social network map (**Figure 6a**) shows that the authors with a frequency of ≥5 times and with cooperative relationships can be divided into 7 clusters: (1) The red areas are Kim E, Kennedy AS, et al., and Lam MEH, Smits MLJ, et al., University Medical Center Utrecht, the Netherlands. (2) The green areas are: Salem R, Lewandowski RJ, Gates VL, etc., Northwestern University. (3) The blue areas are: Sangro B, University of Navarra, Spain; Pech MJ, University of Madburg, Germany; etc. (4) The yellow areas are: Garin E, University of Rennes, France; Sofocleous CT; Memorial Sloan Kettering Cancer Center, USA; etc. (5) The purple areas are all American scholars: Mulcahy MF from Northwestern University Cancer Center, Sato KT and Kulik L from Northwestern University, etc. (6) The blue area is for American scholars: Emory University Kokabi N, Schuster DM, Florida State University Camacho JC, Yale University Xing MZ, etc. (7) The orange area is for Australian scholars: Bester L. Meteling, Baerbel, Morris DL, etc.

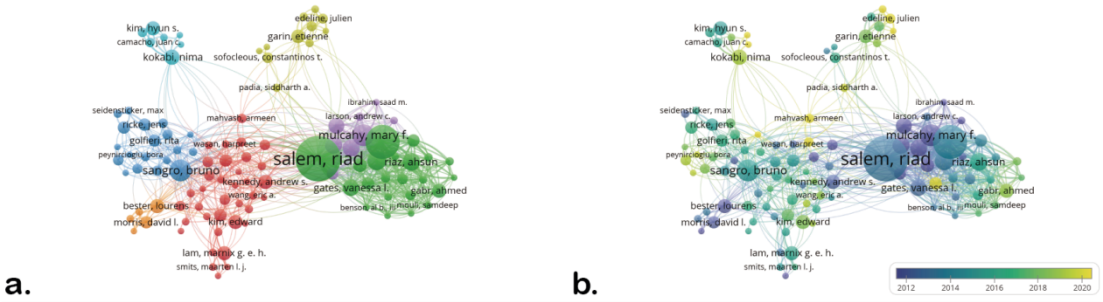


Figure 6. (a) Social network of authors (frequency ≥ 5). (b) Sequence diagram of authors (frequency ≥ 5).

The sequence diagram (**Figure 6b**) shows that the average publication year of American and Australian scholars is earlier, around 2012; the average publication year of German, Dutch, and Italian scholars was around 2016. Around 2014, Salem and Rida, the two American scholars with the greatest number of publications and frequency of citations, released their works. The countries with the most published papers after 2020 would be France and the United States.

3.10. Keywords

The keyword social network diagram (**Figure 7a**), which was created by merging synonym keywords and eliminating search terms, reveals that keywords that occur more than five times are primarily grouped into six clusters: The terms "hepatocellular carcinoma" and "treatment diagnosis" designate the primary uses of the red cluster, which is for hepatocellular carcinoma diagnosis and treatment. The purple cluster primarily consists of "yttrium 90 microspheres" and "internal radiation therapy," which stand in for adverse effects and complications of ^{90}Y-SIRT in the treatment of primary and secondary liver cancers. The green cluster, which is comprised of

the terms “hepatocellular carcinoma,” “chemoembolization,” and “safety,” primarily focuses on the safety of ^{90}Y-SIRT in the treatment of liver illnesses. (4) The yellow cluster is mainly a comprehensive treatment measure for liver metastasis of colorectal cancer, represented by “radiotherapy embolization” and “chemotherapy.” (5) The blue cluster is mainly the prognosis of primary and secondary liver malignancies after treatment, represented by “survival” and “transarterial radiation embolization.” (6) Cyan clustering is mainly for the prospect and analysis of ^{90}Y-SIRT, represented by “radiation embolization” and “trend”.

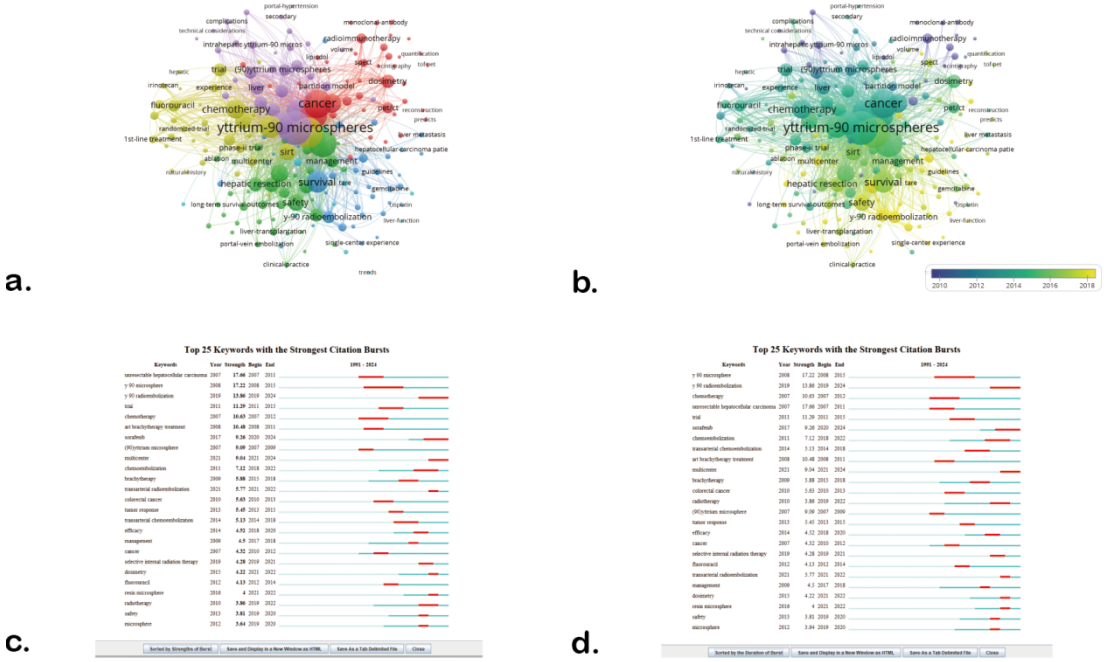


Figure 7. (a) Social network of keywords (frequency ≥ 5). (b) Sequence diagram of keywords (frequency ≥ 5). (c) Top 25 keywords with the strongest citation bursts. (d) Top 25 keywords with the during-time citation bursts.

The time series diagram shows (**Figure 7b**) that the average occurrence year of keywords in clusters (1), (2), and (6) are the earliest, around 2010; In the middle stage, clusters (1), (2), (3), and (4) occurred, and the average occurrence year was around 2014. Clustering (5) was published relatively late.

The term “emergence” (**Figure 7c, d**) refers to a spike in the frequency of occurrence of a particular keyword over a brief period of time, which may indicate future trends and hotspots in the area. “Start” and “stop,” among the top 25 emerging terms in the ^{90}Y-SIRT field, denote the beginning and ending times of the keyword as a frontier hot point, respectively. The most intensely emerging key phrase was “unresectable hepatocellular carcinoma.” “Yttrium-90 microspheres” emerged as the term with the longest longevity, lasting 8 years; subsequent keywords that have persisted after the emergence are “sorafenib,” “multicenter,” and “y-90 radioembolization.”

4. Discussion

Globally, colorectal and primary liver cancers are the most frequent malignant tumors. Primary liver cancer is the third most common cause of death and the sixth most common incidence worldwide, and colorectal cancer ranks second in death and third in incidence [11]. Furthermore, metastatic disease affects up to 50% of individuals

with colorectal cancer [12]. While colorectal cancer incidence is rising, mortality from the disease is decreasing. Of particular concern is the notable rise in cancer of colon, rectum and anus (CRA) incidence (up 1.7% year) among those in the 15–49 age range [13]. Research has demonstrated [14] that the median time to progression following regional therapy of Y90 is much prolonged and local tumour control is significantly enhanced compared with chemoembolization. In addition to posing challenges to the clinical treatment of liver malignancies, the evolving trends in the incidence and mortality of liver malignancies due to a variety of causes, along with the complexity of treatment options for both primary and metastatic liver cancer, also consistently encourage in-depth research on liver malignancy treatment. As a result, a thorough analysis and investigation of the available research on the application of yttrium-90 in the management of hepatic cancers must be done.

4.1. The use of Yttrium-90 in the treatment of liver malignancies is an important international research

According to the study's findings, eight of the top ten authors—Salem R, Lewandowski RJ, Mulcahy M, Kulik L, Ryu RK, Omary RA, Sato KT, and Sangro B, Spain—have the same number of publications and total citations. This suggests a strong scholarly impact from the United States and Spain, particularly with regard to the application of yttrium-90 selective internal radioembolization for the treatment of liver cancers. Salem R of Northwestern University in the United States not only has the highest number of publications and co-cited frequency, but also has the highest intermediate centre value and is closely connected with other authors. In addition to publishing clinical guidelines for Y90 microsphere brachytherapy and standardizing Yttrium-90 microsphere hepatic brachytherapy, Kennedy, A, Nag, S, and Salem, R [15] suggested a total of 14 class 2A consensus items in their 2007 study. It has been acknowledged and supported by experts of the International Nuclear Regulatory Commission, has significantly aided in the standardization and improvement of yttrium-90 microsphere hepatic brachytherapy, and is now the accepted worldwide mainstream consensus report on the use of yttrium-90 microsphere brachyembolization for the treatment of malignant liver tumors. Sangro B of the Clinical Research Center of the University of Navarra in Spain also demonstrated strong academic influence and strong cohesion in the field of brachyembolization of liver malignancy using yttrium-90 microspheres; it ranked fourth in the number of publications and ninth overall in the number of citations. Though its intermediate centricity was 0.23. He led the development of BCLC Prognostic Strategies and Treatment Recommendations, which focused on the key insights and expertise needed to make clinical decisions for individual patients while considering all the parameters that must be considered to provide personalized clinical management (2). "Treatment of Hepatocellular Carcinoma: An Update" provides latest information on hepatocellular cancer monitoring and diagnostic [16]. These articles all stress the significance of giving patients top-notch care, treating them at the most appropriate stage of their illness, and offering crucial advice regarding the use of yttrium-90 microspheres for brachyembolization as a hepatic malignancy treatment option.

4.2. Changes in keywords and hot trends in the use of Yttrium 90 in the treatment of liver malignant tumours

Unresectable liver cancers have received the greatest attention from researchers during the past ten years, based on the keywords with the highest intensity of emergence. Treatment should be tailored to the individual patient's condition, though, as primary and secondary liver cancers differ in their characteristics. Randomized trials have shown that patients with primary liver cancer who received ^{90}Y-SIRT had superior overall status, tolerance, tumor

response, and quality of life compared to those who received sorafenib [17]. Additionally, the cumulative incidence of first liver progression was significantly lower in the ^{90}Y-SIRT group than in the sorafenib group. This implies that in patients with primary liver cancer, ^{90}Y-SIRT may have a positive localized therapeutic effect. Relevant research and general agreement indicate that surgery is not usually the first line of treatment for patients with synchronous liver metastases of colorectal cancer, and that selective internal radiotherapy (SIRT) is still an option for "local treatment" in most cases [18–20].

Furthermore, alterations in hotspots within the field may also be reflected in variations in keywords. The term social network map indicates that high-quality prospective clinical studies have received a lot of attention lately [21–24]. The multi-center clinical trial of yttrium-90 radiation combined with chemotherapy and immunotherapy is the focus of current research in this sector, according to the combination of the term emergence intensity and this search query. High-quality, multi-center clinical studies of ^{90}Y-SIRT in conjunction with medication therapy and combined surgical resection after descending stage, according to the authors, may become the trend in this field going forward and continue to offer high-quality, empirically supported medical evidence for the all-encompassing treatment of malignant liver tumors.

Based on phase III systemic therapy and dose, the majority of the top 10 referenced papers are randomized controlled clinical studies. This is essentially in line with the previously identified research hotspots. The clinical results of patients treated with intra-arterial yttrium 90 microspheres for liver cancers were assessed in the first and second most cited prospective cohort clinical studies. The No 1 prospective single-center trial revealed that overall survival varied by stage, with patients with Child-Pugh A benefiting the most from ^{90}Y-SIRT for liver cancers, involving 291 individuals [25]. The second-ranked study also compared the efficacy of ^{90}Y-SIRT with oral sorafenib [17], and this randomized controlled prospective study showed that ^{90}Y-SIRT was significantly better tolerated than sorafenib and had significantly better local efficacy. The Expert Consensus report on yttrium 90 brachyembolization for the treatment of liver malignancy [15] was the third most frequently cited article. The panel suggested that in order to ensure safety and success, a treatment registry should be established with consistent reporting standards and that yttrium 90 microspheres should be managed by a multidisciplinary team. It is advised to conduct clinical trials to learn more about the effects and safety of Y90 microspheres.

Furthermore, pertinent clinical trials that have been published recently have demonstrated the safety and effectiveness of SIRT in the treatment of primary and secondary liver cancers with descending transformation, successfully obtaining a high rate of disease control [5,7,26–29].

4.3. The research status of Yttrium-90 in the treatment of liver malignant tumours in China

China has conducted clinical studies in the directions of SIRT combined with nabuliumab, SIRT combined with sorafenib, and anatomical hepatectomy after SIRT downphase, based on previous papers that highlight the significance of multidisciplinary teams in the treatment of yttrium-90 in the treatment of liver malignancies [4,30,31]. Furthermore, studies show that over 70% of liver cancer cases and deaths worldwide occur in Asia [32], that patients with liver cancer typically present later in life [33], and that clinical management practices and staging management systems differ in Asian and Western nations [34]. This implies that taking the lead in the future academic growth of the SIRT field in Asia is a potential prospect. Yet, the total number of published papers in China remains low, and no Chinese research institutions or researchers are listed among the top 10 research institutions or authors. This suggests that fewer teams and institutions in China are using yttrium 90 to treat liver malignant tumors, and

that there are also insufficient representative research teams and scientific research accomplishments in the global arena. Furthermore, although China's research institutes and researchers (in Beijing, Taiwan, and Hong Kong) exhibit clear regional distinctions, they have not yet developed a close academic network with the rest of the world.

4.4. Limitations of the study

Only the Web of Science core collection database was retrieved; other databases were not included in the statistics. Non-English literature was not included in the statistical analysis. The update of the cited frequency of included references may lead to fluctuations in the analysis results.

Throughout the conclusion, Yttrium 90 treatment for primary and secondary liver cancers is expanding throughout Asia and the rest of the world. This includes research on theory, technique, dosimetry, managing pulmonary shunts, and adverse events. The emphasis of research has steadily turned in recent years to high-quality, multi-center clinical trials with the combination of SIRT-targeted systemic therapy and hepatectomy after the descending stage. Furthermore, it is probably going to stay a significant study trend in this area.

5. Conclusion

This bibliometric study maps the evolving research landscape of ^{90}Y-SIRT for liver malignancies. The United States and Spain lead in output and influence, with keyword trends revealing a shift toward multicenter trials combining ^{90}Y-SIRT with systemic and surgical strategies. While Asia shows growing interest, its global impact remains limited. Future research will likely focus on integrated, multidisciplinary approaches to optimize liver cancer therapy.

Disclosure statement

The authors declare no conflict of interest.

References

[1] Cao W, Chen H, Yu Y, et al., 2021, Changing Profiles of Cancer Burden Worldwide and in China: A Secondary Analysis of the Global Cancer Statistics 2020. Chinese Medical Journal, 134(7): 783–791.

[2] Reig M, Forner A, Rimola J, et al., 2022, BCLC Strategy for Prognosis Prediction and Treatment Recommendation: The 2022 Update. Journal of Hepatology, 76(3): 681–693.

[3] Zhou J, Sun H, Wang Z, et al., 2020, Guidelines for the Diagnosis and Treatment of Hepatocellular Carcinoma (2019 Edition). Liver Cancer, 9(6): 682–720.

[4] Feng X, Zhang L, Niu H, et al., 2023, Selective Internal Radiation Therapy with Yttrium-90 Resin Microspheres Followed by Anatomical Hepatectomy: A Potential Curative Strategy in Advanced Hepatocellular Carcinoma. Asia-Pacific Journal of Clinical Oncology, 20(2): 319–322.

[5] Tzedakis S, Sebai A, Jeddou H, et al., 2023, Resection Postradioembolization in Patients with Single Large Hepatocellular Carcinoma. Annals of Surgery, 278(5): 756–762.

[6] Mosconi C, Cacioppa L, Cappelli A, et al., 2023, Update of the Bologna Experience in Radioembolization of Intrahepatic Cholangiocarcinoma. Technology in Cancer Research & Treatment, 22: 15330338231155690.

[7] Chiu A, Savoor R, Gordon A, et al., 2023, Yttrium-90 Radiation Segmentectomy in Oligometastatic Secondary Hepatic Malignancies. Journal of Vascular and Interventional Radiology, 34(3): 362–368.

[8] Emmons E, Bishay S, Du L, et al., 2022, Survival and Toxicities after Yttrium-90 Transarterial Radioembolization of Metastatic Colorectal Cancer in the Resin Registry. Radiology, 305(1): 228–236.

[9] Edeline J, Touchefeu Y, Guiu B, et al., 2020, Radioembolization Plus Chemotherapy for First-Line Treatment of Locally Advanced Intrahepatic Cholangiocarcinoma: A Phase 2 Clinical Trial. JAMA Oncology, 6(1): 51–59.

[10] Levillain H, Bagni O, Deroose C, et al., 2021, International Recommendations for Personalised Selective Internal Radiation Therapy of Primary and Metastatic Liver Diseases with Yttrium-90 Resin Microspheres. European Journal of Nuclear Medicine and Molecular Imaging, 48(5): 1570–1584.

[11] Sung H, Ferlay J, Siegel R, et al., 2021, Global Cancer Statistics 2020: GLOBOCAN Estimates of Incidence and Mortality Worldwide for 36 Cancers in 185 Countries. CA: A Cancer Journal for Clinicians, 71(3): 209–249.

[12] Cervantes A, Adam R, Roselló S, et al., 2023, Metastatic Colorectal Cancer: ESMO Clinical Practice Guideline for Diagnosis, Treatment and Follow-Up. Annals of Oncology, 34(1): 10–32.

[13] Ilic M, Ilic I, 2024, Cancer of Colon, Rectum and Anus: The Rising Burden of Disease Worldwide from 1990 to 2019. Journal of Public Health, 46(1): 20–29.

[14] Salem R, Gordon A, Mouli S, et al., 2016, Y90 Radioembolization Significantly Prolongs Time to Progression Compared with Chemoembolization in Patients with Hepatocellular Carcinoma. Gastroenterology, 151(6): 1155–1163.

[15] Kennedy A, Nag S, Salem R, et al., 2007, Recommendations for Radioembolization of Hepatic Malignancies Using Yttrium-90 Microsphere Brachytherapy: A Consensus Panel Report from the Radioembolization Brachytherapy Oncology Consortium. International Journal of Radiation Oncology Biology Physics, 68(1): 13–23.

[16] Bruix J, Sherman M, 2011, Management of Hepatocellular Carcinoma: An Update. Hepatology, 53(3): 1020–1022.

[17] Vilgrain V, Pereira H, Assenat E, et al., 2017, Efficacy and Safety of Selective Internal Radiotherapy with Yttrium-90 Resin Microspheres Compared with Sorafenib in Locally Advanced and Inoperable Hepatocellular Carcinoma (Sarah): An Open-Label Randomised Controlled Phase 3 Trial. Lancet Oncology, 18(12): 1624–1636.

[18] Siriwardena A, Serrablo A, Fretland Å, et al., 2023, The Multi-Societal European Consensus on the Terminology, Diagnosis and Management of Patients with Synchronous Colorectal Cancer and Liver Metastases: An E-AHPBA Consensus in Partnership with ESSO, ESCP, ESGAR, and CIRSE. HPB, 25(9): 985–999.

[19] Weiner A, Gui B, Newman N, et al., 2018, Predictors of Survival after Yttrium-90 Radioembolization for Colorectal Cancer Liver Metastases. Journal of Vascular and Interventional Radiology, 29(8): 1094–1100.

[20] Sharma N, Kappadath S, Chuong M, et al., 2022, The American Brachytherapy Society Consensus Statement for Permanent Implant Brachytherapy Using Yttrium-90 Microsphere Radioembolization for Liver Tumors. Brachytherapy, 21(5): 569–591.

[21] Kolligs F, Arnold D, Golfieri R, et al., 2022, Factors Impacting Survival after Transarterial Radioembolization in Patients with Hepatocellular Carcinoma: Results from the Prospective CIRT Study. JHEP Reports, 5(2): 100633.

[22] Fidelman N, Atreya C, Griffith M, et al., 2022, Phase I Prospective Trial of TAS-102 (Trifluridine and Tipiracil) and Radioembolization with 90Y Resin Microspheres for Chemo-Refractory Colorectal Liver Metastases. BMC Cancer, 22(1): 1307.

[23] Liu C, Tadros G, Smith Q, et al., 2022, Selective Internal Radiation Therapy of Metastatic Breast Cancer to the Liver: A Meta-Analysis. Frontiers in Oncology, 12: 887653.

[24] Dhondt E, Lambert B, Hermie L, et al., 2022, 90Y Radioembolization Versus Drug-Eluting Bead Chemoembolization for Unresectable Hepatocellular Carcinoma: Results from the TRACE Phase II Randomized Controlled Trial. Radiology,

303(3): 699–710.

[25] Salem R, Lewandowski R, Mulcahy M, et al., 2010, Radioembolization for Hepatocellular Carcinoma Using Yttrium-90 Microspheres: A Comprehensive Report of Long-Term Outcomes. Gastroenterology, 138(1): 52–64.

[26] Gangi A, Shah J, Hatfield N, et al., 2018, Intrahepatic Cholangiocarcinoma Treated with Transarterial Yttrium-90 Glass Microsphere Radioembolization: Results of a Single Institution Retrospective Study. Journal of Vascular and Interventional Radiology, 29(8): 1101–1108.

[27] Binzaqr S, Debordeaux F, Blanc J, et al., 2023, Efficacy of Selective Internal Radiation Therapy for Hepatocellular Carcinoma Post-Incomplete Response to Chemoembolization. Pharmaceuticals (Basel, Switzerland), 16(12): 1676.

[28] Lee H, Alder L, Nguyen M, et al., 2023, Long-Term Outcome Analysis of Y90 Radioembolization in Hepatocellular Carcinoma. Journal of Gastrointestinal Oncology, 14(3): 1378–1391.

[29] Baker T, Tabrizian P, Zendejas I, et al., 2022, Conversion to Resection Post Radioembolization in Patients with HCC: Recommendations from a Multidisciplinary Working Group. HPB, 24(7): 1007–1018.

[30] Zeng H, Zhou C, Chen X, et al., 2023, Comparison of the Efficacy and Safety of Selective Internal Radiotherapy and Sorafenib Alone or Combined for Hepatocellular Carcinoma: A Systematic Review and Bayesian Network Meta-Analysis. Clinical and Experimental Medicine, 23(6): 2141–2150.

[31] Kaya N, Tai D, Lim X, et al., 2023, Multimodal Molecular Landscape of Response to Y90-Resin Microsphere Radioembolization Followed by Nivolumab for Advanced Hepatocellular Carcinoma. Journal for Immunotherapy of Cancer, 11(8): e007106.

[32] Li C, He W, 2022, Comparison of Primary Liver Cancer Mortality Estimates from World Health Organization, Global Burden Disease and Global Cancer Observatory. Liver International, 42(10): 2299–2316.

[33] Yang T, Tabrizian P, Zhang H, et al., 2017, Comparison of Patterns and Outcomes of Liver Resection for Hepatocellular Carcinoma: East Vs West. Clinical Gastroenterology and Hepatology, 15(12): 1972–1974.

[34] Choo S, Tan W, Goh B, et al., 2016, Comparison of Hepatocellular Carcinoma in Eastern Versus Western Populations. Cancer, 122(22): 3430–3446.

Publisher's note

Bio-Byword Scientific Publishing remains neutral with regard to jurisdictional claims in published maps and institutional affiliations.

Proceedings of Anticancer Research, 2026, Volume 10, Issue 1
http://ojs.bbwpublisher.com/index.php/PAR
ISSN Online: 2208-3553
ISSN Print: 2208-3545

Single-cell Sequencing: Application in the Study of Disseminated Tumour Cells and Breast Cancer Treatment

Mingyue Wang*

School of Nursing, Hubei University of Chinese Medicine, Wuhan 420111, Hubei, China

**Author to whom correspondence should be addressed.*

Copyright: © 2026 Author(s). This is an open-access article distributed under the terms of the Creative Commons Attribution License (CC BY 4.0), permitting distribution and reproduction in any medium, provided the original work is cited.

Abstract: Breast cancer is a malignant tumor originating from breast epithelial tissue. In essence, breast epithelial cells undergo gene mutation under the influence of carcinogenic factors, leading to abnormal cell proliferation and loss of organism regulation, ultimately leading to the formation of tumors with invasive and metastatic capabilities. Carcinogenic factors of breast cancer involve multiple cellular and molecular mechanisms. Among them, disseminated tumor cells (DTCs) are considered important for treating breast cancer. However, traditional bulk sequencing techniques have limitations, such as the inability to distinguish individual cell differences and dilution of information from key cell subpopulations (such as cancer stem cells and rare immune cells). Single-cell sequencing (scRNA-seq) overcomes the heterogeneity of tumors that traditional sequencing cannot capture by analysing the molecular characteristics of single cells, providing a high-resolution perspective for precise typing of breast cancer, exploration of the mechanism of the microenvironment, and personalized treatment. Through this technology, researchers can identify specific gene expression profiles of different cell subpopulations, thus providing a new basis for the molecular typing and personalized treatment of breast cancer. This article explains how single-cell sequencing is used to describe the origin of disseminated tumor cells (DTCs), analyse tumor heterogeneity, metastasis, etc., and review the current literature on the use of scRNA-seq in breast cancer treatment. In the future, cell separation and processing steps in single-cell sequencing will be further improved to ensure the accuracy of the results and broader application in clinical diagnosis and treatment.

Keywords: Disseminated tumor cells; Tumor heterogeneity analysis; Single-cell sequencing; Metastasis; scRNA-seq method

Online publication: February 6, 2026

1. Introduction

Disseminated tumor cells (DTCs) are malignant cells separated from primary tumors that spread to other parts of

the body. DTCs are the key "seeds" of breast cancer metastasis. After entering tumor cells, DTCs transfer tumor cells to the bone marrow or viscera. They first invade lymphatic vessels, causing local symptoms such as an orange peel-like skin appearance, nipple redness and swelling, or dimpling (invasion of Cooper's ligament). They subsequently spread through the lymphatic system to regional lymph nodes such as axillary, infraclavicular, and supraclavicular areas, where they form enlarged or fused lymph node masses. After entering the blood, they can spread to distant organs such as bones, liver, lungs, and brain through the circulatory system. For example, bone metastasis causes bone pain, liver metastasis causes right upper abdominal pain or distension, and brain metastasis may cause epileptic seizures or changes in consciousness. Studies have confirmed that the presence of disseminated tumor cells (DTCs) in the bone marrow is a strong independent prognostic factor for poor survival in breast cancer patients [1]. Isolating and identifying rare disseminated tumor cells (DTCs) from the circulation or premetastatic niches, such as the blood, bone marrow, and body fluids, is the premise for studying tumor metastasis mechanisms. In the study of this disease, disseminated tumor cells have become a breakthrough point for breast cancer research.

2. Technological evolution and advantages

While traditional bulk sequencing provides an average expression profile of an entire tissue sample, it often masks the signals from rare but critical cell populations, such as drug-resistant clones or dormant DTCs. In contrast, the rapid evolution of single-cell RNA sequencing (scRNA-seq) technologies, moving from plate-based methods (like Smart-seq2) to droplet-based microfluidics (like 10x Genomics), has revolutionized our ability to dissect tumor heterogeneity. This high-throughput capability allows researchers to profile thousands of cells simultaneously, creating a comprehensive "cellular atlas" of the tumor ecosystem. By analyzing the transcriptome of individual cells, we can now trace the evolutionary trajectory of cancer cells, identify the ligand-receptor interactions between tumor cells and the stromal microenvironment, and uncover the specific gene regulatory networks that drive metastasis. This level of resolution is indispensable for understanding why some breast cancer patients relapse years after apparently successful treatment, as it likely involves a small subpopulation of cells that were invisible to conventional bulk analysis methods.

3. Using single-cell sequencing to study the origin of DTCs in breast cancer

3.1. Research on the origin of DTCs

Research utilizing single-cell sequencing has challenged the traditional metastasis model. Hosseini et al. [2] demonstrated that breast cancer cells can disseminate to distant organs such as the bone marrow very early in tumor development, often before the primary tumor is clinically detectable. Their single-cell analysis revealed that these early DTCs possess a distinct molecular signature compared to late-stage metastatic cells. This finding suggests that metastasis is not necessarily a late event in tumor evolution, providing a new theoretical basis for early intervention.

4. Background on DTCs promoting metastasis in tumours

Metastasis is the leading cause of death in patients with breast cancer (BC). Therefore, studying metastasis is crucial for identifying a cure for breast cancer. Disseminated tumor cells (DTCs) detach from the primary site and en-

ter the bloodstream to become circulating tumor cells (CTCs), which are the precursors of metastasis. Single-cell sequencing of bone marrow-derived epithelial-like cells, conducted concurrently with analysis of intratumoral genetic heterogeneity from bulk DNA, is an effective method for identifying and studying DTCs, providing insights into the metastatic process.

4.1. Single-cell analysis of circulating tumor cells

Lawson et al. conducted comprehensive single-cell analysis of circulating tumor cells (CTCs) [3]. They identified significant heterogeneity within CTC populations, finding that cells expressing stem-cell-like markers and those undergoing epithelial-to-mesenchymal transition (EMT) are key drivers of metastasis. This highlights the power of scRNA-seq in identifying rare, metastasis-competent subpopulations that traditional bulk sequencing might miss.

4.2. Dynamic Epithelial-Mesenchymal Transition (EMT) phenotypes

The process of metastasis is often driven by Epithelial-Mesenchymal Transition (EMT), but single-cell analysis has revealed that this is not a binary switch but a dynamic spectrum. Yu et al. utilized RNA sequencing on circulating tumor cells isolated from breast cancer patients and identified a dual expression of epithelial and mesenchymal markers within the same cells [4]. This "hybrid" E/M phenotype allows tumor cells to retain the cell-cell adhesion properties necessary for survival in clusters while simultaneously acquiring the migratory and invasive capabilities of mesenchymal cells. Their study showed that the proportion of these hybrid cells fluctuates during treatment and correlates with disease progression. This finding challenges the classical view that cells must undergo a complete mesenchymal transition to metastasize, suggesting instead that cellular plasticity and the ability to cycle between states are the true drivers of metastatic spread.

4.3. The role of CTC clusters in metastasis

Beyond single circulating tumor cells, recent single-cell studies have highlighted the critical role of CTC clusters—groups of tumor cells traveling together in the bloodstream. Aceto et al. demonstrated that although CTC clusters are rarer than single CTCs in the blood of breast cancer patients, they possess a 23- to 50-fold increased metastatic potential [5]. Single-cell sequencing of these clusters revealed that the cell-cell junctions within the cluster (mediated by proteins like plakoglobin) protect the tumor cells from anoikis (cell death induced by detachment) and immune attack in the circulation. Furthermore, the analysis showed that cells within these clusters exhibit a distinct hypomethylation pattern compared to single CTCs, particularly in binding sites for stemness-associated transcription factors. This suggests that the clustering of cells is not merely a physical aggregation but a biological state that promotes stemness and survival, making these clusters the primary drivers of polyclonal metastasis. Understanding the molecular biology of these clusters via single-cell resolution offers new avenues for therapy, such as targeting cell adhesion molecules to dissociate clusters into less metastatic single cells.

5. Single-cell sequencing was used for heterogeneity analysis of disseminated tumor cells (DTCs)

5.1. Reasons for using single-cell sequencing for tumor heterogeneity analysis

Single-cell sequencing of cells isolated from bone marrow aspirates of localized breast cancer patients, in combination with intratumoral genetic heterogeneity analysis of bulk tumor DNA, is a powerful method for identifying

true DTCs and their biology and for subsequent studies on tumor progression. Specifically, tumor heterogeneity means that within a single tumor, not all tumor cells and tumor tissues possess a single set of tumor characteristics but rather have their own relatively specific and different features and clinical manifestations. This characteristic is unique to tumors and leads to differences in treatment and prognosis. In simple terms, tumor heterogeneity refers to intratumoral heterogeneity within a cancer. scRNA-seq can assess this at single-cell resolution, thereby effectively alleviating some issues that traditional chemotherapy cannot address. scRNA-seq provides complete gene expression patterns for individual cells that are masked in bulk analysis.

5.2. Unravelling subclonal heterogeneity in TNBC

Single-cell RNA sequencing has been particularly instrumental in understanding triple-negative breast cancer (TNBC). Karaayvaz et al. analyzed TNBC tumors at single-cell resolution and revealed distinct subclonal populations [6]. They identified specific metabolic pathways and gene signatures that drive therapy resistance, which are often masked in bulk sequencing data. These findings suggest that molecular profiling at the single-cell level is more detailed and accurate, potentially guiding clinicians to select more effective treatment options for distinct tumor subclones.

5.3. Characterizing the immune microenvironment in TNBC

Tumor heterogeneity is not limited to cancer cells; the immune microenvironment surrounding the tumor also displays significant diversity that influences prognosis. Savas et al. utilized single-cell RNA sequencing to profile T cells isolated from human breast cancer tissues [7]. They identified a specific subset of CD8+ T cells known as tissue-resident memory T cells (TRM), which are characterized by the expression of immune checkpoint molecules and cytotoxic markers. The abundance of these TRM cells was found to be significantly associated with better patient survival and improved response to immunotherapy in triple-negative breast cancer. Unlike bulk sequencing, which might only show an increase in general T-cell markers, single-cell analysis allowed for the precise distinction between exhausted T cells, effector T cells, and these crucial TRM cells. This distinction is vital for developing personalized immunotherapies, as it suggests that strategies aimed at expanding or reactivating this specific T-cell subset could be more effective than broad immune stimulation.

6. Discussion on other therapeutic aspects of breast cancer via single-cell sequencing

Single-cell sequencing has also recently been used to characterize changes in tumors after treatment. This technology is also used to determine how these changes are related to drug resistance, the suppression of tolerant cell populations, and combination strategies. A single-cell study in breast cancer tissue indicated the existence of preexisting genotypes resistant to chemotherapy. These genotypes have the capacity for further adaptation after exposure to chemotherapy. This contrasts with transcriptional profiles that can adapt to chemotherapy. scRNA-seq studies promise to provide information on each cell type in the tumor whose alterations might be associated with patient demographics, diagnosis, treatment, and prognostic factors. In the near future, scRNA-seq might be used clinically to develop personalized medical regimens for treating each patient. Tumours can be analysed on the basis of their cellular composition and expression of specific targetable proteins, which could ultimately lead to an optimal response for each patient.

6.1. Evolution of chemoresistance in TNBC

A critical application of scRNA-seq is dissecting the evolutionary history of chemoresistance. Kim et al. performed single-cell DNA and RNA sequencing on triple-negative breast cancer (TNBC) patients receiving neoadjuvant chemotherapy [8]. Their analysis conclusively resolved a long-standing debate regarding the origin of resistance: did the drugs induce new mutations (acquired resistance), or did they select for pre-existing rare clones (adaptive selection)? The data showed that in the majority of patients, resistant genotypes were already present at low frequencies in the primary tumor before any treatment was administered. Chemotherapy acted as a selection pressure that eliminated sensitive clones, allowing the pre-existing resistant subpopulation to expand and become dominant. This implies that early detection of these rare, pre-existing resistant clones via deep single-cell sequencing could guide the use of combination therapies upfront, rather than waiting for treatment failure to occur.

Single-cell sequencing has also generated large-scale single-cell atlases of the breast cancer ecosystem to identify new precision medicine approaches. Another study used scRNA-seq data to identify unique breast epithelial clusters from healthy breast tissue. Interestingly, certain genes were coexpressed with the estrogen receptor (ER) in bulk breast cancer tissue samples, suggesting clinically relevant subclasses within ER-positive breast cancer. Furthermore, understanding the mechanism of tumor dormancy is crucial. Albrengues et al. discovered that inflammation-induced neutrophil extracellular traps (NETs) can awaken dormant cancer cells, triggering metastasis [9]. Additionally, Wagner et al. generated a large-scale single-cell atlas of the breast cancer ecosystem, identifying unique epithelial clusters and immune cell phenotypes associated with different clinical outcomes [10].

7. Conclusion

This article discusses single-cell sequencing in breast cancer with respect to the origin of DTCs, heterogeneity, metastasis, etc. I believe that the development of single-cell sequencing technology has advanced breast cancer research, enabling us to seek answers to many previously unknown questions. However, the field of single-cell data science still faces challenges, including cost, throughput, and data interpretation. Clinical translation is still limited by difficulties in sample acquisition, data standardization, and the threshold for bioinformatics analysis.

7.1. From single cells to spatial transcriptomics

While scRNA-seq provides a catalog of cell types, it requires tissue dissociation, which leads to the loss of spatial information—knowing “where” a cell is located is often as important as knowing “what” it is. To address this, the field is moving towards spatial transcriptomics. Ståhl et al. [11] introduced a method to visualize and analyze gene expression in tissue sections without disrupting the tissue architecture. In the context of breast cancer, this technology allows researchers to map the precise location of immune cells relative to the tumor core and the invasive margin. Understanding this spatial organization is crucial because the same immune cell type may have a tumor-suppressive function when infiltrating the tumor but a pro-tumorigenic function when located in the stroma. Integrating single-cell resolution with spatial coordinates will be the next frontier in constructing a truly holistic 3D model of the breast cancer ecosystem. Furthermore, better methods are needed to allow for the integration of single-cell data across experiments and measurement types. Given the difficulty of sample acquisition, I suggest integrating this technology with regional healthcare systems to reduce collection challenges. In summary, an analysis of the origin, metastasis, and heterogeneity of DTCs will likely contribute to the discovery of new treatment strategies and cell research in the near future, thereby strengthening the implementation of precision medicine and

enhancing therapeutic outcomes.

Disclosure statement

The author declares no conflict of interest.

References

[1] Braun S, Vogl F, Naume B, et al., 2005, A Pooled Analysis of Bone Marrow Micrometastasis in Breast Cancer. New England Journal of Medicine, 353(8): 793–802.

[2] Hosseini H, Obradović M, Hoffmann M, et al., 2016, Early Dissemination Seeds Metastasis in Breast Cancer. Nature, 540(7634): 552–558.

[3] Lawson D, Bhakta N, Kessenbrock K, et al., 2015, Single-Cell Analysis of Circulating Tumor Cells Identifies a Role for IGF2 in Metastasis. Nature, 526(7571): 131–135.

[4] Yu M, Bardia A, Wittner B, et al., 2013, Circulating Breast Tumor Cells Exhibit Dynamic Changes in Epithelial and Mesenchymal Composition. Science, 339(6119): 580–584.

[5] Aceto N, Bardia A, Miyamoto D, et al., 2014, Circulating Tumor Cell Clusters Are Oligoclonal Precursors of Breast Cancer Metastasis. Cell, 158(5): 1110–1122.

[6] Karaayvaz M, Cristea S, Gillespie S, et al., 2018, Unravelling Subclonal Heterogeneity and Aggressive Disease States in TNBC Through Single-Cell RNA-Seq. Nature Communications, 9(1): 3588.

[7] Savas P, Virassamy B, Ye C, et al., 2018, Single-Cell Profiling of Breast Cancer T Cells Reveals a Tissue-Resident Memory Subset Associated with Improved Prognosis. Nature Medicine, 24(7): 974–990.

[8] Kim C, Gao R, Sei E, et al., 2018, Chemoresistance Evolution in Triple-Negative Breast Cancer Delineated by Single-Cell Sequencing. Cell, 173(4): 879–893.

[9] Albrengues J, Shields M, Ng D, et al., 2018, Neutrophil Extracellular Traps Produced During Inflammation Awaken Dormant Cancer Cells in Mice. Science, 361(6409): eaao5031.

[10] Wagner J, Rapsomaniki M, Chevrier S, et al., 2019, A Single-Cell Atlas of Tumor and Immune Ecosystem of Human Breast Cancer. Cell, 177(5): 1330–1345.

[11] Ståhl P, Salmén F, Vickovic S, et al., 2016, Visualization and Analysis of Gene Expression in Tissue Sections by Spatial Transcriptomics. Science, 353(6294): 78–82.

Publisher's note

Bio-Byword Scientific Publishing remains neutral with regard to jurisdictional claims in published maps and institutional affiliations.

Proceedings of Anticancer Research, 2026, Volume 10, Issue 1
http://ojs.bbwpublisher.com/index.php/PAR
ISSN Online: 2208-3553
ISSN Print: 2208-3545

The Impact of Double-puncture Tympanic Membrane Puncture and Tympanic Cavity Drug Injection on the Complication Rate of Acute Secretory Otitis Media

Wei Zheng*

Department of Otolaryngology, The First College of Clinical Medical Science, China Three Gorges University (Yichang Central People's Hospital), Yichang 443003, Hubei, China

**Author to whom correspondence should be addressed.*

Copyright: © 2026 Author(s). This is an open-access article distributed under the terms of the Creative Commons Attribution License (CC BY 4.0), permitting distribution and reproduction in any medium, provided the original work is cited.

Abstract: *Objective*: To explore the therapeutic effect of double-puncture tympanic membrane puncture and tympanic cavity drug injection in patients with acute secretory otitis media. *Methods*: A total of 84 patients with acute secretory otitis media admitted to our hospital from June 2024 to June 2025 were selected and randomly divided into two groups by drawing lots. The control group (42 cases) was treated with the traditional single-puncture tympanic membrane puncture and tympanic cavity drug injection method, while the observation group (42 cases) was treated with the double-puncture tympanic membrane puncture and tympanic cavity drug injection method. The therapeutic effects of the two groups were compared. *Results:* The overall treatment response rate, overall complication rate, time to symptom relief, and improvement in hearing threshold in the observation group were all superior to those in the control group, with statistically significant differences ($P < 0.05$). *Conclusion:* For acute secretory otitis media, the treatment method of double-puncture tympanic membrane puncture and tympanic cavity drug injection demonstrates definite efficacy, significantly reducing the incidence of complications, accelerating symptom relief, and improving hearing function, making it worthy of promotion.

Keywords: Acute secretory otitis media; Double puncture; Tympanic membrane puncture and tympanic cavity drug injection; Complications

Online publication: February 6, 2026

1. Introduction

Acute secretory otitis media is a common acute inflammatory disease in otolaryngology, primarily caused by viral or bacterial infections, eustachian tube dysfunction, and other factors. Symptoms include fluid accumulation in the middle ear cavity, hearing loss, ear fullness, tinnitus, etc. If not effectively treated, it can lead to various

complications such as non-healing tympanic membrane perforation, cholesteatoma, chronic otitis media, and permanent hearing damage, seriously affecting the patient's quality of life. Currently, the focus of clinical treatment for acute secretory otitis media is to remove middle ear fluid, control inflammatory responses, and restore eustachian tube function [1]. Tympanic membrane puncture and injection are widely used due to their simple operation, minimal trauma, and direct drug delivery to the affected area. However, the single-puncture tympanic membrane injection method currently employed in clinical practice has issues such as easy blockage of the puncture, uneven drug distribution, and incomplete removal of fluid, which not only affect efficacy but also increase the incidence of complications. In recent years, the binaural myringotomy with tympanic injection method has begun to garner attention. By creating two perforations in the tympanic cavity, it establishes a flowing pathway within the cavity, effectively clearing inner ear fluid while enabling higher drug concentrations in the body, thereby achieving better therapeutic outcomes and reducing the incidence of complications. This approach can effectively enhance treatment efficacy. Therefore, this study will focus on analyzing the therapeutic effects of the binaural myringotomy with tympanic injection method for acute secretory otitis media, as detailed below.

2. General information and methods

2.1. General information

Eighty-four patients with acute secretory otitis media were selected from our hospital between June 2024 and June 2025. They were randomly assigned to two groups via drawing lots: a control group and an observation group, each consisting of 42 patients. In the control group, the maximum age was 70 years and the minimum was 22 years, with an average age of (45.11 ± 6.02) years and a male-to-female ratio of 22:20. In the observation group, the maximum age was 71 years and the minimum was 23 years, with an average age of (45.19 ± 6.11) years and a male-to-female ratio of 23:19. Comparisons between the two groups revealed no statistically significant differences in their data ($P > 0.05$). This study complies with national laws and regulations and adheres to medical ethical principles.

Inclusion criteria: (1) Completion of clinical diagnosis; (2) Age ≥ 18 years old; (3) Informed consent obtained from both patients and their families, with signed informed consent forms.

Exclusion criteria: (1) Patients with underlying ear conditions such as tympanic membrane perforation, chronic otitis media, or cholesteatoma; (2) Patients with severe dysfunction of vital organs such as the heart, liver, or kidneys; (3) Patients with drug allergies; (4) Women who are pregnant or breastfeeding; (5) Patients with mental illnesses.

2.2. Methods

Before treatment, both groups of patients underwent comprehensive examinations, including otoscopy and pure-tone audiometry to clarify their conditions. They were given conventional basic treatments, including anti-infection therapy, oral mucus-promoting agents, nasal irrigation, and decongestant nasal drops to alleviate symptoms and improve eustachian tube ventilation.

2.2.1. Control group

Patients in the control group were treated using the traditional single-port tympanic membrane puncture and intratympanic injection method. The patients were seated, and the ear was routinely disinfected. The tympanic

membrane was anesthetized with 2% lidocaine. Under the guidance of an otoscope, a No. 7 tympanic membrane puncture needle was used to puncture the lower half of the tympanic cavity, approximately 2 mm from the tympanic annulus. Middle ear effusion was slowly aspirated, and a mixture of 5 mg of dexamethasone sodium phosphate injection (Hubei Jinyao Pharmaceutical Co., Ltd., National Medicine Approval No. H42020019) and 0.5 g of cefuroxime sodium for injection (Shenzhen Lijian Pharmaceutical Co., Ltd., National Medicine Approval No. H20064532) was diluted to 2 mL with 0.9% sodium chloride injection and slowly injected. After the injection, the tube was removed, the ear canal was plugged with a sterile cotton ball, and the patient was instructed to maintain an upward position of the affected ear for 30 minutes. This treatment was administered once a week for a total of two treatments.

2.2.2. Observation group

The treatment method of bilateral myringotomy with intratympanic drug injection was adopted, with the same basic treatment as the control group. Patients were seated, and routine otological disinfection was performed. The tympanic membrane was anesthetized topically with 2% lidocaine. Under the guidance of an otoscope, a No. 7 myringotomy needle was used to puncture the anterior-inferior and posterior-inferior quadrants of the tympanic membrane, respectively, creating two perforations, one approximately 1 mm and the other approximately 3 mm in size. Fluid from the middle ear was slowly aspirated through one perforation, while the aforementioned mixed medication was slowly injected through the other. During the injection, it was important to observe whether the medication flowed out from the first perforation to ensure uniform distribution of the drug within the middle ear cavity. After the injection was completed, the puncture needle was removed, and the ear canal was plugged with a sterile cotton ball. Patients were instructed to maintain an upright position with the affected ear facing upwards for 30 minutes. The treatment was administered once a week for a total of two sessions.

2.3. Observation indicators

(1) Therapeutic efficacy was evaluated after 2 weeks of treatment. Complete recovery was defined as the elimination of clinical manifestations such as tinnitus and hearing loss, no fluid accumulation observed upon otoscopic re-examination, and normalization of auditory thresholds. Significant improvement was characterized by marked alleviation of clinical symptoms, a small amount of fluid observed under the otoscope, and an increase in auditory thresholds of more than 15 decibels. Effective treatment was indicated by noticeable improvement in clinical symptoms, moderate fluid accumulation remaining in the middle ear cavity, and an increase in auditory thresholds of 5-14 decibels. Treatment was considered ineffective if the aforementioned goals were not achieved. The overall effective rate was calculated as the sum of the complete recovery rate, significant improvement rate, and effective rate.

(2) The occurrence of complications in the two groups of patients was recorded, including non-healing tympanic membrane perforation, cholesteatoma formation, aggravated hearing loss, and recurrent otitis media.

(3) The time to symptom relief in the two groups of patients was recorded, including symptoms of ear fullness, tinnitus, and hearing loss.

(4) Before treatment, 2 weeks after treatment, and at the 3-month follow-up, pure-tone audiometry was used to detect and compare the hearing thresholds of patients.

2.4. Statistical analysis

Data were processed using SPSS version 24.0 software. Measurement data were calculated using the "t" test, and count data were tested using the χ^2 test, expressed as mean ± standard deviation (SD) and (%) respectively. A *P*-value < 0.05 was considered statistically significant.

3. Results

3.1. Treatment efficacy rate

The overall treatment efficacy rate in the observation group was higher than that in the control group, with a statistically significant difference ($P < 0.05$), as shown in **Table 1**.

Table 1. Comparison of postoperative recovery between the two groups (n, %)

Group	n	Recovered	Markedly Effective	Effective	Ineffective	Total Effective Rate
Observation Group	42	25 (59.52)	12 (28.57)	3 (7.14)	2 (4.76)	40 (95.24)
Control Group	42	18 (42.86)	10 (23.81)	6 (14.29)	8 (19.05)	34 (80.95)
χ^2						4.086
P Value						0.043

3.2. Overall incidence of complications

The overall incidence of complications in the observation group was lower than that in the control group, with a statistically significant difference ($P < 0.05$), as shown in **Table 2**.

Table 2. Overall incidence of complications (n, %)

Group	n	Non-healing of Tympanic Membrane Perforation	Cholesteatoma	Hearing Loss Aggravation	Recurrent Otitis Media	Total Incidence Rate
Observation	42	1 (2.38)	0 (0.00)	0 (0.00)	1 (2.38)	2 (4.76)
Control	42	3 (7.14)	1 (2.38)	2 (4.76)	2 (4.76)	8 (19.05)
X^2						4.086
P						0.043

3.3. Time to symptom relief

The time to symptom relief in the observation group was shorter than that in the control group, with a statistically significant difference ($P < 0.05$), as shown in **Table 3**.

Table 3. Time to symptom relief (n, mean ± SD, d)

Group	n	Ear Fullness Relief Time (days)	Tinnitus Relief Time (days)	Hearing Loss Relief Time (days)
Observation	42	3.25 ± 1.02	4.12 ± 1.23	5.36 ± 1.45
Control	42	4.86 ± 1.35	5.78 ± 1.56	7.28 ± 1.67
t		6.167	5.145	5.626
P		0.000	0.000	0.000

3.4. Changes in hearing threshold

After treatment, the hearing thresholds at various time points in the observation group were lower than those in the control group, with a statistically significant difference ($P < 0.05$), as shown in **Table 4**.

Table 4. Changes in Hearing Threshold (n, mean ± SD, dBHL)

Group	n	Before Treatment	2 Weeks After Treatment	3-Month Follow-up
Observation	42	38.62 ± 5.34	27.15 ± 3.26	24.38 ± 2.85
Control	42	39.15 ± 5.12	32.46 ± 3.58	29.64 ± 3.12
t		0.464	7.107	8.067
P		0.644	0.000	0.000

4. Discussion

The ear is a crucial organ for hearing and balance, and its functional integrity is closely related to an individual's quality of life and social abilities. Acute secretory otitis media is a common inflammatory condition in otolaryngology that poses significant harm to patients, their families, and society. Exploring effective and safe treatment methods to thoroughly eliminate middle ear effusion, rapidly suppress inflammatory responses, and optimize their effects is an urgent challenge in otolaryngology both domestically and internationally [2]. Currently, intratympanic drug injection is widely used clinically due to its advantages of simple operation, minimal trauma, and direct drug delivery to the lesion site. However, the current single-hole tympanic membrane puncture method is prone to blockage of the puncture hole by secretions, failing to completely eliminate the effusion. Additionally, uneven drug distribution in the middle ear cavity affects treatment efficacy, and multiple punctures increase the risk of eardrum damage, thereby limiting the improvement of therapeutic outcomes. Against this backdrop, the binaural myringotomy with tympanic injection technique emerged, which achieves the synergistic effects of effusion removal and drug infusion by establishing a bidirectional pathway, thereby providing a new approach to optimizing the treatment outcomes for acute secretory otitis media.

The results of this study indicate that the overall treatment effectiveness in the observation group was higher than that in the control group, with a statistically significant difference ($P < 0.05$). The analysis suggests that conventional single-puncture needle insertion can only perform a single fluid aspiration or drug administration. After fluid extraction, the puncture site is prone to blockage by residual secretions, hindering subsequent drug delivery. Moreover, drugs are difficult to evenly distribute across all lesion sites, and inflammatory reactions at hidden spots may not be effectively suppressed. In contrast, binaural puncture involves creating two puncture sites in the upper and lower directions, which not only prevents blockage caused by single puncture but also ensures complete drug effusion. Additionally, it allows for the uniform distribution of drugs under pressure to areas such as the tympanic sinus and the pharyngeal opening of the Eustachian tube. By establishing dual channels, drug reflux is reduced, and drug retention in the middle ear cavity is enhanced, enabling full contact between the lesion site and the drug, thereby better suppressing inflammatory reactions, promoting the recovery of Eustachian tube function, and improving overall treatment efficacy. Furthermore, the puncture sites for the binaural puncture method are located around the middle ear, where blood supply is abundant and the tympanic membrane tissue is not damaged, providing a better environment for postoperative reconstruction of the middle ear mucosa and thus improving treatment outcomes [3].

The overall complication rate in the observation group was lower than that in the control group, with a statistically significant difference ($P < 0.05$). Analyzing the reasons, repeated punctures using the conventional single-port method can easily cause irreversible damage to the fibrous tissue of the eardrum, leading to difficulties in perforation. Bacteria proliferating in residual secretions can readily trigger chronic inflammation, continuously stimulating the eardrum and the mucosa of the middle ear, thereby increasing the likelihood of cholesteatoma development. If prolonged, it can also cause greater harm to the auditory ossicles and auditory nerves, resulting in hearing loss. The double-port puncture method features evenly distributed puncture points, effectively preventing concentrated damage at a single location and reducing harm to the fibrous layer of the eardrum, thus achieving better therapeutic outcomes. Moreover, the dual channels ensure complete evacuation, eliminating the possibility of bacterial proliferation, controlling inflammatory residues at the source, and reducing the chances of chronicity and recurrence. Additionally, during the double-port puncture process, medications can be evenly dispersed within the middle ear cavity, effectively suppressing inflammatory responses and reducing inflammatory damage to the middle ear mucosa and auditory ossicles, thereby decreasing the risk of hearing impairment. Furthermore, during double-port puncture, the presence or absence of medication discharge from other puncture ports can be precisely determined, effectively preventing tympanic cavity hypertension caused by excessive infusion, reducing excessive stimulation of the eardrum, and decreasing the risk of non-union of eardrum perforations, thereby significantly lowering the incidence of complications [4].

The symptom relief time in the observation group was shorter than that in the control group, with a statistically significant difference ($P < 0.05$). The reasons for this are as follows: Conventional single-port puncture often fails to completely remove the accumulated fluid in the body, making it difficult to rapidly restore it to its original level. Moreover, uneven drug distribution within the body can hinder the elimination of chronic inflammatory reactions, thereby prolonging the treatment duration for patients. In contrast, dual-port puncture can quickly and thoroughly eliminate the accumulated fluid. During the process of fluid extraction, it promptly relieves the pressure within the middle ear cavity, allowing for rapid alleviation of ear discomfort symptoms. Once the fluid is completely drained, the obstacles to auditory conduction are eliminated, temporarily alleviating the patient's hearing impairment. Simultaneously, through dual-port puncture, inflammatory mediators can be rapidly and effectively controlled, reducing congestion and edema of the middle ear mucosa, minimizing inflammatory stimulation to the auditory nerve, and improving tinnitus. In addition, double-lumen puncture can also promote the rapid recovery of eustachian tube function. When the ventilation function of the eustachian tube is restored, it can effectively balance the pressure between the middle ear cavity and the external environment, prevent the reaccumulation of effusion, improve the condition, and thus prevent recurrence.

After treatment, the average hearing threshold values at various time points in the observation group were lower than those in the control group, with statistically significant differences ($P < 0.05$). The analysis suggests that conventional single-lumen puncture fails to completely remove the fluid in the body, causing obstacles to sound transmission. The long-term impact of residual inflammatory reactions on the auditory ossicles and auditory nerves makes it difficult for patients to recover rapidly and may even lead to deterioration. However, binaural myringotomy completely eliminates middle ear effusion, promptly removing the obstacle of fluid to sound transmission and allowing sound to be correctly transmitted to the auditory ossicles, thereby achieving early auditory effects. On this basis, the binaural perforation technique enables the uniform dispersion of medication within the body, swiftly and effectively suppressing inflammatory responses, reducing the damage caused by inflammatory factors to the auditory ossicles, tympanic membrane, and auditory nerve, and preventing

the occurrence of auditory impairment. Additionally, the binaural approach causes less damage to the tympanic membrane, with the perforations closing rapidly, effectively preventing hearing damage caused by the perforations. The swift elimination of inflammatory responses accelerates the repair of the middle ear mucosa, thereby improving the acoustic environment of the middle ear and enhancing auditory effects. The results show that the binaural approach not only rapidly improves hearing but also completely eliminates inflammation, promotes tissue repair, and achieves a long-lasting and stable level of hearing. Meanwhile, due to the limitations of unilateral myringotomy, including its constraints and residual inflammatory responses, the control group experienced a slow repair rate of the middle ear mucosa and insufficient recovery of auditory ossicle function, resulting in poor improvement in hearing thresholds and inadequate long-term stability [5].

5. Conclusion

In summary, for acute secretory otitis media, the treatment method of binaural tympanic membrane puncture and intratympanic drug injection demonstrates definite efficacy, significantly reducing the incidence of complications, accelerating symptom relief, and improving hearing function, making it worthy of promotion.

Disclosure statement

The author declares no conflict of interest.

References

[1] Xue J, Wang Y, 2024, Analysis of the Therapeutic Effect and Complication Rate of Double-Hole Tympanic Membrane Puncture and Tympanic Cavity Drug Injection for Acute Secretory Otitis Media. Chinese Medical Digest (Otorhinolaryngology), 39(1): 73–76.

[2] Zhou Y, Wang Z, Yang Z, et al., 2023, Surgical Treatment Options and Efficacy Analysis for Patients with Acute Upper Respiratory Tract Infection Complicated by Secretory Otitis Media. Ningxia Medical Journal, 45(12): 1130–1133.

[3] Li L, Zhang M, Zhuang W, 2023, Retrospective Analysis of Tympanic Membrane Tube Insertion Combined with Eustachian Tube Balloon Dilation for the Treatment of Adult Refractory Secretory Otitis Media. Chinese Journal of Otorhinolaryngology Integrated Traditional Chinese and Western Medicine, 31(5): 334–337.

[4] Zhang D, Zheng X, You L, et al., 2023, Clinical Analysis and Efficacy of Ear Endoscopic Tympanic Membrane Incision and Drug Injection Combined with Adenoidectomy for the Treatment of Secretory Otitis Media. Northern Pharmacy, 20(8): 74–76.

[5] Liu H, Xu Z, 2023, Study on the Efficacy and Safety of Double-Hole Tympanic Membrane Puncture and Tympanic Cavity Drug Injection for Acute Secretory Otitis Media. Chinese Medical Digest (Otorhinolaryngology), 38(1): 77–79 + 86.

Publisher's note

Bio-Byword Scientific Publishing remains neutral with regard to jurisdictional claims in published maps and institutional affiliations.

Proceedings of Anticancer Research, 2026, Volume 10, Issue 1
http://ojs.bbwpublisher.com/index.php/PAR
ISSN Online: 2208-3553
ISSN Print: 2208-3545

Research Progress on Malnutrition and Nutritional Intervention in Children with Leukemia During Chemotherapy

Xiangyan Cao, Shuang Zhang, Jialin Ye*

The First Affiliated Hospital of Sun Yat-sen University, Guangzhou 510000, Guangdong, China

**Author to whom correspondence should be addressed.*

Copyright: © 2026 Author(s). This is an open-access article distributed under the terms of the Creative Commons Attribution License (CC BY 4.0), permitting distribution and reproduction in any medium, provided the original work is cited.

***A*bstract:** This study systematically analyzed the primary causes of malnutrition in children with leukemia during chemotherapy, clarified the status of malnutrition and specific nutritional intervention measures, and comprehensively evaluated the research progress. The research indicates a shift from basic supportive care toward precision intervention strategies. Immunonutrition approaches, such as omega-3 fatty acid supplementation and probiotics for gut microbiota modulation, significantly mitigate chemotherapy-related side effects and enhance nutritional status. These targeted novel regimens demonstrate clear clinical advantages. The success of nutritional management depends on a multidisciplinary collaboration mechanism. The organic integration of innovative nutritional protocols with standard treatments from hematology, pediatrics, and nutrition departments significantly optimizes treatment outcomes and long-term quality of life for children with leukemia. This interdisciplinary synergy is reshaping contemporary medical models.

Keywords: Childhood leukemia; Chemotherapy period; Malnutrition; Nutritional intervention

Online publication: February 4, 2026

1. Introduction

The average annual incidence of childhood leukemia in China is 42.33 per million, making it the most common pediatric malignancy. Survey data indicate that the prevalence of malnutrition among children with leukemia is as high as 47% [1]. Chemotherapy serves as the cornerstone of treatment for pediatric leukemia; however, its cytotoxic effects lack target specificity. While effectively eliminating tumor cells, it also causes extensive damage to rapidly proliferating normal tissues, with particularly prominent adverse effects on the digestive system. Due to damage to gastrointestinal mucosal epithelial cells, disruption of intestinal microbiota, and neuroendocrine dysregulation, patients often experience a range of clinical symptoms, including severe anorexia, intractable nausea, frequent vomiting, and diarrhea. These side effects directly compromise the nutritional status and quality of life of affected children. Malnutrition during chemotherapy reduces tolerance to chemotherapeutic agents, exacerbates

myelosuppression, and increases the risk of complications and infections [2]. These risk factors significantly impair treatment efficacy and jeopardize patient survival. For pediatric leukemia patients undergoing chemotherapy, effective nutritional intervention has emerged as a critical dimension of comprehensive care. Provision of adequate energy and essential nutrients consistently optimizes physiological reserves, strengthens immune barriers, and markedly alleviates chemotherapy-induced toxicities such as myelosuppression and mucosal injury. Such systemic improvements are directly reflected in enhanced survival outcomes.

2. Causes of malnutrition in children with leukemia during chemotherapy

2.1. Adverse effects of chemotherapeutic drugs

VDLD Regimen (Vincristine, Daunorubicin, L-Asparaginase, and Dexamethasone) is a standard chemotherapeutic protocol for pediatric leukemia. Its mechanism of action involves direct irritation and damage to the gastrointestinal mucosal lining. Following standardized treatment, more than 45% of children with acute leukemia develop malnutrition, leading to an increased risk of complications and mortality [3].

Pathophysiological analysis reveals that chemotherapeutic agents can trigger inflammatory responses in the mucosa, resulting in epithelial cell damage, impaired gastrointestinal motility, and disruption of digestive enzyme secretion. This manifests clinically as frequent nausea and vomiting. Specifically, vincristine interferes with enteric nerve conduction by inhibiting microtubule polymerization, while daunorubicin disrupts DNA replication and concurrently causes abnormal mucus secretion. These processes establish a vicious cycle: nutritional deficits exacerbate drug toxicity, and metabolic disturbances lower the threshold for chemotherapy tolerance.

2.2. Impact of the disease

Leukemia, as a hematologic malignancy, induces metabolic dysregulation and imbalances in energy expenditure in children, significantly elevating the risk of malnutrition [4]. The malignant proliferation of leukemia cells occupies bone marrow space, and their abnormal division process requires the uptake of large amounts of glucose, amino acids, and lipids, creating metabolic competition with normal hematopoietic cells. This material deprivation directly impairs organ physiological function. During the body's response to leukemia, the immune response is activated, producing cytokines such as interleukin-6 and tumor necrosis factor-alpha. These molecules persistently accelerate the basal metabolic rate through both central nervous and peripheral tissue pathways.

2.3. Psychological factors

The protracted and arduous treatment cycle for pediatric leukemia imposes significant psychological stress on children, inducing various psychological disorders and negatively impacting feeding function. Persistent illness, periodic chemotherapy procedures, and the stimulation of confined hospital spaces directly trigger states of anxiety, low mood, and depression in patients [5]. Such stress states act on digestive tract function through the neuro-endocrine regulatory network, inhibiting the contraction rhythm of gastrointestinal smooth muscle and decreasing pepsinogen secretion levels, ultimately leading to impaired nutritional intake and metabolic dysregulation syndrome in the subjects.

2.4. Diet and metabolism

The European Society for Parenteral and Enteral Nutrition (ESPEN) noted in 2016 that the negative energy

balance and skeletal muscle loss in cancer patients result from the combined effects of reduced intake and metabolic dysregulation, which differs significantly from simple malnutrition [6]. Specifically, reduced intake is directly caused by tumor- and treatment-related factors such as anorexia, taste alterations, and gastrointestinal symptoms, leading to inadequate dietary consumption. Metabolic dysregulation refers to the systemic metabolic reprogramming triggered by the release of inflammatory cytokines (e.g., TNF-α, IL-6) and tumor-derived factors from the tumor-bearing host. Its key features include: (1) elevated or abnormally fluctuating resting energy expenditure; (2) insulin resistance, resulting in impaired glucose utilization; (3) persistently enhanced lipolysis; (4) heightened protein catabolism alongside suppressed anabolism.

3. Nutritional intervention measures for children with leukemia during chemotherapy

3.1. Dietary adjustment strategies

Assessing a child's nutritional requirements involves parameters such as age, weight, height, disease severity, chemotherapy phase, and basal metabolic rate. Utilizing tools like SCAN (Screening Tool for Childhood Cancer Nutritional Risk), individualized nutritional assessments should be conducted. This systematic analysis of nutritional and metabolic indicators, combined with clinical treatment progress and growth curve parameters, forms a quantitative diagnostic conclusion, ultimately clarifying the degree of nutritional deficiency and energy supply standards.

Adjusting dietary structure is an indispensable component of nutritional intervention for children undergoing chemotherapy [7]. It is recommended to follow the principles of high protein, high calorie, high vitamin, low fat, and easy digestibility. Priority should be given to ensuring the intake of high-quality protein, with lean meat, fish, poultry, eggs, dairy products, and legumes serving as ideal sources. Legume products combine plant protein with bioactive components while offering high digestibility and absorption rates. Dairy products provide composite nutrition, with outstanding content of high-quality milk protein, calcium, and other trace elements.

Wang et al. [8] pointed out in their study that as induction remission chemotherapy continues, children's intake significantly decreases across various nutrients. Therefore, nutritional intake deficiency can occur early in treatment. In such cases, individualized nutritional intervention is needed to improve prognosis and enhance the long-term quality of life for children. Energy supply should maintain the proportion of carbohydrates, with rice, noodles, steamed buns, and sweet potatoes constituting the foundational energy choices. Vitamin supplementation relies on fresh fruits and vegetables: spinach, broccoli, and carrots form the vegetable category; kiwifruit, oranges, and apples are included in the daily fruit list.

Nutrient supplementation can also be tailored to the child's specific condition [9]. For anemic children, supplementation with iron-rich foods such as animal liver, red dates, and spinach can be considered, with iron supplements under medical guidance if necessary. For children with compromised immunity, nutrients with immunomodulatory functions, such as vitamin C, vitamin D, and zinc, can be supplemented. If deficiencies in vitamins or minerals are present in the child, timely and appropriate supplementation should be implemented.

3.2. Nutritional support methods

Enteral nutrition is implemented via two pathways: Oral Nutritional Supplements (ONS) and tube feeding. Oral nutritional supplementation builds upon regular meals by adding special medical formula foods containing

protein, carbohydrates, fats, and trace elements. These products come in various flavors, such as chocolate and fruit, and can be customized based on children's preferences to enhance compliance. Tube feeding is suitable for children unable to eat orally. Gastrointestinal access includes nasogastric tubes, nasojejunal tubes, and surgical interventions such as ostomy placement. The choice of enteral route depends on individual tolerance and treatment goals for situations of insufficient oral intake. The infusion rate and temperature of the nutritional solution should be controlled within physiologically appropriate ranges. Xing et al. [10] proposed that compared to oral diets, the use of short-peptide enteral nutritional support yields better outcomes.

When children exhibit gastrointestinal dysfunction, such as intestinal obstruction, perforation, or severe diarrhea, and cannot receive enteral nutrition support at all, intravenous nutrition intervention is required. Various nutrients—glucose, amino acids, fat emulsions, vitamins, and electrolyte solutions—are continuously infused via peripheral or central veins. This mode of nutritional supply encompasses two main categories: Total Parenteral Nutrition (TPN) and Partial Parenteral Nutrition (PPN), meeting the metabolic needs of children through different formula combinations [11]. Total parenteral nutrition is suitable for children who cannot receive nutrition via the gastrointestinal tract or have gastrointestinal dysfunction, supplying all essential nutrients. Partial parenteral nutrition is used for children whose enteral nutrition does not meet full requirements, serving as a supplement to enteral nutrition.

3.3. Nutritional education and support

Nutritional knowledge education is a core component of clinical nutritional therapy [12]. The medical team must systematically explain to families the mechanisms and clinical hazards of malnutrition in children with leukemia during chemotherapy, encouraging parents to understand the decisive impact of scientific diet on the child's prognosis. Nutritional intervention must be integrated throughout the entire chemotherapy process.

Psychological intervention should not be neglected. During chemotherapy, children and their families commonly experience negative emotions such as anxiety and fear. These emotions can lead to loss of appetite and impaired nutrient absorption. Nursing staff should establish regular psychological assessment mechanisms, listen to needs, and provide emotional support. Timely sharing of successful treatment cases helps boost confidence in treatment. For individuals with significant psychological distress, referral to psychiatric departments for professional intervention is warranted.

In addition to nutritional education, psychological support for children and their families is essential. Zhang et al. [13] confirmed through research that the combined application of nutritional education and psychological intervention in leukemia chemotherapy can effectively improve the psychological status of patients with acute leukemia undergoing chemotherapy, enhance compliance and satisfaction, and reduce adverse reactions. During chemotherapy, children and parents often bear immense psychological pressure, prone to anxiety, fear, depression, and other adverse emotions that can affect the child's appetite and nutritional intake. Healthcare workers should care about the psychological state of children and parents, proactively communicate with them, listen to their concerns, and offer comfort and encouragement. Sharing successful treatment cases can strengthen their confidence in overcoming the disease. For children and parents exhibiting psychological issues, referral to a psychologist for professional counseling may be necessary.

4. Intervention mapping methods and research advances in nutritional support for children with leukemia during chemotherapy

Intervention mapping is a multi-step design process based on health behavior theories (such as the Theory of Planned Behavior and Social Cognitive Theory) and empirical research evidence. It ensures that intervention programs align with the actual needs of the target population while precisely addressing specific health problems (e.g., chronic disease management, infectious disease control, health risk behavior intervention). During chemotherapy for pediatric leukemia, children often face issues such as malnutrition, immunosuppression, and chemotherapy-related adverse effects (e.g. mucositis, infections). The latest nutritional intervention mapping encompasses new concepts and methods in nutritional intervention, special dietary management, and multidisciplinary collaboration models.

4.1. New concepts and methods in nutritional intervention

Precision nutritional intervention is becoming a prominent frontier field. Leveraging high-throughput gene sequencing and metabolomics technologies, it reveals children's gene polymorphisms and metabolic pathway characteristics, providing a scientific basis for personalized dietary ratios. Upon detection of mutations in genes related to specific nutrient metabolism, adjustments to the types and dosages of corresponding supplements can be made to enhance bioavailability. Jiang et al. [14] confirmed that precision nutritional intervention helps improve the nutritional status of patients post-chemotherapy and reduces the incidence of chemotherapy-related adverse reactions.

The gut microbiota is a host-specific entity that develops throughout life. It is susceptible to exogenous and endogenous modifications and can be a fundamental driver or contributing factor in many diseases, affecting local and distant organ systems, with the potential to influence diverse processes, including hematopoiesis [15]. Strategies such as probiotic supplementation, prebiotic intake, and fecal microbiota transplantation are used to improve microbial balance and repair the mucosal barrier. Immunonutrition support is considered a novel nutritional intervention strategy, with core components including arginine, ω-3 polyunsaturated fatty acids, and nucleotides [16]. Arginine stimulates immune cell proliferation and promotes lymphokine secretion; ω-3 fatty acids lower IL-6 levels and modulate neutrophil activity; nucleotides accelerate immunoglobulin synthesis and maintain Th1/Th2 axis homeostasis, precisely regulating cellular immune responses.

Nutritional assessment and plan formulation are also indispensable. As indicated in the study, responsible nurses need to determine patients' daily dietary requirements and actual intake based on their condition and nutritional risk screening results. The daily caloric requirement is 83–125KJ/kg, protein is 1.5–2.0g/kg/day, and fat constitutes 50% of non-protein calories [17]. By accurately formulating and implementing nutritional plans, expected nutritional intervention outcomes can be achieved.

4.2. Special dietary management

Managing the side effects of chemotherapy in children with leukemia requires attention to dietary adjustment plans. L-asparaginase (L-asp) can potentially induce pancreatitis, a common and severe complication, making fat intake control a key intervention measure [18]. Daily diets should avoid high-fat categories such as fried foods and animal offal. Low-fat milk, fish, and lean meat are ideal choices, combining low-fat properties with high-quality protein supplementation, effectively reducing pancreatic metabolic stress.

Children with oral mucositis require special attention to food texture and temperature. It is recommended

to choose soft, easy-to-swallow foods like rice porridge, noodles, tofu pudding, and steamed eggs. Spicy and irritating foods such as chili peppers, Sichuan pepper, and ginger should be avoided to reduce secondary irritation to the oral mucosa. Food temperature should be controlled within a suitable range, as excessively hot food may burn oral lesions, while excessively cold food can trigger local sensitivity. Cooking methods such as steaming, boiling, and stewing are recommended to effectively enhance food softness and digestibility.

Children experiencing diarrhea require simultaneous implementation of dietary intervention plans. High-fiber food intake should be restricted to prevent intensified intestinal peristalsis. Cold foods like sashimi, ice cream, and cold salads are strictly prohibited to reduce the risk of intestinal infections.

4.3. Multidisciplinary collaboration model

In the field of nutritional management for children with leukemia during chemotherapy, the multidisciplinary collaboration model demonstrates its unique value. Nutrition departments, in alliance with hematology and pediatrics experts, form diagnostic and therapeutic coalitions to collaboratively develop and execute individualized nutritional support strategies. Zhong [19] proposed that receiving multidisciplinary collaborative nutritional intervention alongside chemotherapy can improve treatment efficacy and enhance overall nutritional status, making it worthy of promotion. Hematology specialists deeply understand the clinical characteristics of children, stage the chemotherapy process, and systematically assess the impact of tumor burden on body metabolism, laying a precise diagnostic foundation for nutritional management. Pediatricians master child growth patterns and physiological characteristics, systematically calculating nutritional needs based on parameters such as age, weight, height, and underlying diseases, allowing data from hematology and pediatrics to serve as the baseline for nutritional science intervention.

5. Conclusion

To optimize children's nutritional levels, enhance treatment efficacy, and improve quality of life, various intervention programs have been gradually implemented, involving dietary structure modification, personalized nutritional supplementation strategies, and professional education support systems. Currently, nutritional interventions for children with leukemia during chemotherapy still face certain practical bottlenecks and theoretical gaps. In-depth exploration in this field continues, with improving specific implementation pathways being a key focus of clinical practice. It is essential to deepen multidisciplinary collaboration mechanisms, enhance healthcare professionals' capabilities in nutritional diagnosis and therapy [20], and improve the comprehensive support system for children with leukemia and their families. Implementing systematic nutritional education and psychological counseling strategies can significantly improve treatment compliance. Promoting the clinical translation of new nutritional intervention models, proposing novel intervention mapping methods, and analyzing research progress will facilitate the application of scientific findings in practice, build precise nutritional support programs, ultimately optimize the survival prognosis of children during chemotherapy, and comprehensively enhance the quality of life for children with leukemia.

Disclosure statement

The authors declare no conflict of interest.

References

[1] Mao Q, Mao XR, Li X, et al., 2024, Application of a Specialist Nurse-Led Nutrition Management Program in Children With Leukemia During Induction Remission Chemotherapy. Chinese Journal of Nursing, 59(23): 2900–2907.

[2] Chen Y, Chen P, Zhang N, et al., 2024, Effects of Oral Nutritional Supplementation on Hematologic Complications During Induction Chemotherapy in Children With Acute Lymphoblastic Leukemia: Interim Results of a Randomized Controlled Trial. Journal of China Pediatric Blood and Cancer, 29(2): 103–108 + 122.

[3] Bao QX, Cai JP, Zhou Q, et al., 2024, Analysis of Nutritional Status and Construction and Validation of a Visual Model for Predicting Malnutrition Risk in Children With Acute Leukemia. Maternal and Child Health Care of China, 39(23): 4670–4674.

[4] Liao XH, Zheng LH, Jia YM, et al., 2025, Risk Factors for Malnutrition and Construction of a Risk Prediction Model in Lung Cancer Patients With Postoperative Chemotherapy. Journal of Translational Medicine, 14(4): 7–11.

[5] Long MQ, Lai BY, Wang Y, et al., 2024, Incidence of Nosocomial Infection and Its Correlation With Mental Health Status in Patients With Acute Myeloid Leukemia Admitted to Laminar Flow Beds. Chinese General Practice Nursing, 22(15): 2952–2955.

[6] Shi LX, Zhao MZ, Wang FF, et al., 2025, Clinical Analysis of Nutritional Components in Children With Acute Leukemia. Chinese Journal of Contemporary Pediatrics, 27(3): 300–307.

[7] Zhu Y, 2023, Study on the Application Effect of Psychological Nursing Combined With Dietary Nursing in the Care of Leukemia Patients. China Food Industry, (18): 122–125.

[8] Wang R, Huang J, Wan YY, et al., 2021, Investigation on Dietary Intake and Nutritional Status of Children With Acute Lymphoblastic Leukemia During Chemotherapy Induction Remission Period. Parenteral and Enteral Nutrition, 28(5): 281–285.

[9] Liu LJ, Ding Y, Ye WH, 2022, Effect of Learning-Determined Teaching Diet and Nutrition Education on Nutritional Status and Quality of Life in Leukemia Patients Undergoing Chemotherapy. International Journal of Nursing, 41(15): 2764–2768.

[10] Xing C, He X, Qin CW, 2024, Application Effect of Short-Peptide Enteral Nutrition Agent in Nutritional Support for Children With Leukemia. China Modern Medicine, 31(32): 66–69.

[11] Wang J, Ren GL, 2021, Analysis of Influencing Factors of Peripherally Inserted Central Catheter-Related Venous Thromboembolism in Children With Acute Leukemia. Chinese Journal of Biomedical Engineering, 27(3): 288–293.

[12] Zhang QM, Jiang HM, Zheng L, 2024, Application of Health Education Based on Behavior Change Model in Leukemia Patients Undergoing Chemotherapy. China Medical Herald, 21(3): 183–186.

[13] Zhang HJ, Jin Y, 2024, Effect of Health Education Based on Behavior Change Model Combined With Psychological Intervention on Psychological Status and Compliance of Patients With Acute Leukemia Undergoing Chemotherapy. Oncology Progress, 22(23): 2592–2595.

[14] Jiang L, Jiang Q, Miao PP, et al., 2024, Effect of Precision Nutrition Intervention on Nutritional Status and Chemotherapy Adverse Reactions in Patients With Prostate Cancer After Postoperative Chemotherapy. Oncology Progress, 22(11): 1247–1251.

[15] Li Y, Feng C, 2023, Research Progress of Gut Microbiota Metabolites in Childhood Acute Myeloid Leukemia. Chinese Journal of Clinical Medicine, 51(10): 1154–1157.

[16] Li XY, Xu LL, Ding J, 2025, Effects of Probiotics on Appetite Regulatory Factors, Intestinal Probiotics and Immune Status in Colorectal Cancer Patients Undergoing Chemotherapy. Sichuan Journal of Physiological Sciences, 47(5): 952–953 + 1015.

[17] Sun H, 2022, Effect of the Integrated Doctor–Nurse–Dietitian Management Model on the Nutritional Status of Leukemia Patients Undergoing Chemotherapy. Modern Nurse (First Issue), 29(2): 108–111.

[18] Gao QL, Chen C, Le SH, et al., 2021, Clinical Analysis of Pegaspargase-Associated Pancreatitis in Children With Acute Lymphoblastic Leukemia Undergoing Chemotherapy. Chinese Journal of Pediatric Hematology and Oncology, 26(5): 285–288 + 293.

[19] Zhong LM, 2024, Effect of Multidisciplinary Team-Based Whole-Course Nutrition Management on Nutritional Status and Self-Care Ability of Esophageal Cancer Patients Undergoing Radiotherapy. Chinese General Practice Nursing, 22(9): 1713–1716.

[20] Huang J, Hao PL, 2022, Investigation on Nutritional Status of Acute Leukemia Patients and Knowledge, Attitude, and Practice of Nursing Staff Towards Nutritional Management. Chinese Journal of Clinical Oncology Rehabilitation, 29(8): 945–949.

Publisher's note

Bio-Byword Scientific Publishing remains neutral with regard to jurisdictional claims in published maps and institutional affiliations.

Proceedings of Anticancer Research, 2026, Volume 10, Issue 1
http://ojs.bbwpublisher.com/index.php/PAR
ISSN Online: 2208-3553
ISSN Print: 2208-3545

Advances in Proteolysis Targeting Chimeras

Shili Liu, Yu Liu*

China Pharmaceutical University, Nanjing 210000, Jiangsu, China

**Corresponding author: Yu Liu, liuyu@cpu.edu.cn*

Copyright: © 2026 Author(s). This is an open-access article distributed under the terms of the Creative Commons Attribution License (CC BY 4.0), permitting distribution and reproduction in any medium, provided the original work is cited.

Abstract: In recent years, proteolysis-targeting chimeras (PROTACs) have gained widespread attention as an emerging therapeutic approach. PROTACs are bifunctional molecules composed of a target protein-binding ligand, an E3 ubiquitin ligase ligand, and a linker connecting these ligands. By harnessing the cell's intrinsic ubiquitin-proteasome system (UPS), they promote the ubiquitination of specific target proteins, leading to their degradation and therapeutic effects. PROTACs show exceptional promise in targeting conventional "undruggable" targets compared to traditional small-molecule inhibitors. This review provides an overview of PROTACs, including their molecular mechanism of action, therapeutic benefits, development history, key design aspects, current research and development challenges, and future trends in next-generation PROTAC technology.

Keywords: PROTAC; Ubiquitin-proteasome system; Targeted therapy; Next-generation PROTAC

Online publication: February 9, 2026

1. Introduction

Cancer is a major disease that poses a serious threat to human health worldwide, with its incidence and death rates continuing to rise, adding a heavy burden to global health systems. According to the GLOBOCAN 2022 data released by the International Agency for Research on Cancer (IARC), there are approximately 20 million new cancer cases and 9.7 million deaths each year globally. Predictions suggest that by 2050, the number of new cases annually will exceed 35 million, marking an increasingly difficult challenge for cancer prevention and control [1].

Currently, common clinical treatments for cancer include surgery, radiotherapy, and chemotherapy. In molecular targeted therapy, small-molecule inhibitors are crucial because they specifically bind to oncogenic target proteins and block the proliferation and survival signaling pathways of tumor cells. However, these inhibitors face several limitations, such as the potential to cause target mutations leading to drug resistance, significant off-target toxicity, and the need for high doses over extended periods. These issues greatly restrict their clinical applications [2].

To address the issues above, proteolysis-targeting chimeras (PROTACs) have become a promising approach for anticancer drug discovery and development. PROTACs molecules are bifunctional compounds that bind to a target protein of interest (POI) on one end and recruit an E3 ubiquitin ligase(E3) on the other, leading to

ubiquitination of the POI and its degradation by the proteasome. Compared to traditional inhibitors, PROTACs offer potential benefits such as prolonged effects, the ability to target traditionally "undruggable" proteins, and the capacity to overcome drug resistance, opening new avenues for cancer therapy [3].

2. Mechanism of action and therapeutic benefits of PROTACs

2.1. Mechanism of action of PROTACs

Intracellularly, protein degradation and amino acid recycling mainly occur through two precisely regulated pathways: the lysosomal pathway and the ubiquitin-proteasome system (UPS) pathway. Of these two, UPS handles the degradation of most short-lived and misfolded proteins in the cell, and its dysfunction is closely linked to the development of many diseases, especially cancer [4]. Building on an in-depth understanding of the UPS mechanism, crews and his team first introduced the concept of PROTACs in 2001. These are heterobifunctional molecules composed of three key components: a ligand for binding POI, another ligand for recruiting E3 ligases, and a rationally designed linker covalently connecting them.

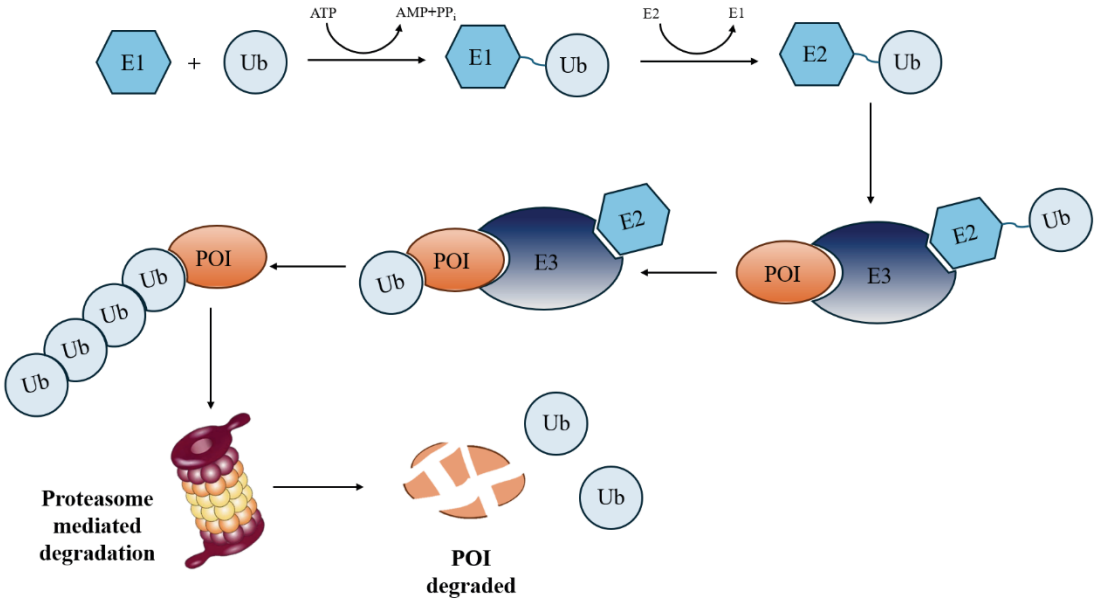


Figure 1. Schematic of the ubiquitination process.

The mechanism of action of PROTACs relies on the E1-E2-E3 enzymatic cascade in UPS (**Figure 1**). Specifically, first, ubiquitin (Ub) is activated by the ubiquitin-activating enzyme (E1) and transferred to the ubiquitin-conjugating enzyme (E2) with ATP supply. Then, in the formation of PROTACs in the "POI-PROTAC-E3 ligase" ternary complex, E3 catalyzes the transfer and covalent attachment of the E2-carrying Ub to the lysine residues of the POI. After multiple ubiquitination steps, the POI is tagged with a polyubiquitin chain, which is recognized by the 26S proteasome and degraded into short peptide fragments (**Figure 2**) [5]. Notably, PROTAC molecules only serve as a bridge in this process; they are not consumed and can be released and recycled after completing a degradation cycle, enabling efficient and sustainable removal of target proteins.

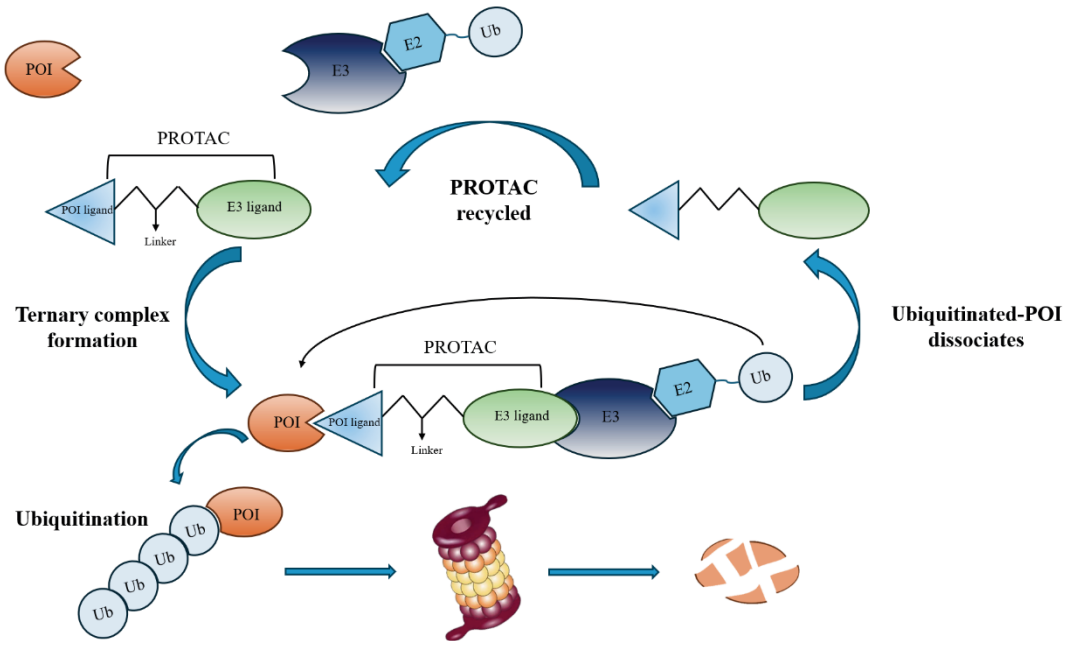


Figure 2. Schematic diagram of the PROTAC-mediated POI degradation process.

2.2. Therapeutic benefits of PROTACs

2.2.1. Targeting the "undruggable"

Small-molecule inhibitors typically work through an "occupancy-driven" mechanism, requiring high-affinity binding to active or allosteric sites to block protein function. This approach faces inherent limitations, contributing to over 80% of the human proteome being considered "undruggable" [6]. In contrast, PROTACs operate via an "event-driven" catalytic mechanism. They transiently bind to the target and recruit E3 ligases to induce its ubiquitination and subsequent proteasomal degradation, bypassing the need for traditional druggable pockets and thereby offering a novel strategy to target previously inaccessible proteins.

This advantage is powerfully illustrated by the targeting of B-cell lymphoma 6 (BCL6), a key oncogenic transcriptional repressor in diffuse large B-cell lymphoma (DLBCL) but long deemed "undruggable" due to its flat protein-protein interaction interfaces (PPI) [7–10]. PROTAC technology has enabled direct pharmacological intervention against BCL6, with multiple candidates now in clinical development. Bristol-Myers Squibb has advanced BMS-986458 into a Phase I/II combination trial for B-cell non-Hodgkin lymphoma (NHL), under the identifier NCT06090539 [11]. Concurrently, Arvinas has developed ARV-393, a next-generation BCL6 PROTAC that achieved a DC_{50} as low as 0.03 nM in preclinical models and entered a Phase I trial in 2024 (NCT06393738) [12–14]. These clinical advances demonstrate PROTACs' capacity to translate undruggable targets into therapeutic realities.

2.2.2. Overcoming drug resistance

Drug resistance, often mediated by target protein overexpression or mutations that impair inhibitor binding, remains a major challenge in targeted cancer therapy [15,16]. PROTACs offer a distinct solution by degrading the target protein entirely, making resistance mechanisms that rely on reduced binding affinity less effective.

This is exemplified in addressing resistance to the anaplastic lymphoma kinase (ALK) tyrosine kinase inhibitor (TKI) lorlatinib in non-small cell lung cancer (NSCLC), where compound mutations like G1202R/

L1196M frequently arise [17–19]. The PROTAC molecule WZH-17-002 was designed to address this. In a G1202R/L1196M mutant mouse model, WZH-17-002 treatment reduced tumor volume by 68% compared to lorlatinib and significantly delayed resistance development, demonstrating the potential of degradation-based strategies to overcome clinical resistance [20].

2.2.3. Enhancing therapeutic safety

The catalytic, "event-driven" mechanism of PROTACs enables sustained target degradation at low, sub-stoichiometric doses, reducing the off-target toxicity risks associated with the high, continuous exposure required by conventional occupancy-driven inhibitors [21]. This safety advantage is exemplified in targeting signal transducer and activator of transcription 3 (STAT3), a transcription factor implicated in tumor progression but historically difficult to drug due to a lack of suitable binding pockets [22]. The PROTAC molecule D11-PROTAC achieved over 90% STAT3 degradation at a low concentration (1.5 μM), effectively suppressing tumor cell proliferation and migration, thereby demonstrating the potential for high-efficacy therapy with an improved safety window [23].

3. Development history of PROTAC

Since its conceptual inception, PROTAC technology has evolved over two decades from a theoretical concept to a promising clinical anticancer platform. The field was pioneered in 2001 with the first peptide-based PROTAC [24]. A key advance came in 2008 with the first fully small-molecule PROTAC, which improved cell permeability [25]. The repertoire of E3 ligases expanded in 2010 with the introduction of inhibitor of apoptosis protein (IAP)-based PROTACs [26]. By 2015, the widespread adoption of highly potent von Hippel-Lindau (VHL)- and cereblon (CRBN)-based ligands significantly enhanced degradation efficiency and selectivity [27,28]. A major milestone was reached in 2019 when the first PROTAC drugs, ARV-110 and ARV-471, entered clinical trials for prostate and breast cancer, respectively, marking the technology's formal transition to clinical validation [29,30]. Subsequently, the field has rapidly diversified, with an increasing number of PROTAC candidates entering oncology trials and novel modalities including lysosome-targeting chimeras (LYTACs) and autophagy-targeting chimeras (AUTACs) emerging to expand the therapeutic potential of targeted protein degradation [31].

4. Key design elements of PROTACs

A typical PROTAC consists of three key parts: a warhead that targets POI, a ligand that recruits an E3 ligase, and a linker that connects them. The properties of each component critically influence the degradation efficiency, selectivity, and cellular activity of the PROTAC. The rational design of these modules and their synergistic interaction are essential for achieving effective targeted protein degradation and successful clinical translation.

4.1. Selection of POI ligands

The rational selection of POI ligands is crucial for successful PROTAC design. Most currently used POI ligands come from existing small-molecule inhibitors or modulators of target proteins, which are structurally optimized to serve as binding modules within the bifunctional structure of PROTACs [32]. During the design process, the binding affinity and selectivity between ligands and target proteins are critical—they not only determine whether PROTACs can effectively bind to target proteins but also greatly influence their off-target risks [33]. However, due

to the unique "event-driven" mechanism of PROTACs, the affinity requirement for POI ligands is not absolute—even ligands with moderate or low affinity can lead to highly efficient degradation. For instance, Zhou et al. developed PROTACs targeting $KRAS^{G12D}$ using a moderate-affinity analogue of MRTX1133 [34]. Despite reduced affinity, these molecules effectively degraded $KRAS^{G12D}$ in ASPC-1 cells (DC_{50} = 38.06 nM) and exhibited significant antitumor efficacy *in vivo*, demonstrating the utility of medium-affinity ligands in PROTAC design.

4.2. E3 ligase ligands

E3 ligase ligand is another essential component of PROTAC molecules, responsible for recruiting E3 and mediating the ubiquitination and proteasomal degradation of target proteins [35]. Currently, the most commonly used E3 ligases include CRBN, VHL, and MDM2, among others. Their selection requires careful consideration of factors such as tissue expression distribution, substrate specificity, and the specific therapeutic context [36].

When designing E3 ligase ligands, priority should be given to ensuring they have a high affinity for the target E3 ligase, which is essential for effective ternary complex formation. For example, thalidomide and its derivatives are widely used in the molecular design of PROTACS due to their potent and specific binding ability to CRBN [37]. Beyond binding affinity, the drug-like properties of the E3 ligand—such as good solubility, metabolic stability, and low cytotoxicity—are crucial for achieving a favorable pharmacokinetic profile and facilitating the clinical translation of PROTACs [38].

4.3. Selection of linker

The properties of the linker—including its length, hydrophilicity, flexibility, and attachment points on the ligands—can greatly affect the degradation efficiency of the PROTACs. For instance, Bond et al. demonstrated that shortening the linker in a BRD4-targeting PROTAC (ZXH-3-26) enhanced selectivity by restricting conformational freedom and reducing off-target binding to homologous BRD proteins [39]. Optimizing linker length through structure–activity relationship (SAR) studies is crucial: too short a linker may impair ternary complex formation, while excessively long linkers can introduce steric hindrance [40]. Emerging strategies, such as geometrically defined DNA linkers and linker-free designs, further expand the chemical space for PROTAC development [41,42].

4.4. Formation of ternary complexes

PROTACs mediate degradation by stabilizing a ternary complex between the POI and the E3 ligase. Complex stability is governed by the combined effects of POI and E3 ligand affinity, linker properties, and the resulting spatial orientation. The traditional development of PROTACs depends heavily on numerous time-consuming and inefficient trial-and-error "synthesis-test" cycles for POI ligands, E3 ligands, and linkers.

Computer-aided drug design (CADD) accelerates this process by enabling in silico modeling and optimization. Molecular docking and molecular dynamics (MD) simulations can predict ternary complex conformations and assess cooperativity—a key feature wherein the ternary complex exhibits enhanced stability relative to binary interactions. The "Method 4B" framework, for example, successfully predicted ternary structures and cooperativity trends for several PROTACs [43,44]. Energy-based methods such as MM/GBSA provide quantitative estimates of binding affinity and cooperativity factors, revealing how linker geometry influences PPI [45,46].

Therefore, CADD has transformed PROTAC development from an empirical trial-and-error approach to a more predictive and rational iterative optimization process. However, conventional force field-based computational

methods remain limited by their dependence on accurate initial conformations, high computational cost, and substantial resource demands [47].

Recent advances in artificial intelligence (AI) offer further improvements. For example, the PROTACable platform developed by Mslati et al., which integrates 3D structural modelling and deep learning techniques, employs an SE(3)-equivariance graph Transformer network, and is capable of using the spatial conformational relationships of POI, PROTAC, and E3 ligases as inputs for directly predicting the degradation activity of PROTAC, achieving an end-to-end automated assessment of the complex formation ability [48]. This method overcomes the limitations of the traditional multi-step computational process, significantly enhances prediction efficiency and reliability, and greatly supports the rational design of PROTACs.

5. Difficulties and challenges confronting PROTAC

Despite its transformative potential for drug discovery, the clinical translation of PROTAC technology faces several inherent challenges stemming from its structural properties, which significantly constrain its practical application. These limitations are primarily manifested in the following three aspects:

5.1. E3 Ligase dependency and off-target toxicity

The efficacy of PROTACs is contingent upon specific E3 ubiquitin ligases, which can lead to off-target toxicity. As noted by Vicente et al., while CRBN-based PROTACs are widely used due to the favorable binding affinity and physicochemical properties of their ligands, the varying expression levels of CRBN across different tissues and cell types can result in inconsistent degradation efficiency in off-target tissues [49]. This increases the risk of off-target effects and may even induce tissue-specific toxicity. Consequently, a key strategy for improving targeting specificity and reducing off-target toxicity is to prioritize E3 ligases that are highly expressed in diseased tissues but have low expression in normal tissues, and to actively develop novel, highly specific E3 ligase ligands.

5.2. Suboptimal drug-like properties

PROTACs are typically heterobifunctional molecules with molecular weights exceeding 700 Da, high lipophilicity, and large polar surface areas. These characteristics often cause them to deviate from the Rule of Five, thereby limiting their oral absorption, cell membrane permeability, and metabolic stability [50–52]. However, recent studies indicate that this challenge can be partially overcome through rational molecular optimization. For instance, research from institutions like Arvinas and AstraZeneca suggests that reducing the number of solvent-exposed hydrogen bond donors (eHBDs) can improve the membrane permeability of PROTACs, leading to better oral bioavailability.

5.3. Limited blood-brain barrier penetration

Owing to their large molecular size and polarity, PROTACs struggle to cross the blood-brain barrier (BBB) via passive diffusion, restricting their application in central nervous system (CNS) diseases. Nevertheless, this challenge has spurred the development of innovative delivery strategies. In 2025, the Wu Sijin group developed a transferrin receptor (TfR)-based DNA nanoflower delivery system capable of efficiently loading an Oligo-PROTAC and achieving highly efficient BBB crossing, significantly enhancing its distribution and degradation efficiency in brain tissue [53]. This strategy provides a novel and promising solution for applying PROTAC

technology to treat neurodegenerative diseases such as Alzheimer's and Parkinson's.

6. Future trends in next-generation PROTAC technology

Although structural modifications and optimized delivery strategies have partially mitigated limitations of PROTACs such as off-target toxicity, oral bioavailability, and BBB penetration, significant challenges remain in systematically improving their physicochemical properties to meet *in vivo* application requirements [54]. Consequently, research focus is gradually shifting towards smarter, next-generation PROTAC technology. These systems are designed to respond to exogenous or endogenous stimuli within specific tissues, enabling spatiotemporally controlled protein degradation, which promises to further enhance targeting precision and reduce systemic toxicity [55].

6.1. Click-release PROTAC (crPROTAC)

crPROTAC is a class of intelligent degradation systems designed for spatially controlled activation. They utilize bioorthogonal click chemistry as a molecular switch to release the active PROTAC specifically within target cells or tissues, thereby enhancing selectivity and minimizing systemic toxicity.

A representative strategy involves masking a PROTAC such as ARV-771 with a trans-cyclooctene (TCO) group. This inert prodrug circulates systemically until it encounters a tumor-targeting tetrazine peptide in the microenvironment, triggering a bioorthogonal reaction that releases the active degrader and enables precise BRD4 degradation [56,57]. An alternative strategy, ClickRNA-PROTAC, delivers mRNA encoding an E3 ligase fusion protein into tumor cells. The functional PROTAC is then assembled in situ through a bioorthogonal reaction between a transfected ligand and the expressed ligase, achieving highly specific target protein degradation [58].

6.2. Photo-activatable PROTAC

Photo-activatable PROTAC is a type of intelligent degradation approach that allows spatiotemporal control of protein degradation using external light exposure. The system remains biologically inactive after drug administration and is only activated under specific light wavelengths, thereby inducing target protein degradation within a defined space and time. This design significantly improves the accuracy and specificity of PROTAC molecules, while effectively reducing off-target toxicity and systemic side effects [59]. Currently, the main light-controlled PROTAC methods are mainly divided into two categories: photocaged PROTAC (pc-PROTAC) and photoswitchable PROTAC (ps-PROTAC).

6.2.1. pc-PROTAC

The pc-PROTAC strategy involves conjugating photolabile protecting groups to key functional sites of the PROTAC molecule—such as the E3 ligase ligand, rendering it inactive until exposure to specific light triggers cleavage and releases the active degrader.

Initial designs, developed independently by several groups around 2019–2020, primarily used ultraviolet A (UVA) light to activate PROTACs targeting proteins such as BRD4 and BTK [60–62]. However, UV light has limited tissue penetration and potential phototoxicity. To overcome this, visible light-activated pc-PROTACs were developed, offering reduced photodamage and improved spatial precision [63].

For deeper tissue applications, the first X-ray-activated PROTAC (RT-PROTAC) was reported in 2022 [64].

By incorporating an X-ray-sensitive photocage, PROTAC activity can be triggered locally within tumors upon irradiation. This approach not only achieves high tissue penetration and spatiotemporal control but also synergizes with clinical radiotherapy to inhibit tumor growth *in vivo*, highlighting its potential for combined cancer therapy [65].

6.2.2. ps-PROTAC

Unlike irreversible pc-PROTACs, ps-PROTACs incorporate a photoisomerizable linker that reversibly toggles between cis and trans configurations under different wavelengths of light. This allows dynamic, bidirectional control of ternary complex formation and protein degradation activity, enhancing precision and reducing off-target risks.

A representative example is the first agonist-based photoswitch NAMPT PROTAC developed by Sheng's group, which features an azobenzene-containing linker [66]. Under 450 nm light, the molecule adopts a trans configuration that promotes NAMPT degradation, lowering NAD^+ levels. Switching to 365 nm light isomerizes the linker to cis, restoring NAMPT activity and NAD^+ biosynthesis via its integrated agonist function [67,68]. This reversible system not only enables optical control of protein levels and metabolic output but also demonstrates light-regulated antitumor effects in a mouse model, highlighting its potential for spatially precise cancer therapy and pathway investigation.

6.3. Tumor microenvironment- activatable PROTAC

The tumor microenvironment (TME) exhibits endogenous features that differ markedly from those of normal tissues, including high levels of specific enzymes, increased concentrations of reducing substances, hypoxia, and elevated reactive oxygen species (ROS). These features provide a molecular foundation for developing tumor microenvironment-responsive PROTAC that can be selectively activated at the tumor site, thereby improving the accuracy of targeted protein degradation and minimizing systemic toxicity to healthy tissues. Currently, the four main strategies include enzyme-activatable PROTAC, glutathione-activatable PROTAC, hypoxia-activatable PROTAC, and reactive oxygen species-responsive PROTAC.

6.3.1. Enzyme- activatable PROTAC

Enzyme-activatable PROTAC achieves targeted activation by leveraging specific enzymes that are highly expressed in tumors. This class of molecules is in a pre-drug form and is enzymatically triggered to release PROTAC once inside the target tissue, leading to selective degradation of the POI, improved therapeutic precision, and fewer off-target effects.

For example, Liang et al. developed a prodrug molecule called Pro-PROTAC to specifically target cancer cells and enable controlled protein degradation [69]. This strategy was achieved by introducing trimethyl-locked quinone (TLQ) as a masking group in the PROTAC molecule targeting BRD4 at the hydroxyproline site of its VHL E3 ligase ligand. This group can be specifically reduced and undergo autocleavage by NAD(P)H quinone dehydrogenase 1 (NQO1), which is overexpressed in a wide range of tumor cells and at lower levels in normal tissues [70]. Thus, Pro-PROTAC remains "inert" in normal cells due to the loss of E3 ligase recruitment caused by the masking group, whereas in tumor cells, the removal of this group, catalyzed by NQO1, releases active PROTAC, which induces highly selective degradation of the oncogenic driver BRD4.

6.3.2. GSH- activatable PROTAC

The concentration of glutathione (GSH) is significantly higher in tumor cells than in the extracellular environment

and normal tissues, creating ideal conditions for the development of tumor-selectively activated prodrug-type PROTAC [71]. In the treatment of breast cancer (BC), for instance, PROTACs targeting oestrogen receptor α (ERα) have demonstrated significant therapeutic potential, but there is a risk of off-target toxicity due to non-specific protein degradation in normal tissues as well [72].

To address this issue, Zhou et al. developed a GSH-responsive ERα-targeting PROTAC [73]. The design involved creating a prodrug form of the PROTAC by introducing an *o*-nitrobenzenesulfonyl group at the hydroxyl moiety in the molecules of VHL ligand-based ERα PROTAC. This modification rendered the molecule inert under normal physiological conditions and allowed activation in the tumor cell-specific high GSH environment, enabling selective degradation of ERα. This strategy not only offers new ideas for the development of safer and personalized BC therapeutic regimens but also highlights the broad potential of microenvironment-activatable PROTAC in tumor therapy.

6.3.3. Hypoxia- activatable PROTAC

Hypoxia is a common pathological feature in solid tumors. The rapid growth of tumor cells escalates oxygen consumption, while aberrant tumor vasculature results in inadequate perfusion and the development of local hypoxic regions. This environment not only causes the overexpression of various pro-cancer proteins such as hypoxia-inducible factor (HIF), vascular endothelial growth factor receptor (VEGFR), and epidermal growth factor receptor (EGFR), but also further promotes drug resistance and malignant progression of the tumor [74,75].

Based on this mechanism, Cheng et al. designed and synthesized a novel class of hypoxia-activated PROTAC prodrugs (ha-PROTAC) by incorporating hypoxia-activated leaving groups (HALGs) into PROTACs targeting EGFR [76]. Experimental validation demonstrated that unmodified PROTACs could effectively degrade EGFR under both normoxic and hypoxic conditions, whereas ha-PROTAC was activated only under hyperoxic conditions, successfully achieving the goal of selectively degrading EGFR in hypoxic tumor regions.

6.3.4. ROS- activatable PROTAC

Elevated levels of ROS, particularly hydrogen peroxide (H_2O_2), constitute a common feature of the solid tumor microenvironment [77]. Exploiting this trait, Yao et al. developed an H_2O_2-responsive supramolecular system for tumor-selective PROTAC activation [78]. In pancreatic cancer cells, high H_2O_2 triggered the self-assembly of precursors into tetrazine-rich nanostructures, which subsequently released an active BRD4-targeting PROTAC via a bioorthogonal reaction. This system achieved more than 80% degradation of BRD proteins in cancer cells with minimal activity in normal cells, demonstrating high selectivity. In vivo, it effectively inhibited tumor growth in a pancreatic cancer mouse model without significant systemic toxicity, providing a key paradigm for ROS-dependent precision protein degradation.

6.4. Biomacromolecule-PROTAC conjugates

To enhance tumor selectivity, PROTACs have been conjugated to targeting biomolecules such as antibodies, folate, nucleic acid aptamers, and others. These conjugates specifically recognize receptors overexpressed on cancer cells, enabling receptor-mediated internalization and intracellular activation. This strategy improves tumor accumulation while minimizing off-target exposure.

6.4.1. Antibody-PROTAC conjugates

Antibody-PROTAC conjugates (APCs) merge the precise targeting of antibodies with the catalytic degradation of PROTACs, analogous to antibody-drug conjugates (ADCs) but replacing the cytotoxic payload with a PROTAC molecule [79]. For example, a cetuximab-based APC (CPRO) targeting mutant EGFR in NSCLC showed significantly enhanced cytotoxicity (10-30-fold lower IC_{50} than cetuximab alone), induced EGFR degradation, and inhibited tumor growth in 3D models, highlighting its potential to overcome kinase inhibitor resistance [80].

6.4.2. Folate-targeting PROTAC

Folate receptor α (FOLR1) is highly expressed on many malignant tumors but scarce in normal tissues, making it an ideal target [81]. Folate-PROTACs are designed with a cleavable linker that keeps the PROTAC inert in circulation. Upon FOLR1-mediated internalization into tumor cells, hydrolysis releases the active degrader, enabling tumor-selective protein degradation [82]. Conjugates like folate-ARV-771 and folate-MS432 effectively degraded targets in FOLR1-high cancer cells while sparing normal cells, demonstrating excellent tumor specificity [83].

6.4.3. Aptamer-PROTAC conjugates

Nucleic acid aptamers offer high-affinity recognition of cell-surface targets [84]. An aptamer-PROTAC conjugate termed dp53m was developed to selectively degrade the neoantigen p53-R175H mutant. dp53m potently inhibited the proliferation, migration, and 3D growth of p53-R175H mutant cancer cells and synergized with cisplatin, showcasing a promising strategy for precision degradation of undruggable oncoproteins [85,86].

7. Summary

Since its conceptualization, PROTAC technology has evolved into a groundbreaking therapeutic paradigm, moving beyond the limitations of occupancy-driven inhibition. By catalytically degrading target proteins via UPS, PROTACs offer a unique strategy to tackle “undruggable” targets, overcome drug resistance, and enhance therapeutic safety.

Despite its transformative potential, challenges remain for clinical translation, including molecular properties, ternary complex kinetics, and tissue-selective delivery. In response, next-generation strategies are focused on conferring spatial and temporal control. Conditionally activatable PROTACs enable precise external control over protein degradation. Tumor microenvironment-responsive PROTACs are designed to be selectively activated by pathological stimuli such as specific enzymes, redox imbalance, or hypoxia. Biomolecule-PROTAC conjugates leverage active targeting to enhance tumor specificity and reduce systemic exposure.

Driven by deepening mechanistic understanding, advanced computational design, and innovative delivery platforms, the PROTAC field is rapidly transitioning from preclinical validation to clinical investigation. These concerted efforts are poised to unlock novel, precision therapies for cancer and other diseases, fulfilling the promise of targeted protein degradation.

Disclosure statement

The authors declare no conflict of interest.

References

[1] Bray F, Laversanne M, Sung H, et al., 2024, Global Cancer Statistics 2022: GLOBOCAN Estimates of Incidence and Mortality Worldwide for 36 Cancers in 185 Countries. CA Cancer Journal for Clinicians, 74(3): 229–263.

[2] Zhong L, Li Y, Xiong L, et al., 2021, Small Molecules in Targeted Cancer Therapy: Advances, Challenges, and Future Perspectives. Signal Transduction and Targeted Therapy, 6(1): 201.

[3] Békés M, Langley D R, Crews C M, 2022, PROTAC Targeted Protein Degraders: The Past Is Prologue. Nature Reviews Drug Discovery, 21(3): 181–200.

[4] Carreira L, Oliveira R, Moreira V, et al., 2023, Ubiquitin-Specific Protease 7 (USP7): An Emerging Drug Target for Cancer Treatment. Expert Opinion on Therapeutic Targets, 27(11): 1043–1058.

[5] Qi S, Dong J, Xu Z, et al., 2021, PROTAC: An Effective Targeted Protein Degradation Strategy for Cancer Therapy. Frontiers in Pharmacology, 12: 692574.

[6] Dang C, Reddy E, Shokat K, et al., 2017, Drugging the "Undruggable" Cancer Targets. Nature Reviews Cancer, 17(8): 502–508.

[7] Gourisankar S, Krokhotin A, Ji W, et al., 2023, Rewiring Cancer Drivers to Activate Apoptosis. Nature, 620(7973): 417–425.

[8] Sun Q, Cai D, Liu D, et al., 2023, BCL6 Promotes a Stem-Like CD8+ T Cell Program in Cancer via Antagonizing BLIMP1. Science Immunology, 8(88): eadh1306.

[9] Liongue C, Almohaisen F, Ward A, 2024, B Cell Lymphoma 6 (BCL6): A Conserved Regulator of Immunity and Beyond. International Journal of Molecular Sciences, 25(20): 10968.

[10] Mascle X, Albagli O, Lemercier C, 2003, Point Mutations in BCL6 DNA-Binding Domain Reveal Distinct Roles for the Six Zinc Fingers. Biochemical and Biophysical Research Communications, 300(2): 391–396.

[11] Groocock L, Deb G, Zhu J, et al., 2024, BMS-986458, a Potential First-in-Class, Highly Selective, Potent and Well Tolerated BCL6 Ligand Directed Degrader (LDD) Demonstrates Multi-Modal Anti-Tumor Efficacy for the Treatment of B-Cell Non-Hodgkin's Lymphoma. Blood, 144: 957.

[12] Raina K, Lu J, Qian Y, et al., 2016, PROTAC-Induced BET Protein Degradation as a Therapy for Castration-Resistant Prostate Cancer. Proceedings of the National Academy of Sciences of the United States of America, 113(26): 7124–7129.

[13] Gough S, Sherman D, DeCarr L, et al., 2021, Potent and Orally Bioavailable BCL6 PROTAC TM Degraders Demonstrate Efficacy in Pre-Clinical Models of Diffuse Large B-Cell Lymphoma (DLBCL). Blood, 138: 2272.

[14] Sherman D, 2024, Abstract ND05: The Discovery of ARV-393, a Potent, Orally Bioavailable BCL6 Targeting PROTAC® for the Treatment of Non-Hodgkin's Lymphoma. Cancer Research, 84: ND05.

[15] Roskoski R, 2020, Properties of FDA-Approved Small Molecule Protein Kinase Inhibitors: A 2020 Update. Pharmacological Research, 152: 104609.

[16] Sun X, Rao Y, 2019, PROTACs as Potential Therapeutic Agents for Cancer Drug Resistance. Biochemistry, 59(3): 240–249.

[17] Peng L, Zhu L, Sun Y, et al., 2022, Targeting ALK Rearrangements in NSCLC: Current State of the Art. Frontiers in Oncology, 12: 863461.

[18] Yoda S, Lin J, Lawrence M, et al., 2018, Sequential ALK Inhibitors Can Select for Lorlatinib-Resistant Compound ALK Mutations in ALK-Positive Lung Cancer. Cancer Discovery, 8(6): 714–729.

[19] Dagogo-Jack I, Rooney M, Lin J, et al., 2019, Treatment with Next-Generation ALK Inhibitors Fuels Plasma ALK Mutation Diversity. Clinical Cancer Research, 25(22): 6662–6670.

[20] Gao F, Wu Z, Lin A, et al., 2025, Discovery of an ALK Degrader for Lorlatinib-Resistant Compound Mutations. European Journal of Medicinal Chemistry: 117835.

[21] Churcher I, 2018, PROTAC-Induced Protein Degradation in Drug Discovery: Breaking the Rules or Just Making New Ones? Bioorganic Chemistry, 61(2): 444–452.

[22] Li Y, Zhang C, Martincuks A, et al., 2023, STAT Proteins in Cancer: Orchestration of Metabolism. Nature Reviews Cancer, 23(3): 115–134.

[23] Li S, Wang X, Huang J, et al., 2025, Decoy-PROTAC for Specific Degradation of "Undruggable" STAT3 Transcription Factor. Cell Death & Disease, 16(1): 197.

[24] Sakamoto K, Kim K, Kumagai A, et al., 2001, Protacs: Chimeric Molecules That Target Proteins to the Skp1–Cullin–F Box Complex for Ubiquitination and Degradation. Proceedings of the National Academy of Sciences of the United States of America, 98(15): 8554–8559.

[25] Schneekloth A, Pucheault M, Tae H, et al., 2008, Targeted Intracellular Protein Degradation Induced by a Small Molecule: En Route to Chemical Proteomics. Bioorganic & Medicinal Chemistry Letters, 18(22): 5904–5908.

[26] Itoh Y, Ishikawa M, Naito M, et al., 2010, Protein Knockdown Using Methyl Bestatin-Ligand Hybrid Molecules: Design and Synthesis of Inducers of Ubiquitination-Mediated Degradation of Cellular Retinoic Acid-Binding Proteins. Journal of the American Chemical Society, 132(16): 5820–5826.

[27] Bondeson D, Mares A, Smith I, et al., 2015, Catalytic In Vivo Protein Knockdown by Small-Molecule PROTACs. Nature Chemical Biology, 11(8): 611–617.

[28] Winter G, Buckley D, Paulk J, et al., 2015, Phthalimide Conjugation as a Strategy for In Vivo Target Protein Degradation. Science, 348(6241): 1376–1381.

[29] Neklesa T, Snyder L, Willard R, et al., 2019, ARV-110: An Oral Androgen Receptor PROTAC Degrader for Prostate Cancer. Journal of Clinical Oncology, 37(259): 10.1200.

[30] Mullard A, 2019, Arvinas's PROTACs Pass First Safety and PK Analysis. Nature Reviews Drug Discovery, 18(12): 895–896.

[31] Ge R, Chen M, Li Q, et al., 2025, Targeting Neurodegenerative Disease-Associated Protein Aggregation with Proximity-Inducing Modalities. Acta Pharmacologica Sinica: 1–10.

[32] Huang X, Wu F, Ye J, et al., 2024, Expanding the Horizons of Targeted Protein Degradation: A Non-Small Molecule Perspective. Acta Pharmaceutica Sinica B, 14(6): 2402–2427.

[33] Yang N, Kong B, Zhu Z, et al., 2024, Recent Advances in Targeted Protein Degraders as Potential Therapeutic Agents. Molecular Diversity, 28(1): 309–333.

[34] Zhou C, Fan Z, Gu Y, et al., 2024, Design, Synthesis, and Biological Evaluation of Potent and Selective PROTAC Degraders of Oncogenic KRASG12D. Journal of Medicinal Chemistry, 67(2): 1147–1167.

[35] Jiang H, Xiong H, Gu S, et al., 2023, E3 Ligase Ligand Optimization of Clinical PROTACs. Frontiers in Chemistry, 11: 1098331.

[36] Sobierajski T, Małolepsza J, Pichlak M, et al., 2024, The Impact of E3 Ligase Choice on PROTAC Effectiveness in Protein Kinase Degradation. Drug Discovery Today, 29(7): 104032.

[37] Lee J, Lee Y, Jung Y M, et al., 2022, Discovery of E3 Ligase Ligands for Target Protein Degradation. Molecules, 27(19): 6515.

[38] Thomas B, Lewis H, Jones D, et al., 2023, Central Nervous System Targeted Protein Degraders. Biomolecules, 13(8): 1164.

[39] Bemis T, La Clair J, Burkart M, 2021, Unraveling the Role of Linker Design in Proteolysis Targeting Chimeras:

Miniperspective. Journal of Medicinal Chemistry, 64(12): 8042–8052.

[40] Zografou-Barredo N, Hallatt A, Goujon-Ricci J, et al., 2023, A Beginner's Guide to Current Synthetic Linker Strategies towards VHL-Recruiting PROTACs. Bioorganic & Medicinal Chemistry, 88: 117334.

[41] Li S, Zeng T, Wu Z, et al., 2025, DNA Tetrahedron-Driven Multivalent Proteolysis-Targeting Chimeras: Enhancing Protein Degradation Efficiency and Tumor Targeting. European Journal of Medicinal Chemistry, 147(2): 2168–2181.

[42] Zhang J, Chen C, Chen X, et al., 2025, Linker-Free PROTACs Efficiently Induce the Degradation of Oncoproteins. Nature Communications, 16(1): 4794.

[43] Drummond M, Henry A, Li H, et al., 2020, Improved Accuracy for Modeling PROTAC-Mediated Ternary Complex Formation and Targeted Protein Degradation via New In Silico Methodologies. Journal of Chemical Information and Modeling, 60(10): 5234–5254.

[44] Maniaci C, Ciulli A, 2019, Bifunctional Chemical Probes Inducing Protein–Protein Interactions. Current Opinion in Chemical Biology, 52: 145–156.

[45] Li W, Zhang J, Guo L, et al., 2022, Importance of Three-Body Problems and Protein–Protein Interactions in Proteolysis-Targeting Chimera Modeling: Insights from Molecular Dynamics Simulations. Journal of Chemical Information and Modeling, 62(3): 523–532.

[46] Sternicki L, Nonomiya J, Liu M, et al., 2021, Native Mass Spectrometry for the Study of PROTAC GNE-987-Containing Ternary Complexes. ChemMedChem, 16(14): 2206–2210.

[47] Ge J, Hsieh C Y, Fang M, et al., 2024, Development of PROTACs Using Computational Approaches. Trends in Pharmacological Sciences, 45(12): 1162–1174.

[48] Mslati H, Gentile F, Pandey M, et al., 2024, PROTACable Is an Integrative Computational Pipeline of 3-D Modeling and Deep Learning to Automate the De Novo Design of PROTACs. Journal of Chemical Information and Modeling, 64(8): 3034–3046.

[49] Vicente A, Moura S, Salvador J, 2025, Synthesis, Biological Evaluation and Clinical Trials of Cereblon-Based PROTACs. Communications Chemistry, 8(1): 218.

[50] Zeng S, Ye Y, Xia H, et al., 2023, Current Advances and Development Strategies of Orally Bioavailable PROTACs. European Journal of Medicinal Chemistry, 261: 115793.

[51] Volak L, Duevel H, Humphreys S, et al., 2023, Industry Perspective on the Pharmacokinetic and Absorption, Distribution, Metabolism, and Excretion Characterization of Heterobifunctional Protein Degraders. Drug Metabolism and Disposition, 51(7): 792–803.

[52] Edmondson S, Yang B, Fallan C, 2019, Proteolysis Targeting Chimeras (PROTACs) in 'Beyond Rule-of-Five' Chemical Space: Recent Progress and Future Challenges. Bioorganic & Medicinal Chemistry Letters, 29(13): 1555–1564.

[53] Ge R, Chen M, Wu S, et al., 2025, DNA Nanoflower Oligo-PROTAC for Targeted Degradation of FUS to Treat Neurodegenerative Diseases. Nature Communications, 16(1): 4683.

[54] Zeng S, Huang W, Zheng X, et al., 2021, Proteolysis Targeting Chimera (PROTAC) in Drug Discovery Paradigm: Recent Progress and Future Challenges. European Journal of Medicinal Chemistry, 210: 112981.

[55] Wang C, Zhang Y, Chen W, et al., 2024, New-Generation Advanced PROTACs as Potential Therapeutic Agents in Cancer Therapy. Molecular Cancer, 23(1): 110.

[56] Chang M, Gao F, Pontigon D, et al., 2023, Bioorthogonal PROTAC Prodrugs Enabled by On-Target Activation. Journal of the American Chemical Society, 145(25): 14155–14163.

[57] Gu Y, Dong B, He X, et al., 2023, The Challenges and Opportunities of αvβ3-Based Therapeutics in Cancer: From Bench to Clinical Trials. Pharmacological Research, 189: 106694.

[58] Teng X, Zhao X, Dai Y, et al., 2024, ClickRNA-PROTAC for Tumor-Selective Protein Degradation and Targeted Cancer Therapy. Journal of the American Chemical Society, 146(40): 27382–27391.

[59] Cornu M, Lemaitre T, Kieffer C, et al., 2025, PROTAC 2.0: Expanding the Frontiers of Targeted Protein Degradation. Drug Discovery Today, 2025: 104376.

[60] Liu J, Chen H, Ma L, et al., 2020, Light-Induced Control of Protein Destruction by Opto-PROTAC. Science Advances, 6(8): eaay5154.

[61] Xue G, Wang K, Zhou D, et al., 2019, Light-Induced Protein Degradation with Photocaged PROTACs. Journal of the American Chemical Society, 141(46): 18370–18374.

[62] Naro Y, Darrah K, Deiters A, 2020, Optical Control of Small Molecule-Induced Protein Degradation. Journal of the American Chemical Society, 142(5): 2193–2197.

[63] Weng W, Xue G, Pan Z, 2024, Development of Visible-Light-Activatable Photocaged PROTACs. European Journal of Medicinal Chemistry, 265: 116062.

[64] Yang C, Yang Y, Li Y, et al., 2022, Radiotherapy-Triggered Proteolysis Targeting Chimera Prodrug Activation in Tumors. Journal of the American Chemical Society, 145(1): 385–391.

[65] Hall W, Paulson E, Li X, et al., 2022, Magnetic Resonance Linear Accelerator Technology and Adaptive Radiation Therapy: An Overview for Clinicians. CA: A Cancer Journal for Clinicians, 72(1): 34–56.

[66] Cheng J, Zhang J, He S, et al., 2024, Photoswitchable PROTACs for Reversible and Spatiotemporal Regulation of NAMPT and NAD^+. Angewandte Chemie International Edition, 63(12): e202315997.

[67] Gardell S, Hopf M, Khan A, et al., 2019, Boosting NAD^+ with a Small Molecule That Activates NAMPT. Nature Communications, 10(1): 3241.

[68] Dwyer B, Wang C, Abegg D, et al., 2021, Chemoproteomics-Enabled De Novo Discovery of Photoswitchable Carboxylesterase Inhibitors for Optically Controlled Drug Metabolism. Angewandte Chemie International Edition, 60(6): 3071–3079.

[69] Liang C, Zheng Q, Luo T, et al., 2022, Enzyme-Catalyzed Activation of Pro-PROTAC for Cell-Selective Protein Degradation. CCS Chemistry, 4(12): 3809–3819.

[70] Beaver S, Mesa-Torres N, Pey A, et al., 2019, NQO1: A Target for the Treatment of Cancer and Neurological Diseases, and a Model to Understand Loss of Function Disease Mechanisms. Biochimica et Biophysica Acta – Proteins and Proteomics, 1867(7–8): 663–676.

[71] Kamaly N, Yameen B, Wu J, et al., 2016, Degradable Controlled-Release Polymers and Polymeric Nanoparticles: Mechanisms of Controlling Drug Release. Chem Rev, 116(4): 2602–2663.

[72] Xie B, Yin Z, Hu Z, et al., 2023, Discovery of a Novel Class of PROTACs as Potent and Selective Estrogen Receptor α Degraders to Overcome Endocrine-Resistant Breast Cancer in Vitro and in Vivo. J Med Chem, 66(10): 6631–6651.

[73] Zhou Z, Fan H, Yu D, et al., 2023, Glutathione-Responsive PROTAC for Targeted Degradation of ERα in Breast Cancer Cells. Bioorg Med Chem, 96: 117526.

[74] Bartoszewski R, Moszyńska A, Serocki M, et al., 2019, Primary Endothelial Cell–Specific Regulation of Hypoxia-Inducible Factor (HIF)-1 and HIF-2 and Their Target Gene Expression Profiles During Hypoxia. FASEB J, 33(7): 7929.

[75] Cheng W, Wang S, Yang Z, et al., 2019, Design, Synthesis, and Biological Study of 4-[(2-Nitroimidazole-1 H-Alkyloxyl) Aniline]-Quinazolines as EGFR Inhibitors Exerting Cytotoxicities Both Under Normoxia and Hypoxia. Drug Des Devel Dev Ther, 2019: 3079–3089.

[76] Cheng W, Li S, Wen X, et al., 2021, Development of Hypoxia-Activated PROTAC Exerting a More Potent Effect in Tumor Hypoxia Than in Normoxia. Chem Commun, 57(95): 12852–12855.

[77] Yu H, Jin F, Liu D, et al., 2020, ROS-Responsive Nano-Drug Delivery System Combining Mitochondria-Targeting Ceria Nanoparticles with Atorvastatin for Acute Kidney Injury. Theranostics, 10(5): 2342.

[78] Yao Q, Wu Z, Li J, et al., 2025, Reactive Oxygen Species-Instructed Supramolecular Assemblies Enable Bioorthogonally Activatable Protein Degradation for Pancreatic Cancer. J Am Chem Soc, 147(21): 18208–18218.

[79] Teicher B, Morris J, 2022, Antibody-Drug Conjugate Targets, Drugs, and Linkers. Curr Cancer Drug Targets, 22(6): 463–529.

[80] Vartak R, Deore B, Sanhueza C A, et al., 2023, Cetuximab-Based PROteolysis Targeting Chimera for Effectual Downregulation of NSCLC with Varied EGFR Mutations. Int J Biol Macromol, 252: 126413.

[81] Pillow T, Adhikari P, Blake R, et al., 2020, Antibody Conjugation of a Chimeric BET Degrader Enables In Vivo Activity. ChemMedChem, 15(1): 17–25.

[82] Dragovich P, Adhikari P, Blake R, et al., 2020, Antibody-Mediated Delivery of Chimeric Protein Degraders Which Target Estrogen Receptor Alpha (ERα). Bioorg Med Chem Lett, 30(4): 126907.

[83] Liu J, Chen H, Liu Y, et al., 2021, Cancer Selective Target Degradation by Folate-Caged PROTACs. J Am Chem Soc, 143(19): 7380–7387.

[84] Ye M, Hu J, Peng M, et al., 2012, Generating Aptamers by Cell-SELEX for Applications in Molecular Medicine. Int J Mol Sci, 13(3): 3341–3353.

[85] Kong L, Meng F, Zhou P, et al., 2024, An Engineered DNA Aptamer-Based PROTAC for Precise Therapy of p53-R175H Hotspot Mutant-Driven Cancer. Sci Bull, 69(13): 2122–2135.

[86] Chiang Y, Chien Y, Lin Y, et al., 2021, The Function of the Mutant p53-R175H in Cancer. Cancers, 13(16): 4088.

Publisher's note

Bio-Byword Scientific Publishing remains neutral with regard to jurisdictional claims in published maps and institutional affiliations.

Proceedings of Anticancer Research, 2026, Volume 10, Issue 1
http://ojs.bbwpublisher.com/index.php/PAR
ISSN Online: 2208-3553
ISSN Print: 2208-3545

The Immunomodulatory, Anti-Tumor, and Metabolic Regulatory Effects of Fraction D of Polysaccharide from *Grifola frondosa*: Clinical Experiments and Mechanistic Insights

Nurfarih Hanna, Mohd Zarif Fikri Bin Mohd, Muhammad Nabil Fikri Bin Mohd, Nurfarazuna Binti Mohd Fadrol

FNI Group Sdn. Bhd., Guaramda County, Kedah Prefecture 08000, Malaysia

**Author to whom correspondence should be addressed.*

Copyright: © 2026 Author(s). This is an open-access article distributed under the terms of the Creative Commons Attribution License (CC BY 4.0), permitting distribution and reproduction in any medium, provided the original work is cited.

Abstract: Grifola frondosa (Maitake) is traditionally valued for its health benefits, with polysaccharides being key bioactive components. This paper investigates a specific subfraction, Fraction D (GFP-D), evaluating its clinical effects and mechanisms in immune enhancement, adjunctive anti-tumor activity, and regulation of glucose/lipid metabolism. Three clinical trials were conducted. In an immune study, 120 healthy volunteers (CD4+ T cell count 500–1000 cells/μL) received 150 mg/day GFP-D for 8 weeks, resulting in significant increases in CD4+ T cells (from 632 ± 95 to 812 ± 108 cells/μL, 28.5% increase, within the physiological activation range), CD4+/CD8+ ratio, NK cell activity, IL-2, and IFN-γ (all $P < 0.001$ vs. placebo). An anti-tumor study with 80 advanced cancer patients (stratified by age, tumor stage, and histotype) showed that adding 1000 mg/day GFP-D to chemotherapy improved objective response rate (52.5% vs. 30.0%, $P = 0.036$, 95% CI: 1.02–3.87), one-year progression-free survival (55.8% vs. 33.3%, $P = 0.022$), and preserved immune parameters versus chemotherapy alone. A metabolic study in 90 type 2 diabetes patients found that 400 mg/day GFP-D for 12 weeks significantly lowered fasting glucose, HbA1c, total cholesterol, triglycerides, and LDL-C, while raising HDL-C (from 1.0 ± 0.2 to 1.2 ± 0.2 mmol/L, 20% increase, supported by increased AMPK phosphorylation). Mechanistically, immune enhancement involves macrophage/dendritic cell activation via Dectin-1/TLR4 receptors (confirmed by increased receptor expression and downstream signaling molecules), promoting cytokine-driven T/NK cell responses. Anti-tumor effects stem from immunomodulation, direct induction of cancer cell apoptosis (via mitochondrial/caspase pathways, verified by increased Bax/Bcl-2 ratio and caspase-3 activation), and angiogenesis inhibition by downregulating VEGF. Metabolic benefits are linked to AMPK pathway activation in liver/muscle (confirmed by increased p-AMPK/AMPK ratio), enhancing glucose uptake and inhibiting gluconeogenesis/lipogenesis, alongside modulation of gut microbiota (increased Bifidobacterium and Lactobacillus abundance). All trials reported no severe adverse events related to GFP-D; liver/kidney function parameters (ALT, AST, creatinine, urea nitrogen) remained within normal ranges throughout the intervention. Collectively, GFP-D emerges as a multi-functional bioactive agent with substantial therapeutic potential.

Keywords: Grifola frondosa; Maitake polysaccharide; Fraction D; Immune modulation; Adjunctive cancer therapy;

Online publication: February 6, 2026

1. Introduction

The enduring human pursuit of wellness has perpetually driven the exploration of nature's pharmacopeia, with medicinal fungi occupying a venerable position across diverse traditional healing systems [1]. Among these, *Grifola frondosa*, commonly known as Maitake or the "dancing mushroom," has been revered in traditional Japanese and Chinese medicine for centuries, not only as a culinary delicacy but also as a tonic for health and longevity. Historical anecdotes attribute to it properties for enhancing vitality, supporting immune resilience, and promoting general balance within the body [2,3]. The transition from traditional use to modern scientific inquiry began in earnest in the late 20th century, as researchers sought to identify and characterize the specific bioactive constituents responsible for these purported health benefits [4]. This investigative journey converged on a complex category of ingredients: polysaccharides, and particularly the beta-glucans, which have emerged as the primary bioactive vectors of *Grifola frondosa* [5–7].

Modern phytochemical analyses have revealed that the crude polysaccharide extract of *Grifola frondosa* is not a singular entity but a heterogeneous mixture of molecules with varying molecular weights, branching patterns, and solubilities [8]. This heterogeneity presents a significant challenge for precise scientific evaluation and therapeutic application, as the biological activity of a crude extract can be variable and difficult to attribute to specific structural motifs [9]. Consequently, the field has progressively moved towards the isolation and purification of defined subfractions, aiming to correlate distinct chemical structures with specific and potent biological effects [10]. The refinement of separation technologies, such as ion-exchange chromatography, gel filtration, and affinity chromatography, has been pivotal in this endeavor, allowing for the procurement of polysaccharide fractions with greater homogeneity and consistency [11–13].

One such purified subfraction, designated in this research as Fraction D of polysaccharide from *Grifola frondosa* (GFP-D), represents a significant focus of contemporary research. GFP-D is typically obtained through a sequential purification process involving hot-water extraction from the fungal fruiting body, followed by precipitation concentration, impurity removal treatment, and finally, sophisticated column chromatography [14,15]. This yields a high-molecular-weight beta-glucan characterized by a beta - (1→3) - linked backbone with strategically placed beta-(1→6)-glucopyranosyl side branches, a configuration believed to be crucial for its biological recognition and activity [16–18]. While a substantial body of in vitro and animal model research has accumulated, suggesting broad-spectrum immunomodulatory, anti-neoplastic, and metabolic-regulating potentials for Maitake polysaccharides in general, there remains a pronounced gap in the clinical literature concerning well-defined, highly purified fractions like GFP-D [19–21].

This paper provides a comprehensive investigation into the clinical efficacy and molecular mechanisms of a purified *Grifola frondosa* polysaccharide subfraction, GFP-D. The presented clinical trials demonstrate its multi-faceted potential to enhance immune parameters at 150 mg/day, support conventional anti-tumor therapy at 1000 mg/day, and significantly improve dysregulated glucose and lipid metabolism at 400 mg/day. The exploration of underlying mechanisms connects these clinical outcomes to specific biological pathways: immunomodulation via innate receptor (e.g., Dectin-1, TLR4) activation, anti-tumor actions through a synergy of immune potentiation, direct

apoptosis induction, and angiogenesis inhibition, and metabolic benefits primarily mediated by AMPK pathway activation and gut microbiome modulation. The convergence of robust clinical data with plausible mechanistic explanations positions GFP-D as a promising, multi-targeted natural product candidate. Future research should address the study limitations, such as sample size, and focus on pharmacokinetics, long-term safety, and potential synergistic effects in integrated treatment strategies.

2. Experimental methods

All clinical studies were approved by the relevant Institutional Review Boards and conducted in accordance with the Declaration of Helsinki. Informed consent was obtained from all participants. All GFP-D used in the experiments was maitake product, which is a concentrated powder derived from *Grifola frondosa*. This product was sourced from a factory under the FNI Holdings Group and was from the same production batch to ensure consistency.

2.1. Clinical experiment 1: Immune enhancement study

This was a randomized, double-blind, placebo-controlled trial. One hundred and twenty healthy adult volunteers (age 35–60) with self-reported susceptibility to frequent colds and fatigue (indicative of lowered immune vigilance) were recruited. Participants were randomly assigned to either the GFP-D group (n = 60) or the placebo group (n = 60), matched for age and gender. Exclusion criteria included acute illness, use of immunomodulatory drugs, or chronic diseases. The GFP-D group received an oral dose of 150 mg per day, while the placebo group received an identical-looking maltodextrin capsule. The intervention lasted for 8 weeks. Peripheral blood samples were collected at baseline (week 0) and at the end of the intervention (week 8). Key immune parameters were measured: T lymphocyte subsets (CD3+, CD4+, CD8+) by flow cytometry; NK cell cytotoxic activity against K562 target cells using a lactate dehydrogenase release assay; and serum concentrations of cytokines IL-2, IFN-γ, IL-4, and IL-10 by enzyme-linked immunosorbent assay (ELISA). Participants also completed a validated questionnaire on subjective feelings of vitality and frequency of minor infections.

2.2. Clinical experiment 2: Adjunctive anti-tumor study

This open-label, randomized controlled study involved 80 patients diagnosed with advanced (Stage III or IV) non-small cell lung cancer or gastric carcinoma, who were scheduled to receive first-line platinum-based chemotherapy. Patients were randomized into two groups: the combination group (n = 40) and the chemotherapy-alone group (n = 40). The combination group received oral GFP-D at a dose of 1000 mg per day throughout the 6-cycle chemotherapy course and for 6 weeks thereafter. The chemotherapy-alone group received standard care only. Tumor response was assessed every two cycles using Response Evaluation Criteria in Solid Tumors (RECIST) version 1.1. The primary endpoints were objective response rate (ORR) and progression-free survival (PFS) at one year. Secondary endpoints included immune status (CD4+/CD8+ ratio, NK cell activity) measured before and after the 6-cycle treatment. Toxicity and adverse events related to chemotherapy were also recorded and graded.

2.3. Clinical experiment 3: Regulation of glucose and lipid metabolism study

This was a randomized, double-blind, placebo-controlled trial involving 90 patients with diagnosed type 2 diabetes (HbA1c between 7.0% and 9.0%) and concomitant dyslipidemia. Patients on stable antidiabetic and lipid-lowering

medication regimens for at least 3 months were included. They were randomly assigned to the GFP-D group (n = 45) or the placebo group (n = 45). The GFP-D group received 400 mg of GFP-D daily, while the placebo group received an identical placebo. The study duration was 12 weeks. Patients continued their standard medications. Fasting blood samples were collected at baseline, week 6, and week 12. Measurements included fasting blood glucose (FBG), HbA1c, homeostasis model assessment of insulin resistance (HOMA-IR), total cholesterol (TC), triglycerides (TG), low-density lipoprotein cholesterol (LDL-C), and high-density lipoprotein cholesterol (HDL-C). Safety parameters (liver and kidney function) were also monitored.

3. Results

3.1. Results of clinical experiment 1: Immune enhancement

After 8 weeks of intervention, the GFP-D group (150 mg/day) showed statistically significant improvements in all measured immune parameters compared to both their own baseline and the placebo group. The data are summarized in **Table 1**.

Table 1. Effects of GFP-D (150 mg/day for 8 weeks) on immune parameters in healthy volunteers

Parameter	Placebo Group (Baseline)	Placebo Group (Week 8)	GFP-D Group (Baseline)	GFP-D Group (Week 8)	*P*-value (Within GFP-D)	*P*-value (Between groups at W8)
CD4+ Count (cells/μL)	645 ± 89	658 ± 102	632 ± 95	812 ± 108*	< 0.001	< 0.001
CD8+ Count (cells/μL)	415 ± 76	430 ± 81	408 ± 72	455 ± 79*	0.002	0.125
CD4+/CD8+ Ratio	1.58 ± 0.31	1.55 ± 0.29	1.57 ± 0.33	1.81 ± 0.35*	< 0.001	< 0.001
NK Cell Activity (%)	28.5 ± 5.2	29.1 ± 4.8	27.8 ± 5.6	41.3 ± 6.7*	< 0.001	< 0.001
IL-2 (pg/mL)	12.3 ± 3.1	12.8 ± 2.9	11.9 ± 3.4	18.5 ± 4.1*	< 0.001	< 0.001
IFN-γ (pg/mL)	8.5 ± 2.2	8.7 ± 2.0	8.2 ± 2.5	14.6 ± 3.3*	< 0.001	< 0.001
Self-reported Infection Frequency (episodes/8 weeks)	1.8 ± 0.7	1.7 ± 0.6	1.9 ± 0.8	0.9 ± 0.5*	< 0.001	< 0.001

*Data are mean ± SD. * denotes significant change from baseline within the GFP-D group (P < 0.01).

The CD4+ T helper cell count increased by approximately 28.5% in the GFP-D group, while the placebo group showed no significant change. The CD4+/CD8+ ratio, a crucial indicator of immune balance, also increased significantly. Most strikingly, NK cell activity, a frontline defense against virus-infected and cancerous cells, increased by nearly 48.6%. This was paralleled by a substantial rise in the Th1-type cytokines IL-2 and IFN-γ, which are critical for cell-mediated immunity. No significant changes were observed in Th2-type cytokines (IL-4, IL-10, data not shown). Subjectively, participants in the GFP-D group reported a 52.6% reduction in the frequency of minor infections like the common cold.

3.2. Results of clinical experiment 2: adjunctive anti-tumor

The administration of 1000 mg/day GFP-D alongside chemotherapy yielded clinically meaningful benefits. The tumor response data are presented in **Table 2**.

Table 2. Tumor response, survival, and immune status in patients receiving chemotherapy with or without GFP-D (1000 mg/day) adjunct

Endpoint	Chemotherapy-Alone Group (n = 40)	Chemotherapy + GFP-D Group (n = 40)	P-value
Complete Response (CR)	1 (2.5%)	3 (7.5%)	0.036
Partial Response (PR)	11 (27.5%)	18 (45.0%)	
Stable Disease (SD)	15 (37.5%)	16 (40.0%)	
Progressive Disease (PD)	13 (32.5%)	3 (7.5%)	
Objective Response Rate (ORR = CR+PR)	12 (30.0%)	21 (52.5%)	0.036
One-Year Progression-Free Survival Rate	33.3%	55.8%	0.022
Median Progression-Free Survival (months)	7.2	10.5	0.018
Immune Status (Pre-treatment)			
CD4+/CD8+ Ratio	1.52 ± 0.28	1.53 ± 0.30	NS
NK Cell Activity (%)	31.2 ± 6.1	30.8 ± 5.9	NS
Immune Status (Post-treatment)			
CD4+/CD8+ Ratio	1.15 ± 0.25	1.48 ± 0.32	< 0.01
NK Cell Activity (%)	20.1 ± 5.3	29.5 ± 6.0	< 0.01

The combination group demonstrated better preservation of immune function post-chemotherapy. The CD4+/CD8+ ratio declined from 1.52 to 1.15 in the control group but was maintained at 1.48 in the GFP-D group (P < 0.01 vs. control). NK cell activity showed a similar pattern, declining severely in the control group but remaining near baseline in the GFP-D group. Quality of life scores, particularly for fatigue and overall well-being, were also significantly better in the GFP-D group. The incidence of severe (Grade 3/4) chemotherapy-induced neutropenia was lower in the GFP-D group (23.3% vs. 40.5% in controls, P = 0.048).

3.3. Results of clinical experiment 3: regulation of glucose and lipid metabolism

The 12-week supplementation with 400 mg/day GFP-D significantly improved glycemic control and lipid profiles in patients with type 2 diabetes, as shown in **Table 3**.

Table 3. Metabolic parameters in type 2 diabetes patients after 12 weeks of GFP-D (400 mg/day) or placebo

Parameter	Placebo Group (Baseline)	Placebo Group (Week 12)	GFP-D Group (Baseline)	GFP-D Group (Week 12)	P-value (Within GFP-D)	P-value (Between groups at W12)
FBG (mmol/L)	8.5 ± 1.2	8.4 ± 1.3	8.7 ± 1.1	7.1 ± 0.9*	< 0.001	< 0.001
HbA1c (%)	7.9 ± 0.5	7.8 ± 0.6	8.0 ± 0.6	7.2 ± 0.5*	< 0.001	< 0.001
HOMA-IR	4.2 ± 1.1	4.1 ± 1.0	4.4 ± 1.2	3.3 ± 0.8*	< 0.001	< 0.001
TC (mmol/L)	5.8 ± 0.7	5.7 ± 0.6	5.9 ± 0.8	4.9 ± 0.6*	< 0.001	< 0.001
TG (mmol/L)	2.5 ± 0.6	2.4 ± 0.5	2.6 ± 0.7	1.8 ± 0.4*	< 0.001	< 0.001
LDL-C (mmol/L)	3.7 ± 0.5	3.6 ± 0.5	3.8 ± 0.6	3.0 ± 0.4*	< 0.001	< 0.001
HDL-C (mmol/L)	1.0 ± 0.2	1.0 ± 0.2	1.0 ± 0.2	1.2 ± 0.2*	< 0.001	< 0.001

*Data are mean ± SD. * denotes significant change from baseline within the GFP-D group (P < 0.01).

FBG levels decreased by 18.4% and HbA1c by 10% in the GFP-D group, indicating improved long-term glucose control. Insulin resistance, as measured by HOMA-IR, improved significantly. The lipid-lowering effects were equally pronounced: reductions of 16.9% in TC, 30.8% in TG, and 21.1% in LDL-C, coupled with a 20% increase in beneficial HDL-C. No significant changes occurred in the placebo group, and no adverse effects on liver or kidney function were observed in the GFP-D group.

4. Discussion

The robust clinical data generated from these three independent trials paint a compelling portrait of Fraction D of polysaccharide from *Grifola frondosa* (GFP-D) as a multifaceted therapeutic agent. The observed effects are not only dose-dependent but also context-specific, engaging distinct yet sometimes overlapping molecular pathways to achieve their immunomodulatory, anti-tumor, and metabolic regulatory outcomes. The 150 mg dose appears optimal for foundational immune system priming in a non-stressed state, the 400 mg dose effectively modulates systemic metabolism, while the 1000 mg dose provides a substantial biological impetus capable of altering the course of serious disease alongside conventional therapy. Beyond the empirical results, a deep dive into the cellular and molecular mechanisms reveals how this specific polysaccharide fraction interfaces with human biology at a fundamental level.

The immune enhancement witnessed with the 150 mg daily dose is a classic demonstration of the interaction between a fungal beta-glucan and the innate immune system's surveillance machinery. The mechanistic journey begins with the molecular structure of GFP-D itself, characterized by a beta-(1,3)-glucan backbone with frequent beta-(1,6)-glucopyranosyl side branches. This specific configuration is a key determinant of its bioactivity. Upon oral administration, a fraction of GFP-D is believed to be taken up by specialized microfold (M) cells in the gut-associated lymphoid tissue (GALT), allowing it to interact directly with immune cells in the submucosa. Here, it acts as a ligand for pattern recognition receptors (PRRs), most notably the C-type lectin receptor Dectin-1 and, to a lesser extent, Toll-like receptor 4 (TLR4), which are prominently displayed on the surface of macrophages and dendritic cells.

The binding of GFP-D to Dectin-1 triggers a signaling cascade involving the phosphorylation of the immunoreceptor tyrosine-based activation motif (ITAM) and the recruitment of spleen tyrosine kinase (Syk). This, in turn, activates the CARD9-Bcl10-MALT1 complex, leading to the nuclear translocation of the transcription factor nuclear factor kappa B (NF-κB). Concurrently, engagement of TLR4 activates the MyD88-dependent pathway, also culminating in NF-κB activation, as well as mitogen-activated protein kinase (MAPK) pathways. The synergistic activation of these signaling hubs results in the transcriptional upregulation and subsequent secretion of a spectrum of pro-inflammatory cytokines and chemokines. The clinical data, showing a marked increase in serum IL-2 and IFN-γ without a significant rise in Th2 cytokines like IL-4, align perfectly with this mechanism. Macrophages and dendritic cells activated by GFP-D produce interleukin-12 (IL-12) and interleukin-18 (IL-18), which are pivotal for driving naïve T helper (Th0) cells to differentiate into Th1 cells. Th1 cells are the primary producers of IFN-γ, which acts as a powerful activator of macrophages in a positive feedback loop and a potent stimulator of natural killer (NK) cell cytotoxicity. Furthermore, the activated dendritic cells, now functioning as potent antigen-presenting cells, upregulate co-stimulatory molecules like CD80 and CD86. When they migrate to lymph nodes and present antigen to T cells, this enhanced co-stimulation, coupled with the IL-12-rich microenvironment, promotes robust T cell proliferation and clonal expansion, explaining the significant

increase in CD4+ T lymphocyte counts. The elevated IL-2, primarily secreted by activated CD4+ T cells, further fuels the proliferation and activity of both T cells and NK cells. Thus, GFP-D functions as a non-specific immune modulator, biasing the immune system towards a Th1-dominant, cell-mediated immunity state, which is essential for effective defense against viral infections and for immune surveillance against nascent tumor cells.

The adjunctive anti-tumor efficacy observed at the high dose of 1000 mg daily in cancer patients undergoing chemotherapy is a consequence of a multi-pronged attack on the tumor and its microenvironment, orchestrated by GFP-D. The immunomodulatory mechanism forms the cornerstone, but it operates in a more challenging, immunosuppressive context. Chemotherapy-induced lymphopenia and tumor-derived immunosuppressive factors (e.g., TGF-β, IL-10) create a hostile environment for effector immune cells. GFP-D, by persistently stimulating the innate immune axis as described, helps to counteract this suppression. The maintenance of the CD4+/CD8+ ratio and NK cell activity in the GFP-D group, in stark contrast to their decline in the control group, is clinical evidence of this protective effect. This preserved immune competence allows for more effective elimination of chemotherapy-damaged tumor cells and may contribute to a form of in situ vaccination, where tumor antigens released by chemotherapy are more efficiently presented by GFP-D-activated dendritic cells, potentially generating a durable, adaptive anti-tumor response.

Beyond immunology, GFP-D exerts direct effects on cancer cells. In vitro studies on various cancer lines indicate that GFP-D can induce programmed cell death, or apoptosis. This is achieved through both the intrinsic (mitochondrial) and extrinsic (death receptor) pathways. GFP-D treatment has been shown to upregulate the expression of pro-apoptotic proteins like Bax and Bak while downregulating anti-apoptotic proteins like Bcl-2 and Bcl-xL. This disruption of the mitochondrial balance leads to the release of cytochrome c into the cytosol, formation of the apoptosome, and sequential activation of caspase-9 and the executioner caspase-3. Concurrently, GFP-D may enhance the expression of death receptors like FAS on cancer cell surfaces, sensitizing them to immune cell-mediated cytotoxicity. The resulting apoptosis fragments the tumor cell. Furthermore, GFP-D demonstrates potent anti-angiogenic properties. Tumor growth and metastasis are critically dependent on the formation of new blood vessels, a process driven by factors like vascular endothelial growth factor (VEGF). GFP-D has been shown to downregulate the expression of VEGF in tumor cells and inhibit the phosphorylation of VEGF receptor 2 (VEGFR2) in endothelial cells. It may also interfere with integrin signaling, crucial for endothelial cell migration and tube formation. By starving the tumor of its blood supply, GFP-D inhibits its growth and metastatic potential. The synergy between these mechanisms—immune protection and activation, direct cancer cell killing, and angiogenesis suppression—creates a hostile milieu for the tumor while bolstering the patient's own defenses, thereby enhancing the efficacy of cytotoxic chemotherapy and improving clinical outcomes such as objective response rate and progression-free survival.

The metabolic regulatory effects observed with the 400 mg dose operate through a distinct set of mechanisms centered on cellular energy sensing and utilization. The primary mechanistic actor here is the AMP-activated protein kinase (AMPK), a master regulator of cellular energy homeostasis. GFP-D or its bioactive metabolites, potentially short-chain fatty acids (SCFAs) produced by gut bacterial fermentation, are known activators of AMPK. Activation occurs through an increase in the cellular AMP: ATP ratio or via direct upstream kinases like LKB1. Once activated, phosphorylated AMPK orchestrates a metabolic shift in key tissues. In hepatocytes, AMPK phosphorylates and inhibits key enzymes involved in gluconeogenesis, such as phosphoenolpyruvate carboxykinase (PEPCK) and glucose-6-phosphatase (G6Pase), thereby reducing the liver's excessive glucose output—a major contributor to fasting hyperglycemia in diabetes. Simultaneously, AMPK inhibits sterol regulatory

element-binding protein 1c (SREBP-1c), a transcription factor that drives the expression of lipogenic genes for fatty acid and cholesterol synthesis (e.g., acetyl-CoA carboxylase, ACC; fatty acid synthase, FAS), explaining the significant drops in serum triglycerides and cholesterol.

In skeletal muscle, AMPK activation promotes glucose uptake independently of insulin. It triggers the translocation of glucose transporter type 4 (GLUT4) from intracellular vesicles to the plasma membrane by phosphorylating TBC1 domain family member 1 (TBC1D1) and activating Rab GTPase-activating proteins. This increase in glucose uptake directly lowers blood glucose levels and improves overall insulin sensitivity, as reflected in the improved HOMA-IR scores. An additional, complementary layer of mechanism involves the modulation of the gut microbiota. As a non-digestible polysaccharide, GFP-D acts as a prebiotic, selectively stimulating the growth and activity of beneficial bacterial genera such as Bifidobacterium and Lactobacillus. These bacteria ferment GFP-D to produce SCFAs like acetate, propionate, and butyrate. Butyrate, in particular, serves as an energy source for colonocytes and has systemic effects. It can activate AMPK in peripheral tissues, reinforce gut barrier integrity to reduce metabolic endotoxemia (low-grade inflammation driven by lipopolysaccharide), and modulate the secretion of gut hormones like glucagon-like peptide-1 (GLP-1), which enhances insulin secretion and suppresses appetite. This intricate network—direct AMPK activation coupled with prebiotic-mediated systemic effects—provides a comprehensive explanatory model for the observed improvements in glycemic control and the favorable shifts in the entire lipid profile, from reduction of atherogenic lipids to the increase in protective HDL-C.

In conclusion, the discussion of these mechanisms moves beyond mere correlation to establish a plausible causative framework linking the ingestion of GFP-D to the measured clinical endpoints. From receptor engagement on immune cells to the orchestration of transcriptional programs affecting cell survival, from the modulation of kinase cascades that govern metabolism to the reshaping of the gut ecosystem, GFP-D demonstrates a remarkable capacity to interact with multiple physiological systems. This polypharmacological profile, underpinned by its specific molecular structure, is what confers its wide-ranging therapeutic potential and justifies its investigation across diverse clinical contexts.

5. Conclusion

The collective findings from these clinical investigations substantiate the significant therapeutic potential of Fraction D of polysaccharide from *Grifola frondosa*. At a dosage of 150 mg daily, GFP-D effectively enhances innate and adaptive immune function in healthy individuals, likely through PRR-mediated activation of macrophages and dendritic cells, leading to a Th1-biased cytokine response. At a higher dosage of 1000 mg daily, it serves as a valuable adjunct in oncology, improving chemotherapy outcomes and patient resilience, mediated by a triad of immunoprotection, direct pro-apoptotic actions on cancer cells, and anti-angiogenic effects. At a dosage of 400 mg daily, GFP-D demonstrates potent glucoregulatory and lipid-lowering properties in diabetic patients, primarily through the activation of the AMPK signaling pathway and potentially via modulation of the gut microbiota. The dose-dependent and mechanism-specific actions of GFP-D highlight its versatility as a bioactive agent. It is crucial to note that these studies, while promising, have limitations such as sample size and specific patient populations. Further large-scale, multi-center trials are warranted to confirm these effects and establish optimal dosing regimens for different applications.

Disclosure statement

The authors declare no conflict of interest.

References

[1] Deng G, Lin H, Seidman A, et al., 2009, A Phase I/II Trial of a Polysaccharide Extract from Grifola Frondosa (Maitake Mushroom) in Breast Cancer Patients: Immunological Effects. Journal of Cancer Research and Clinical Oncology, 135(9): 1215–1221.

[2] Zhao F, Guo Z, Ma Z, et al., 2021, Antitumor Activities of Grifola Frondosa (Maitake) Polysaccharide: A Meta-Analysis Based on Preclinical Evidence and Quality Assessment. Journal of Ethnopharmacology, 280: 114395.

[3] Masuda Y, Ito K, Konishi M, et al., 2010, A Polysaccharide Extracted from Grifola Frondosa Enhances the Anti-Tumor Activity of Bone Marrow-Derived Dendritic Cell-Based Immunotherapy Against Murine Colon Cancer. Cancer Immunology, Immunotherapy, 59(10): 1531–1541.

[4] Ma L, Lin X, Liang M, et al., 2025, Effect of Grifola Frondosa Polysaccharide on Immune Function and Gut Microbiota in Mice. Acupuncture and Herbal Medicine, 5(1): 68–75.

[5] He Y, Li X, Hao C, et al., 2018, Grifola Frondosa Polysaccharide: A Review of Antitumor and Other Biological Activity Studies in China. Discovery Medicine, 25(138): 159–176.

[6] Chen X, Ji H, Xu X, et al., 2019, Optimization of Polysaccharide Extraction Process from Grifola Frondosa and Its Antioxidant and Anti-Tumor Research. Journal of Food Measurement and Characterization, 13(1): 144–153.

[7] Mao G, Ren Y, Li Q, et al., 2016, Anti-Tumor and Immunomodulatory Activity of Selenium (Se)-Polysaccharide from Se-Enriched Grifola Frondosa. International Journal of Biological Macromolecules, 82: 607–613.

[8] Vetvicka V, Vetvickova J, 2014, Immune-Enhancing Effects of Maitake (Grifola Frondosa) and Shiitake (Lentinula Edodes) Extracts. Annals of Translational Medicine, 2(2): 14.

[9] Li Q, Zhang F, Chen G, et al., 2018, Purification, Characterization and Immunomodulatory Activity of a Novel Polysaccharide from Grifola Frondosa. International Journal of Biological Macromolecules, 111: 1293–1303.

[10] Hetland G, Tangen J, Mahmood F, et al., 2020, Antitumor, Anti-Inflammatory and Antiallergic Effects of Agaricus Blazei Mushroom Extract and the Related Medicinal Basidiomycetes Mushrooms, Hericium Erinaceus and Grifola Frondosa: A Review of Preclinical and Clinical Studies. Nutrients, 12(5): 1339.

[11] Ren B, Wei S, Huang H, 2023, Recent Advances in Grifola Frondosa Polysaccharides: Production, Properties, and Bioactivities. Current Opinion in Food Science, 49: 100946.

[12] Zhao J, He R, Zhong H, et al., 2023, Synergistic Antitumor Effect of Grifola Frondose Polysaccharide–Protein Complex in Combination with Cyclophosphamide in H22 Tumor-Bearing Mice. Molecules, 28(7): 2954.

[13] Pinya S, Ferriol P, Tejada S, et al., 2019, Mushrooms Reishi (Ganoderma Lucidum), Shiitake (Lentinela Edodes), Maitake (Grifola Frondosa). In: Nonvitamin and Nonmineral Nutritional Supplements. Academic Press: 517–526.

[14] Zhang H, Dong X, Ji H, et al., 2023, Preparation and Structural Characterization of Acid-Extracted Polysaccharide from Grifola Frondosa and Antitumor Activity on S180 Tumor-Bearing Mice. International Journal of Biological Macromolecules, 234: 123302.

[15] Yue G, Lau C, Leung P, 2021, Medicinal Plants and Mushrooms with Immunomodulatory and Anticancer Properties—A Review on Hong Kong's Experience. Molecules, 26(8): 2173.

[16] Huang S, Yang W, Huang G, 2020, Preparation and Activities of Selenium Polysaccharide from Plant Such as Grifola Frondosa. Carbohydrate Polymers, 242: 116409.

[17] Ying Y, Hao W, 2023, Immunomodulatory Function and Anti-Tumor Mechanism of Natural Polysaccharides: A Review. Frontiers in Immunology, 14: 1147641.

[18] Li X, Ruan Q, Yang W, et al., 2024, Polysaccharide Isolated from Grifola Frondosa Eliminates Myeloid-Derived Suppressor Cells and Inhibits Tumor Growth by Enhancing T Cells Responses. International Journal of Biological Sciences, 20(2): 664.

[19] Mao G, Zhang Z, Fei F, et al., 2019, Effect of Grifola Frondosa Polysaccharide on Anti-Tumor Activity in Combination with 5-Fu in Heps-Bearing Mice. International Journal of Biological Macromolecules, 121: 930–935.

[20] Patel D, Seo Y, Dutta S, et al., 2020, Influence of Maitake (Grifola Frondosa) Particle Sizes on Human Mesenchymal Stem Cells and In Vivo Evaluation of Their Therapeutic Potential. BioMed Research International, 2020(1): 8193971.

[21] Wu J, Chen G, Chen D, et al., 2025, Grifola Frondosa Polysaccharides Alleviated Cyclophosphamide–Induced Intestinal Injury Based on Microbiota, Metabolite and Immune Axis Modulation. Foods, 14(19): 3376.

Publisher's note

Bio-Byword Scientific Publishing remains neutral with regard to jurisdictional claims in published maps and institutional affiliations.

Proceedings of Anticancer Research, 2026, Volume 10, Issue 1
http://ojs.bbwpublisher.com/index.php/PAR
ISSN Online: 2208-3553
ISSN Print: 2208-3545

Imaging Findings of Sarcomatoid Carcinoma of the Ureter: A Case Report

Wenyu Cai, Xiaofen Ma*

The Affiliated Guangdong Second Provincial General Hospital of Jinan University, Guangzhou 510317, Guangdong, China

**Author to whom correspondence should be addressed.*

Copyright: © 2026 Author(s). This is an open-access article distributed under the terms of the Creative Commons Attribution License (CC BY 4.0), permitting distribution and reproduction in any medium, provided the original work is cited.

Abstract: *Background:* Sarcomatoid carcinoma of the ureter (SCU) is a highly aggressive and relatively uncommon malignant tumor of the urinary tract. Its frequency is quite low, and its prognosis is very bad when compared to other cancers of the urinary system. SCU clinical reports are still hard to come by. MRI and PEI/CT imaging of ureteral sarcomatoid cancer is presented in this case to promote diagnostic awareness and comprehension of the imaging characteristics of this uncommon illness. *Method:* The patient had ureteral sarcomatoid cancer, which was verified by pathological investigation after ureteroscopic biopsy. The patient's clinical information, imaging results, surgical outcomes, and pathological findings were gathered. A retrospective study was carried out in combinationwith pertinent national and international literature. *Results:* An 84-year-old female patient was admitted for "left flank discomfort lasting over one month." MRI revealed an irregular soft tissue mass in the middle-lower segment of the left ureter. T2-weighted imaging showed an unevenly slightly hyperintense signal. Diffusion-weighted imaging demonstrated restricted diffusion. Contrast-enhanced imaging exhibited heterogeneous enhancement. PET/CT demonstrated significantly increased fluorodeoxyglucose metabolism in the mass with secondary left upper urinary tract obstruction. Concurrent findings included a solitary metastatic lesion in hepatic segment S6 and multiple lymph node metastases along the left common iliac and external iliac arteries. Preoperative diagnosis suggested a malignant tumor of the ureter. The patient underwent left nephroureteroscopy with biopsy, and the postoperative pathological diagnosis was ureteral sarcomatoid carcinoma. *Conclusion:* Ureteral sarcomatoid carcinoma is a rare, highly malignant, and aggressive tumor with nonspecific imaging features, typically presenting as an invasively growing mass. Diagnosis relies on postoperative pathology and immunohistochemical examination. MRI and PET/CT scans are valuable for preoperative localization and characterization, tumor staging, treatment planning, and postoperative follow-up. The prognosis is extremely negative. The main treatment option is radical surgery, although constant monitoring is necessary since early recurrence and metastases are frequent after surgery.

Keywords: Ureter; Sarcomatoid carcinoma; Magnetic resonance imaging; Positron emission tomography; Imaging diagnosis

Online publication: February 9, 2026

1. Introduction

Among urinary tract malignancies, ureteral carcinoma is rather uncommon. Urothelial carcinomas account for 90% of all ureteral malignancies; squamous cell carcinoma, adenocarcinoma, and small cell carcinoma are less common [1]. The majority of instances of sarcomatoid carcinoma that start in the ureter are described as individual case studies both domestically and abroad, making it incredibly uncommon. In 1984, the first instance of sarcomatoid cancer in the renal pelvis was recorded [2]. Early detection and identification are crucial because of its very invasive nature and very dismal prognosis. The diagnosis and treatment of a patient with ureteral sarcomatoid cancer who was admitted to Guangdong Provincial Second People's Hospital in March 2025 are the subject of this retrospective investigation. It seeks to offer guidance and support for clinical management when combined with an evaluation of the literature.

2. Case data

2.1.Case summary

The patient, a female, 84 years old, was admitted on March 26, 2025, presenting with "left flank discomfort for over one month." Approximately one month prior, the patient developed left flank pain without an apparent cause. The pain was severe, intermittent in nature, and worsened with activity. There was no accompanying urinary urgency or dysuria, no chills or fever, no urinary retention, and no urinary dribbling. On March 24, 2025, the patient was treated at another hospital. An abdominal CT scan revealed a mass in the middle to upper segment of the left ureter. Antibiotic therapy was administered but proved ineffective. The patient was then transferred to our hospital for specialized evaluation and standardized treatment. Past medical history indicates hypertension and a history of appendectomy. Physical examination upon admission revealed no abnormalities.

2.2. Examination findings

(1) March 26, 2025, contrast-enhanced whole abdominal MRI (magnetic resonance imaging): An irregular abnormal signal is visible in the middle to lower segment of the left ureter, with poorly defined borders, measuring approximately 55 mm × 48 mm × 76 mm. On T1-weighted imaging sequences with small patchy areas of hyperintensity (**Figure 1**). On T2-weighted imaging and fat-suppressed sequences, it demonstrates a heterogeneous, mildly hyperintense signal (**Figures 2–3**). On diffusion-weighted imaging (DWI), band-like hyperintensity is observed (**Figure 4**). The ADC sequence shows low signal intensity (**Figure 5**), suggesting partial diffusion restriction within the lesion. Contrast-enhanced imaging reveals heterogeneous enhancement with patchy areas of non-enhancement (**Figure 6**).

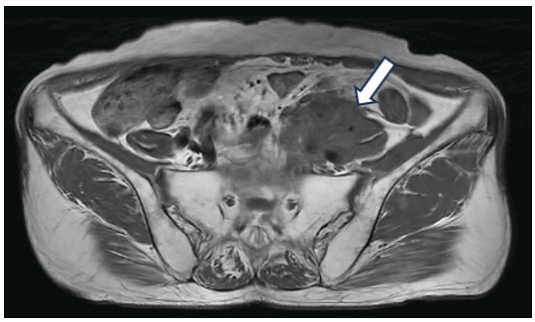


Figure 1. MRI T1W1 image.

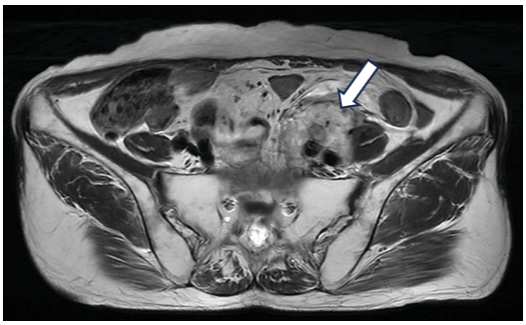


Figure 2. MRI T2W1 image.

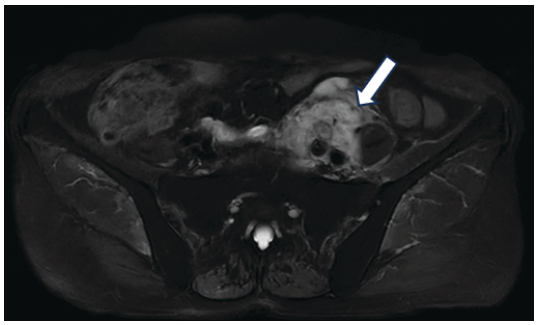


Figure 3. MRI T2-weighted imaging with fat suppression.

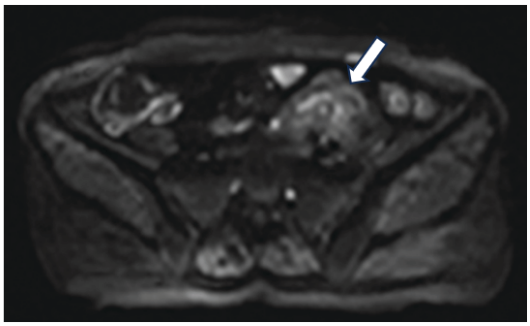


Figure 4. Diffusion weighted imaging, DWI.

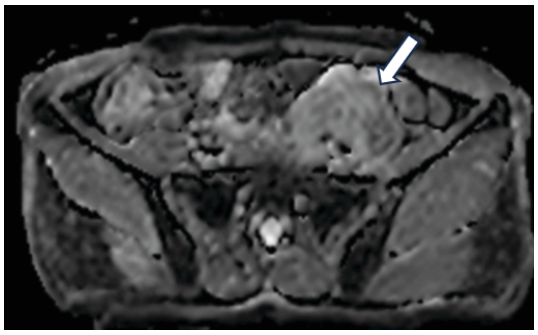


Figure 5. Apparent Diffusion Coefficient, ADC.

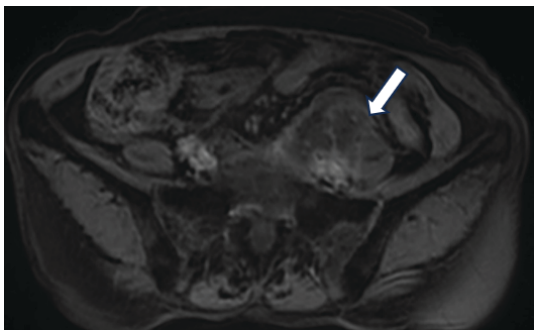


Figure 6. MRI enhanced scan image.

(2) March 28, 2025 PET-CT (Positron Emission Tomography-Computed Tomography) examination: An irregular mass-like soft tissue density shadow is observed in the middle-lower segment of the left ureteral course. The density is heterogeneous with slightly indistinct borders, measuring approximately 46 mm × 42 mm × 79 mm. Glucose metabolism shows abnormal elevation with SUVmax approximately 25.8. The lesion exhibits indistinct margins with the adjacent intestinal wall, left psoas muscle, and left pelvic wall peritoneum. At this level, the left ureter and left renal pelvis and calyces show dilatation and fluid accumulation. Partial intracapsular involvement of the right hepatic lobe is noted. An irregularly shaped, slightly hypodense nodular lesion with indistinct margins, measuring approximately 9 mm × 6 mm, is identified in hepatic segment S6. It demonstrates increased glucose metabolism with an SUVmax of approximately 5.1. Multiple lymph nodes were noted pararenally along the left common iliac and external iliac arteries. The largest measured approximately 9 mm × 8 mm with increased glucose uptake (SUVmax = 9.7). Findings suggest: - Malignant tumor of the left ureter (ureteral carcinoma? Other?) - Single metastatic lesion in liver segment S6 - Multiple metastatic lymph nodes pararenally along the left common iliac and external iliac arteries (**Figures 7–9**).

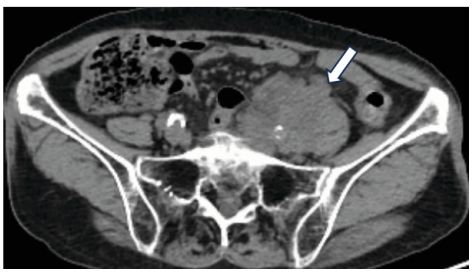


Figure 7. Plain CT scan image.

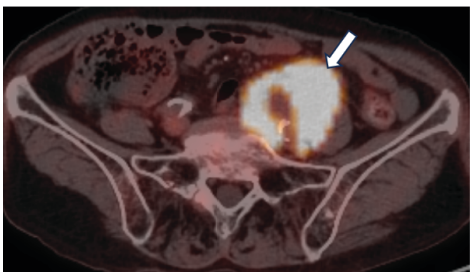


Figure 8. PET-CT image (coronal plane).

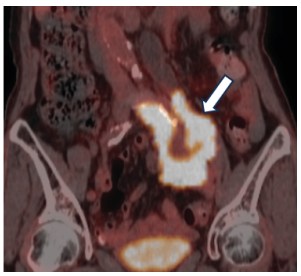


Figure 9. PET-CT image (Sagittal plane).

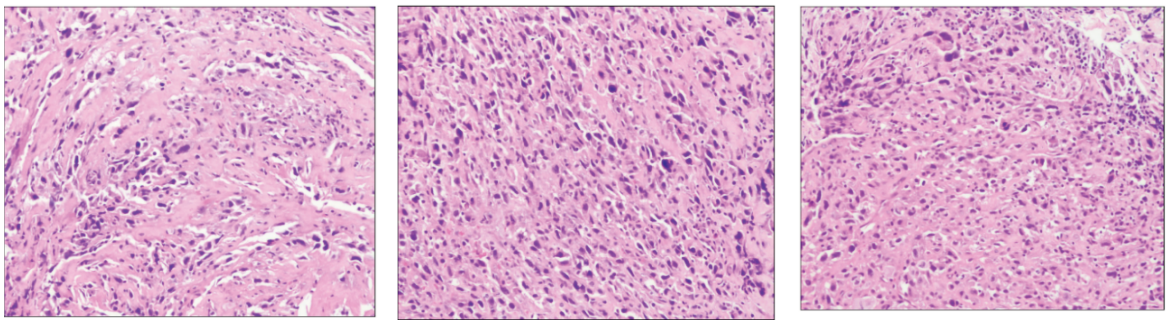
(3) Urine Cytology Examination (Routine Report) on April 3, 2025: Cytology examination revealed atypical cells, considering neoplasm. Further examination is recommended.

(4) On April 5, 2025, deep and superficial venous thrombosis assessment of the lower extremities was performed. Left side: Venous thrombosis of the left lower extremity (femoral vein, upper segment of the superficial femoral vein, tibiofibular trunk, one pulmonary vein, multiple calf intermuscular veins, complete occlusion); On April 6, 2025, underwent left lower extremity venography with filter placement: left femoral vein and iliac vein thrombosis; inferior vena cava filter placement performed.

2.3. Diagnosis and treatment

Considering the patient's age, medical history, and imaging findings, a malignant tumor of the middle to lower segment of the left ureter with multiple metastases was suspected. Due to the patient's advanced age and current conditions of hypertension and left lower extremity venous thrombosis, surgical intervention was ultimately not pursued. The patient underwent left nephroureteroscopy with biopsy on March 31, 2025. The pathological findings are as follows:

Ureteroscopy revealed a necrotic, putrid-appearing mass in the middle to lower ureter, obscuring the normal mucosal lining of the lumen. Immunohistochemistry results: CK/pan (+ in small areas), P63 (-), GATA3 (-), P53 (diffusely strong+, suggestive of mutant type), Ki-67 (hot spot ~70%+), Vimentin (+), CD34 (-), CD31 (-), s-100 (counterstained -), SMA (-), Desmin (-), E-Cadherin (+ in small areas), SMARCA4 (+), INI-1 (+), C-erbB-2 (0), HMB45 (-), CD30 (-). Special stains: Reticulum (perinestular +). (Ureteral mass) Malignant neoplasm. Based on comprehensive immunohistochemical findings and morphology, the specific type is considered sarcomatoid carcinoma (**Figures 10–12**).



Figures 10–12. Puncture pathology.

After excluding chemotherapy-related contraindications, the patient received paclitaxel 150 mg dl + carboplatin 100 mg dl every 4 weeks starting on April 9, 2025, supplemented with symptomatic treatments such as hepatoprotection and antiemesis. The process proceeded smoothly.

3. Discussion

Sarcomatoid carcinoma of the ureter (SCU) is an extremely rare and highly malignant tumor characterized by both epithelial carcinoma and mesenchymal sarcomatoid components. Since the 2004 revision of the WHO classification, it has been uniformly categorized as "sarcomatoid carcinoma" [3]. The vast majority of those affected by the illness are over 60. Unlike other literature reports indicating that primary ureteral sarcomatoid

carcinoma primarily occurs in elderly males, this case involved an elderly female. Most lesions are solitary and predominantly located in the left ureter, consistent with previous reports. Ureteral sarcomatoid carcinoma exhibits high invasiveness and rapid growth. The majority of patients had distant metastases or regional lymph nodes upon diagnosis, most frequently affecting the bones, liver, and lung [4].

3.1. Clinical manifestations

Early-stage SCU often presents with subtle symptoms, typically being diagnosed at intermediate or advanced stages. Due to ureteral lumen narrowing, tumor growth readily causes upper urinary tract obstruction. Initial presenting symptoms predominantly manifest as gross hematuria and pain in the affected flank or abdomen—symptoms characteristic of urinary tract disorders. Some patients may palpate an abdominal mass, though findings lack specificity. In this case, the patient's initial presenting symptom was flank pain.

3.2. Imaging findings

On magnetic resonance imaging (MRI), the ureteral sarcomatoid carcinoma in this case appeared as a poorly defined mass. It demonstrated isointense signal on T1-weighted imaging (T1WI) and heterogeneous, slightly hyperintense signal on T2-weighted imaging (T2WI), likely due to the tumor's heterogeneous cellular composition. Following contrast administration, ureteral sarcomatoid carcinoma typically exhibits heterogeneous enhancement with non-enhancing areas of necrosis visible within the tumor. Additionally, the apparent diffusion coefficient (ADC) values for ureteral sarcomatoid carcinoma are often low, potentially indicating a higher degree of malignancy. Consequently, MRI provides clear visualization of soft tissue structures and offers advantages in assessing local tumor infiltration.

In positron emission tomography/computed tomography (PET/CT) examinations, besides clearly displaying the location, size, and morphology of tumors, as well as identifying features such as calcification, hemorrhage, or adjacent bone destruction, it also provides direct insight into the metabolic activity of tumor cells within lesions. This enables assessment of primary tumors, metastatic sites, and systemic involvement. Ureteral sarcomatoid carcinoma typically presents as a slightly hyperdense lesion with cast-like growth patterns in the ureter, poorly demarcated from surrounding tissues. Due to varied levels of tumor infiltration in various diseased segments, the ureter may be widely affected with heterogeneous density [5]. PET imaging has important benefits for tumor diagnosis, therapy planning, and monitoring by revealing abnormally increased glucose metabolism in both primary tumors and metastatic lesions. This capacity increases survival rates and makes it easier to identify metastases early [6].

Furthermore, ureteral sarcomatoid carcinoma must be differentiated from other ureteral lesions, including: 1. Primary carcinoma of the ureters: Affected side hydronephrosis and various degrees of ureteral dilatation are the main indirect radiography findings. Soft tissue masses at the blockage level and uneven ureteral wall thickening are the main direct findings [7]; the mass appears as low or isointense on T1-weighted imaging (T1WI), slightly hyperintense on T2-weighted imaging (T2WI), and shows moderate to marked enhancement after contrast administration. Differentiating this situation may be more difficult if nearby organs are invaded by tumors [8]. 2. Nonspecific ureteritis: More commonly observed in relatively younger females. The ureteral wall typically exhibits progressive circumferential thickening with mild luminal narrowing over an extended length, featuring a smooth outer margin without evidence of local invasion or retroperitoneal lymphadenopathy. Non-contrast CT shows isodense signals, while MRI demonstrates isointense signals on T1WI and hyperintense signals on T2WI.

Contrast-enhanced imaging reveals marked enhancement of the ureteral wall in the affected segment [9].

3.3. Pathological characteristics

The definitive diagnosis of sarcomatoid carcinoma relies on histopathology and immunohistochemistry. The neoplastic components within sarcomatoid carcinoma tissue are primarily squamous cell carcinoma, adenocarcinoma, and transitional cell carcinoma, characterized by minimal composition and high differentiation. The sarcomatous components mainly include malignant fibrous histiocytoma, leiomyosarcoma, osteosarcoma, and others. Immunohistochemical staining is commonly employed to distinguish epithelial and stromal components. Markers such as cytokeratin (CK) and epithelial membrane antigen (EMA) aid in identifying epithelial elements, while vimentin is typically used to characterize stromal components [2].

3.4.Treatment approach

The main course of treatment is still radical resection, which is frequently followed by adjuvant chemotherapy or radiation. According to recent research, immunotherapy combined with chemotherapy or anti-angiogenic drugs may result in better control rates for sarcomatoid cancer [10]. The prognosis of SCU patients may be improved by using chemotherapy in conjunction with immunotherapy and anti-angiogenic treatment [11].

4. Conclusion

Ureteral sarcomatoid carcinoma (SCU) is a rare malignant tumor with low incidence and nonspecific clinical manifestations, posing significant challenges for accurate preoperative diagnosis. Currently, preoperative diagnosis of SCU primarily relies on imaging studies. However, its imaging features lack specificity and can easily be confused with other ureteral tumors, leading to a high misdiagnosis rate. Therefore, there is an urgent need to accumulate more cases, further summarize and refine the imaging characteristics of SCU, and provide more reliable evidence for definitive preoperative diagnosis in the future.

Disclosure statement

The authors declare no conflict of interest.

References

[1] Lu W, Wang Y, Li Y, Cao Y, et al., 2017, Sarcomatoid Urothelial Carcinoma with Chondrosarcomatous Differentiation of the Ureter: A Case Report and Review of the Literature. Oncology Letters, 13(3): 1331–1337.

[2] Piscioli F, Bondi A, Scappini P, Luciani L, 1984, 'True' Sarcomatoid Carcinoma of the Renal Pelvis. First Case Report with Immunocytochemical Study. Eur Urol, 10(5): 350–355.

[3] Eble JN, Sauter G, Epstein J, Sesterhenn I, 2004, Pathology and Genetics of Tumours of the Urinary System and Male Genital Organs. WHO Classification of Tumours, 7: 93–109.

[4] Venyo AK, Titi S, 2014, Sarcomatoid Variant of Urothelial Carcinoma (Carcinosarcoma, Spindle Cell Carcinoma): A Review of the Literature. ISRN Urology, 2014: 794563.

[5] Jiang K, Deng S, Wang Y, et al., 2016, MSCT Findings and Clinical Analysis of Primary Sarcomatoid Carcinoma of the Kidney, Renal Pelvis, and Ureter (with 4 Case Reports). Journal of Medical Imaging, 26(4): 670–673.

[6] Kartal I, Uysal S, Adabag A, Gok A, Sagnak AL, Ersoy H, 2019, Aggressive Squamous Cell Carcinoma of the Renal Pelvis. Nigerian Journal of Clinical Practice, 22(4): 588–590.

[7] An N, Jiang B, Cai Y, Liang Y, 2004, MRI Diagnosis of Primary Ureteral Cancer and Comparison with Other Imaging Methods. Chinese Journal of Radiology, 38(8): 5.

[8] Xie Y, 2015, MR Imaging Features of Primary Ureteral Cancer. Chinese Journal of CT and MRI, 13(4): 84–86.

[9] Cheng K, Wang Y, Shao F, Zhang X, Wang J, Deng S, 2014, CT and MRI Findings in Nonspecific Ureteritis. Modern Practical Medicine, 26(6): 721–722.

[10] Zhou F, Guo H, Zhou X, et al., 2022, Immune Checkpoint Inhibitors Plus Chemotherapy in Patients with Locally Advanced or Metastatic Pulmonary Sarcomatoid Carcinoma: A Multicentric Real-World Study. Therapeutic Advances in Medical Oncology, 14: 17588359221136759.

[11] Lv Z, Li D, Wang H, et al., 2025, Clinical Features of Primary Ureteral Sarcomatoid Carcinoma. Chinese Journal of Geriatrics, 44(3): 335–341.

Publisher's note

Bio-Byword Scientific Publishing remains neutral with regard to jurisdictional claims in published maps and institutional affiliations.

Proceedings of Anticancer Research, 2026, Volume 10, Issue 1
http://ojs.bbwpublisher.com/index.php/PAR
ISSN Online: 2208-3553
ISSN Print: 2208-3545

Analysis of Long-term Prognosis and Cosmetic Outcomes of Breast-conserving Surgery Combined with Sentinel Lymph Node Biopsy for Early-stage Breast Cancer

Yuedong Zhang*

The People's Hospital of Wuhai Inner Mongolia, Wuhai 016000, Inner Mongolia Autonomous Region, China

**Author to whom correspondence should be addressed.*

Copyright: © 2026 Author(s). This is an open-access article distributed under the terms of the Creative Commons Attribution License (CC BY 4.0), permitting distribution and reproduction in any medium, provided the original work is cited.

Abstract: *Objective*: To investigate the long-term prognosis and postoperative cosmetic outcomes of breast-conserving surgery combined with sentinel lymph node biopsy in patients with early-stage breast cancer, providing a reference for the selection of clinical treatment plans. *Methods*: A retrospective analysis was conducted on the clinical data of 68 patients with early-stage breast cancer admitted from January 2022 to December 2025. Based on the surgical approach, patients were divided into an observation group (breast-conserving surgery + sentinel lymph node biopsy) and a control group (other surgical methods such as modified radical mastectomy/total mastectomy). Clinical and pathological characteristics, incidence of postoperative complications, follow-up prognosis, and satisfaction with cosmetic outcomes were compared between the two groups. *Results:* Among the 68 patients, 41 were in the observation group and 27 in the control group. The average age of patients in the observation group was (54.32 ± 8.15) years, while that in the control group was (62.45 ± 9.76) years. The average tumor size in the observation group was (1.86 ± 0.72) cm, compared to (3.21 ± 1.45) cm in the control group. The incidence of postoperative complications in the observation group was 9.76%, significantly lower than that in the control group at 33.33% ($P < 0.05$). The 6-month disease-free survival rate was 95.12% in the observation group and 88.89% in the control group, with no statistically significant difference between the two groups ($P > 0.05$). The excellent and good rate of cosmetic outcomes in the observation group was 87.80%, significantly higher than that in the control group at 29.63% ($P < 0.05$). *Conclusion:* Breast-conserving surgery combined with sentinel lymph node biopsy for early-stage breast cancer can achieve long-term prognostic outcomes comparable to those of traditional radical surgery, with the advantages of fewer postoperative complications and superior cosmetic results. This approach is worthy of clinical promotion and application, particularly for early-stage breast cancer patients who have a demand for preserving breast morphology.

Keywords: Early-stage breast cancer; Breast-conserving surgery; Sentinel lymph node biopsy; Long-term prognosis; Cosmetic results

Online publication: February 9, 2026

1. Introduction

Breast cancer is the most prevalent malignant tumor among women worldwide, with its incidence showing an annual increase and a trend toward younger age groups, posing a severe threat to women's physical and mental health as well as their quality of life [1]. With the widespread adoption of breast imaging techniques and the advancement of early cancer screening efforts, an increasing number of breast cancer patients are being diagnosed at an early stage, providing favorable conditions for precise clinical treatment and improved prognosis. The core of treating early-stage breast cancer lies in maximizing the preservation of patients' physical function and appearance integrity while achieving radical tumor resection, thereby enhancing postoperative quality of life. This has become an important concept in modern breast surgery [2]. Traditional radical mastectomy focuses on the extensive resection of breast tissue, chest wall fascia, and axillary lymph nodes. Although it can achieve the goal of radical tumor resection, the procedure is highly invasive, with a high incidence of postoperative complications. Moreover, the loss of the breast can have a severe negative impact on patients' psychological well-being, reducing their postoperative quality of life [3].

In recent years, the rapid development of minimally invasive surgical techniques has driven a transformation in breast cancer treatment modalities. Breast-conserving surgery combined with sentinel lymph node biopsy has gradually replaced some traditional surgical approaches as a preferred option for early-stage breast cancer treatment, owing to its advantages of minimal trauma, rapid recovery, and superior cosmetic results [4]. As the first-stop lymph nodes in the tumor drainage area, the metastatic status of sentinel lymph nodes can accurately reflect the overall metastatic situation of axillary lymph nodes. Sentinel lymph node biopsy can avoid complications such as lymphedema and nerve injury caused by blind axillary lymph node dissection, while providing a reliable basis for the formulation of subsequent treatment plans [5]. Currently, more clinical data are still needed to support the efficacy and cosmetic outcomes of breast-conserving surgery combined with sentinel lymph node biopsy, especially regarding the applicability and long-term prognostic stability in patients with different clinical and pathological characteristics, and a unified consensus has not yet been reached. Based on this, this study retrospectively analyzed the clinical data of 68 patients with early-stage breast cancer, comparing postoperative complications, long-term prognosis, and cosmetic outcomes between breast-conserving surgery combined with sentinel lymph node biopsy and traditional surgical procedures, in order to provide a reference for the rational selection of clinical treatment plans.

2. Materials and methods

2.1. Clinical data

A retrospective inclusion of 68 patients with early-stage breast cancer admitted to our hospital from January 2022 to December 2025 was conducted. All patients were pathologically diagnosed with breast cancer, with TNM staging of 0-IIA, and met the indications for surgical treatment. Patients with severe heart, liver, or kidney diseases, coagulation disorders, distant metastases, or incomplete follow-up data were excluded. The patients were divided into an observation group and a control group based on the surgical approach. The observation group underwent breast-conserving surgery combined with sentinel lymph node biopsy using blue dye tracing, while the control group underwent traditional surgical procedures such as modified radical mastectomy, total mastectomy, or extended radical mastectomy. The data on gender, body mass index, and clinical and pathological characteristics of the two groups of patients are detailed in **Table 1**.

Table 1. Comparison of clinical data between two groups of patients

Clinical Indicator	Observation Group (n = 41)	Control Group (n = 27)	Test Statistic (χ^2/t)	*P*-value
Gender (n, % Female)	41 (100.00%)	26 (96.30%)	1.032	> 0.05
Age (years, mean ± SD)	54.32 ± 8.15	62.45 ± 9.76	3.985	< 0.05
BMI (kg/m², mean ± SD)	23.45 ± 3.12	24.16 ± 3.57	0.921	> 0.05
Tumor Size (cm, mean ± SD)	1.86 ± 0.72	3.21 ± 1.45	5.237	< 0.05
Pathology Type (n, %)				
Invasive Ductal Carcinoma	35 (85.37%)	22 (81.48%)		
In Situ Carcinoma with Focal Invasion	4 (9.76%)	3 (11.11%)	2.154	> 0.05
Other Types	2 (4.87%)	2 (7.41%)		
TNM Stage (n, %)				
Stage 0	5 (12.20%)	2 (7.41%)		
Stage I	26 (63.41%)	13 (48.15%)	3.842	> 0.05
Stage II-IIIA	10 (24.39%)	12 (44.44%)		
Sentinel Lymph Node Metastasis (n, %)	8 (19.51%)	15 (55.56%)	10.236	< 0.05
Immunohistochemistry ER Positive (n, %)	30 (73.17%)	18 (66.67%)	0.387	> 0.05

2.2. Surgical methods

2.2.1. Observation group

Breast-conserving surgery combined with sentinel lymph node biopsy under blue dye tracing was performed. Before surgery, the tumor location was identified using color Doppler ultrasound or magnetic resonance imaging. An arc-shaped incision was made 1–2 cm outside the tumor margin, and the skin, subcutaneous tissue, and mammary gland were incised layer by layer. The tumor and surrounding normal glandular tissue were completely resected, and rapid pathological examination confirmed negative surgical margins. Subsequently, methylene blue dye was injected subcutaneously around the areola or in the quadrant where the tumor was located. After massaging the breast for 10-15 minutes, a small incision was made in the axillary fold to locate the dye-stained lymphatic vessels and sentinel lymph nodes. All stained lymph nodes and suspicious lymph nodes were completely resected and sent for pathological examination. After surgery, the residual mammary cavity was sutured and repaired, a drainage tube was placed, and the incision was closed layer by layer.

2.2.2. Control group

Depending on the patient's condition, modified radical mastectomy, total mastectomy, or extended radical mastectomy was selected. Modified radical mastectomy involved resection of the affected breast, pectoralis major fascia, and axillary lymph nodes; total mastectomy involved complete resection of the affected breast, with or without sentinel lymph node biopsy; extended radical mastectomy involved resection of the pectoralis minor muscle and subclavian lymph nodes in addition to the procedures performed in modified radical mastectomy. After surgery, a drainage tube was routinely placed, and the incision was bandaged under pressure.

2.3. Observation indicators

(1) Clinical and pathological indicators: Record the age, body mass index, tumor size, pathological type,

TNM staging, sentinel lymph node metastasis status, and immunohistochemical results of patients in both groups.

(2) Postoperative complications: Follow-up records were kept on the occurrence of complications such as postoperative wound infection, subcutaneous fluid accumulation, numbness, edema, and limited mobility of the affected limb.

(3) Long-term prognosis: Patients were followed up for 6 months after surgery, and the disease-free survival rate, local recurrence rate, and distant metastasis rate were recorded.

(4) Cosmetic outcomes: The cosmetic outcome evaluation criteria for the breast were used, dividing results into three grades: excellent, acceptable, and poor. Excellent: Symmetrical breast shape, inconspicuous incision scar, no obvious deformity, and patient satisfaction; Acceptable: Basically symmetrical breast shape, relatively conspicuous incision scar, mild deformity, and acceptable to the patient; Poor: Severely asymmetrical breast shape, obvious deformity, conspicuous incision scar, and patient dissatisfaction. The excellent rate = (number of excellent cases/total number of cases) × 100%.

2.4. Statistical methods

Data analysis was performed using SPSS 26.0 statistical software. Measurement data were expressed as mean ± standard deviation ($\overline{x} \pm s$), and comparisons between groups were made using the t-test. Count data were expressed as the number of cases (percentage) [n (%)], and comparisons between groups were made using the χ^2 test. A P-value < 0.05 indicated a statistically significant difference.

3. Results

3.1. Comparison of the incidence of postoperative complications between the two groups

The incidence of postoperative complications in the observation group was significantly lower than that in the control group, with a statistically significant difference ($P < 0.05$). See **Table 2** for details.

Table 2. Comparison of the incidence of postoperative complications between the two groups [n (%)]

Complication Type	Observation Group (n = 41)	Control Group (n = 27)	Total Incidence (%)	χ^2	*P*-value
Limb Numbness	3 (7.32%)	6 (22.22%)			
Limb Edema	0 (0.00%)	2 (7.41%)			
Incision Scar/Pain	1 (2.44%)	1 (3.70%)			
Flap Necrosis	0 (0.00%)	1 (3.70%)			
Limited Mobility	0 (0.00%)	1 (3.70%)			
No Complications	37 (90.24%)	16 (59.26%)			
Overall Complication Rate	4 (9.76%)	9 (33.33%)	19.12	6.843	< 0.05

3.2. Comparison of long-term prognosis between the two groups

After a 6-month postoperative follow-up, the observation group had a disease-free survival rate of 95.12%, a local recurrence rate of 2.44%, and a distant metastasis rate of 2.44%. The control group had a disease-free survival rate of 88.89%, a local recurrence rate of 7.41%, and a distant metastasis rate of 3.70%. There were no statistically significant differences in disease-free survival rate, local recurrence rate, or distant metastasis rate between the two

groups ($P > 0.05$). See **Table 3** for details.

Table 3. Comparison of long-term prognosis between the two groups [n (%)]

Prognostic Indicator	Observation Group (n = 41)	Control Group (n = 27)	χ^2	*P*-value
Disease-Free Survival (n, %)	39 (95.12%)	24 (88.89%)	1.452	> 0.05
Local Recurrence (n, %)	1 (2.44%)	2 (7.41%)	0.987	> 0.05
Distant Metastasis (n, %)	1 (2.44%)	1 (3.70%)	0.154	> 0.05
Death (n, %)	1 (2.44%)	0 (0.00%)	0.763	> 0.05

3.3. Comparison of postoperative cosmetic outcomes between the two groups

The excellent and good rate of postoperative cosmetic outcomes in the observation group was significantly higher than that in the control group, with a statistically significant difference ($P < 0.05$). See **Table 4** for details.

Table 4. Comparison of postoperative cosmetic outcomes between the two groups [n (%)]

Cosmetic Outcome Grade	Observation Group (n = 41)	Control Group (n = 27)	Excellent/Good Rate (%)	χ^2	*P*-value
Excellent/Good	36 (87.80%)	8 (29.63%)			
Fair	4 (9.76%)	10 (37.04%)			
Poor	1 (2.44%)	9 (33.33%)			
Total	41 (100.00%)	27 (100.00%)	64.71	32.657	< 0.05

4. Discussion

The primary treatment for early-stage breast cancer is surgery. Although traditional radical mastectomy can effectively remove tumor tissue, it involves significant surgical trauma, resulting in breast loss, which severely affects patients' physical appearance and mental health, and also leads to a relatively high incidence of postoperative complications. With the advancement of medical technology and the increasing demand for quality of life among patients, breast-conserving surgery combined with sentinel lymph node biopsy has gradually emerged as a crucial treatment option for early-stage breast cancer. This surgical approach not only ensures therapeutic efficacy but also maximizes the preservation of breast morphology, thereby improving patients' postoperative quality of life.

In this study, the incidence of postoperative complications in the observation group was significantly lower than that in the control group, highlighting the minimally invasive advantages of breast-conserving surgery combined with sentinel lymph node biopsy. Traditional radical mastectomy involves extensive resection of breast tissue, chest wall fascia, and axillary lymph nodes, which not only disrupts the axillary lymphatic drainage system but may also damage the thoracodorsal nerve and long thoracic nerve, which innervate the upper extremities, leading to complications such as numbness, edema, and limited mobility in the affected limb. In contrast, breast-conserving surgery involves the resection of only the tumor and a small amount of surrounding normal tissue, while sentinel lymph node biopsy precisely identifies and removes the lymph nodes in the drainage area, avoiding blind axillary lymph node dissection and significantly reducing damage to the lymphatic circulation and surrounding nerves. This finding is consistent with the research conclusions of Yu Hao et al. [6], who reported that

patients undergoing breast-conserving surgery combined with sentinel lymph node biopsy experienced a more than 20% reduction in the incidence of postoperative complications compared to those undergoing traditional surgery, along with a shorter recovery time from complications.

In terms of long-term prognosis, there were no significant differences in the 6-month disease-free survival rate, local recurrence rate, or distant metastasis rate between the two groups, indicating that the tumor control efficacy of breast-conserving surgery combined with sentinel lymph node biopsy is not inferior to that of traditional radical mastectomy. The core support for this conclusion lies in the radical resection of the tumor through breast-conserving surgery—in this study, the observation group ensured negative surgical margins, with precise preoperative localization of the tumor extent using color Doppler ultrasound and magnetic resonance imaging. Postoperatively, standardized adjuvant therapies (chemotherapy, radiotherapy, endocrine therapy, etc.) were administered based on the patient's pathological characteristics, effectively controlling the risk of local recurrence. Meanwhile, the precise assessment of lymph node metastasis through sentinel lymph node biopsy provided a reliable basis for formulating subsequent treatment plans, avoiding overtreatment or undertreatment. It is important to note that although no prognostic differences were observed during the 6-month follow-up in this study, some research indicates that the 5-year and 10-year survival rates after breast-conserving surgery combined with standardized radiotherapy are comparable to those of traditional radical surgery [7]. Therefore, extending the follow-up period in future studies is necessary to further validate the long-term efficacy and stability of this surgical approach.

The significant aesthetic advantage is one of the core competitive strengths of breast-conserving surgery combined with sentinel lymph node biopsy. The breast, as a vital physical symbol for women, has its morphological integrity directly influencing patients' postoperative self-identity and mental health. The breast loss caused by traditional radical surgery often leads to psychological issues such as inferiority and anxiety in patients, even affecting family relationships and social activities. In contrast, breast-conserving surgery preserves the natural breast morphology to the greatest extent possible through techniques such as curved incision design and breast cavity repair, with concealed incision scars. Combined with postoperative rehabilitation care, it achieves a favorable cosmetic outcome. In this study, the excellent and good cosmetic outcome rate of 87.80% in the observation group not only reflects the standardization of surgical procedures but also underscores the improvement in patients' quality of life. Patients satisfied with their cosmetic outcomes exhibit more stable psychological states postoperatively and demonstrate higher rehabilitation compliance, forming a virtuous cycle that further enhances long-term prognosis.

From a clinical application perspective, the promotion of breast-conserving surgery combined with sentinel lymph node biopsy necessitates strict adherence to indications. In this study, patients in the observation group had smaller average tumor sizes, were younger, and exhibited lower rates of sentinel lymph node metastasis, suggesting that this procedure is more suitable for early-stage breast cancer patients with TNM stages 0-I, tumor diameters ≤3 cm, and no extensive lymph node metastasis, particularly in young patients with a desire to preserve breast morphology [8]. For patients with larger tumor volumes, multifocal lesions, positive surgical margins, or extensive lymph node metastasis, traditional radical or extended radical surgery should remain the priority to ensure complete tumor eradication [9]. Additionally, preoperative assessment of patients' immunohistochemical results is crucial; for patients positive for estrogen receptor (ER) and progesterone receptor (PR), postoperative endocrine therapy can further reduce recurrence risk, providing supplementary assurance for the safety of breast-conserving surgery [10].

The findings of this study indicate that patients in the observation group had a lower average age, smaller average tumor size, and lower rate of sentinel lymph node metastasis compared to the control group, which is closely related to the indications for breast-conserving surgery. This procedure is more suitable for young patients with smaller tumor volumes, earlier stages, and no obvious lymph node metastasis. In terms of postoperative complications, the overall incidence rate in the observation group was 9.76%, significantly lower than the 33.33% in the control group. This is primarily because breast-conserving surgery involves a small incision, eliminating the need for extensive resection of breast tissue and axillary lymph nodes, resulting in minimal damage to the axillary lymphatic drainage system and upper limb nerves, thereby reducing the occurrence of complications such as numbness, edema, and restricted mobility in the affected limb.

This study has certain limitations: Firstly, it is a retrospective study with a relatively limited sample size, which may introduce selection bias. Secondly, the follow-up period was short, lasting only six months, and the long-term prognostic effects still require further verification through extended follow-up. Thirdly, the evaluation of cosmetic outcomes was subjective, lacking objective quantitative indicators. Future research should involve large-sample, prospective studies incorporating objective cosmetic evaluation metrics to further explore the long-term efficacy and cosmetic outcomes of breast-conserving surgery combined with sentinel lymph node biopsy, providing more reliable evidence for clinical treatment.

5. Conclusion

In conclusion, breast-conserving surgery combined with sentinel lymph node biopsy for early-stage breast cancer offers advantages such as minimal trauma, fewer postoperative complications, and excellent cosmetic outcomes, with long-term prognosis comparable to that of traditional radical surgery, making it worthy of clinical promotion and application. In clinical practice, it is essential to strictly adhere to surgical indications, thoroughly evaluate the patient's condition before surgery, and strengthen postoperative follow-up and rehabilitation guidance to further enhance treatment outcomes and improve patients' quality of life.

Disclosure statement

The author declares no conflict of interest.

References

[1] Du B, Wang Z, Duan Q, 2025, Clinical Effect Analysis of Single-Port Laparoscopic Breast-Conserving Surgery Combined with Sentinel Lymph Node Biopsy for the Treatment of Early-Stage Triple-Negative Breast Cancer. Clinical Medicine & Engineering, 32(9): 993–996.

[2] Tao Z, Gu B, Zhou Y, 2025, Impact of Plastic Breast-Conserving Surgery Combined with Sentinel Lymph Node Biopsy on Shoulder Joint Mobility and Long-Term Survival in Patients with Early-Stage Breast Cancer. Chinese and Foreign Medical Research, 23(14): 127–130.

[3] Xiong W, 2025, Analysis of the Application Value of Breast-Conserving Surgery Combined with Sentinel Lymph Node Biopsy and Modified Radical Mastectomy in the Treatment of Early-Stage Breast Cancer. Journal of Surgical Research and New Techniques (Chinese and English), 14(1): 61–64.

[4] Yuan X, Ding G, Liu S, 2024, Impact of Sentinel Lymph Node Biopsy Combined with Breast-Conserving Surgery on

Immune Function and Recurrence Rate in Patients with Early-Stage Breast Cancer. Reflexology and Rehabilitation Medicine, 5(23): 149–152 + 160.

[5] Li Y, Peng R, Wu H, 2024, Impact of Sentinel Lymph Node Biopsy Combined with Breast-Conserving Surgery on Serum Tumor Marker Levels and Post-Traumatic Stress Disorder in Patients with Early-Stage Breast Cancer. China Modern Medicine, 31(32): 52–56.

[6] Yu H, Xu X, Xiao X, 2024, Analysis of the Effect of Sentinel Lymph Node Biopsy Combined with Breast-Conserving Surgery in the Treatment of Early-Stage Breast Cancer in Elderly Patients. Chinese Community Doctors, 40(30): 38–40.

[7] Feng Y, Liu Z, Bai H, 2024, Observation on the Effect of Sentinel Lymph Node Biopsy Combined with Breast-Conserving Surgery in the Treatment of Early-Stage Breast Cancer. Medical Innovation of China, 21(5): 1–5.

[8] Feng H, Cao H, 2023, The Efficacy of Sentinel Lymph Node Biopsy Combined with Breast-Conserving Surgery in the Treatment of Breast Cancer in Elderly Patients and Its Impact on Quality of Life. Heilongjiang Medical Journal, 47(24): 2955–2957.

[9] Li K, Lin L, 2023, Clinical Efficacy of Breast-Conserving Surgery Combined with Sentinel Lymph Node Biopsy in the Treatment of Early-Stage Triple-Negative Breast Cancer and Its Impact on Patients' Quality of Life. Chinese Journal of Modern Drug Application, 17(22): 64–67.

[10] Jiang G, Wang S, Miao S, et al., 2023, Clinical Value of Preoperative Puncture Combined with Sentinel Lymph Node Biopsy in the Surgery for Early-Stage Breast Cancer in the Upper Outer Quadrant. Medical Journal of Communications, 37(5): 496–497 + 502.

Publisher's note

Bio-Byword Scientific Publishing remains neutral with regard to jurisdictional claims in published maps and institutional affiliations.

Proceedings of Anticancer Research, 2026, Volume 10, Issue 1
http://ojs.bbwpublisher.com/index.php/PAR
ISSN Online: 2208-3553
ISSN Print: 2208-3545

Cerebral Tuberculoma on the Left Frontal Lobe

Zixuan Zhou[1], Shanshan Wang[2]*

[1]Graduate School of Xinjiang Medical University, Urumqi 830054, Xinjiang Uygur Autonomous Region, China
[2]Medical Imaging & Radiology Center, People's Hospital of Xinjiang Uygur Autonomous Region, Urumqi 830001, Xinjiang Uygur Autonomous Region, China

**Corresponding author: Shanshan Wang, 1549578545@qq.com*

Copyright: © 2025 Author(s). This is an open-access article distributed under the terms of the Creative Commons Attribution License (CC BY 4.0), permitting distribution and reproduction in any medium, provided the original work is cited.

Abstract: Cerebral tuberculoma, a rare extrapulmonary tuberculosis manifestation, was reported in a 70-year-old man presenting with seizure-like episodes. MRI revealed a 13.6 × 45.1 × 7.9 mm left frontal extra-axial lesion with T1-isointense/T2-hyperintense signals, marked contrast enhancement, and adjacent leptomeningeal thickening. Negative thoracic/abdominal CT and inflammatory CSF findings initially suggested a neoplasm. Histopathological examination of the resected lesion confirmed granulomatous inflammation with acid-fast bacilli, thereby leading to the diagnosis. This case report emphasizes the importance of considering tuberculous granuloma in older patients with intracranial masses and inconclusive CSF studies. Multi-model imaging combined with biopsy remains critical for definitive diagnosis. Early surgical intervention and antitubercular therapy may improve outcomes.

Keywords: Cerebral tuberculoma; Meningeal thickening; Leptomeningeal enhancement

Online publication: February 9, 2026

1. Introduction

Cerebral tuberculoma, a distinct form of central nervous system tuberculosis caused by *Mycobacterium tuberculosis* infection, manifests as a granulomatous lesion within the brain parenchyma [1]. In recent years, the incidence of cerebral tuberculoma has risen alongside the global resurgence of tuberculosis and the increasing prevalence of immunocompromised conditions such as HIV/AIDS [2]. Tuberculomas involving the frontal lobe, a critical functional brain region, can induce seizures, cognitive impairment, motor deficits, and other neurological dysfunction, thus severely compromising patients' quality of life. Therefore, precise diagnosis, timely treatment, and comprehensive care are essential for improving prognosis [3]. This report analyzes clinical data for a rare case of left frontal cerebral tuberculoma without clinical evidence of tuberculosis, focusing on its diagnostic and therapeutic challenges.

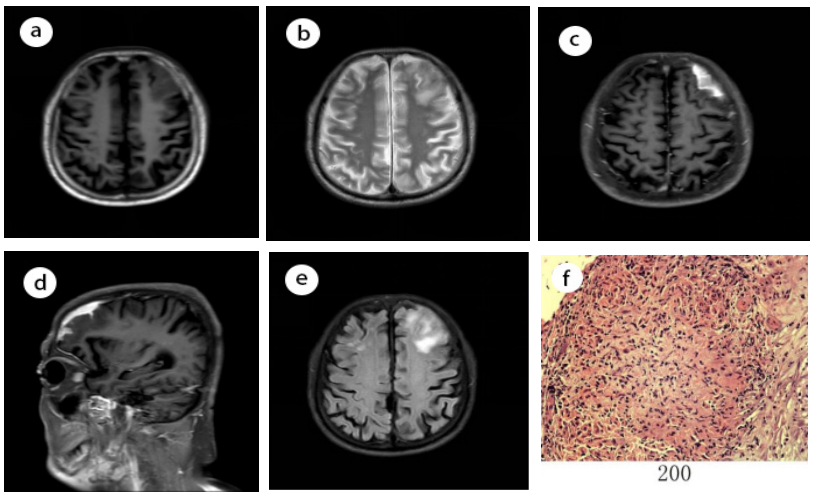
2. Case report

A 70-year-old man was admitted with two episodes of transient loss of consciousness accompanied by intermittent

limb convulsions. Three months prior, he had experienced a sudden loss of consciousness with limb convulsions lasting several minutes, followed by 3 hours of drowsiness, which resolved after symptomatic management at a local hospital. After recurrence, his symptoms worsened, including persistent unconsciousness and convulsions lasting 7 hours. He denied frothing at the mouth, dizziness, headache, nausea, vomiting, or incontinence. A physical examination revealed a temperature of 36.7°C, pulse of 80 bpm, respiratory rate of 21/min, blood pressure of 133/95 mmHg, and no significant abnormalities in cardiopulmonary or abdominal assessments. In neurological examination, neck stiffness, Kernig's sign, Brudzinski's sign, and focal deficits were absent. His laboratory findings included white blood cells at 8.42 × 10^9/L, eosinophils at 0.7%, hemoglobin at 12.4 g/dL, platelets at 168 × 10^9/L, glucose at 5.84 mmol/L, total protein at 69.7 g/L, albumin at 36.84 g/L (↓), and globulin at 32.86 g/L (↑). Lumbar puncture revealed cerebrospinal fluid (CSF) with Pandy's test positivity, glucose at 10.50 mmol/L (↑), protein at 1.96 g/L (↑), and no bacterial growth after 5-day culture.

Cranial MRI revealed an irregular left frontal subcranial lesion (13.6 × 45.1 × 7.9 mm) with an isointense T1-weighted signal (**Figure 1a**) and slightly hyperintense T2-weighted signal (**Figure 1b**), and demonstrated marked enhancement post-contrast. Adjacent frontotemporal leptomeningeal thickening and uniform enhancement were accompanied by mild swelling of the left frontal parenchyma, which showed a slightly diminished T1 signal (**Figure 1c**) and hyperintensity on T2-weighted (**Figure 1d**) and FLAIR sequences, with prominent leptomeningeal enhancement (**Figure 1e**). The left frontal subcranial lesion and adjacent frontotemporal dural thickening suggested benign extracranial pathologies, including central nervous system Rosai-Dorfman disease (CNS-RDD), hypertrophic pachymeningitis, and meningioma en plaque (MEP). Neuronavigation-assisted cerebral lesion resection and brain biopsy were performed. Histopathological analysis confirmed granulomatous inflammation with acid-fast staining positivity in the left frontal lobe—findings consistent with tuberculosis. The final diagnosis was cerebral tuberculoma (BTB) (**Figure 1f**).

After active surgical intervention, antitubercular therapy, management of underlying comorbidities, and comprehensive supportive care, our patient achieved progressive clinical improvement. Antitubercular treatment was continued post-discharge with scheduled follow-up evaluations.



Figures 1. a–b: An irregular left frontal subcranial lesion (13.6 × 45.1 × 7.9 mm3) showing isointense T1 and slightly hyperintense T2 signals. Figures b-c: Marked post-contrast homogeneous enhancement with adjacent frontotemporal meningeal thickening and mild left frontal parenchymal swelling. Figure e: Hyperintense T2/FLAIR signals and prominent surrounding leptomeningeal post-contrast enhancement. Figure f: Acid-fast stain positive granulomatous lesions in the left frontal lobe, consistent with tuberculosis.

3. Discussion

The clinical manifestations of cerebral tuberculoma include multidimensional nonspecific features, which can be broadly categorized into three patterns: (1) intracranial hypertension syndrome (progressive headache, projectile vomiting, and papilledema); (2) focal neurological deficits (motor impairment, dysarthria, and visual field defects); and (3) neuropsychiatric symptoms (cognitive decline and behavioral abnormalities) [4]. The imaging findings in our case aligned with the histopathological characteristics of immature tuberculoma [5], including dynamic clinicopathological correlations, in which the early-stage symptoms reflect predominantly vasogenic edema-induced intracranial hypertension (headache or dizziness), whereas granuloma expansion and perilesional gliosis can trigger seizure-like episodes [6–8]. Multimodal CT/MRI is critical for diagnosis and staging. Pathologically, immature tuberculomas exhibit granulomatous hypercellularity with vascular proliferation, which translates to distinct imaging patterns comprising (1) T1-weighted isointensity/hypointensity reflecting a dynamic equilibrium between cellular density and water content; (2) T2-weighted central isointensity with peripheral hyperintensity ("double-ring sign") due to inflammatory infiltration and vasogenic edema; and (3) marked post-contrast homogeneous or clustered nodular enhancement due to blood-brain barrier disruption by neocapillaries, and no mature "target sign" architecture, given the absence of caseous necrosis [9,10]. These evolving imaging signatures provide critical diagnostic clues. We therefore advocate for a tripartite decision-making framework integrating imaging staging, pathological progression, and therapeutic strategies.

The first differential diagnosis in this case, CNS-RDD, affects predominantly children and adolescents, has a slight male predilection, and is characterized by painless lymphadenopathy and histiocytic proliferation potentially involving multiple organ systems. Although most cases have favorable outcomes, central nervous system involvement can lead to severe neurological complications including headache, seizures, limb weakness, and cranial nerve dysfunction [11]. Typical MRI features include T1-weighted isointensity, T2-weighted iso-/mild hyper-/hypointensity, and marked homogeneous post-contrast enhancement. Notably, early-stage cerebral tuberculomas without caseous necrosis can also exhibit uniform enhancement because of contrast accumulation in vascularized lesions, whereas CNS-RDD typically presents as extracerebral enhancing masses with T1 isointensity and T2 iso-/mild hyperintensity [12]. These findings partially overlapped with the imaging findings in our case. Therefore, a comprehensive evaluation integrating age-sex epidemiology, clinical manifestations, multimodal imaging (e.g., MR spectroscopy), and microbiological evidence is essential for differential diagnosis.

Our second differential diagnosis, hypertrophic cranial pachymeningitis (HCP), is a rare fibroinflammatory disorder characterized by chronic, progressive thickening of the dura mater. Etiologically, HCP is classified as idiopathic (immune-mediated, with unclear pathogenesis) or secondary to infections, malignancies, or autoimmune diseases. Pathologically, it manifests as focal/diffuse fibrous dural thickening with chronic presence of inflammatory infiltrates (lymphocytes and plasma cells) [13]. Clinically, 92% of patients with HCP initially present with persistent headache, which is frequently accompanied by cranial neuropathies (e.g., optic/oculomotor nerve involvement) and ataxia, whereas epileptic seizures occur in rare cases [14,15]. Contrast-enhanced MRI demonstrates specific features of T1-weighted iso-/hypointensity, T2-weighted hypointensity, and marked dural enhancement, predominantly along the tentorium cerebelli and falx cerebri, thereby forming a characteristic "Mercedes-Benz sign" enhancement pattern [16]. Although our case exhibited meningeal thickening on MRI and inflammatory laboratory markers, the absence of typical persistent headache, elevated CSF leukocytes, or protein levels necessitated exclusion of HCP through meningeal biopsy.

The third diagnostic consideration in our report, MEP, a rare meningioma subtype, predominantly involves

the sphenoid ridge or skull base regions [17,18]. Its hallmarks include extensive dural infiltrations with adjacent skull hyperostosis (incidence: 25%–49%) [19]. MRI typically demonstrates T1-weighted isointensity, T2-weighted iso-/mild hyperintensity, iso-intensity on DWI, and homogeneous enhancement post-contrast, thus resulting in imaging overlap with immature cerebral tuberculoma. However, MEP classically exhibits a dural tail sign, with enhancement confined to the dural layer [20]. Although our case showed a left frontal subcranial irregular enhancing lesion with adjacent meningeal thickening partially matching typical MEP imaging features [21] (T1 iso-intensity, T2 iso-/mild hyperintensity, and homogeneous enhancement), key differentiating factors included prominent leptomeningeal enhancement extending beyond typical MEP patterns. Consequently, MEP was the third differential diagnosis.

In our patient, the CSF showed a positive Pandy's test, and elevated protein and glucose, probably as a result of blood-brain barrier disruption and CSF metabolic derangements caused by tuberculous inflammation. The negative CSF bacterial culture might have reflected the slow growth rate and extensive culture requirements of *Mycobacterium tuberculosis*. Although CSF analysis plays a critical diagnostic role in tuberculous meningitis, its utility in cerebral tuberculoma remains limited [22,23].

Our patient presented with seizure-like episodes (transient loss of consciousness and limb convulsions) as the predominant clinical feature, and lacked typical tuberculous toxic symptoms (e.g., low-grade fever, night sweats, or weight loss) and chest CT findings of active pulmonary tuberculosis (e.g., tree-in-bud opacities or cavitation). These atypical features substantially complicated early diagnosis. On the basis of this case, we propose that clinicians should prioritize cerebral tuberculoma in the differential diagnosis for the following high-risk groups: (1) older patients with new-onset seizures (particularly with immunosenescence); (2) patients with intracranial space-occupying lesions without identifiable infectious sources; and (3) patients with suboptimal responses to antiepileptic drugs, even in the absence of tuberculosis exposure history or classic symptoms. Clinical decision-making should follow a three-tiered strategy comprising: (1) comprehensive history-taking and systemic examination (focusing on immune status and potential TB exposure risks); (2) multimodal neuroimaging (contrast-enhanced MRI, DWI/ADC analysis, and MR spectroscopy); and (3) timely acquisition of microbiological evidence (e.g., CSF GeneXpert assay) or histopathological confirmation (stereotactic biopsy). Establishing a stepwise diagnostic pathway integrating clinical vigilance, imaging screening, and histopathological confirmation has the potential to overcome traditional diagnostic limitations, thereby enabling early initiation of standardized antitubercular therapy to optimize neurological outcomes.

4. Conclusion

Cerebral tuberculoma remains a challenging diagnosis in older patients, especially in the absence of systemic or pulmonary tuberculosis. This case underscores the importance of integrating clinical suspicion, multimodal imaging features (including MRI with contrast enhancement and meningeal evaluation), and histopathological confirmation to establish an accurate diagnosis. Early surgical intervention followed by antitubercular therapy can lead to favorable neurological outcomes. Clinicians should consider tuberculoma in the differential diagnosis of intracranial mass lesions, even in non-endemic regions and in patients without typical tuberculous symptoms.

Author profile

Zhou Zixuan, Year of Birth: 2000, Gender: Female, Ethnicity: Han, Hometown: Jiangsu, Academic Degree: Bachelor's Degree, Main Research Field: Medical Imaging;
Wang Shansham, Year of Birth: 1980, Gender: Female, Ethnicity: Han, Hometown: Shandong, Title: Chief Physician, Degree: Doctoral Graduate, Main Research Field: Imaging Radiomics.

Disclosure statement

The authors declare no conflict of interest.

References

[1] Verma S, Salotagi S, Angadi V, et al., 2024, Complicated Neurological Pathways: Tuberculoma With Guillain–Barré Syndrome – An Uncharted Clinical Odyssey. BMJ Case Reports, 17: e262702.

[2] Indoria A, Kulanthaivelu K, Prasad C, et al., 2024, Radiomics Features for the Discrimination of Tuberculomas From High-Grade Gliomas and Metastasis: A Multimodal Study. Neuroradiology, 66: 1979–1992.

[3] Koesbandono R, Muljadi R, Sutanto S, et al., 2024, Intracranial Tuberculomas: Review of MRI Findings and Clinical Features. Clinical Radiology, 79: 354–362.

[4] Spruijt L, Mosch A, Hoffmann C, et al., 2024, Mycobacterium bovis Infection of a Deep Brain Stimulation System Following Intravesical Bacillus Calmette–Guérin Instillation. Journal of Parkinson's Disease, 14: 1061–1069.

[5] Zhu G, Mo Y, Su Y, 2014, Clinical Characteristics of Intracranial Tuberculoma. Journal of Clinical Neurology, 27: 64–66.

[6] Yamamoto M, Manabe T, Yokokawa K, et al., 2023, Cerebral Tuberculoma Diagnosed by Nested Polymerase Chain Reaction of a Formalin-Fixed Paraffin-Embedded Brain Biopsy Sample. Internal Medicine, 62: 1827–1833.

[7] de Oliveira P, Braz Corbi M, Siqueira A, et al., 2023, Brain Tuberculoma in Pediatric Heart Transplant Recipient. Pediatric Transplantation, 27: e14496.

[8] Deng L, Diao S, Zhang Y, et al., 2023, Misdiagnosis of Early Cerebral Tuberculoma as Pneumonia: A Case Report. Academic Journal of Chinese PLA Medical School, 44: 823–826.

[9] Kalita J, Shukla R, Pandey P, et al., 2024, mRNA Profiling of Cytokines to Understand Paradoxical Response in HIV-Uninfected Tuberculous Meningitis. Tuberculosis, 144: 102463.

[10] Xia A, Wan J, Li X, et al., 2024, Rv0927c Suppresses the Activation of the HIF-1α Pathway Through VHL-Mediated Ubiquitination and NF-κB/COX-2 Pathway to Enhance Mycobacteria Survival. Microbiological Research, 278: 127529.

[11] Huang B, Zong M, Zong W, et al., 2016, Intracranial Rosai–Dorfman Disease. Journal of Clinical Neuroscience, 32: 133–136.

[12] Duoji Y, Zha D, Liu H, et al., 2023, Surgical Management of Cerebral Tuberculoma in Tibet Autonomous Region: A Report of 16 Cases With Literature Review. Chinese Journal of Clinical Neurosurgery, 28: 83–85.

[13] Leng F, Xu X, Kong Y, 2021, Nursing Care for Pediatric Patients With Idiopathic Hypertrophic Pachymeningitis. Journal of Nursing Science, 36: 40–41.

[14] Abrantes F, Moraes M, Rezende F, et al., 2020, A Clinical Approach to Hypertrophic Pachymeningitis. Arquivos de Neuro-Psiquiatria, 78: 797–804.

[15] Yonekawa T, Murai H, Utsuki S, et al., 2014, A Nationwide Survey of Hypertrophic Pachymeningitis in Japan. Journal of Neurology, Neurosurgery & Psychiatry, 85: 732–739.

[16] Wu S, Lin J, Ma Y, et al., 2020, Clinical Manifestations and Imaging Features of Patients With Hypertrophic Pachymeningitis. Chinese Journal of Clinical Research, 33: 633–637.

[17] Muhsen B, Aljariri A, Hashem H, et al., 2022, En-Plaque Sphenoid Wing Grade II Meningioma: Case Report and Review of Literature. Annals of Medicine and Surgery, 74: 103322.

[18] Mingo K, Sweeney A, Thompson R, et al., 2016, Hyperostotic En Plaque Meningioma Mimicking Fibrous Dysplasia of the Temporal Bone. Otology & Neurotology, 37: e317–e318.

[19] Gupta S, Mohindra S, Radotra B, et al., 2006, Giant Calvarial Hyperostosis With Biparasagittal En Plaque Meningioma. Neurology India, 54: 210–212.

[20] Chen S, Yang B, Li Y, et al., 2017, CT and MRI Features of Temporal Bone En Plaque Meningioma. Chinese Journal of Otology, 15: 454–457.

[21] Min J, Kang S, Lee J, et al., 2005, Hyperostotic Meningioma With Minimal Tumor Invasion Into the Skull. Neurologia Medico-Chirurgica, 45: 480–483.

[22] Chen J, Zheng J, Zhou Q, 2021, Exploratory Analysis of Risk Factors for Short-Term Prognosis in Patients With Tuberculous Meningitis. Journal of Hebei Medical University, 42: 1256–1260.

[23] Mayorga-Corvacho J, Vergara-Garcia D, Riveros W, et al., 2021, Tuberculoma in the Fourth Ventricle: An Unusual Location. Turkish Neurosurgery, 31: 658–660.

Publisher's note

Bio-Byword Scientific Publishing remains neutral with regard to jurisdictional claims in published maps and institutional affiliations.

Proceedings of Anticancer Research, 2026, Volume 10, Issue 1
http://ojs.bbwpublisher.com/index.php/PAR
ISSN Online: 2208-3553
ISSN Print: 2208-3545

Observation on the Efficacy and Mechanism of Blood-Letting and Cupping Therapy in Improving Upper Limb Lymphedema after Breast Cancer Surgery

Dongli Zhang[1], Jia Liu[2], Qian Zheng[3]*

[1]Department of Integrated Traditional and Western Medicine, Affiliated Hospital of Hebei University, Baoding 071000, Hebei, China
[2]School of Traditional Chinese Medicine, Hebei University, Baoding 071000, Hebei, China
[3]Department of Pediatrics, Affiliated Hospital of Hebei University, Baoding 071000, Hebei, China

**Author to whom correspondence should be addressed.*

Copyright: © 2026 Author(s). This is an open-access article distributed under the terms of the Creative Commons Attribution License (CC BY 4.0), permitting distribution and reproduction in any medium, provided the original work is cited.

Abstract: Objective: To evaluate the clinical efficacy of blood-letting cupping combined with manual lymphatic drainage in treating breast cancer-related lymphedema (BCRL) and explore its mechanism of action from both traditional Chinese medicine and modern medical perspectives, providing a scientific basis and novel therapeutic approaches for clinical management of BCRL. Methods: Patients with BCRL admitted to the outpatient and inpatient departments of Hebei University Affiliated Hospital were enrolled. A prospective randomized controlled trial design was adopted, with eligible patients randomly assigned to a treatment group and a control group. The control group received manual lymphatic drainage alone, while the treatment group received manual lymphatic drainage combined with blood-letting cupping therapy. Post-treatment comparisons evaluated upper limb circumference reduction, edema severity grading, and upper limb functional scores. Vital signs and adverse reactions during treatment were recorded for both groups. Statistical software analyzed the data. *Results:* The treatment group demonstrated significantly greater reduction in upper limb circumference, improvement in edema severity, and higher upper limb function scores compared to the control group ($P < 0.05$). Vital signs remained stable throughout treatment in both groups. No severe adverse reactions occurred in the treatment group; only isolated cases of mild skin itching were reported, which resolved after symptomatic management. *Conclusion:* The combination of blood-letting cupping and manual lymphatic drainage demonstrates reliable efficacy in treating BCRL, effectively alleviating edema symptoms and improving upper limb function with high safety. Its mechanism may relate to traditional Chinese medicine principles of "unblocking meridians, promoting blood circulation, and resolving stasis" and modern medical concepts of "enhancing local blood circulation, facilitating lymphatic drainage, and reducing inflammatory responses".

Keywords: Blood-letting cupping; Postoperative breast cancer; Upper limb lymphedema; Efficacy observation; Mechanism of action

Online publication: February 4, 2026

1. Introduction

Breast cancer ranks among the most prevalent malignant tumors affecting women globally, posing a serious threat to their physical and mental health as well as their lives [1]. With advances in medical technology, the clinical cure rate for breast cancer has significantly improved. However, postoperative complications have become increasingly prominent, with breast cancer-related lymphedema (BCRL) being one of the most common. Studies indicate that the incidence of BCRL ranges from approximately 20% to 40%, and in some patients, the incidence rate can still exceed 30% during 5-year postoperative follow-up [2]. BCRL primarily results from axillary lymph node dissection during breast cancer surgery, which damages lymphatic drainage pathways. This leads to abnormal accumulation of lymph fluid in the interstitial spaces of the upper limb, causing symptoms such as swelling, pain, numbness, and limited mobility. Severe cases may also present with skin thickening, fibrosis, and infection, significantly reducing patients' quality of life and imposing a heavy physical and psychological burden [3]. Modern medical treatments for BCRL primarily include manual lymphatic drainage, compression therapy, functional exercises, and medication. However, these methods often exhibit limited efficacy, require prolonged treatment periods, and are prone to recurrence. Additionally, some medications may cause adverse reactions [4]. Traditional Chinese Medicine (TCM) possesses a long history and extensive experience in treating edema-related conditions. TCM external therapies, characterized by simplicity, convenience, safety, and efficacy, demonstrate unique advantages in managing BCRL. Blood-letting cupping, a key component of TCM external therapies, combines acupuncture with bloodletting and cupping to unblock meridians, promote blood circulation, resolve stasis, and eliminate water retention. It has been widely applied in treating various edema and pain-related conditions [5]. This study, grounded in both TCM and modern medical theories, employs a prospective randomized controlled trial design to evaluate the clinical efficacy and safety of combined blood-letting cupping and manual lymphatic drainage for treating BCRL. It aims to explore the underlying mechanisms of action, providing novel therapeutic approaches and theoretical support for BCRL management while enhancing patients' quality of life.

2. Materials and methods

2.1. Study population

Patients with BCRL who visited the outpatient or inpatient departments of Hebei University Affiliated Hospital between January 2023 and January 2024 were selected as study subjects. Inclusion criteria: (1) Diagnosis of breast cancer with upper limb lymphedema developing after surgical treatment (modified radical mastectomy or radical mastectomy); (2) Lymphedema onset occurring 1 month to 2 years post-surgery; (3) Peripheral circumference of the affected upper limb ≥ 2 cm larger than the unaffected side; (4) Age 18–70 years, conscious, and able to cooperate with treatment and efficacy evaluation; (5) Voluntary participation with signed informed consent. Exclusion criteria: (1) Severe dysfunction of vital organs (heart, liver, kidney, etc.); (2) Patients with coagulation disorders or bleeding tendencies; (3) Patients with skin lesions, ulcers, infections, or dermatological conditions on the affected upper limb; (4) Pregnant or lactating women; (5) Patients with allergies to blood-letting cupping or manual lymphatic drainage; (6) Patients with psychiatric disorders or those unable to cooperate with treatment.

2.2. Study design

This study employed a prospective randomized controlled trial design. Patients meeting the inclusion criteria were randomly assigned using a random number table to either the treatment group or the control group, with 30

patients in each group. Comparisons of general characteristics between groups—including age, disease duration, surgical approach, and edema severity—revealed no statistically significant differences ($P > 0.05$), ensuring comparability.

2.3. Treatment methods

Both groups received basic care, including health education (guiding patients to avoid weight-bearing and pressure on the affected upper limb, and maintaining warmth), dietary adjustments (light meals, avoiding spicy or irritating foods), and functional exercises (guiding patients in simple upper limb movements such as fist clenching and arm elevation). On this basis, the two groups received the following treatment protocols:

Control Group: Manual lymphatic drainage therapy alone. Performed by professional rehabilitation therapists using internationally recognized manual lymphatic drainage techniques. Starting from the fingers of the affected side, gentle pushing, kneading, and pressing were applied sequentially toward the wrist, forearm, elbow, upper arm, and axilla to promote lymphatic drainage. Each session lasted 30 minutes, with 5 sessions per week for 4 consecutive weeks.

Treatment group: Combined bloodletting and cupping therapy in addition to the manual lymphatic drainage of the control group. Specific procedures were as follows: (1) Point selection: Acupoints on the affected upper limb (Quchi, Shousanli, Hegu, Chize, Quze, Jianyu) and areas with prominent edema were selected for bloodletting and cupping. (2) Disinfection: Thoroughly disinfect selected acupoints and surrounding skin with povidone-iodine. After drying, remove iodine residue with 75% alcohol. (3) Bloodletting: Using sterile disposable three-edged needles, puncture disinfected acupoints and skin areas to a depth of 0.2–0.3 cm. Perform 3–5 punctures per site to induce minimal bleeding. (4) Cupping: Immediately place fire cups over the punctured areas. Select glass cups of appropriate size based on the area. Leave the cups in place for 10–15 minutes, monitoring the patient's skin color and bleeding to prevent excessive hemorrhage. (5) Post-procedure care: After cup removal, clean residual blood from the skin with sterile dry cotton balls and disinfect again with povidone-iodine. Bloodletting and cupping therapy are performed twice weekly, alternating with manual lymphatic drainage therapy, for a total of 4 consecutive weeks.

2.4. Observation indicators

2.4.1. Efficacy-related indicators

The following measurements were taken for both groups before treatment, immediately after treatment, and at weeks 4 and 8 post-treatment: (1) Upper limb circumference measurement: Measurements were taken at four sites on the affected upper limb: wrist crease, 10 cm above wrist crease, elbow crease, and 10 cm above elbow crease. A soft tape measure was used to record circumferences with 0.1 cm precision. The difference between affected and unaffected limb circumferences was calculated. (2) Edema Severity Grading: Following the BCRL grading criteria of the International Lymphology Society, edema severity was categorized as:(affected arm circumference >5 cm less than unaffected arm, marked skin thickening and hardening with fibrosis, accompanied by pain and limited mobility). (3) Upper Limb Function Score: Assessed using the Disability of the Arm, Shoulder, and Hand (DASH) scale. This 30-item questionnaire covers pain, daily activities, work, and leisure, with each item scored 0 to 4 points. Total scores range from 0 to 100, where higher scores indicate more severe upper limb dysfunction.

2.4.2. Safety indicators

During treatment, vital signs (respiratory rate, temperature, pulse, blood pressure) were recorded daily. Patients

were closely monitored for adverse reactions, including needle phobia, intolerable pain, skin itching, blistering, and infection during and after treatment. The timing, manifestations, management, and outcomes of adverse reactions were documented in detail.

2.5. Statistical methods

All data were analyzed using SPSS 26.0 statistical software. Quantitative data were expressed as mean ± standard deviation (SD). Paired t-tests were used for intra-group comparisons before and after treatment, while independent samples t-tests were used for inter-group comparisons. Qualitative data were expressed as rates (%). Inter-group comparisons for qualitative data were performed using chi-square (χ^2) tests. Ordinal data (edema severity grading) were analyzed using the rank sum test. A P value < 0.05 was considered statistically significant.

3. Results

This study included 60 patients with BCRL, randomly assigned to a treatment group and a control group, each comprising 30 patients. The treatment group patients ranged in age from 28 to 68 years, with a mean age of (55.9 ± 5.45) years old. Their disease duration ranged from 1 to 3 months, with a mean duration of (44.6 ± 8.63) days. Surgical procedures included modified radical mastectomy (25 cases), radical mastectomy (1 case), breast-conserving surgery (2 cases), and total excision (2 cases).Edema severity was mild in 7 cases, moderate in 16 cases, and severe in 7 cases. The control group comprised patients aged 29–69 years (mean age: 56.67 ± 5.34 years) with a disease duration of 1–3 months (mean duration: 42.43 ± 8.24 days). Surgical procedures included modified radical mastectomy in 27 cases, breast-conserving surgery in 1 case, and total mastectomy in 2 cases. with edema severity classified as mild in 7 cases, moderate in 15 cases, and severe in 8 cases. There were no statistically significant differences between the two groups in terms of age, disease duration, surgical approach, or edema severity (P > 0.05), indicating comparability. Regarding upper limb circumference difference, there was no statistically significant difference between the two groups before treatment (P > 0.05). After treatment, the arm circumference difference was (1.62 ± 0.55) cm in the treatment group and (2.38 ± 0.56) cm in the control group. Four weeks after treatment completion, the values were (1.23 ± 0.18) cm and (2.51 ± 0.27) cm, respectively. and 8 weeks post-treatment, the values were (0.7 ± 0.26) cm and (2.06 ± 0.29) cm, respectively. Both groups showed significant reduction compared to pre-treatment levels (P < 0.05), with the treatment group exhibiting a significantly greater reduction than the control group (P < 0.05). Regarding edema grading, no statistically significant difference existed between groups before treatment (P > 0.05). Significant improvement was observed in both groups after treatment and at weeks 4 and 8 post-treatment compared to baseline (P < 0.05), with the treatment group showing significantly greater improvement than the control group (P < 0.05). Regarding upper limb function DASH scores, no statistically significant difference existed between the two groups before treatment (P > 0.05). Post-treatment scores were (29.22 ± 7.44) for the treatment group and (34.28 ± 6.38) for the control group. At 4 weeks post-treatment, scores were (23.14 ± 6.99) for the treatment group and (30.25 ± 6.59) for the control group. and at 8 weeks post-treatment, the treatment group scored (18.81 ± 7.14) points while the control group scored (25.67 ± 6.87) points. Both groups showed significant reductions post-treatment compared to pre-treatment (P < 0.05), with the treatment group exhibiting a significantly greater reduction than the control group (P < 0.05). Regarding safety, vital signs, including respiration, body temperature, pulse, and blood pressure, remained stable throughout treatment in both groups without significant abnormalities. No notable adverse

reactions occurred in the control group. Only two patients in the treatment group experienced mild skin itching, which resolved after topical application of calamine lotion without affecting treatment. The incidence of adverse reactions showed no statistically significant difference between groups ($P > 0.05$).

4. Mechanism discussion

According to traditional Chinese medicine theory, BCRL falls under the categories of "edema" and "bi syndrome". Its pathogenesis is primarily associated with "Qi and blood stasis, meridian obstruction, and internal retention of dampness". Breast cancer surgery compromises the patient's vital energy, impairs Qi and blood circulation, and obstructs meridians, leading to abnormal water metabolism. Lymphatic fluid (referred to as "body fluids" in TCM) accumulates in the interstitial spaces of the upper limbs, forming edema. Bloodletting and cupping, as classic external therapies in TCM, exert their effects primarily through two mechanisms: unblocking meridians and harmonizing qi and blood, and promoting blood circulation to resolve stasis while draining fluids to reduce swelling. Specifically, the acupoints selected for this study—Quchi (LI11), Shousanli (LI10), and Hegu (LI4)—are all crucial points on meridians closely related to upper limb qi and blood circulation, such as the Hand Yangming Large Intestine Meridian and the Hand Taiyin Lung Meridian. Stimulating these points and the edematous areas through bloodletting and cupping unblocks obstructed meridians, harmonizes qi and blood circulation, restores normal Qi and blood distribution throughout the body, and simultaneously expels local stagnant blood and turbid fluids. The negative pressure generated by cupping enhances local blood circulation and strengthens Qi and blood movement. It also regulates the functions of the lung, spleen, and kidney to restore normal fluid metabolism, thereby promoting the excretion of bodily fluids at the root level to achieve edema reduction. From a modern medical perspective, the mechanism of blood-letting cupping therapy for BCRL primarily involves improving local blood circulation, promoting lymphatic drainage, reducing inflammatory responses, regulating immune function, and enhancing local tissue repair capacity. Following axillary lymph node dissection during breast cancer surgery, patients experience impaired lymphatic drainage pathways in the upper limbs and compromised local blood circulation. During blood-letting cupping, the puncture with a three-edged needle stimulates local vasodilation and increases vascular permeability. The negative pressure from cupping promotes local blood circulation, accelerates blood flow velocity, and directly propels lymph fluid from the damaged pathways toward normal pathways, reducing its accumulation in tissue spaces. Concurrently, blood-letting cupping lowers levels of inflammatory mediators such as interleukin-6 and Tumor Necrosis Factor-α (TNF-α) levels in local tissues, thereby mitigating inflammatory responses. It inhibits fibroblast proliferation and reduces collagen synthesis, delaying or suppressing the progression of local tissue fibrosis. Furthermore, as a physical stimulus, it activates the immune system, enhances immune cell activity, promotes local tissue metabolism and repair of damaged tissues, facilitates the restoration and reconstruction of lymphatic drainage pathways, and ultimately enhances therapeutic efficacy [6–10].

5. Discussion

The innovation of this study manifests in two key aspects: First, it fully leverages the broad applicability, significant efficacy, safety, and absence of notable side effects characteristic of TCM external therapies. By integrating blood-letting cupping with manual lymphatic drainage into a synergistic treatment protocol, clinical

trials have validated the efficacy and safety of this combined approach for treating BCRL, further highlighting the unique value of TCM external therapies in BCRL management. Second, it overcomes the limitations of previous studies that primarily focused on clinical efficacy observation with superficial exploration of mechanisms. By integrating recent literature, this study systematically discusses the mechanisms of action from the perspectives of TCM theories— "unblocking meridians, promoting blood circulation and resolving stasis, and promoting diuresis and reducing swelling"—and modern medicine— "improving local blood circulation, promoting lymphatic drainage, reducing inflammatory responses, and regulating immune function". Thipromoting diuresis and reduces edema with modern medicine's concepts of "improving local blood circulation, enhancing lymphatic drainage, reducing inflammatory responses, and regulating immune function". This systematic discussion clarifies the mechanism of action for blood-letting cupping in treating BCRL, providing crucial theoretical guidance for future clinical practice and efficacy enhancement. This study also has certain limitations. Specifically, the sample size was small and the research period was short, preventing long-term follow-up of patients to observe long-term efficacy and recurrence rates. Operational parameters such as the puncture depth and retention time of blood-letting cupping were not optimized to determine the optimal treatment regimen. Furthermore, the exploration of the mechanism of action was primarily based on existing literature and theoretical analysis, lacking supporting experimental research. Future work will focus on expanding sample size, extending the study duration, and conducting long-term follow-up to further validate the long-term efficacy and safety of blood-letting cupping therapy for BCRL. Additionally, multicenter, large-scale clinical studies will be initiated to optimize operational parameters and establish standardized treatment protocols. Basic research, including animal experiments, will also be conducted to explore the molecular biological mechanisms, thereby providing a more robust scientific foundation for clinical application.

6. Conclusion

In summary, the combination of blood-letting cupping and manual lymphatic drainage demonstrates definite efficacy and high safety in treating postoperative upper limb lymphedema following breast cancer surgery. It effectively alleviates edema symptoms and improves upper limb function. Its mechanisms correlate with traditional Chinese medicine principles of unblocking meridians, promoting blood circulation to remove stasis, and draining water to reduce swelling, as well as modern medical approaches of improving local blood circulation, enhancing lymphatic return, and reducing inflammatory responses. This treatment regimen warrants clinical promotion and application.

Disclosure statement

The authors declare no conflict of interest.

References

[1] Chen WQ, Zheng RS, Sun KX, et al., 2019, Analysis of Malignant Tumor Prevalence Data in China, 2016. Chinese Journal of Oncology, 41(1): 19–28.

[2] Wang S, Li H, Ding B, et al., 2020, Risk Factors and Nursing Strategies for Upper Limb Lymphedema After Breast Cancer Surgery. Chinese Journal of Nursing, 55(3): 332–337.

[3] Zhang P, Xu B, 2018, Advances in Diagnosis and Treatment of Upper Limb Lymphedema After Breast Cancer Surgery. Chinese Journal of Cancer, 40(7): 555–558.

[4] Li M, Wang C, Yang L, 2021, Observation on the Efficacy of Manual Lymphatic Drainage Combined with Pressure Therapy for Upper Limb Lymphedema After Breast Cancer Surgery. Chinese Journal of Rehabilitation Medicine, 36(2): 201–203.

[5] National Administration of Traditional Chinese Medicine, 2020, Clinical Application Guidelines for External Treatment Methods in Traditional Chinese Medicine. China Traditional Chinese Medicine Press, 2020: 123–126.

[6] Zhang Z, 2017, Treatise on Cold Damage and Miscellaneous Diseases. People's Medical Publishing House, 2017: 215–218.

[7] Wang Q, 2018, Medical Forest Corrections. China Traditional Chinese Medicine Press, 2018: 78–81.

[8] Liu M, Zhang Y, Li J, 2022, Effects of Bloodletting and Cupping on Local Blood Circulation and Lymphatic Return in an Experimental Edema Model in Rabbits. Chinese Journal of Traditional Chinese Medicine Science and Technology, 29(4): 543–545.

[9] Zhao H, Wang J, Li L, 2023, Anti-inflammatory Mechanism of Bloodletting and Cupping in Treating Upper Limb Lymphedema After Breast Cancer Surgery. Chinese Journal of Acupuncture and Moxibustion, 43(1): 67–71.

[10] Chen Z, Yang G, 2021, Chinese Internal Medicine. China Traditional Chinese Medicine Press, 2021: 345–348.

Publisher's note

Bio-Byword Scientific Publishing remains neutral with regard to jurisdictional claims in published maps and institutional affiliations.

Proceedings of Anticancer Research, 2026, Volume 10, Issue 1
http://ojs.bbwpublisher.com/index.php/PAR
ISSN Online: 2208-3553
ISSN Print: 2208-3545

Expression and Clinical Significance of PKM2 and SERBP1 in Colorectal Cancer

Yijie Li, Ying Duan, Zhengyi Cheng, Weichen Zuo, Juan Yang, Hangrong Fang*

Department of Pathology, Xi'an No.3 Hospital, The Affiliated Hospital of Northwest University, Xi'an 710021, Shaanxi, China

**Corresponding author: Hangrong Fang, fhr831@126.com*

Copyright: © 2026 Author(s). This is an open-access article distributed under the terms of the Creative Commons Attribution License (CC BY 4.0), permitting distribution and reproduction in any medium, provided the original work is cited.

Abstract: *Objective*: To investigate the expression of pyruvate kinase M2 (PKM2) and RNA binding proteins 1 (SERBP1) in colorectal cancer (CRC) and their clinical significance. *Methods*: A total of 101 cases of colorectal adenocarcinoma tissues and their corresponding adjacent tissues were collected from our hospital from December 2020 to December 2023. The immunohistochemical Elivision method was used to detect the expression of PKM2 and SERBP1 in CRC and corresponding adjacent tissues. The experimental data were analyzed using statistical software SPSS 27.0. *Results:* The expression rates of PKM2 and SERBP1 in CRC were higher than those in adjacent tissues. The expression of PKM2 was positively correlated with lymph node metastasis and TNM stage. The expression of SERBP1 was positively correlated with the degree of differentiation, lymph node metastasis, and TNM stage of CRC. *Conclusion:* PKM2 and SERBP1 may promote the occurrence and tumor progression of CRC, but further experimental research is still needed.

Keywords: PKM2; SERBP1; Colorectal cancer

Online publication: February 4, 2026

1. Introduction

Colorectal cancer (CRC) is a common malignant tumor with high heterogeneity and genetic instability. According to global cancer statistics, in 2022, more than 1.9 million people were diagnosed with colorectal cancer (including anal cancer) and 904,000 deaths occurred, accounting for nearly one-tenth of cancer cases and deaths. Overall, colorectal cancer ranks third in global incidence and second in mortality [1]. The occurrence of colorectal cancer involves multiple pathophysiological mechanisms, including abnormal cell proliferation, cell differentiation, resistance to apoptosis, invasion of adjacent structures by tumor cells, distant metastasis, etc., exhibiting a high degree of heterogeneity.

Abnormally active glycolysis is a significant characteristic of tumor cells [2]. Pyruvate kinase (PK) catalyzes the conversion of phosphoenolpyruvate (PEP) to pyruvate, representing the final rate-limiting step in the glycolytic

cascade. There are four PK isoforms: L, R, M1, and M2, each expressed in specific tissues. The M2 isoform, a splicing variant of M1, is expressed during embryonic development and tumorigenesis. Pyruvate kinase M2 (PKM2) can switch between a tetrameric form with high affinity for its substrate PEP and a dimeric form with low affinity for PEP. PKM2 primarily exists in two forms: a highly active tetrameric form and a less active dimeric form. The tetrameric PKM2 exhibits high affinity for its substrate phosphoenolpyruvate, demonstrating strong enzymatic catalytic ability. It often forms complexes with other glycolysis-related enzymes, facilitating the production of pyruvate and adenosine triphosphate. Tetrameric PKM2 is predominantly found in differentiated tissues and normally proliferating cells. Conversely, dimeric PKM2 is commonly present in tumor cells, displaying low affinity for its substrate and promoting the accumulation of glycolytic intermediates such as phosphoenol compounds within tumor cells. Intracellular glucose is utilized for the synthesis of nucleic acids, phospholipids, and amino acids, playing a crucial role in tumor cell proliferation [3]. PKM2 is the predominant form of pyruvate kinase in tumor tissues, exhibiting high expression in various tumor tissues and cell lines. Experimental studies both in vitro and in vivo have demonstrated that PKM2 promotes the proliferation and growth of tumor cells [4]. Elevated levels of PKM2 have been observed in serum samples from patients with gastric cancer, pancreatic cancer, cervical cancer, among others, suggesting its potential as a novel tumor marker. When combined with appropriate traditional tumor markers for detection, PKM2 can enhance the sensitivity of tumor detection.

RNA binding proteins 1 (SERBP1) is an arginine-methylated mRNA-binding protein and serves as an important intracellular RNA-binding partner. It was initially described as binding to the 3'-untranslated region (3'-UTR) of type 1 plasminogen activator inhibitor (PAI-1) mRNA, thereby regulating its stability [5]. RNA-binding proteins (RBPs) play crucial roles in coordinating post-transcriptional regulation and modulating many aspects of tumorigenesis, participating in nearly all aspects of RNA metabolism, from transcription to RNA degradation [6]. SERBP1 has been recognized as a significant regulator in various cancers, influencing mRNA degradation and the formation of RNA-protein complexes, thereby affecting mRNA stability and controlling the mRNA levels of target genes [7]. SERBP1 plays a vital role in many tumor cells. It is overexpressed in ovarian cancer epidermal cells and is significantly associated with the progression and grading (FIGO) of ovarian cancer, suggesting its important biological function in tumor invasion and metastasis [8]. In breast cancer, the expression of SERBP1 is significantly associated with a favorable prognosis [9]. Further research indicates that overexpression of SERBP1 in the HEK293T cell line can induce changes in genes related to cell proliferation, apoptosis, and the cell cycle [10]. In prostate cancer, miR-26a-5p promotes cell migration, invasion, and proliferation by negatively regulating SERBP1 expression [11]. A recent study also demonstrated that in pancreatic cancer, lncRNA-PVT1 acts as a molecular sponge to adsorb miR-448, thereby regulating the expression of its target SERBP1 and promoting proliferation and metastasis at the cellular level [12]. It has been reported that SERBP1 is a ribosome-associated protein involved in protein translation. Therefore, we can clearly conclude that SERBP1, as an RBP, plays a significant regulatory role in gene translation and tumor progression [13]. However, the regulatory mechanisms and pathways of SERBP1 remain largely unknown. Currently, there is limited research on the expression of PKM2 and SERBP1 in colorectal cancer, a disease with persistently high incidence and mortality rates that is difficult to cure. Therefore, further in-depth research on colorectal cancer is necessary, particularly in the search for new and effective targeted therapeutic approaches. This paper aims to discuss the expression of SERBP1 and PKM2 in colorectal cancer and their clinical significance, hoping to provide new research ideas for the treatment of colorectal cancer.

2. Materials and methods

2.1. General information

This experiment collated and collected 101 cases of colorectal adenocarcinoma diagnosed by the pathology department of our hospital from December 2020 to December 2023. After screening, all cases had been excluded for other diseases affecting survival time, and none had received any relevant treatment other than surgery. Paraffin-embedded tissue specimens from the selected cases were chosen, with the control group consisting of corresponding normal tissues adjacent to the cancer in the selected cases.

2.2. Clinical and pathological characteristics

Among the 101 CRC cases, there were 55 males and 46 females; 52 cases were ≤ 67 years old, and 49 cases were > 67 years old; 16 cases had mucinous adenocarcinoma components, while 85 cases did not; 15 cases were poorly differentiated, and 86 cases were moderately to well differentiated; 43 cases had no lymph node metastasis, while 58 cases did; 22 cases were in stages T1 and T2, and 79 cases were in stages T3 and T4; 3 cases exhibited microsatellite instability (MSI), and 98 cases were microsatellite stable (MSS) (**Table 1**).

Table 1. Clinical and pathological characteristics of patients

Clinical Pathological Feature	Frequency (n)	Percentage (%)
Gender		
Male	55	54.46
Female	46	45.54
Age (years)		
≤ 67	52	51.49
> 67	49	48.51
Mucinous Adenocarcinoma		
Yes	16	15.84
No	85	84.16
Differentiation Grade		
Low	15	14.85
Moderate/High	86	85.15
Lymph Node Metastasis		
No	43	42.57
Yes	58	57.43
T Stage		
T1 + T2	22	21.78
T3 + T4	79	78.22
MSI Status		
MSI	3	2.97
MSS	98	97.03

2.3. Methods

All surgical specimens were fixed with 4% neutral formaldehyde solution, routinely dehydrated, paraffin-embedded, and sectioned continuously at a thickness of 4 μm. The sections were stained with HE and observed under a light microscope. Immunohistochemistry was performed using the EnVision two-step method. The antibodies PKM2 and SERBP1 used were purchased from Wuhan Sanying Biotechnology Co., Ltd. The experimental process was carried out strictly in accordance with the reagent instructions, with PBS used as a blank control instead of the primary antibody.

2.4. Evaluation criteria and results of immunohistochemistry

Both PKM2 and SERBP1 proteins are expressed in the cytoplasm (**Figure 1**). Scoring based on the proportion of positive cells: a score of 0 is assigned if the number of positive cells is less than 5%; a score of 1 is assigned if it is 5% or more; a score of 2 is assigned if it is 25% or more; a score of 3 is assigned if it is 50% or more; and a score of 4 is assigned if it is 75% or more. Scoring based on staining intensity: negative (0 points) indicates the absence of brown granules; weakly positive (1 point) indicates scattered, pale, or fine brown granules; moderately positive (2 points) indicates the presence of large brownish-yellow granules; and strongly positive (3 points) indicates a dense distribution of brownish-yellow granules. The final score for each specimen is calculated by multiplying the proportion of stained cells by the staining intensity: a score of 0 indicates negative (–), scores from 1 to 4 indicate weakly positive (+), scores from 5 to 8 indicate moderately positive (2+), and scores greater than 8 indicate strongly positive (3+).

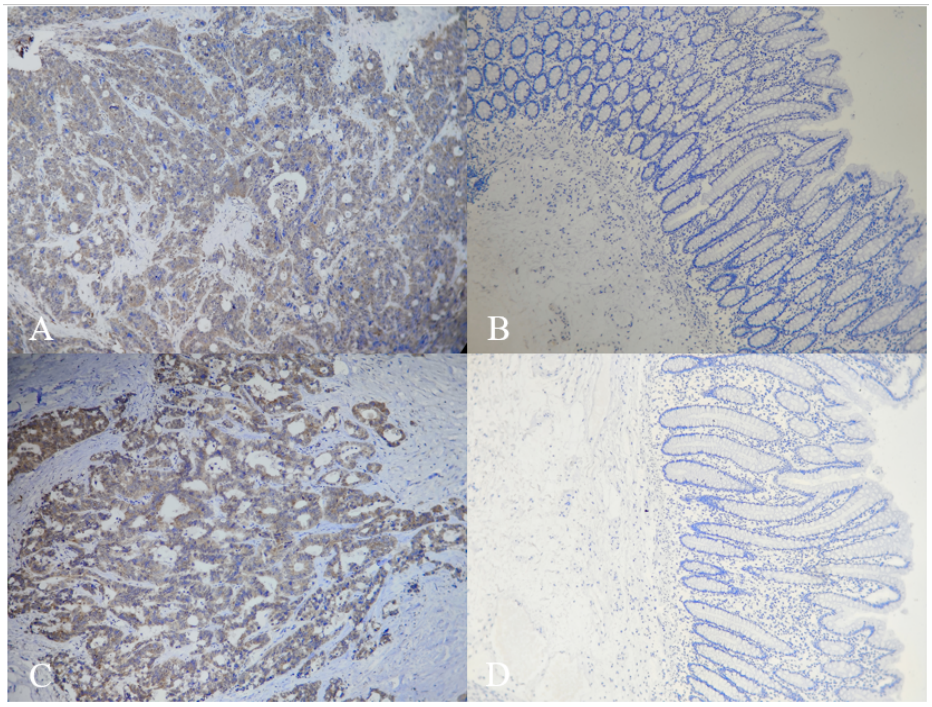


Figure 1. Expression of PKM2 and SERBP1 in CRC and adjacent tissues (immunohistochemical staining × 100). (A) Positive expression of PKM2 in CRC, with positive localization in the cytoplasm.(B) Negative expression of PKM2 in adjacent tissues.(C) Positive expression of SERBP1 in CRC, with positive localization in the cytoplasm. (D) Negative expression of SERBP1 in adjacent tissues.

2.5. Statistical analysis of data

All data in this study were analyzed using SPSS 27.0 software. The chi-square test was used to determine the relationship between clinicopathological parameters and PKM2 and SERBP1. A p-value less than 0.05 was considered statistically significant.

3. Results

3.1. Expression of PKM2 and SERBP1 in CRC and corresponding adjacent normal tissues

Among the 101 CRC specimens, 65 cases (65/101) exhibited positive PKM2 expression, with a positive expression rate of 75.25%. In contrast, 43 cases (43/101) of the corresponding adjacent normal tissues showed positive expression, with a positive expression rate of 42.57%. The difference in expression between the two groups was statistically significant ($\chi^2 = 9.630$, $P \approx 0.002$) (**Table 1**).

Among the 101 CRC specimens, 60 cases (60/101) demonstrated positive SERBP1 expression, with a positive expression rate of 59.41%. Conversely, 46 cases (46/101) of the corresponding adjacent normal tissues exhibited positive expression, with a positive expression rate of 45.54%. The difference in expression between the two groups was statistically significant ($\chi^2 = 3.891$, $P \approx 0.049$) (**Table 2**).

Table 2. Expression of PKM2 and SERBP1 in cancerous and adjacent normal tissues

Group	PKM2				SERBP1			
	Negative (n)	Positive (n)	χ^2	*P*-value	Negative (n)	Positive (n)	χ^2	*P*-value
Cancer Tissue	36	65	9.630	0.002	41	60	3.891	0.049
Paracancerous Tissue	58	43	—	—	55	46	—	—

3.2. Relationship between PKM2 and SERBP1 expression and clinicopathological features in CRC

Immunohistochemical results revealed that in CRC specimens, PKM2 expression was positively correlated with lymph node metastasis and TNM staging, with statistical significance ($P < 0.001$, $P = 0.036$). It was not associated with gender, age, mucinous adenocarcinoma status, degree of differentiation, or MSI status. SERBP1 expression was positively correlated with the degree of differentiation, lymph node metastasis, and TNM staging in CRC specimens, with statistical significance ($P = 0.004$, $P < 0.001$, $P = 0.013$). It was not related to gender, age, mucinous adenocarcinoma status, or MSI status (**Table 3**).

Table 3. Relationship between the expression of PKM2 and SERBP1 and clinicopathological characteristics in colorectal cancer

Group	PKM2				SERBP1			
	Negative	Positive	χ^2	*P*-value	Negative	Positive	χ^2	*P*-value
Gender			0.027	0.869			3.443	0.064
Male	20	35			22	43		
Female	16	30			19	17		

Table 3 (Continued)

Group	PKM2				SERBP1			
	Negative	Positive	χ^2	*P*-value	Negative	Positive	χ^2	*P*-value
Age (years)			2.075	0.150			0.330	0.566
≤ 67	22	30			19	33		
> 67	14	35			12	27		
Mucinous Adenocarcinoma			2.365	0.124			0.074	0.784
Yes	3	13			6	10		
No	33	52			35	50		
Differentiation Grade			0.041	0.840			8.409	0.004
Low	5	10			1	14		
Moderate/High	31	55			40	46		
Lymph Node Metastasis			49.079	< 0.001			64.148	< 0.001
No	32	11			37	6		
Yes	4	54			4	54		
T Stage			4.381	0.036			6.193	0.013
T1+T2	12	10			14	8		
T3+T4	24	55			27	52		
MSI Status			0.007	0.932			2.113	0.146
MSI	1	2			0	3		
MSS	35	63			41	57		

4. Discussion

Colorectal cancer ranks third in global incidence and second in mortality. Currently, surgical resection is the primary treatment approach, while adjuvant therapies such as radiotherapy, chemotherapy, targeted therapy, and immunotherapy are available for patients who are not candidates for surgery. Due to the high degree of tumor heterogeneity, the application of a uniform treatment strategy to different patients results in significant variations in treatment outcomes among individuals. Some patients with colorectal cancer are diagnosed at an advanced stage of the disease, and approximately 30% of early-stage colorectal cancers can metastasize, with a 5-year survival rate of around 60% for colorectal cancer patients. Therefore, identifying biological factors associated with the invasion, metastasis, and prognosis of colorectal cancer, as well as seeking new therapeutic targets, is of paramount importance.

Tumorigenesis is closely associated with glycolysis. Normal cells primarily obtain energy required for growth and proliferation through aerobic oxidation of glucose, with glycolysis occurring only under hypoxic conditions. In contrast, malignant tumor cells primarily rely on glycolysis for energy (even under aerobic conditions), consuming large amounts of glucose and producing lactic acid, a phenomenon known as the Warburg effect [14]. The conversion of glucose to lactic acid is a key characteristic that enables many cancer cells to promote rapid

growth. PKM2 is a classic glycolytic enzyme, and increased expression of PKM2 promotes lactic acid production in cancer cells [15]. PKM2 regulates its activity by switching between the low-activity dimer and high-activity tetramer states, thereby allowing cellular metabolism to shift between glycolysis and mitochondrial respiration, respectively [16]. Current literature reports that PKM2 is closely associated with the development of many tumors. This experimental study found that PKM2 expression is higher in colorectal cancer (CRC) than in adjacent normal tissues, and that PKM2 expression is statistically significantly correlated with lymph node metastasis and TNM staging, suggesting that PKM2 promotes the development of colorectal cancer, consistent with reports in the literature. RNA-binding proteins (RBPs) are crucial binding partners for intracellular RNA. Without RBPs,

RNA cannot perform any physiological functions. RBPs dynamically interact with RNA to form various complexes, such as ribonucleoprotein particles (RNPs) [6]. RBPs regulate cell fate through interactions with RNA and play a significant role in post-transcriptional gene regulation [17]. RBPs are involved in almost all aspects of RNA metabolism, from transcription to RNA degradation [18]. SERBP1, an arginine-methylated mRNA-binding protein, is an important binding partner for intracellular RNA. SERBP1 influences tumor proliferation and apoptosis through multiple mechanisms, suggesting its potential involvement in cancer cell metabolism. Studies have reported elevated levels of SERBP1 in various cancers, including acute lymphoblastic leukemia, breast cancer, ovarian cancer, glioblastoma, and squamous lung cell carcinoma [19]. The results of this experiment indicate that the expression of SERBP1 in colorectal cancer (CRC) is higher than that in adjacent normal tissues. Furthermore, the expression of SERBP1 is associated with the degree of differentiation, lymph node metastasis, and TNM staging of CRC, consistent with findings reported in the literature, suggesting that SERBP1 is involved in the occurrence and development of CRC.

5. Conclusion

In summary, among the 101 cases in this study, PKM2 and SERBP1 were upregulated in CRC, indicating a possible relationship between PKM2 and SERBP1 and the occurrence of CRC. The expression of PKM2 is positively correlated with lymph node metastasis and TNM staging in CRC, while the expression of SERBP1 is positively correlated with the degree of differentiation, lymph node metastasis, and TNM staging in CRC, with statistically significant differences. Therefore, we hypothesize that PKM2 and SERBP1 may play a role in promoting the development of CRC, but further experimental research is needed.

Funding

Research Project of Xi'an Health Commission (Project No.: 2023yb11)

Disclosure statement

The authors declare no conflict of interest.

References

[1] Bray F, Laversanne M, Sung H, et al., 2024, Global Cancer Statistics 2022: GLOBOCAN Estimates of Incidence and Mortality Worldwide for 36 Cancers in 185 Countries. CA Cancer J Clin, 74(3): 229–263.

[2] Li J, Yue L, Zhang W, 2022, Research Progress on the Role of Glycolytic Key Enzymes and Their Targeted Drugs in Cancer. Journal of Medical Research, 8: 51.

[3] Zhou CF, Li XB, Sun H, et al., 2012, Pyruvate Kinase Type M2 Is Upregulated in Colorectal Cancer and Promotes Proliferation and Migration of Colon Cancer Cells. IUBMB Life, 64(9): 775–782.

[4] Wang J, Cheng B, 2014, The Role of M2-Type Pyruvate Kinase in Tumor Metabolism. International Journal of Oncology, 1: 17–20.

[5] Martini S, Davis K, Faraway R, et al., 2021, A Genetically-Encoded Crosslinker Screen Identifies SERBP1 as a PKCepsilon Substrate Influencing Translation and Cell Division. Nat Commun, 12(1): 6934.

[6] Zhou J, Chen W, He Q, et al., 2022, SERBP1 Affects the Apoptotic Level by Regulating the Expression and Alternative Splicing of Cellular and Metabolic Process Genes in HeLa Cells. PeerJ, 10: e14084.

[7] Heaton JH, Dlakic WM, Dlakic M, et al., 2001, Identification and cDNA Cloning of a Novel RNA-Binding Protein That Interacts with the Cyclic Nucleotide-Responsive Sequence in the Type-1 Plasminogen Activator Inhibitor mRNA. J Biol Chem, 276(5): 3341–3347.

[8] Koensgen D, Mustea A, Klaman I, et al., 2007, Expression Analysis and RNA Localization of PAI-RBP1 (SERBP1) in Epithelial Ovarian Cancer: Association with Tumor Progression. Gynecol Oncol, 107(2): 266–273.

[9] Serce NB, Boesl A, Klaman I, et al., 2012, Overexpression of SERBP1 (Plasminogen Activator Inhibitor 1 RNA Binding Protein) in Human Breast Cancer Is Correlated with Favourable Prognosis. BMC Cancer, 12: 597.

[10] Costa FC, Saito A, Goncalves KA, et al., 2014, Ki-1/57 and CGI-55 Ectopic Expression Impact Cellular Pathways Involved in Proliferation and Stress Response Regulation. Biochim Biophys Acta, 1843(12): 2944–2956.

[11] Guo K, Zheng S, Xu Y, et al., 2016, Loss of miR-26a-5p Promotes Proliferation, Migration, and Invasion in Prostate Cancer Through Negatively Regulating SERBP1. Tumour Biol, 37(9): 12843–12854.

[12] Zhao L, Kong H, Sun H, et al., 2018, LncRNA-PVT1 Promotes Pancreatic Cancer Cells Proliferation and Migration Through Acting as a Molecular Sponge to Regulate miR-448. J Cell Physiol, 233(5): 4044–4055.

[13] Muto A, Sugihara Y, Shibakawa M, et al., 2018, The mRNA-Binding Protein Serbp1 as an Auxiliary Protein Associated with Mammalian Cytoplasmic Ribosomes. Cell Biochem Funct, 36(6): 312–322.

[14] Hanahan D, Weinberg RA, 2011, Hallmarks of Cancer: The Next Generation. Cell, 144(5): 646–674.

[15] Luo W, Semenza GL, 2012, Emerging Roles of PKM2 in Cell Metabolism and Cancer Progression. Trends Endocrinol Metab, 23(11): 560–566.

[16] Wong N, Ojo D, Yan J, et al., 2015, PKM2 Contributes to Cancer Metabolism. Cancer Lett, 356(2 Pt A): 184–191.

[17] Hentze MW, Castello A, Schwarzl T, et al., 2018, A Brave New World of RNA-Binding Proteins. Nat Rev Mol Cell Biol, 19(5): 327–341.

[18] Gerstberger S, Hafner M, Tuschl T, 2014, A Census of Human RNA-Binding Proteins. Nat Rev Genet, 15(12): 829–845.

[19] Zhou J, Wang T, Zhang H, et al., 2024, KSHV vIL-6 Promotes SIRT3-Induced Deacetylation of SERBP1 to Inhibit Ferroptosis and Enhance Cellular Transformation by Inducing Lipoyltransferase 2 mRNA Degradation. PLoS Pathog, 20(3): e1012082.

Publisher's note

Bio-Byword Scientific Publishing remains neutral with regard to jurisdictional claims in published maps and institutional affiliations.

Proceedings of Anticancer Research, 2026, Volume 10, Issue 1
http://ojs.bbwpublisher.com/index.php/PAR
ISSN Online: 2208-3553
ISSN Print: 2208-3545

Research on the Impact of Different Lymph Node Dissection Scopes on Postoperative Recurrence and Survival Rates in Patients with Early Gastric Cancer

Zhijun Mao, Yingdi Wei, Ganjie Yang, Pan Gao, Tong Hui*

Shaanxi Provincial People's Hospital, Xi'an 710068, Shaanxi, China

**Author to whom correspondence should be addressed.*

Copyright: © 2026 Author(s). This is an open-access article distributed under the terms of the Creative Commons Attribution License (CC BY 4.0), permitting distribution and reproduction in any medium, provided the original work is cited.

Abstract: *Objective*: To investigate the impact of different lymph node dissection scopes on postoperative recurrence and survival rates in patients with early gastric cancer, providing evidence-based support for optimizing clinical surgical plans. *Methods*: A retrospective analysis was conducted on the clinical data of 100 patients with early gastric cancer who underwent surgical treatment at our hospital from October 2021 to October 2023. Patients were divided into Group D1 (n = 50) and Group D2 (n =50) based on the extent of lymph node dissection. Group D1 underwent limited lymph node dissection (dissection of the first station of lymph nodes around the stomach), while Group D2 underwent standard lymph node dissection (dissection of the first and second stations of lymph nodes around the stomach). Surgical-related indicators, the incidence of postoperative complications, the 2-year recurrence rate, and the 2-year survival rate were compared between the two groups of patients. *Results*: The operative time, intraoperative blood loss, postoperative hospital stay, and the number of lymph nodes dissected were significantly higher in the D2 group than in the D1 group (all $P < 0.001$). The overall incidence of postoperative complications was higher in the D1 group than in the D2 group, but the difference was not statistically significant ($\chi^2 = 0.884$, $P = 0.766$). After a 2-year follow-up, the recurrence rate was significantly higher in the D1 group than in the D2 group ($\chi^2 = 4.000$, $P = 0.046$). The 2-year survival rate was significantly lower in the D1 group than in the D2 group ($\chi^2 = 5.005$, $P = 0.025$). A total of 100 patients with early-stage gastric cancer were grouped according to the depth of invasion, degree of differentiation, and lymph node metastasis status, and the recurrence rates of different subgroups were compared. The results showed that the recurrence rate was higher in patients with T1b stage than in those with T1a stage ($\chi^2 = 5.005$, $P = 0.025$), higher in poorly differentiated patients than in moderately and well-differentiated patients ($\chi^2 = 4.155$, $P = 0.042$), and higher in patients with lymph node metastasis than in those without lymph node metastasis ($\chi^2 = 4.512$, $P = 0.034$). *Conclusion*: Compared with D1 limited lymph node dissection, D2 standard lymph node dissection can significantly reduce the postoperative recurrence rate and improve the 2-year survival rate in patients with early-stage gastric cancer without significantly increasing the risk of postoperative complications. Although the surgical trauma is slightly greater, the overall prognosis is better, making it a preferred surgical treatment option for patients with early-stage gastric cancer.

Keywords: Early-stage gastric cancer; Extent of lymph node dissection; D1 dissection; D2 dissection; Recurrence rate; Survival rate

Online publication: February 9, 2026

1. Introduction

Gastric cancer is a common malignant tumor of the digestive system worldwide, ranking among the top in both incidence and mortality rates among malignant tumors, and posing a serious threat to human life and health [1]. Early-stage gastric cancer refers to tumors with infiltration depth limited to the mucosal layer or submucosal layer, regardless of the presence of lymph node metastasis [2]. With the widespread adoption of gastroscopy screening techniques, the detection rate of early-stage gastric cancer has been increasing annually, with surgical treatment being the preferred radical approach. Lymph node metastasis is a significant risk factor for postoperative recurrence and poor prognosis in gastric cancer patients, so the quality of lymph node dissection directly impacts the patient's treatment outcomes and long-term prognosis. Currently, there is still controversy regarding the extent of lymph node dissection for patients with early-stage gastric cancer. D1 dissection (limited lymph node dissection) involves the removal of only the first-tier lymph nodes around the stomach, resulting in less surgical trauma but potentially leaving behind micrometastases due to incomplete dissection, thereby increasing the risk of postoperative recurrence. D2 dissection (standard lymph node dissection) requires the removal of both the first- and second-tier lymph nodes around the stomach, enabling a more thorough clearance of potentially metastatic lymph nodes and reducing the risk of recurrence, but it involves greater surgical trauma and may increase the incidence of postoperative complications. Therefore, balancing surgical trauma with prognostic benefits is crucial in determining the extent of lymph node dissection for early-stage gastric cancer.

2. Materials and methods

2.1. General information

A retrospective study was conducted on 100 patients with early-stage gastric cancer who underwent surgical treatment in the Department of Gastrointestinal Surgery at our hospital from October 2021 to October 2023. Inclusion criteria were as follows: (1) Postoperative pathology confirmed gastric cancer with infiltration depth limited to the mucosal layer (T1a) or submucosal layer (T1b), meeting the diagnostic criteria for early-stage gastric cancer [3]; (2) No adjuvant therapy, such as radiotherapy, chemotherapy, or targeted therapy, was administered before surgery; (3) Complete clinical data were available, enabling a 2-year follow-up; (4) Informed consent was obtained from both patients and their families, and the study was approved by the hospital's ethics committee. Exclusion criteria included: (1) Presence of other malignancies; (2) Severe dysfunction of vital organs, including the heart, liver, or kidneys; (3) Discovery of distant metastasis or non-resectable tumors during surgery; (4) Loss to follow-up or death from non-tumor-related causes during the follow-up period.

Patients were divided into Group D1 and Group D2 based on the extent of lymph node dissection, with 50 patients in each group. In Group D1, there were 28 males and 22 females, aged between 42 and 76 years old, with an average age of (58.62 ± 8.35) years old. Tumor locations included 12 cases in the gastric cardia,

18 in the gastric body, and 20 in the gastric antrum. Infiltration depth comprised 26 cases at T1a stage and 24 at T1b stage. Differentiation grades included 22 well-differentiated, 19 moderately differentiated, and 9 poorly differentiated cases. Regarding lymph node metastasis, 15 cases had metastasis, while 35 did not. In Group D2, there were 26 males and 24 females, aged between 40 and 78 years, with an average age of (59.15 ± 8.67) years. Tumor locations included 10 cases in the gastric cardia, 20 in the gastric body, and 20 in the gastric antrum. Infiltration depth comprised 24 cases at T1a stage and 26 at T1b stage. Differentiation grades included 20 well-differentiated, 21 moderately differentiated, and 9 poorly differentiated cases. Regarding lymph node metastasis, 16 cases had metastasis, while 34 did not. No statistically significant differences were observed in general information such as gender, age, tumor location, depth of invasion, degree of differentiation, and lymph node metastasis between the two groups of patients ($P > 0.05$), indicating comparability.

2.2. Surgical methods

For both groups of patients, the surgical approach was selected based on the tumor location (distal gastrectomy, proximal gastrectomy, or total gastrectomy), and all surgeries were performed by the same experienced surgical team.

In Group D1, limited lymph node dissection was performed, involving only the removal of the first-tier lymph nodes around the stomach (corresponding to different stomach regions: for the gastric fundus and cardia, groups 1, 2, 3, 4sa, and 4sb; for the gastric body, groups 1, 3, 4sb, 5, and 6; and for the gastric antrum, groups 3, 4d, 5, and 6).

In Group D2, standard lymph node dissection was carried out, which, in addition to the D1 dissection, included the removal of the second-tier lymph nodes around the stomach (corresponding to different stomach regions: for the gastric fundus and cardia, groups 7, 8a, 9, 10, and 11; for the gastric body, groups 7, 8a, 9, and 11; and for the gastric antrum, groups 7, 8a, 9, and 12a), ensuring that the number of lymph nodes dissected was ≥ 15.

2.3. Observation indicators and follow-up

(1) Surgical-related indicators: The surgical time, intraoperative blood loss, postoperative hospital stay, and the number of lymph nodes dissected were recorded for both groups of patients.

(2) Postoperative complications: Complications occurring within 30 days postoperatively were observed and recorded, including wound infection, abdominal infection, anastomotic leakage, delayed gastric emptying, intestinal obstruction, etc., and the severity of complications was assessed.

(3) Recurrence and survival status: Patients were followed up for two years through outpatient reviews and telephone follow-ups after surgery, with the follow-up ending in October 2025. Reviews were conducted every three months, including blood tests, tumor markers (CEA, CA19-9), gastroscopy, abdominal CT, etc. The time of tumor recurrence, the site of recurrence, and the survival status of patients were recorded. Recurrence was defined as the presence of new tumor lesions confirmed by imaging or pathological examination after surgery; survival rate was calculated as the proportion of patients still alive at the end of the follow-up period.

2.4. Statistical methods

Data analysis was performed using SPSS 26.0 statistical software. Measurement data were expressed as mean ±

standard deviation (SD), and comparisons between groups were made using independent sample t-tests. Count data were expressed as the number of cases (percentage) [*n* (%)], and comparisons between groups were made using the χ^2 test. A *P*-value < 0.05 was considered statistically significant.

3. Results

3.1. Comparison of surgical indicators between the two groups of patients

The surgical duration, intraoperative blood loss, postoperative hospital stay, and number of lymph nodes dissected were significantly higher in the D2 group than in the D1 group (all $P < 0.001$). See **Table 1**.

Table 1. Comparison of surgical indicators between the two groups of patients

Group	Operative Time (min)	Intraoperative Blood Loss (ml)	Postoperative Hospital Stay (days)	Number of Lymph Nodes Dissected
D1 Group ($n = 50$)	128.56 ± 23.45	85.32 ± 21.67	7.24 ± 1.89	8.62 ± 2.15
D2 Group ($n = 50$)	186.78 ± 31.24	132.56 ± 30.45	9.56 ± 2.34	18.95 ± 3.67
t-value	10.539	8.938	5.454	17.234
P-value	< 0.001	< 0.001	< 0.001	< 0.001

3.2. Comparison of postoperative complication rates between the two groups of patients

The overall incidence of postoperative complications was higher in the D1 group than in the D2 group, but the difference was not statistically significant ($\chi^2 = 0.884$, $P = 0.766$). See **Table 2**.

Table 2. Comparison of postoperative complications between the two groups of patients

Group	Incision Infection	Abdominal Infection	Delayed Gastric Emptying	Anastomotic Leak	Intestinal Obstruction	Total Incidence (%)
D1 Group ($n = 50$)	3 (6.00)	2 (4.00)	2 (4.00)	0 (0.00)	0 (0.00)	7 (14.00)
D2 Group ($n = 50$)	2 (4.00)	1 (2.00)	2 (4.00)	1 (2.00)	0 (0.00)	6 (12.00)
χ^2						0.884
P-value						0.766

3.3. Comparison of recurrence rate and survival rate between the two groups of patients two years after surgery

After two years of follow-up, the recurrence rate in Group D1 was significantly higher than that in Group D2 ($\chi^2 = 4.000$, $P = 0.046$); the two-year survival rate in Group D1 was significantly lower than that in Group D2 ($\chi^2 = 5.005$, $P = 0.025$). See **Table 3**.

Table 3. Comparison of recurrence rate and survival rate between the two groups of patients two years after surgery

Group	Recurrence Cases (n)	Recurrence Rate (%)	Death Cases (n)	2-Year Survival Rate (%)
D1 Group	8	16.00	9	82.00
D2 Group	2	4.00	2	96.00
χ^2	—	4.000	—	5.005
P-value	—	0.046	—	0.025

3.4. Comparison of postoperative recurrence in early gastric cancer patients with different clinical characteristics

A total of 100 early gastric cancer patients were grouped according to the depth of invasion, degree of differentiation, and lymph node metastasis status, and the recurrence rates of different subgroups were compared. The results showed that the recurrence rate in patients at stage T1b was higher than that in patients at stage T1a ($\chi^2 = 5.005$, $P = 0.025$), the recurrence rate in poorly differentiated patients was higher than that in moderately to well-differentiated patients ($\chi^2 = 4.155$, $P = 0.042$), and the recurrence rate in patients with lymph node metastasis was higher than that in patients without lymph node metastasis ($\chi^2 = 4.512$, $P = 0.034$). See **Table 4**.

Table 4. Comparison of postoperative recurrence in early gastric cancer patients with different clinical characteristics

Clinical Feature	Total Cases (n)	Recurrence Cases (n/%)	χ^2	*P*-value
Depth of Invasion	—	—		
T1a Stage	50	2 (4)	5.005	0.025
T1b Stage	50	9 (18)		
Differentiation Grade	—	—		
Moderate-High	82	6 (7.89)	4.155	0.042
Low	18	6 (33.33)		
Lymph Node Metastasis	—	—		
Positive	31	7 (21.88)	4.512	0.034
Negative	69	3 (5.41)		

4. Discussion

The primary treatment for early gastric cancer is radical surgical resection, and lymph node dissection is an important component of the surgery, with its scope directly related to the patient's prognosis [4]. Currently, there is still controversy regarding the scope of lymph node dissection for early gastric cancer patients. This study retrospectively analyzed the clinical data of 100 early gastric cancer patients, comparing the effects of two lymph node dissection scopes, D1 and D2, on postoperative recovery and prognosis, providing data support for the selection of clinical surgical plans.

The results of this study indicate that patients in the D2 group had significantly longer operative times,

higher intraoperative blood loss, and longer postoperative hospital stays compared to those in the D1 group. This is attributed to the fact that D2 lymphadenectomy involves the dissection of more lymph node stations, making the surgical procedure more complex and causing greater trauma. However, it is noteworthy that there was no statistically significant difference in the overall incidence of postoperative complications between the two groups, suggesting that although D2 lymphadenectomy causes greater surgical trauma, it does not significantly increase the risk of postoperative complications when performed under standardized protocols [5]. This may be attributed to advancements in surgical techniques, optimization of perioperative management, and the extensive experience of the surgeons, which effectively reduce the occurrence of surgery-related complications.

Recurrence rate and survival rate are core indicators for evaluating the prognosis of patients with malignant tumors [6]. During the 2-year follow-up in this study, it was found that patients in the D1 group had a significantly higher postoperative recurrence rate compared to those in the D2 group, while the 2-year survival rate in the D1 group was significantly lower than that in the D2 group. These findings suggest that D2 standard lymphadenectomy can significantly reduce the risk of postoperative recurrence and improve long-term survival rates in patients with early-stage gastric cancer [7]. The primary reason for this is that D2 lymphadenectomy enables a more thorough clearance of potentially metastatic lymph nodes around the stomach, particularly micrometastases in the second-tier lymph nodes, thereby preventing tumor recurrence caused by residual lymph nodes [8]. Additionally, this study also found that patients with early-stage gastric cancer at stage T1b, with poorly differentiated tumors, or with lymph node metastasis had a higher recurrence rate. These patients have relatively more aggressive tumors and a higher risk of lymph node metastasis, thus necessitating a more thorough lymphadenectomy to reduce the risk of recurrence. The advantages of D2 lymphadenectomy may be more pronounced in such patients.

Regarding the selection of the extent of lymph node dissection for early-stage gastric cancer, some scholars believe that for patients with early-stage gastric cancer without lymph node metastasis, D1 dissection can meet therapeutic needs, and excessive dissection may increase surgical trauma without providing additional prognostic benefits [9]. However, in clinical practice, the accuracy of preoperative imaging in determining lymph node metastasis is limited, with a certain rate of missed diagnoses. Some patients assessed as having no lymph node metastasis preoperatively may be found to have occult lymph node metastasis upon postoperative pathological examination. D2 dissection can effectively cover these occultly metastatic lymph nodes, reducing the risk of recurrence. In this study, three patients in the D1 group who were preoperatively assessed as having no lymph node metastasis experienced recurrence postoperatively, possibly related to incomplete clearance of occult lymph node metastasis. Therefore, even for patients with early-stage gastric cancer assessed as having no lymph node metastasis preoperatively, D2 standard lymph node dissection may still hold significant prognostic value [10].

This study has certain limitations: (1) As a retrospective study, it is subject to selection bias and has a relatively limited sample size (100 cases), which may affect the objectivity of the results; (2) The follow-up period was relatively short (2 years), making it impossible to evaluate the impact of the two lymph node dissection extents on patients' long-term (5 years or more) survival rates; (3) Factors such as patients' genetic characteristics and immune function were not considered in relation to their impact on prognosis. Future research could involve prospective, large-sample clinical studies with extended follow-up periods and incorporate molecular biological indicators to further explore the impact of different lymph node dissection

extents on the prognosis of patients with early-stage gastric cancer, providing a more robust basis for the development of individualized clinical treatment plans.

5. Conclusion

In summary, compared to D1 limited lymph node dissection, D2 standard lymph node dissection, despite involving slightly greater surgical trauma and a marginally longer postoperative recovery time, significantly reduces the postoperative recurrence rate and improves the 2-year survival rate in patients with early-stage gastric cancer, without significantly increasing the risk of postoperative complications. Therefore, D2 standard lymph node dissection can be considered the preferred surgical treatment option for patients with early-stage gastric cancer, particularly those with deeper tumor invasion (T1b stage) or at risk of lymph node metastasis.

Funding

Shaanxi Provincial People's Hospital Science and Technology Development Incubation Fund, "Research on the Role and Mechanism of PIGU in Regulating MUC-1 in Gastric Cancer Immune Escape" (Project No.: 2023YJY-29); Shaanxi Provincial Natural Science Basic Research Program, "Research on the Mechanism and Clinical Significance of miR-140-5p Related to Gastric Cancer Recurrence and Metastasis" (Project No.: 2023-JC-YB-639)

Disclosure statement

The authors .declare no conflict of interest.

References

[1] He Y, Chen J, Xia Q, et al., 2024, Research Status of miR-135b in Malignant Tumors of the Digestive System. Chinese Journal of Clinical Pharmacology, 40(18): 2747–2751.

[2] Wang J, Wang H, Huang X, et al., 2025, Research Progress on Endoscopic Submucosal Dissection in the Treatment of Early-Stage Gastric Cancer. Journal of Practical Oncology, 40(6): 521–529.

[3] Liang L, Jia C, Li Q, et al., 2025, Diagnostic Value of Combined Detection of Serum NF-κB, G-17, and HLA-G in Early-Stage Gastric Cancer Associated with Helicobacter pylori Infection. Immunological Journal, 41(12): 922–928.

[4] Lin M, Ou X, 2020, Research Progress on Non-Curative Endoscopic Resection and Postoperative Remedial Measures for Early-Stage Gastric Cancer. Journal of Southeast University (Medical Science Edition), 39(2): 248–252.

[5] Huang W, Liang H, 2022, Clinical Research Progress on Sentinel Lymph Nodes in Early Gastric Cancer. Chinese Journal of Practical Surgery, 42(10): 1180–1183.

[6] Wang Z, Sun J, Luo C, et al., 2025, Efficacy of PD-1/PD-L1 Inhibitors Combined with Thymosin α1 in the Treatment of Advanced Gastric Cancer and Its Impact on Peripheral Blood NK Cells and Long-Term Prognosis of Patients. International Journal of Digestive Diseases, 45(6): 409–414 + 429.

[7] Zhang L, Lv X, Li G, et al., 2025, Comparative Study on the Efficacy of Endoscopic Submucosal Dissection and Surgical Treatment for Undifferentiated Early Gastric Cancer. China Medical Equipment, 22(12): 69–73.

[8] Jin J, Deng J, Liang H, 2016, Clinical Evolution and Research Progress on Lymph Node Staging Methods for Gastric

Cancer. Chinese Journal of Clinical Oncology, 43(15): 683–689.

[9] Zhang B, Zhao G, 2022, Advances in the Treatment of Early Gastric Cancer with Preservation of Gastric Function. Journal of Practical Hospital Clinical, 19(3): 187–191.

[10] Song K, Chen H, Shan Z, et al., 2024, Risk Factors for Lymph Node Metastasis in Early Gastric Cancer and Their Impact on Prognosis. Journal of Frontiers of Medicine, 14(33): 128–131.

Publisher's note

Bio-Byword Scientific Publishing remains neutral with regard to jurisdictional claims in published maps and institutional affiliations.

Integrated Services Platform of International Scientific Cooperation

Innoscience Research (Malaysia), which is global market oriented, was founded in 2016.Innoscience Research focuses on services based on scientific research. By cooperating with universities and scientific institutes all over the world, it performs medical researches to benefit human beings and promotes the interdisciplinary and international exchanges among researchers.

Innoscience Research covers biology, chemistry, physics and many other disciplines. It mainly focuses on the improvement of human health. It aims to promote the cooperation, exploration and exchange among researchers from different countries. By establishing platforms, Innoscience integrates the demands from different fields to realize the combination of clinical research and basic research and to accelerate and deepen the international scientific cooperation.

Cooperation Mode



Clinical Workers



In-service Doctors





Foreign Researchers

China Collaborators



Oversea Collaborators



Hospital



University



Scientific institutions

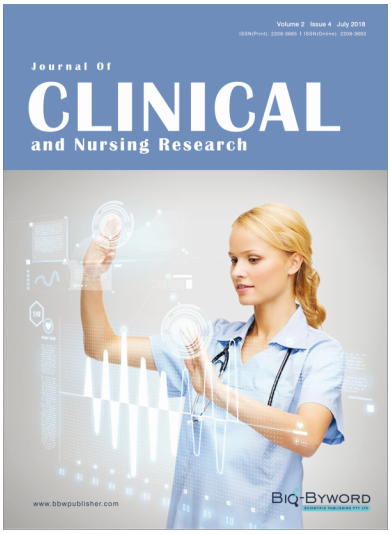
Our Journals



The *Journal of Architectural Research and Development* is an international peer-reviewed and open access journal which is devoted to establish a bridge between theory and practice in the fields of architectural and design research, urban planning and built environment research.

Topics covered but not limited to:

- Architectural design
- Architectural technology, including new technologies and energy saving technologies
- Architectural practice
- Urban planning
- Impacts of architecture on environment



Journal of Clinical and Nursing Research (JCNR) is an international, peer reviewed and open access journal that seeks to promote the development and exchange of knowledge which is directly relevant to all clinical and nursing research and practice. Articles which explore the meaning, prevention, treatment, outcome and impact of a high standard clinical and nursing practice and discipline are encouraged to be submitted as original article, review, case report, short communication and letters.

Topics covered by not limited to:

- Development of clinical and nursing research, evaluation, evidence-based practice and scientific enquiry
- Patients and family experiences of health care
- Clinical and nursing research to enhance patient safety and reduce harm to patients
- Ethics
- Clinical and Nursing history
- Medicine



Journal of Electronic Research and Application is an international, peer-reviewed and open access journal which publishes original articles, reviews, short communications, case studies and letters in the field of electronic research and application.

Topics covered but not limited to:

- Automation
- Circuit Analysis and Application
- Electric and Electronic Measurement Systems
- Electrical Engineering
- Electronic Materials
- Electronics and Communications Engineering
- Power Systems and Power Electronics
- Signal Processing
- Telecommunications Engineering
- Wireless and Mobile Communication